A ROCKET DRIVE
FOR
LONG RANGE BOMBERS

(Über einen Raketenantrieb für Fernbomber)

by

E. Sänger and J. Bredt

Ainring, August 1944

Deutsche Luftfahrtforschung

UM 3538

Translated by M. HAMERMESH
RADIO RESEARCH LABORATORY

Reproduced by
TECHNICAL INFORMATION BRANCH
BUAER NAVY DEPARTMENT

A Note by the Publisher

Toward the end of the last century a few farsighted individuals became thoroughly convinced that man could fly. Today their names are all but forgotten but their technical achievements will endure for centuries.

Today we are on the threshold of manned flight between the planets. Drs. Eugen Sänger and Irene Bredt are prominent among the handful of pioneers whose dedicated efforts have made possible this vista.

"Uber einen Raketenantrieb fur Fernbomber" is based on more than a decade of effort by the authors. The material is condensed. This report contains only about one-third of the information which the authors had available at the time of writing; all of the mathematical derivations and much of the supporting and supplementary information were omitted.

In spite of this fact, the report is, in effect, a definitive treatise. It catalogs new problems and outlines solutions to the more important ones. For years to come it will serve as a storehouse of vital concepts for the serious student of rocket science. For these reasons, its publication at this time seems warranted.

Since 1945, Dr. Irene Bredt (now Sänger-Bredt) and Dr. Eugen Sänger have lived in Paris, where they are employed by the Arsenal de l'Aeronautique. Dr. Sänger is also president of the International Astronautical Federation.

While the Technical Information Branch, BUAER, Navy Department, has very generously furnished copies of their translation of "Uber einen Raketenantrieb fur Fernbomber" to many public libraries and research institutions, this is the first time the report has been available for public sale. The publisher would like to thank the U. S. Navy, without whose permission this publication would not have been possible.

Robert Cornog
Santa Barbara, California
16 November 1952

FOREWORD

The application of pure rocket propulsion to aeronautics suffers at present from limitations imposed on exhaust speed and flight velocity by constructional difficulties.

Because of the thermal stresses on the engines, the exhaust speed is not raised to the physically possible limits.

Because of the mechanical stresses on the airframe, the velocity of flight has not yet gone beyond the velocity of sound.

On the basis of extensive physical and physico-chemical studies, we shall discuss some possibilities which are opened for the rocket propulsion of long-range military aircraft when these two limits are surpassed.

In addition several suggestions as to construction are made, which should facilitate overcoming the present limitations.

These investigations on the problem of long-range military rocket aircraft originated as a joint work of the two authors during the years 1937-1941 and were intended, together with the material of report UM-3509, to be a second volume of "Rocket Flight Technique", by the senior author.

As a result of circumstances caused by the war, publication was postponed and the results of the work issued in abstract form in the present report.

Sänger

(sig.)

Bredt

Ainring (Upper Bavaria), August 1944

TABLE OF CONTENTS

Page 3

I. Fundamentals

II. The Aircraft
1. Characteristics of the Motor
2. Effective Exhaust Speed of the Motor
3. Properties of the Air-Frame
4. The Glide-number of the Air-frame

III. Launching and Climb
1. Acceleration of the Aircraft
2. Catapult take-off
3. Climb Path

IV. Gliding Flight and Landing
1. Supersonic Path of Gliding Flight
2. Path of Subsonic Gliding Flight and Landing

V. Projection of Bombs
1. Types of Projection
2. Flight Path of the Bomb
3. Ballistics of Impacts

VI. Types of Attack
1. Basic Types of Attack
2. Point Attack with Two Propulsion Periods and Reversal of Path
3. Point Attack with Two Propulsion Periods, Partial Turn and Auxiliary Point
4. Point Attack with Sacrifice of the Bomber
5. Area Attack with Full Turn
6. Area Attack with Partial Turn and Auxiliary Point.
7. Area Attack with Antipodal Auxiliary Point
8. Area Attack with Circumnavigation
9. Evaluation of Procedures for Attack

VII. The Line of Development of the Rocket Bomber
1. Development of the Combustion Chamber and Jet of the Motor
2. Development of Special Fuels for Rocket Motors
3. Development of the Auxiliary Engines of the Rocket Bomber
4. Development of Test Model of Complete Rocket Motor
5. Wind-Tunnel and Tow-Tests on Models of the Air-frame
6. Constructional Development of the Vehicle
7. Bench Tests on Interaction of Motor and Air-frame
8. Development and Test of the Take-off Arrangement
9. Takeoff and Landing Tests on the Bomber
10. Flight Tests of the Bomber
11. Navigation Tests on the Rocket Bomber
12. Bomb Release Trials

Bibliography

Table of Most Important Symbols

I. Fundamentals

The range of flight-speeds several times the velocity of sound is the exclusive province of the pure rocket, which develops the propulsive jet entirely from the fuel carried on board the aircraft. The pure rocket can also compete in cost at lower speeds, if propulsive forces of great magnitude or short duration are required, or if no surrounding air is available, e.g. under water or outside the perceptible atmosphere of the earth. These special characteristics give rocket propulsion a broad domain of application to military techniques, which can be outlined as follows:

Propulsion of projectiles or bombs, in which the relatively strong, short duration propulsive forces can be achieved in most cases by powder-rockets.

Auxiliary drive for propeller-, or jet-aircraft, with operating periods generally under a minute, for which liquid rockets with compression-drive can be used.

Auxiliary or principal propulsion for vessels with period of operation of several minutes, so that rocket motors having fuel pumps, but without high exhaust speed, are required.

Main drive of aerial torpedoes against land, sea, or air targets, with moderate to long times of operation, in which high exhaust speeds are important only for quite large ranges.

Main drive of fighter or bomber aircraft, e.g. for fighter defense at very high altitudes or for military aircraft operating over very great distances. Both propulsion-time and exhaust speed set extreme requirements for the rocket motor. The last-mentioned application, the rocket bomber, is treated in more detail in the present report.

Pure-rocket engines make only very incomplete use of the energy made available by the fuel. However since the craft is not loaded down by the energy carried on board but rather by the weight of the fuel, this disadvantage can be counteracted by use of fuels with the maximum possible energy content per unit weight. Thus rocket fuels represent, on the one hand, carriers of energy with maximum concentration of energy per unit mass and per unit tank space; on the other hand, they are the carriers of those masses from which the jet of the engine is developed.

According to the method of feeding the fuel (which, in the tank, is liquid or solid) into the combustion chamber of the rocket, we can distinguish between various modes of operation of the rocket motor; e.g. rockets with periodic propulsion, which are characterized by moderate values of the work for feeding the fuel, the temperature stresses in the walls in contact with the flame, the exhaust speed and the thrust; and rockets with continuous propulsion, with arbitrarily high constant flame-pressures, high constant exhaust speed, maximum thrust for given dimensions and maximum thermal stresses of the furnace walls.

The type of construction of the walls in contact with the flame is determined by these stresses.

The type of construction using the heat capacity of the wall-material gives very simple solutions, which are however applicable only to periodic propulsion, or to continuous propulsion over short periods at moderate furnace temperatures. For example, the 20 mm. thick metal wall of the jet-throat of a powder-rocket at 2800°K and having thermal conductivity 4000 k cal/$m^2 h^\circ$, begins to melt on the side in contact with the flame after 2, 4, 8, 10, 14 or 90 sec, if it is made of Al, Ag, Cu, Fe or Ni, Pt, or Ir, resp; this can be shown by calculation and can be qualitatively checked by tests on welding torches.

Designs of combustion chamber walls using the best refractory materials give somewhat more complicated arrangements and longer propulsion times, which are in general limited mainly by chemical changes in the wall material. The best heat resistant materials, (melting points given in °C) which would be of interest in this connection are for example: beryllium oxide (2500), molybdenum (2600), zirconium oxide (2700), magnesium oxide (2800), thorium oxide (3050), titanium carbide (3140), rhenium (3170), tungsten (3380), zirconium carbide (3500), tantalum and hafnium carbide (3700) and graphite (4000). With these materials, using non-stationary thermal conditions, the driving times can be extended further than the values given previously.

Design using condenser jackets around the combustion-chamber walls is similar to that used in internal combustion engines for controlling the hot, strongly superheated combustion gases; it is however limited to moderate combustion temperatures and pressures for which the heat flow through the wall is everywhere less than 1 h.p./cm^2 so that the velocity of the coolant need not be raised above about 10 m/sec.

$4 = 4.5 \frac{BTU}{in^2 sec}$

Fire-wall construction using forced circulation of the refrigerant in channels, of preferably one-dimensional extent, which cover practically without gaps all the wall surfaces couched by the flame, gives the possibility of controlling also those high heat transfers through the chamber walls which occur unavoidably in using high-grade rocket fuels in uniform-pressure rockets, and which go far above 1 h.p/$_{cm}$2, and can be even 10 h.p/$_{cm}$2 or more in the jet throat. This type of firewall for rocket motor construction is used in the designs of the present work.

Aside from design of firewalls, the supply of fuel to the combustion chamber is, for uniform-pressure rockets, a special problem for the solution of which various methods have been used.

Placing the whole fuel supply in the combustion chamber has proved suitable in short-period powder rockets. Pressure tank feed of liquid fuel, because of the considerable weights of the tanks and compressed air, is possible only for moderate driving periods and fire gas pressures. Fuel supply through gas-pressure pumps limits the tank size and gives longer driving periods at moderate flame pressures. Fuel supply with ordinary pumps and turbine drive requires special propellants or exhaust gas removal from the combustion chamber and results in increased fuel requirement per unit momentum; nevertheless, it does give high driving periods and flame pressures. Fuel supply with ordinary pumps using a turbine driven by steam from the refrigerant, where the steam for the turbine is developed by vaporizing the coolant in the canals of the chamber walls and fire-jet, limits neither driving period, driving pressure, or flame temperature, and permits the use of the greatest exhaust speeds. This method is the basis of the rocket motors described here.

Finally, one of the most essential construction problems for uniform pressure rocket motors is the choice of furnace pressure. The high-pressure rockets with furnace pressures above 50 atm. (which are necessary because of the high exhaust speeds required), are in practise driven up to 100 atm. They have small dimensions per unit thrust and are especially valuable combined with highest grade fuels, where the already high exhaust velocity can be increased by 22% through a furnace pressure increase from 10 to 100 atm., and by 6% through a change from 50 to 100 atm. Its domain of application is therefore especially that of rocket flight, e.g. for rocket bombers, where the requirement of high exhaust speed is most stringent. The high requirements on the fuel feed system are no trouble when they are taken care of by the coolant-steam turbine mentioned above, which uses the heat from the forced cooling of the furnace. As a result of increased gas-density,-velocity,-temperature, and - radiation, the specific heatflow from the flame through the furnace walls rises proportionally with the furnace pressure. This has as consequence the decisive difficulty that the protection of the walls in contact with the flame becomes more critical as the furnace pressure increases, since the heat transfer from furnace wall to coolant only increases as the 0.4 power of the coolant pressure, so that a practical limit of furnace pressure is reached at about 100 atm.

Similar general considerations apply to the air-frame. To the fundamental question, whether explosive propulsion by rockets over large distances shall be used with wingless, unmanned rocket-torpedos or with winged and man carrying rocket aircraft, it may be said that for the "returning" aircraft, the range of use and the total destructive energy brought to the target (weight of bomb % energy of explosive) is as large as for the rocket torpedo for equal initial flight speed, so that the conserving of the empty craft for repeated use and the probably greater bombing accuracy speak in favor of the aircraft. Since the initial cost of the empty craft is far greater than that for the bomb and fuel load, this is the basis for the choice. If the rocket bomber doesn't return to its place of takeoff, its range for equal v_0 will be much greater than that of the rocket torpedo, though, of course, the % weight of destructive energy brought to the target decreases. The extreme ranges possible with the rocket bomber are completely forbidden to the rocket torpedo.

The rocket bomber will differ from the present-day propeller-driven bombing aircraft in the following essential points: in place of the propeller propulsion from the fuselage front it has the rocket propulsion in the fuselage stern; the fuselage is in the shape of a bullet with tapered hind part, the wings have a thin wedge-shaped profile with sharp leading and trailing edges and high wing loading at the start of the flight; the cabin is constructed as an airtight stratosphere chamber.

For starting, the use of its own fuel as in the usual propeller-driven aircraft was considered. Because of the great difference in start- and landing-weight this leads to large wing surfaces and too high fuel consumption in the range of speeds below the velocity of sound. Vertical start under its own power has only the last disadvantage, but even in a greater degree. Sling-starting on a horizontal take-off path until the sound velocity is reached appears most favorable and is assumed here. In this type of start by means of external forces, an especially

energy-consuming part of the aircraft acceleration is not obtained at the expense of the fuel carried on board, so that the range of the aircraft catapulted in this fashion rises markedly, while at the same time the flight-characteristics can be matched more easily to the steadily decreasing wing loading during flight.

As methods of flight were considered; acceleration to the point where flight speed equals exhaust speed, and then flight at constant speed; also acceleration to such a speed that the subsequent unpowered glide extends over the entire remaining flight path. For equal fuel cost, the last method gives greater ranges and simpler power plant, and is therefore assumed from now on.

The whole procedure for use takes place somewhat as follows: the rocket bomber at the surface of the earth is brought to a speed of about 500 m/sec. by a ground-fixed rocket drive in a period of 11 seconds over a 3 km. starting path; then climbs at full motor drive to a height of 50-150 km along a path which is inclined at 30° to the horizon at first, but later becomes flatter; thus it reaches final velocities up to more than twice the exhaust speed. The duration of the climb is 4-8 minutes; usually during this time all the fuel supply on board will be consumed. At the end of the climb the rocket motor is turned off, and the aircraft, because of its kinetic and potential energy, continues on its path in a sort of oscillating gliding flight with steadily decreasing amplitude of oscillation. This type of motion is similar to the path of a long-range projectile which from similar heights follows a descending glide-path. Because of its wings the aircraft descending its ballistic curve bounces on the lower layers of the atmosphere and is again kicked upwards, like a flat stone ricocheting on a water surface, though during the entrance into the dense air each time a fraction of the kinetic energy is consumed, so that the initially big jumps steadily become smaller and finally go over into a steady gliding flight. At the same time the flight speed, along the glide path of several thousand kilometers, decreases from its high initial value to normal landing speed. If the descending path (which is within certain limits controllable by the pilot) lies in the direction of the target, the bombs are released at a predetermined moment, and the craft returns to its starting place (or some other landing field) in a wide arc, while the bombs go toward the target along the original direction of flight. Even if the target is very distant from the take off point, the bombs are only dropped near it, so that the scatter of bombs can be compensated for by a large number of releases on the target, which will in this way be covered by a Gaussian distribution of hits. This military use is completely independent of weather and time of day at the target, and of enemy counteraction, because of the possibility of using astronomical navigation in the stratosphere and because of the height and speed of flight.

From the characteristics given for the rocket bomber it follows that this is not the development of an improved military craft, which will gradually replace present types, but rather that a problem has been solved for which no solution existed up to now, namely, bombardment and bombing over distances of 1,000 to 20,000 km. With a single rocket bomber point attacks can be made, e.g. from Central Europe, on distant point targets like a warship on the high seas, a canal lock; even a single man in the other hemisphere can be fired upon.

With a group of 100 rocket bombers, surfaces of the size of a large city at arbitrary places on the earth's surface can be completely destroyed in a few days.

II. The Aircraft

1. Characteristics of the Rocket Motor

The main parts of the basic construction of the rocket motor considered here are shown in Fig. 1. The fuel goes from the fuel tank to the fuel pump, where it is compressed to 150 atm., then fed continuously through valve 5 to the injection head of the combustion chamber. The oxygen goes from the thin-walled uninsulated oxygen tank into the oxygen tank, is compressed to 150 atm. there, then forced through valve 6 and the pipe system of the condensers into the injection head and the combustion chamber, after being warmed to 0° C. There the fuels come together for the first time, mix and burn producing flue gases at a constant pressure of 100 atm. and at 4000° C. In the head of the burner, the flue gas expands to a very low pressure and forms the driving mass-jet with exhaust velocity of 3-4000 m/set, whose reaction for a fuel consumption of 245-327 kg/sec produces a thrust of 100 tons. With a 90 ton fuel supply, the aircraft can be driven with the above thrust for 367-275 seconds.

Aside from this main process with energy conversion of about a million Kcal/sec the secondary process shown schematically in Fig. 2 gives an energy conversion of 20,000 Kcal/sec for driving the feed-pumps. Its parts, visible in Fig 1, can be followed from the water pump which puts about 28 kg/sec of water under 250 atm. pressure, drives this water, at the jet throat, into the cooling pipes of the jet walls, where it flows toward the mouth of the jet and is heated to about 300° C. After coming out of there, while still above the critical pressure, it is (again at the jet throat) driven into the cooling pipes of the combustion chamber wall, where it is again heated and vaporizes in the neighborhood of the critical pressure; finally it is removed at the injection head in the form of highly-compressed superheated steam, led to the steam turbine; there it expands to about 6 atm. and goes to the liquid-oxygen-cooled condensers where it is reconverted to water and gives up considerable energy to the oxygen; then it repeats its cycle going through the water pump. The steam turbine drives all three pumps from the same shaft. During the process valves 3, 4, 5, and 6 are open, and 1, 2 are closed, while 7 serves as a safety valve against too high rotation of the turbine.

The process described can be begun with the aid of the steam-starter, which produces the small amounts of steam required by chemical means; in this process the valves 3 and 4 are closed, 1, 2, 5, 6, and 7 are opened.

Aside from the details given in the literature, (16-30) the following things are important for understanding the proposed construction:

The relative value of different fire-wall materials is determined by the available heat flow $q \approx \lambda(t_f - t_K)/d$ through the walls for a given heat capacity of the walls. If the wall thickness d is proportional to the reciprocal of the breaking strength σ (tensile stress), or to its square root (torsion stress), then the possible heat flow (and also therefore the worth of the material) is proportional to the product $\lambda(t_f - t_K)\sigma$, or $\lambda(t_f - t_K)\sqrt{\sigma}$ resp. Here λ, t_f and σ are pure material constants, while the cool-surface temperature t_K (and so the whole evaluation) depends on the particular arrangement, coolant temperature, etc. In the combustion chamber cooled by live steam, the cool-surface temperatures are 500-600° C. From Fig. 3 one sees that the usual heat-resistant metals chrome-nickel steel, nickel, " ventil"-steel, etc., are favorable (as confirmed by construction experience) while platinum is even more suitable. The theoretically most favorable materials like tantalum, tungsten, and molybdenum are, because of their chemical activity and the difficulty in working them, actually not at all promising. In the hot-water-cooled fire jet the cool-surface temperatures are at 400-500° C, because of the high heat flow; Fig. 4 shows (in accord with practical experience) that copper is unsurpassed as jet-wall material.

The cooling system for the walls in contact with the flame (21) is required because of the high heat flow from the combustion gases to the fire-walls; this is presented in Fig. 5 for a gas-oil-oxygen charge at 100 atm. combustion pressure, on the basis of calculations and practical experience. For example, in order to conduct 5 hp./$_{cm}^2$ from the fire-surface to the cool surface through a 1 mm thick copper wall, a temperature gradient $(t_f - t_K)$ between the two surfaces of 100° C is necessary. In order for such thin walls to withstand the mechanical stresses due to flame-and coolant-pressures, they must be reinforced at very short intervals. At the same time the heat flow through the fire-walls must be assured by a precisely prescribed and carefully maintained high streaming velocity of the coolant behind the fire-wall. Both requirements can be met by the cooling-pipe system shown in Fig. 1, with forced circulation of the coolant in structures of one-dimensional extent. The necessary compromise between the rising forced motion and increased pressures required to drive the coolant when the number of channels is decreased has been so made that the cooling system of the jet consists of several hundred parallel pipes each only a few

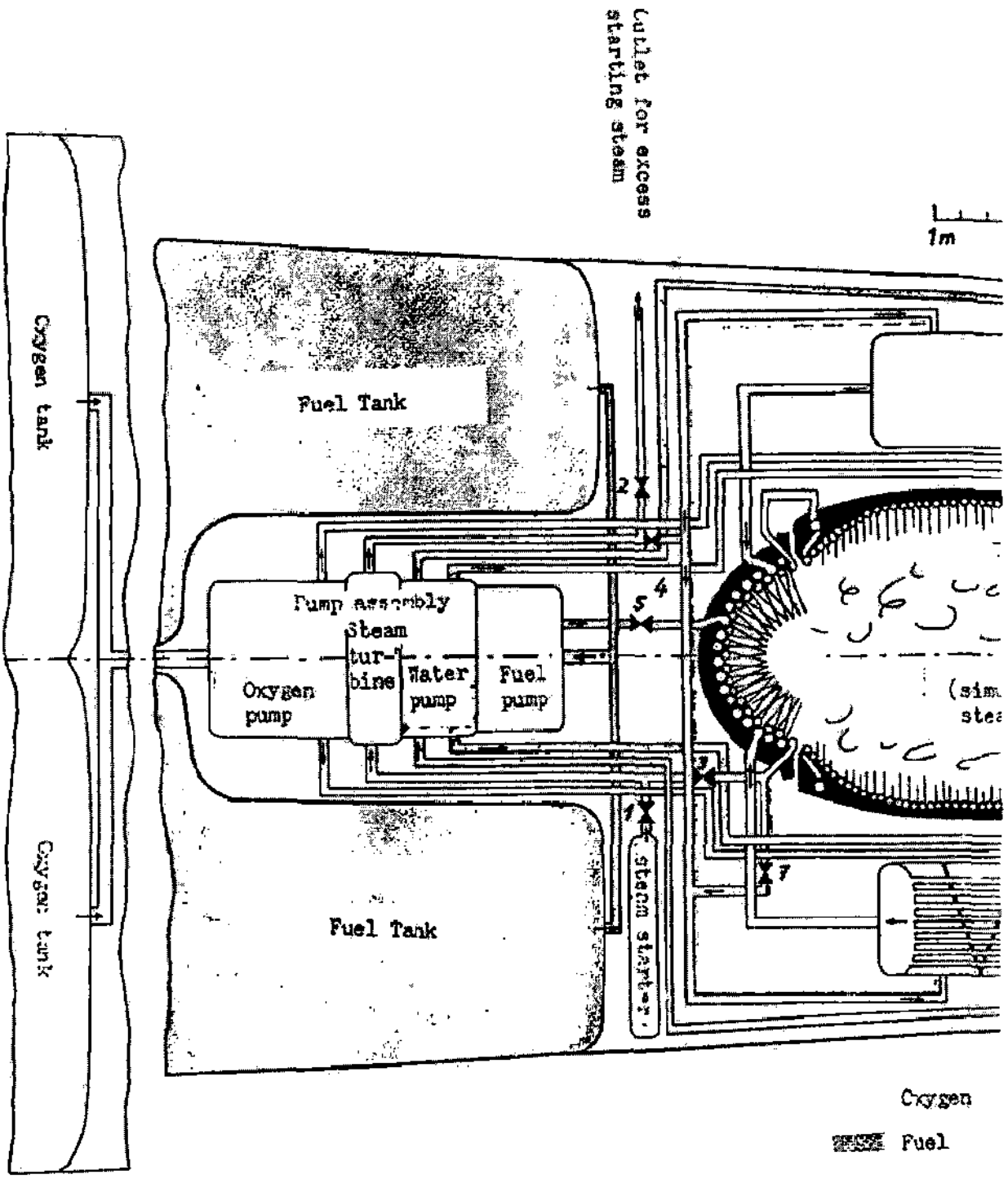

Fig. 1: Systematic representation of the main parts of the rocket mot
of the rocket bomber.

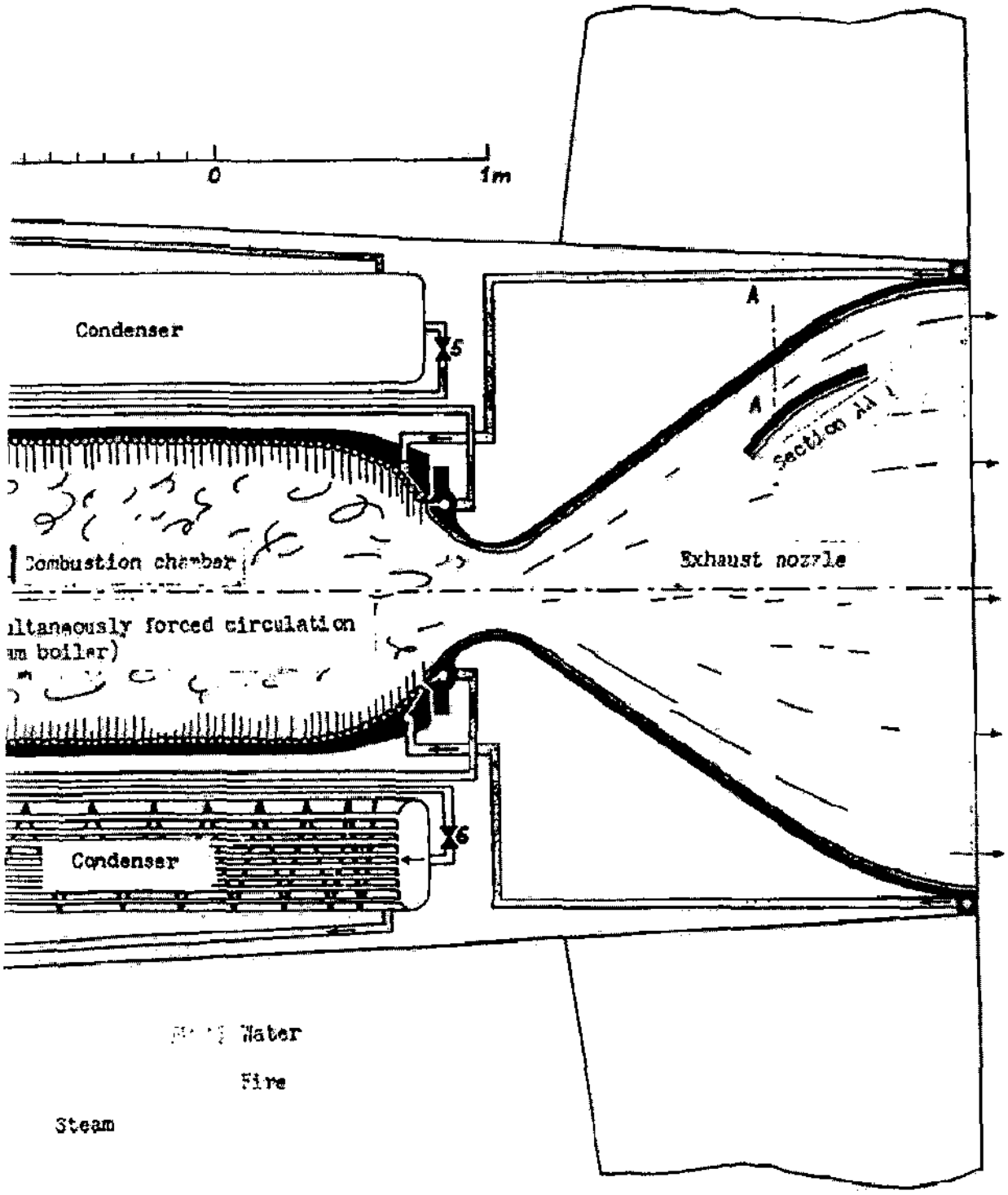

or, drawn in the interior

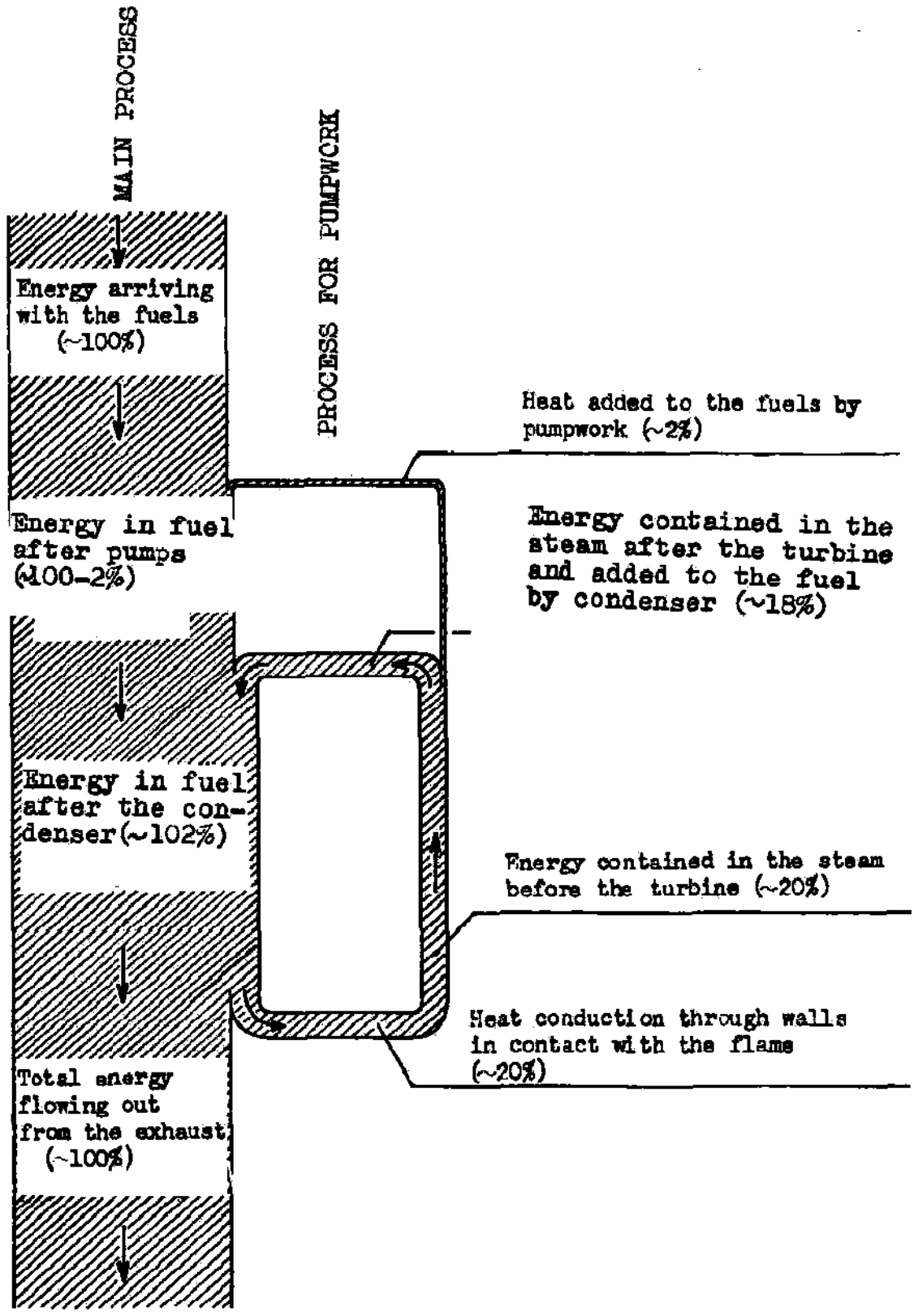

Fig. 2: Energy flow in the working process of the rocket motor.

sq. mm. in cross-section, which join together partially at the jet throat and again branch off in the far parts of the jet mouth so that the small individual cross-section of the pipes is retained; each pipe runs meridionally, and the whole surface of the jet is completely covered with pipes, of which the side toward the flame consists of the smooth and torsion-stressed fire-wall. The requirement of a plane surface does not apply to the furnace surface in contact with the flame, so that there the statically more favorable circular cross-section can be used. This circumstance and the smaller heat-flow through the furnace walls require greater wall-strengths of the fire-wall and thus greater cross-section for the individual cooling pipes, so that the then necessarily few pipes in parallel can assure high circulation of the coolant in the neighborhood of the steam chamber which has varied and unstable flow conditions. These few cooling pipes are wound on the furnace surface in the form of an evaporating coil.

We see, from the above discussion, the requirements on the coolant itself: large heat capacity, heat conductivity and density; for this reason mercury has advantages over water.

The reason why the furnace-jet in Figs. 1, and 5 is shown with the unusually large opening angle of 60° is the following: (22) Aside from the fact that a special coolant, which best suits the requirements, is circulated around the fire-walls, the actual coolant is really the fuel itself, to which the intermediate coolant transfers its heat in the pumps and condensor. The heat-absorptivity of the fuel before it is brought into the combustion chamber is limited, and is only a few percent of the heat which is liberated when it is burned in the combustion chamber. One must therefore take care, that the total heat transfer per sec. from the flue-gas to the coolant through the walls of the furnace and jet, which is given as 20% in the example of Fig. 2, remains less than or equal to the aforementioned absorptivity of the fuel consumed per sec. This total heat transfer which must be regulated is proportional to the total inner surface of the furnace and jet. It can be decreased by diminishing this total surface. Concerning the contribution of furnace and jet to the total surface in contact with the flame, the following is true: all experience shows that over a wide range of values, combustion in a furnace is more complete, and efficiency and exhaust speed are correspondingly larger, the greater the furnace volume Vo as compared to the smallest cross-section f' of the furnace jet. Because the total wall-surface is limited by the heat absorptivity of the fuel used as a coolant, the furnace surface can be increased provided that the jet surface is decreased keeping the sum of the two below the permissible limit. From Figs. 2 and 5, the total heatflow through the 154,000 cm of fire-wall surface represents 2% of the energy developed, which corresponds to the permissible heat absorption of the fuel, so that the heatflow per unit area of the furnace and jet walls is about 0.8 kp/cm^2. If in place of the short 60° throat with 60,000 cm^2 surface we used the customary Laval-throat with a 10° opening angle, its furface (345000 cm^2) could not be completely cooled if the same heatflow and absorptivity of the coolant were maintained; for the furnace there would be no surface cooling available at all. At the same time the length of the Laval-throat could not be decreased below 9720 mm. By using large throat-angles we are enabled to fulfil the requirements of the fuel-cooled rocket motor, and moreover the quantity Vo/f' which determines the completeness of combustion can be increased, so long as the increased efficiency of the furnace $\mathcal{L}/E$ is not overcome by the decrease of jet-efficiency $(Ac^2/2g)/L$ with increasing opening angle.

The pump system of the rocket motor consists of three pumps for fuel, oxygen and coolant, and the driving turbine, for these pumps. The vaporized coolant of the rocket motor is used for feeding the turbine, where the forced circulation used for the combustion chamber permits the chamber to be used as a high-pressure-radiating-steam-boiler with forced circulation in the manner of the Benson -, Lahont -, Velox -, Sulzer - steam boilers. (27) The use of the vaporized coolant for driving the auxiliary turbine has the advantage over the use of a separate energy source that the total fuel consumption per impulse by the rocket motor is not increased by the auxiliary turbine drive; the advantages over feeding the auxiliary turbine from the flue-gas of the rocket motor are that: use of the cooling capacity of the fuel for cooling the combustion gases brings it to temperatures permissible for the turbine drive-rod; the difficulties associated with condensation of, for example, metallic-oxide fumes in the flue gas disappear; the heat absorptivity of the fuel as a coolant is increased by the work done in pumping; the important decrease in momentum of the jet in the emission of a part of the flue-gas and transfer of its heat content to the remaining flue-gas is avoided; finally the construction of a high pressure steam turbine is incomparably simpler than that of a high pressure flue-gas turbine. Since according to Fig. 2, the efficiency of the 12,000 hp. drive of the steam turbine, which uses waste energy, is unimportant, while we do demand very small weights of the installation, the simple Curtis-shaft gives a suitable solution. The 3 pumps can in view of the high total fuel supply of over 1000 $m^3/hr.$, be designed as one-stage turbines (despite the high intake pressures), so that the whole pump assembly including the turbines consists of 4 running from the same shaft, at about 12,000 RPM. Thus the outer dimensions and weight of the whole installation can be kept below 600 x 1200 mm and 500 kg.

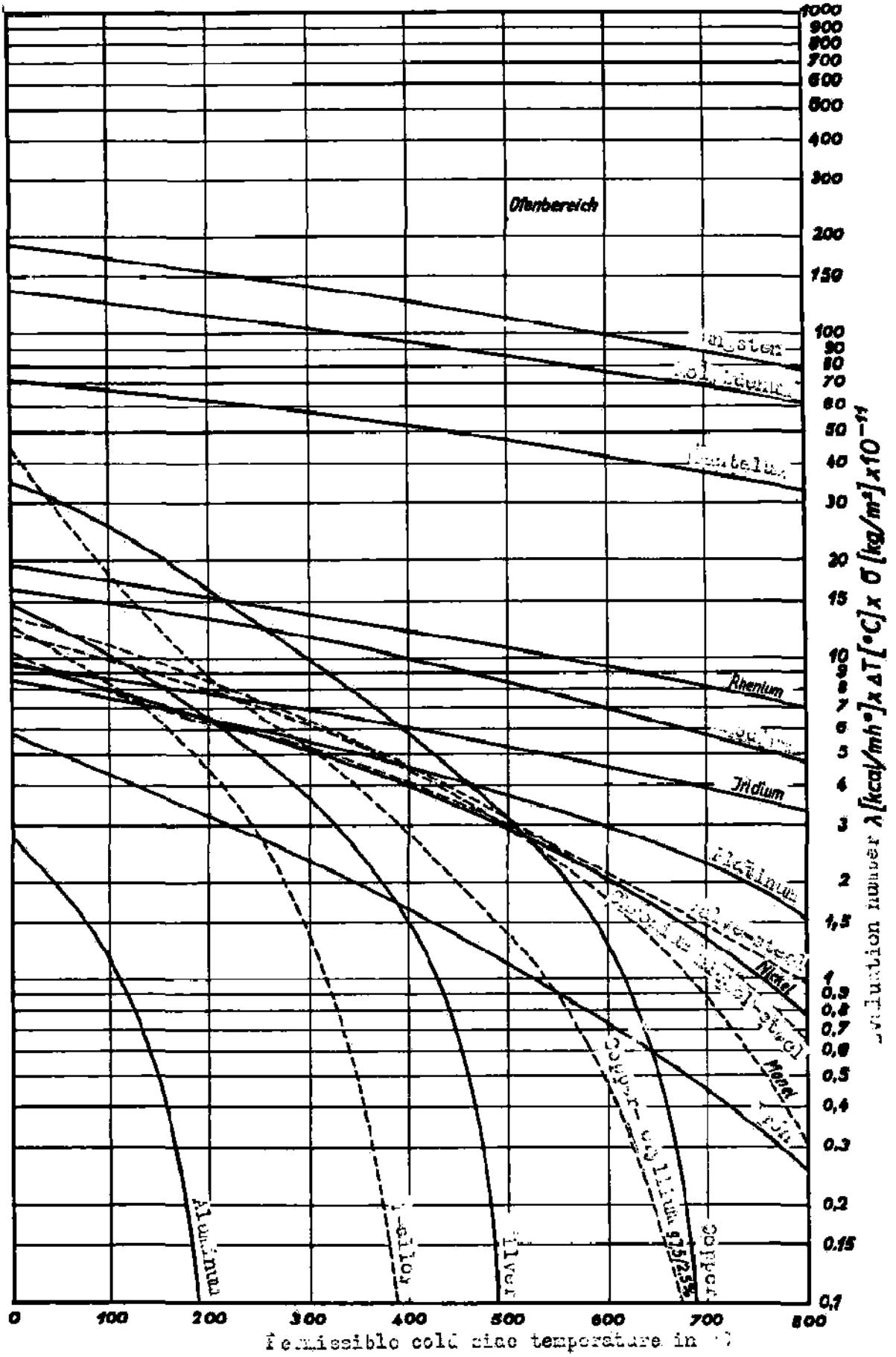

Fig. 3: Relative evaluation number of combustion chamber wall materials subject to tension.

C-84296

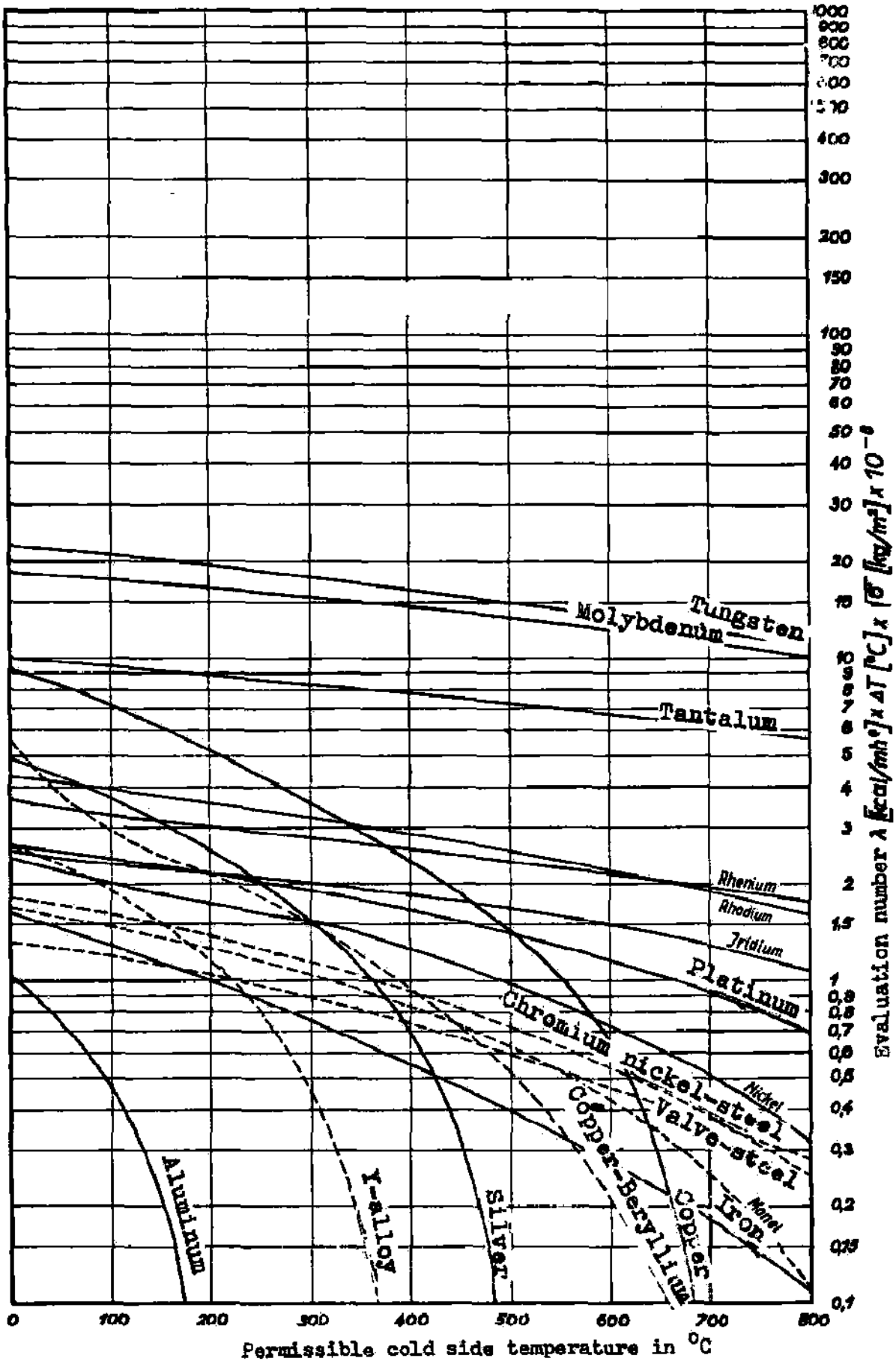

Fig. 4: Relative evaluation numbers of firewall construction materials under bending (exhaust wall materials).

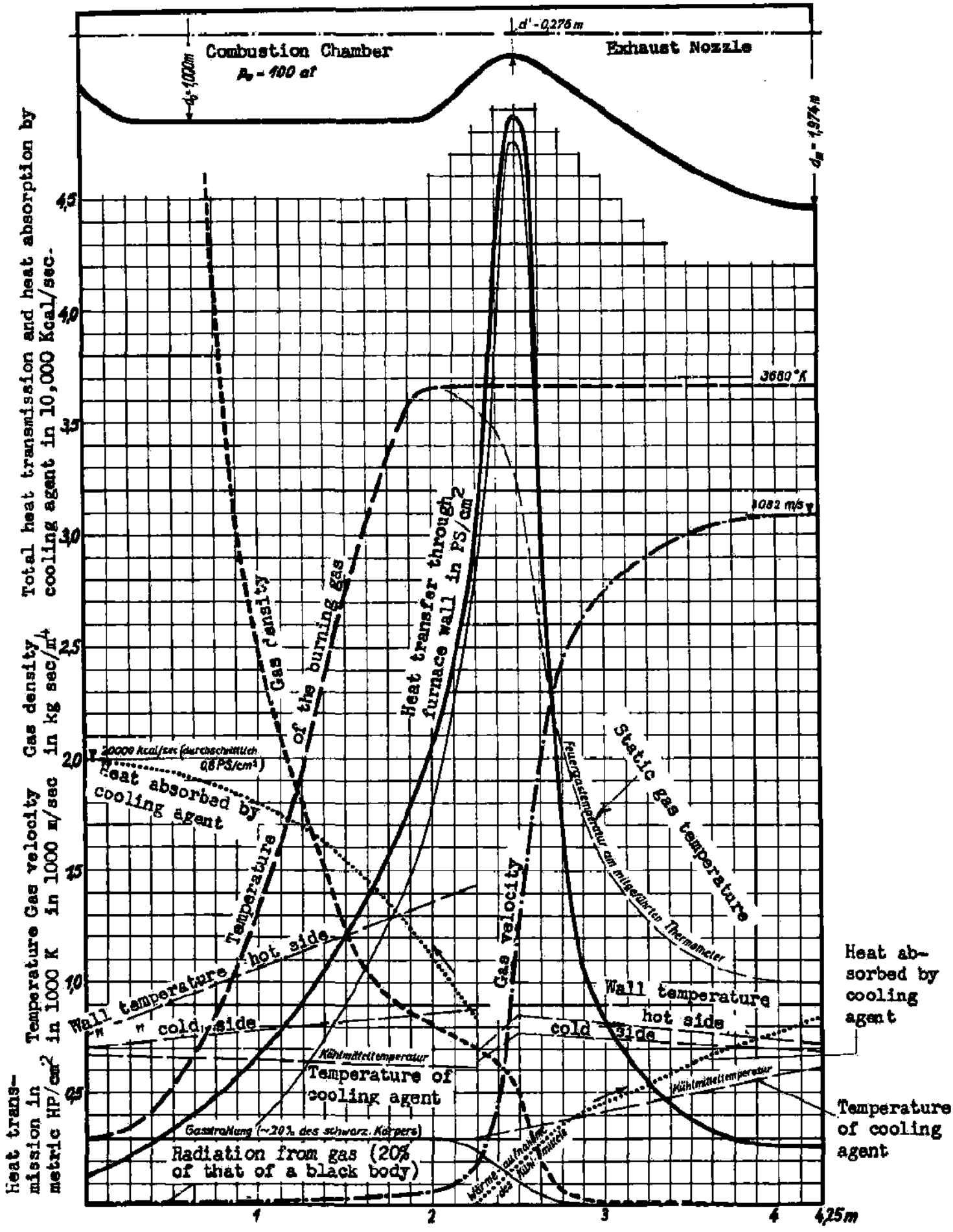

Fig. 5: Conditions in a 100 ton rocket motor operating with oxygen and oil.

C-R1204

Aside from the requirements of extremely light construction the turbine, fuel pump and water pump present no special constructional difficulties, whereas in the construction of the oxygen pump the choice of the construction material, the arrangement of the moving parts and the feeding of the boiling liquid to the pump must be specially considered. As a construction material (for the oxygen pump) which at -180° C will be sufficiently strong, elastic and resistant to impact, sufficiently resistant to corrosion and non-inflammable in liquid oxygen, the nickel-, Al-, and Mn- bronzes, as well as Monel-type alloys and pure nickel have proven satisfactory. In view of the inflammability of all lubricants in liquid oxygen, the problem of arrangement of moving parts was solved by using a floating support for the pump shaft away from the oxygen. In order to drive the boiling liquid O_2 from the tank steadily to the pump, an arrangement was used whereby the oxygen flows toward the pump over a long route in the direction of an acceleration field; e.g., in the test installation, from a higher level; or in the aircraft, from tanks lying far toward the front. Because of the gradual pressure increase in the feed lines, accompanied by only a slight temperature increase, supercooling of the O_2 occurs at the pump intake, so that no more gas is liberated.

Fig. 6 is a photo of the experimental model of a high-pressure liquid- O_2 pump, which as a rotary 6-stage pump with external bearings supplies 5 kg/sec of liquid O_2 at 150 atm. pressure, when running at 15,000 RPM; it has proven its suitability and reliability in hundreds of experiments.

The ignition of the rocket motor is not shown in Fig. 1, because ignition is limited only to starting; once the combustion chamber gets going it operates like a welding-burner. The basic ignition procedure chosen was the injection into the combustion chamber of materials which ignite on contact with O_2 or air. From the pyrophors to be considered, like the phosphorus hydrides, "silanen", halogen-acetylenes, rare earth amalgams, metal alkyls, etc., zinc-diethyl $Zn(C_2 H_5)_2$ was chosen at the suggestion of H. Troitzsch; F. Zohrer developed a suitable ignition fluid by dilution of this with heavy hydrocarbons (e.g., machine oil), and also an ignition apparatus in the form of a small pressure bomb using compressed nitrogen and a remote-controlled valve; by a simple movement of the valve and consequent injection of the ignition fluid into the combustion chamber, arbitrary ignition time and arbitrary repetition of the ignition is possible. This ignition procedure is notable for its sure performance and the very smooth starting of combustion.

The practical work on the development of the rocket motor described in this section was taken up by the senior author in 1933-34 at the Technische Hochschule in Vienna and gave in the first experiments, on small models with 30 kg. thrusts, controllable flame-pressures of 50 atm. and high exhaust speeds; the fuel was O_2 (at up to 150 atm. injection pressure), and gas-oil (at up to 500 atm. injection pressure), and a Laval-throat of small opening angle was used. (19) After a delay of several years, which were spent in constructing larger experimental installations, the tests were recommenced at the Trau Aeronautical Testing Station in 1939. The construction of the experimental installations was under the direction of H. Zborowski; the construction of the components was directed by H. Ziebland; K. Hedfeld directed the experimental work. Fig. 7 shows the testing-shed during an experiment with 1 ton thrust and 5 minutes duration. Among the important parts, one can see at the left on the embankment a cylindrical tank of capacity 2.5 m^3 for the liquid O_2, and just to the right of it the tap for the underground tank of liquid O_2 (see also II, 2). The drive tank, from which the apparatus is directly fed, is an open uninsulated thin-walled metal tank which (out in the open) vaporizes oxygen at the rate of 15 kg/hr. per sq. meter of tank wall, and whose varying weight during the test is shown by an automatically-recording spring balance. From this tank the liquid O_2 flows at slow speed under its own weight to the high-pressure liquid oxygen pump 8 m. below (see fig.). Beyond the feed pump the liquid oxygen, now at 150 atm. pressure, runs through a heat exchanger, in which it is heated by the warm cooling-water coming from the furnace, then goes into the combustion chamber through a large number of injector nozzles. Following the corresponding path of the fuel, we see in the left foreground a $1m^3$ fuel tank, from which the fuel flows under its own weight to the high-pressure fuel pump. For this purpose a cog-wheel pump is used, which compresses the gas-oil to 150 atm. at 3000 RPM. In the experiment shown here, the fuel and oxygen pumps were driven together by a D.C. Motor standing between the pumps; later the coolant-steam turbine was used instead. Beyond the fuel pump the fuel also is forced into the combustion chamber through a large number of nozzles. The fuel - and O_2- streams are directed at 30° to each other and have initial entrance-velocities of about 100 m/sec so that rapid spraying and mixing is forced. In the furnace, the three fluids - oxygen, fuel and ignitor - meet and form the furnace gas. The furnace-gas pressure during the entire run is up to 100 atm, with $V_0/f = 800$ and about 30° opening angle of the provisional expansion-nozzle. The next photos 8 and 9 show a 1-ton trial from the jet side, 10 shows a small model using coolant vaporization; Fig. 11 shows a 1-ton trial in which a high-percent Al-gas-oil suspension was used as fuel. The flame glows brighter in this case, and the resulting aluminium oxide begins to condense to white corundum dust at a few meters from the jet opening, and then thickens into a heavy white cloud. Finally, Fig. 12 shows a short-exposure

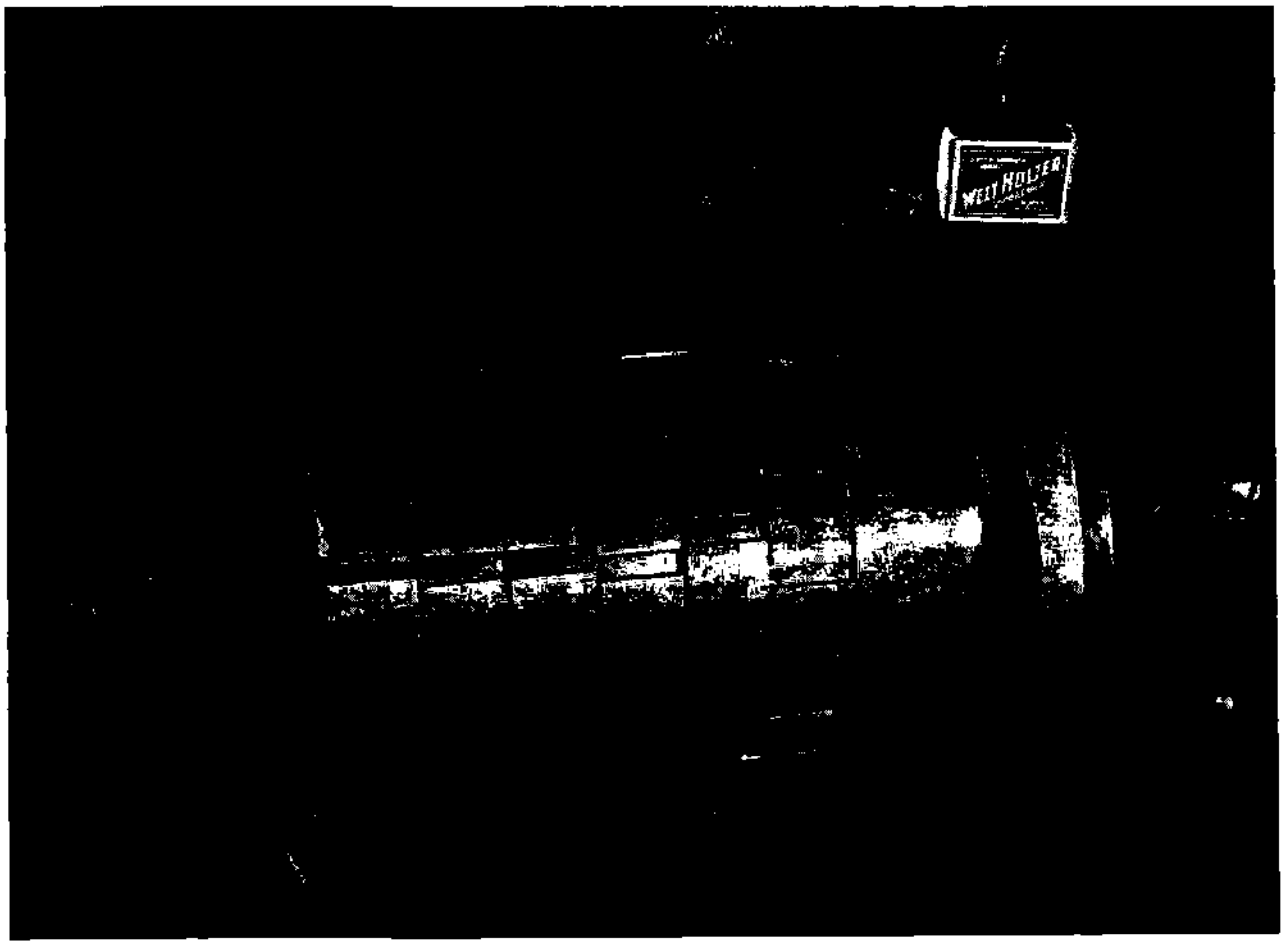

Figure 6; Experimental high pressure liquid O_2 pump which has a 6 stage rotary pump. At 15,000 R.P.M. it is pumping 5 kg/sec of liquid O_2 at 150 atmospheres.

Fig. 7: Overall view of a 1-ton, high pressure combustion chamber experiment using cooling by evaporation. Propellent tanks are above roof to the left. The fuel pumps directly underneath. Combustion chamber is in operation in center. Note the cloud of condensed cooling agent. The observation stand is above on the right.

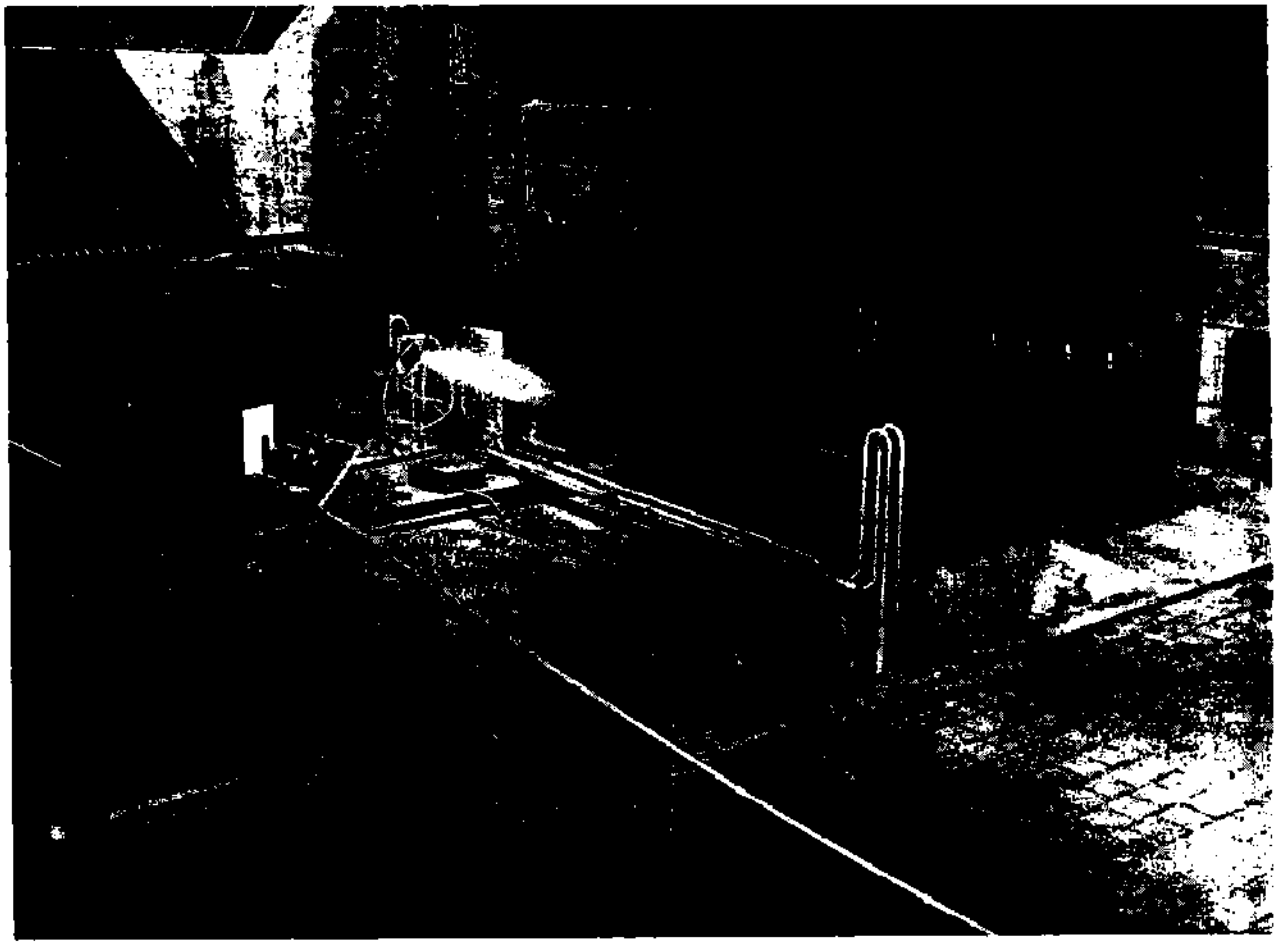

Figure 8: Overall view of a rocket motor test stand. This motor produced 1 ton of thrust for a duration of 5 minutes.

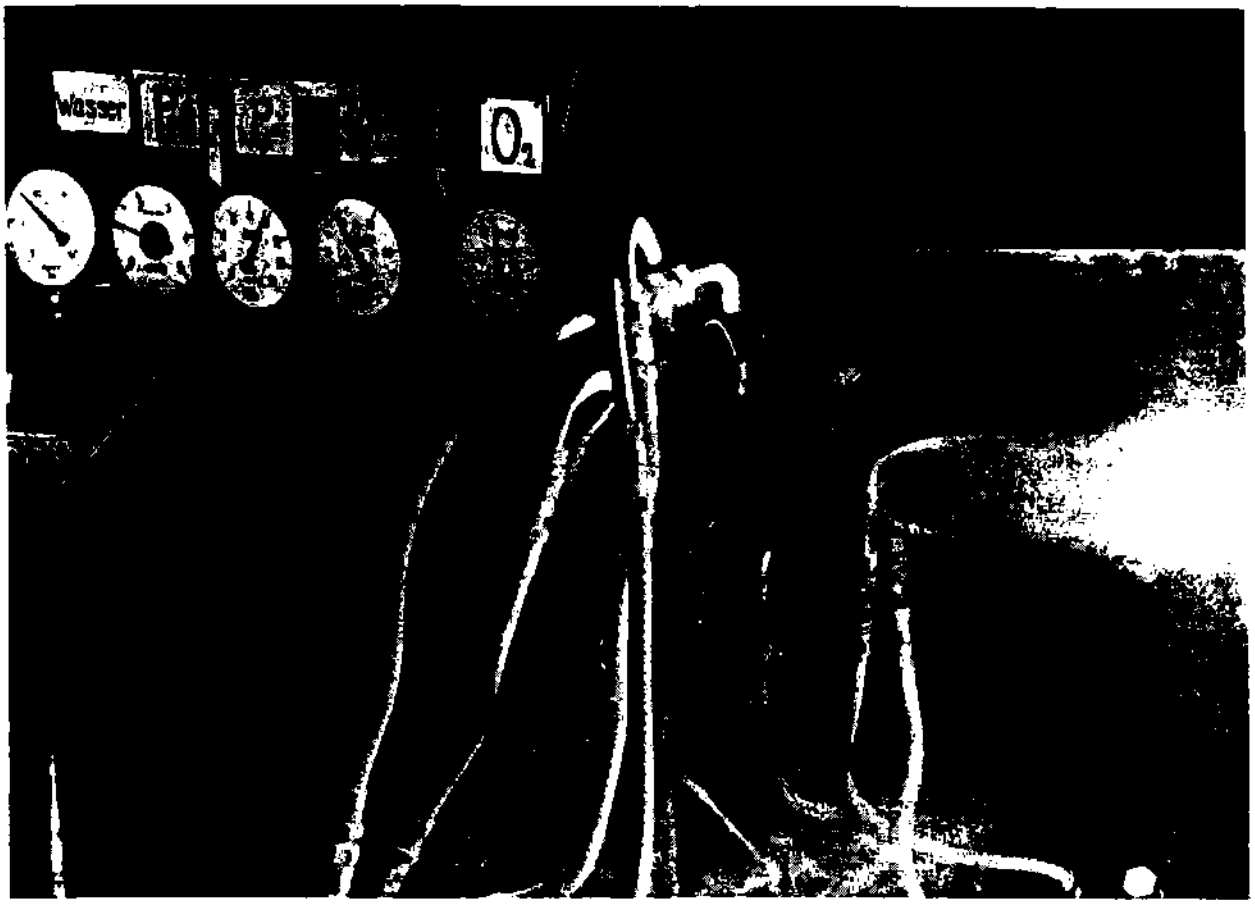

Figure 9; View of instruments and propellent lines. This test was run on the 20th of March 1941. The chamber pressure 100 atmospheres, the thrust 1.1 tons, the duration 3.5 minutes.

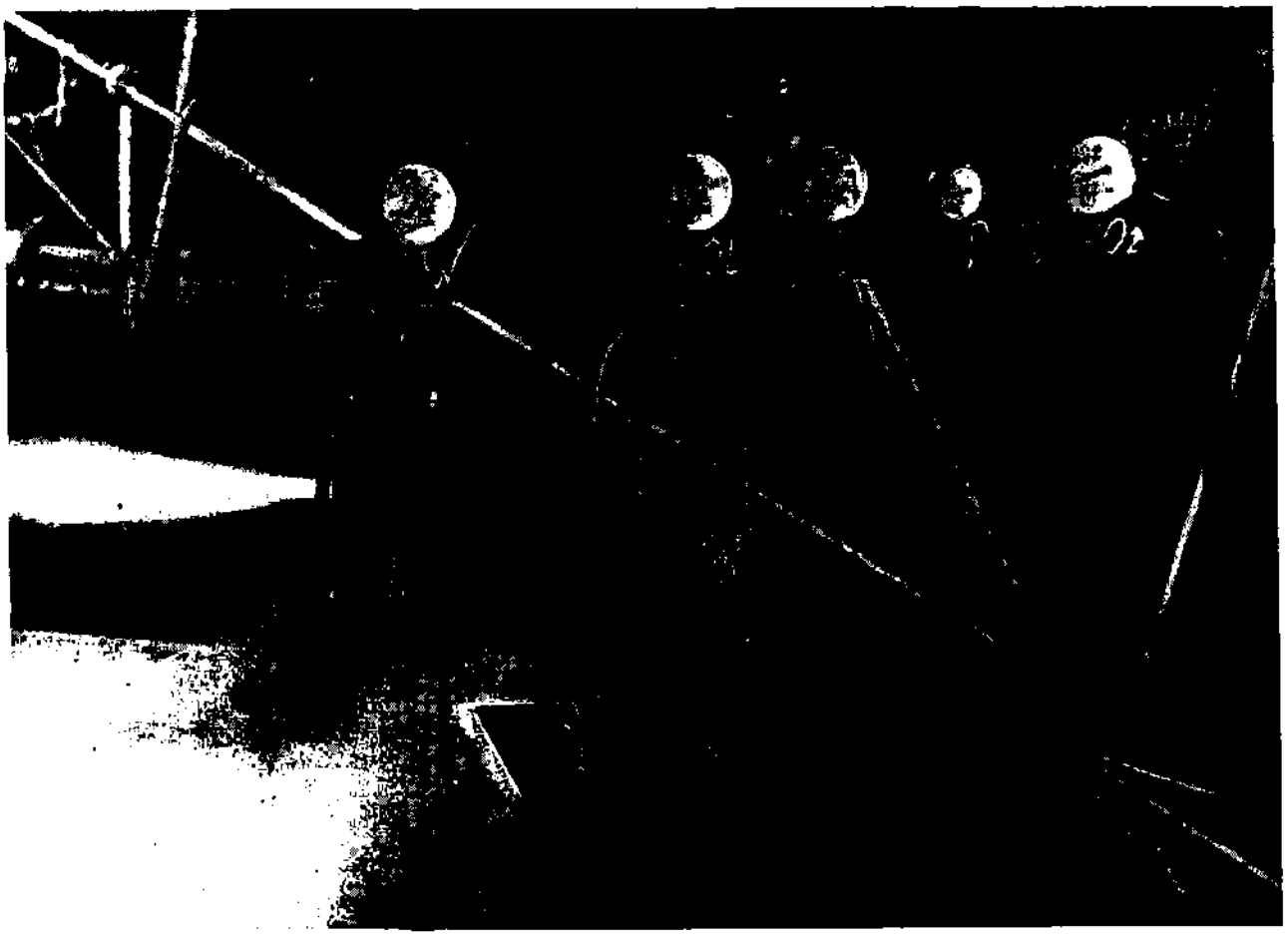

Figure 10; Small water cooled combustion chamber and test instrument in duration test. Water, heated at 400^{0} centigrade at 100 atmospheres pressure in the cooling system.

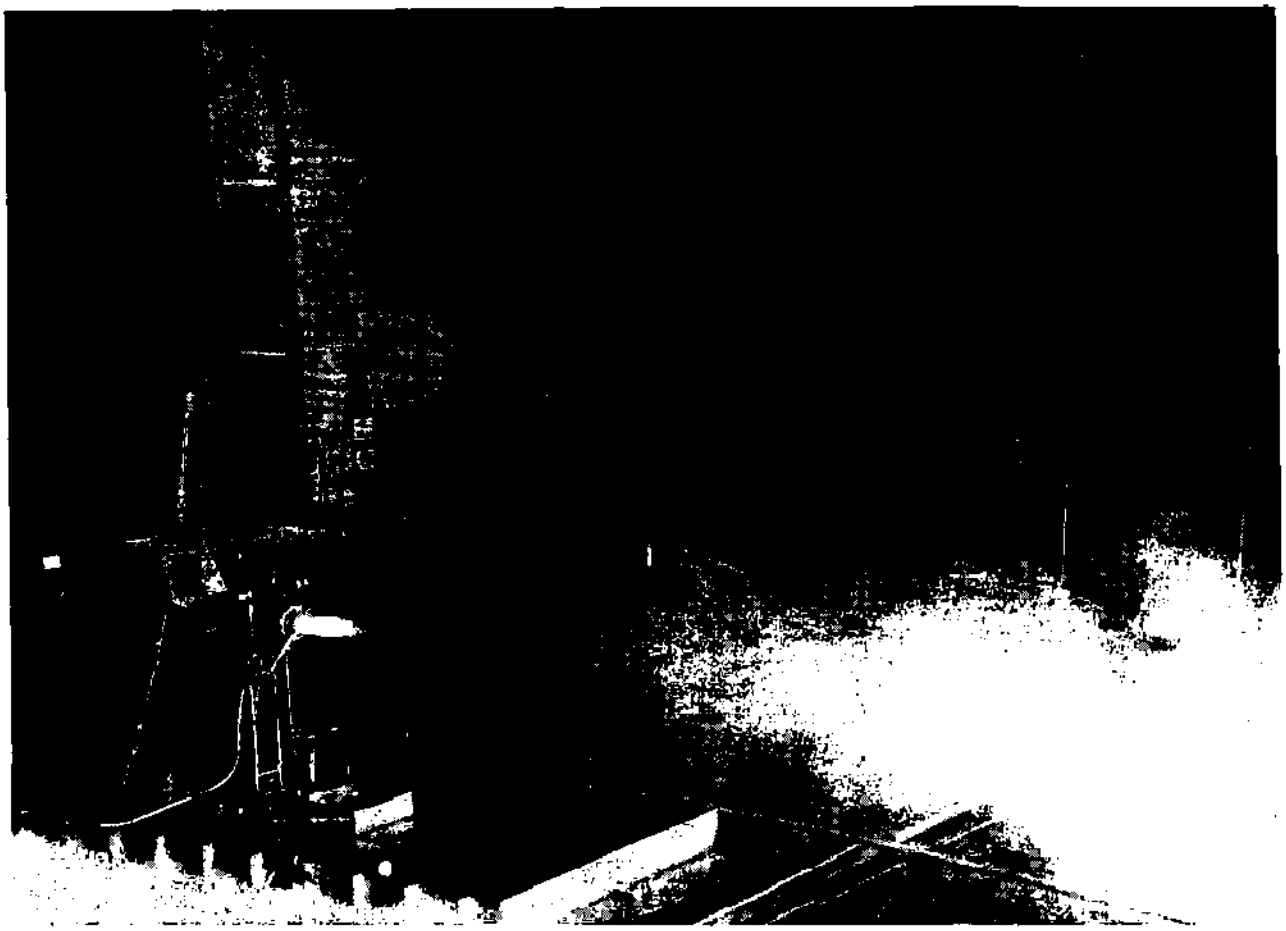

Figure 11; Rocket motor test stand experiment using Aluminum in oil dispersion as fuel. Supersonic exhaust gases from the nozzle of 1-ton experimental rocket motor. Note compression lines.

Fig. 12: Supersonic exhaust gases from the nozzle of the rocket motor during an experimental run. Thrust was 1 ton. Note the compression lines.

Fig. 12a: Experimental construction of the evaporative cooling system of a 100 ton high pressure combustion chamber.

photo of the jet itself, in which one can see with the naked eye the supersonic compression lines which give the exhaust jet the appearance of a large, blue crystal.

The main part of the practical work consisted in the construction of combustion chambers for developing and withstanding of combustion gases with the high energy concentration mentioned No time could as yet be devoted to the conversion of the heat into kinetic energy of a jet, that is to construction of a jet nozzle. Ordinary amounts of fuel consumption in the course of long and steadily run tests, gave effective exhaust speeds of up to 2400 m/sec at about 35 atm flame pressure, with gas-oil-oxygen fuel and for $k=P/p=1.43$ (i.e., still insufficient performance of the extended throat section).

With the relatively low $\varkappa$-values of the combustion gas (about 1.25) carefully constructed fire-jets should, according to Fig. 17, give at least $P/p_{atm}=1.6$ in the test set-up, and about $P/p_{atm}=1.75$ in the aircraft, so that the combustion gas developed corresponds to effective exhaust speeds of 2700 m/sec. on the ground, and near 3000 m/sec. in the aircraft.

Finally, Fig. 12a shows a trial construction of the carburetor of a 100-ton rocket high pressure combustion chamber, which was not however used in the experiments.

2. Effective Exhaust-speed of the Rocket Motor

Statements concerning the form and nature of the physico-chemical processes in the jet of the rocket-furnace, which could give a determination of the effective exhaust speed, assume a knowledge of the processes and of the final state of the combustion gas in the furnace.

One may assume that most of the available time in the furnace space (about 75 millisec) is used up in processes of spraying, heating, vaporization, dissociation, turbulence and diffusion of the injected streams of fuel and oxygen; and only a small part of the time is used for the actual combustion and coming to equilibrium. The fully prepared and mixed fuel-, and oxygen-molecules (or - atoms) collide, and react with each other, but will immediately dissociate again if there is no means of transferring the liberated heat of reaction to internal degrees of freedom, to other bodies, or converting it to translational energy. The last possibility exists for atomic collisions (according to the principle of the conservation of the center mass) only if a third atom or molecule takes part in the collision, so that the particles present after the reaction can repel each other. (Triple collision, wall-catalysis, exchange reaction). A measur for the probability of occurrence of any reaction is the effective number of collisions, which states how many collisions of other particles with the molecule under consideration are required to produce the desired effect. According to an empirical formula of Gaeb (5) Z triple collisions occur in every Z ordinary collisions After each formation of a new molecule, later collisions will supply energy first to its rotational and then to its vibrational degrees of freedom at the expense of its translational energy, till finally in some cases dissociation occurs. In the course of a sufficiently long time, which is dependent on the number of effective collisions which a molecule must undergo for each of these changes, and on the time interval between two such collisions, an equilibrium state (dependent on the pressure, temperature and proportions of fuel and O_2) develops in the furnace, which can be exactly described in terms of the kind, number and energy content of the molecules or atoms present. This state is assumed in the later calculations of the effective exhaust speed.

Since the greatest possible energy content of the translational degrees of freedom of the combustion gas determines the maximum possible value of the effective exhaust speed, one would prefer for the rocket motor a more favorable final state than that of stationary equilibrium, this seems to be attainable, since translation, rotation, vibration, dissociation and recombination take successively longer times to attain equilibrium, and the time during which the fuel remains in the furnace may lie anywhere between these times. According to Jost (8, page 141) it is conceivable that the newly formed molecules may, because of their process of formation, not have their vibrational degrees of freedom completely excited by the end of the combustion process, so that a greater fraction of the energy remains for the K.E. of the center of mass than corresponds to equilibrium; thus temperature and pressure at the end may be higher than that corresponding to equilibrium. (see K. Wohl and M. Magat, Z. Phys. Chem. Vol. 19, p. 117, 1932; also (10) p. 805, fig. 6, "The Approach to Thermal Equilibrium").

While, in the furnace of the rocket at say 100 atm. flame pressure and 3700° K, a molecule experiences an average of 10^{11} collisions per sec, the number of collisions drops after expansion in the jet, with a corresponding decrease in the rate of excitation of the degrees of freedom, the rates of further chemical reactions, such as reburning, and of physical reactions such as condensation or solidification of the combustion products (provided the temperature drops below their static sublimation temperature during the expansion).

The processes in the jet are then treated exactly as those in the furnace, neglecting all wall-effects; the expanding combustion gas is assumed to be an adiabatically closed system with a total energy E kcal/kg corresponding to the heat content of the mixture; i.e. $\Delta E = 0$

Accordingly as the time the streaming gas spends in the jet is long or short compared to the times of development of the various internal energetic and chemical equilibria, three assumptions are possible concerning the expansion:

1. The time spent, or the number of collisions which a molecule undergoes, on its path through the jet, is so small that no energy exchange or changes of vibrational and dissociation energy can occur. The characteristic conditions for this case are $dD = 0$ and $c_{v\,osc}\,dT = 0$; when put into the generally valid energy relations between total energy, E, heat supplied, Q, internal energy, U, heat of dissociation, D, heat of vaporization at 0°K, R_{io}, heat content, J, work done in expansion, ApV, and kinetic energy $Ac^2/2g$, to the equations:

$$dU = c_{v\,trans.}\,dT + c_{v\,rot.}\,dT = -A\,p\,dV;$$

$$p/p_o = (T/T_o)^{\frac{\varkappa_u}{\varkappa_u - 1}} \qquad \text{where} \quad \varkappa_u = 1 + \frac{AR}{c_{v(trans+rot)}} \qquad \text{is}$$

a "smaller" adiabat exponent which results from only translational and rotational specific heats; ($\varkappa$ ordinarily would be $(c_{vrot} + AR)/c_{vrot}$ (note by Transl).

$$\Delta J = \frac{\varkappa_u}{\varkappa_u - 1} AR(T_o - T) \quad \text{and}$$

$$c^2 = \frac{2g}{A}\Delta J = 2gR\frac{\varkappa_u}{\varkappa_u - 1}(T_o - T) = 2gRT_o\frac{\varkappa_u}{\varkappa_u - 1}\left[1 - (p/p_o)^{\frac{\varkappa_u - 1}{\varkappa_u}}\right]$$

gives the variation of the flow-velocity as a function of the pressure drop in the jet.

2. If the time spent by the combustion gas in the jet is such that vibrational states are instantaneously in equilibrium, whereas no chemical processes can reach equilibria corresponding to the changed conditions, then the flow is characterized by $dD = 0$, C_v osc. $dT = f(T)$. From this and the fundamental equations we get the relation:

$$\int_{T_o}^{T} c_{vosc}\,dT + (c_{v\,trans} + c_{v\,rot})\int_{T_o}^{T} dT = A\int_{V_o}^{V} p\,dV$$

For a gas mixture with n vibration frequencies and m different gases,

$$\overline{C_{v_{osc}}} = AR\sum_{i=1}^{n}\left[\frac{(\Theta_i/T)^2 e^{\Theta_i/T}}{(e^{\Theta_i/T} - 1)^2}\cdot\frac{p_i}{p_o}\right] \quad \text{and}$$

$$\overline{C_{v(trans+rot)}} = \sum_{i=1}^{m}\left[M_i c_{vi\,(trans+rot)}\frac{p_i}{p_o}\right] \Big/ \sum_{i=1}^{m}\left[M_i\frac{p_i}{p_o}\right]$$

$$\text{also} \quad \overline{\varkappa_u} = 1 + \frac{AR}{\overline{c_{v(trans+rot)}}}, \text{ where } p_i \text{ is the constant}$$

partial pressure of the gas as compared to p_o and Θ_i the characteristic temperature. The integral for this type of flow is:

$$\frac{\overline{\varkappa_u}}{\varkappa_u - 1}\int_T^{T_o}\frac{dT}{T} + \sum_{i=1}^{n}\left[\frac{p_i}{p_o}\cdot\frac{1}{\Theta_i}\int_T^{T_o}\frac{(\Theta_i/T)^3 e^{\Theta_i/T}}{(e^{\Theta_i/T} - 1)^2}\,dT\right] = \int_p^{p_o}\frac{dp}{p} \quad \text{and its solution is:}$$

$$\frac{\overline{\varkappa_u}}{\varkappa_u - 1}\ln\frac{T_o}{T} + \sum_{i=1}^{n}\frac{p_i}{p_o}\left[\frac{\Theta_i/T_o}{e^{\Theta_i/T_o} - 1} - \frac{\Theta_i/T}{e^{\Theta_i/T} - 1} - \ln\frac{1 - e^{-\Theta_i/T_o}}{1 - e^{-\Theta_i/T}}\right] = \ln\frac{p_o}{p}$$

Furthermore

$$\Delta J = \frac{\overline{\varkappa_u}}{\varkappa_u - 1}AR(T - T_o) + AR\sum_{i=1}^{n}\frac{p_i}{p_o}\Theta_i\left(\frac{1}{e^{\Theta_i/T_o} - 1} - \frac{1}{e^{\Theta_i/T} - 1}\right)$$

and

$$c^2 = 2gR\left[\frac{\overline{\varkappa_u}}{\varkappa_u - 1}(T_o - T) + \sum_{i=1}^{n}\frac{p_i}{p_o}\Theta_i\left(\frac{1}{e^{\Theta_i/T_o} - 1} - \frac{1}{e^{\Theta_i/T} - 1}\right)\right]$$

3. The third possible type of flow in the jet occurs when the time spent in the jet by the combustion gas is so long that all energetic equilibria, including chemical equilibrium, can be attained for the instantaneous values of pressure and temperature. This type of flow is characterized by the conditions: $c_{v\,osc}\,dT = f(T)$, $dD = f(p, T)$

From this and the fundamental equations, we obtain the differential equation:

$$d\left(\int_0^T c_v\,dT\right) + dD + A p\,dV = 0 \quad \text{or} \quad dJ + dD = ART\frac{dp}{p}$$

The function $dD = \varphi(p,T)$ which now contains p, cannot be represented in explicit form, so that no general analytic solution of the differential equation can be given. One must therefore, using the difference equation

$$\Delta J + \Delta D = ART\,\Delta p/p \quad \text{or} \quad J_1 - J_2 + D_1 - D_2 = 3.97\frac{T_1+T_2}{M_1+M_2}\cdot\frac{p_1-p_2}{p_1+p_2} \quad \text{and}$$

as close a collection of values of J, D, and M as functions of p and T as possible, obtain the desired connections point for point. Procedures for calculating such tables for various fuels have been suggested by M. V. Stein.

The behavior of temperature T, heat content J, Dissociation energy D, and the liberated kinetic energy $w^2/2g$ along a pressure drop from $p_o = 100$ atm to $p_m \to 0$ for all three types of flow is shown for the combustion of octane in liquid oxygen in Fig. 13.

The decision as to which of the three possibilities (or an intermediate one) is most probable for the flow of the combustion gases from the rocket furnace is influenced by the following consideration: if the expansion takes place in an experimental short jet 1300 mm. long, then the mean time spent by the combustion gases can be computed to be about 2×10^{-3} sec, corresponding to an average no. of collisions of the molecule on its way through the jet of about 2×10^8. If one considers that 96% of these collisions already occur in the space between the furnace and the smallest cross-section, then one sees by comparison with the effective number of collisions (10^2–10^3) for the various energy interchanges, that we may expect equilibrium of rotations, vibrations and possibly even dissociations for the processes occurring in the initial part of the jet, up to its smallest cross-section. Flow-type 1 becomes the more improbable the higher the furnace pressure and temperature for given velocity, the longer the jet, and the smaller the effective number of collisions of the combustion gas mixture. Therefore flow-type 2 is generally assumed in calculations on rockets; it gives closed integrable formulae. The actually rapidly varying $\varkappa$ can, for rough estimates, using the usual adiabatic flow formulae, be replaced in first approximation by a mean value $\varkappa^* = \frac{J_o/T_o}{J_o/T_o - AR}$ which for stochiometric burning of octane at 100 atm. gives $\varkappa^* = 1.248$

This mean value is strictly valid only for an expansion to $T_m = 0°K$ and $p_m = 0$ atm. If for example the mouth values are to be calculated for an expansion to $p_m = 1$ atm, then two equations are required for a determination of $\varkappa^*/\varkappa_m$ since both $\varkappa^*/\varkappa_o$ and T_m are unknown for a given mouth pressure $p_m \neq 0$ For the example of octane combustion given above, we obtain in this manner from the equations:

$$T_m/T_o = (p_m/p_o)^{\varkappa^*/\varkappa_m\,(\varkappa^*/\varkappa_m - 1)} \quad \text{and}$$

$$\varkappa^*/\varkappa_m = \frac{J/T_m}{J/T_m - AR} = \frac{\dfrac{\varkappa_m}{\varkappa_m - 1} + \sum_{i=1}^{n}\left[\dfrac{p_i}{p_o}\cdot\dfrac{\Theta_i}{T_o - T_m}\left(\dfrac{1}{e^{\Theta_i/T_m} - 1} - \dfrac{1}{e^{\Theta_i/T_m} - 1}\right)\right]}{\dfrac{\varkappa_m}{\varkappa_m - 1} + \sum_{i=1}^{n}\left[\dfrac{p_i}{p_o}\cdot\dfrac{\Theta_i}{T_o - T_m}\left(\dfrac{1}{e^{\Theta_i/T_o} - 1} - \dfrac{1}{e^{\Theta_i/T_m} - 1}\right)\right] - 1}$$

for an expansion to $p_m = 1$ atm, the value $\varkappa^*/\varkappa_m = 1.222$ at $T_m = 1586°$ K. This method gives fairly accurate values of T_m and c_m whereas all intermediate values between T_o and T_m, as well as the corresponding c_m, are more inaccurate. Flow-type 3, in case its consideration can not be avoided, can be represented by the method of Mollier with the aid of entropy charts, which show J + D + R as ordinate and enable c_m and temperature values to be read off. Figure 14 shows such a Mollier-diagram for a combustion gas of gas-oil-oxygen and gas-oil ozone respectively.

The following table shows in summary form for the case of stochiometric combustion of octane in O_2 at 100 atm. pressure, how the important final characteristics of the streaming: mouth velocity c_m, effective exhaust speed C, jet mouth temperature T_m, and the ratio of kinetic energy to total energy supplied (E), differ for the three types of flow and for different jet end-pressures.

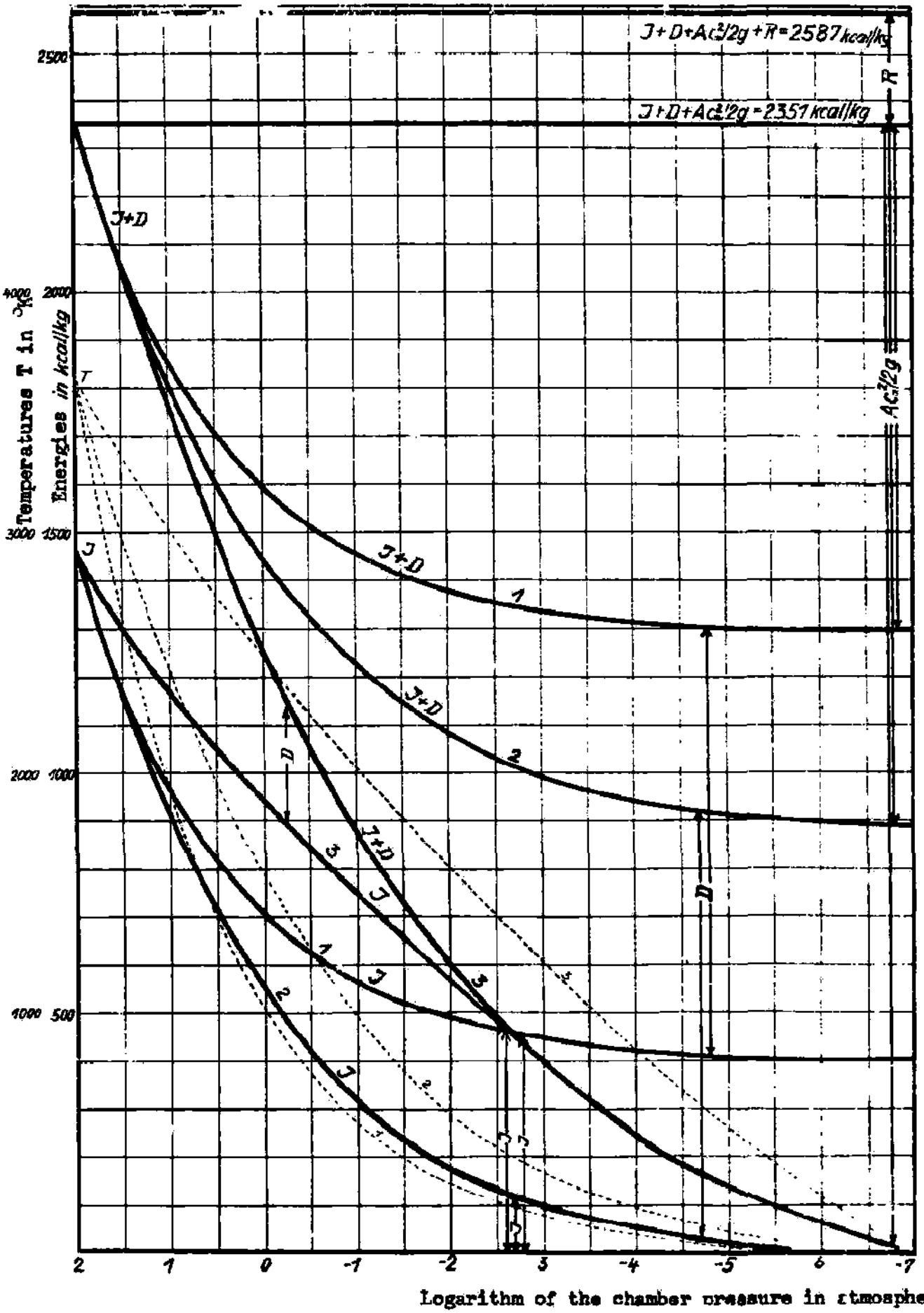

Figure 13; Temperature T, Heat content J, Dissociation loss Dpt, and gain in kinetic energy plotted against the logarithm of the pressure p according to the three possible streaming gradients in the nozzle. (See text p.24 & FF). The gasses entering the nozzle are assumed to be a completely burned stoichiometric mixture of the octane and O_2 at a pressure of 100 atmospheres.

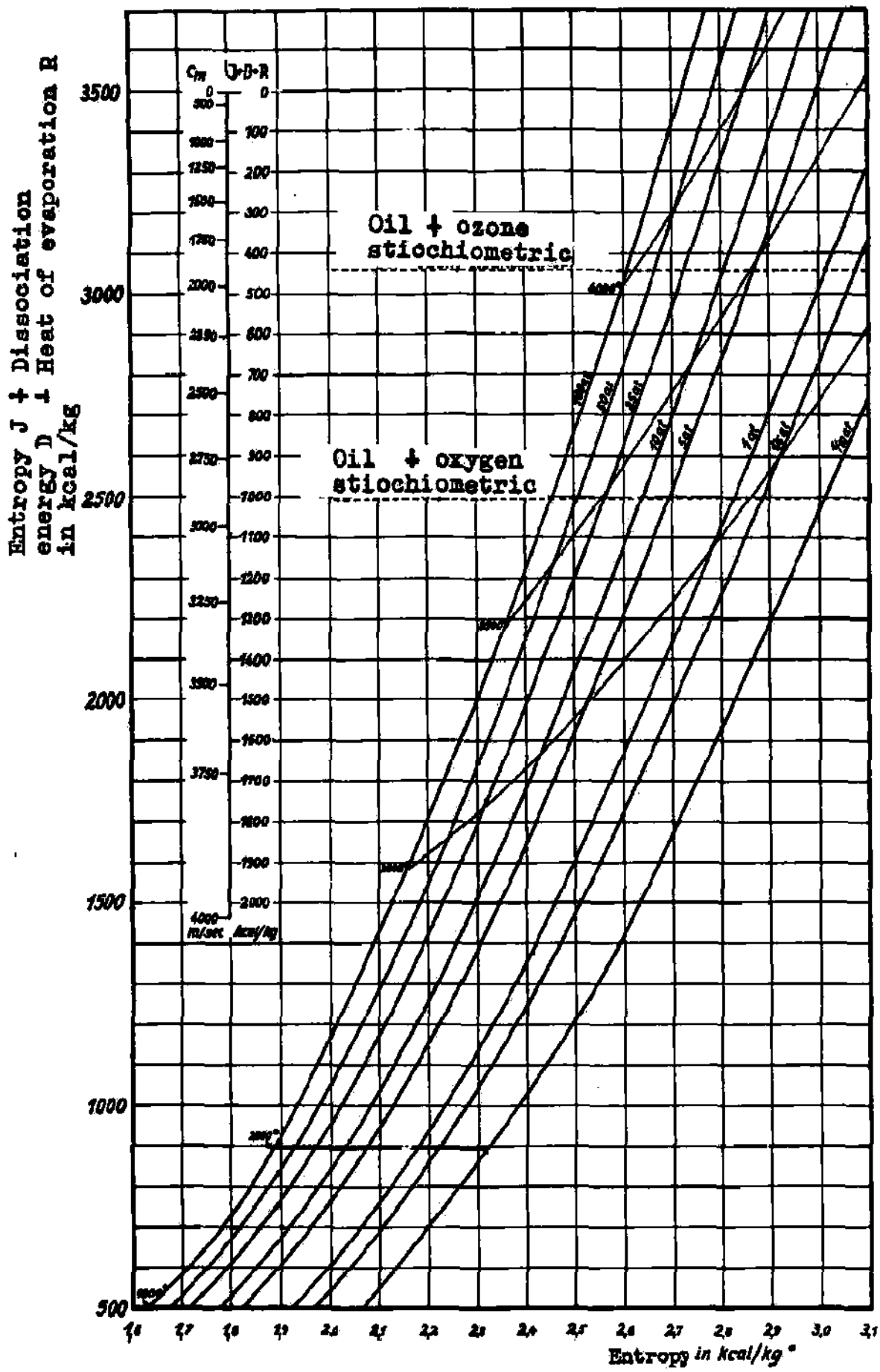

Figure 14; Entropy diagram after M. von Stein for the Nozzle stream gradient and oil combustion. II 3

Streaming process Art (1,380) 2. Art 3. Art

Test stand conditions:

p_m =	1 at	1 at	1 at
T_m =	1030°K	1577°K	2500°K
c_m =	2518 m/sec	2759 m/sec	3020 m/sec
c =	2654 m/sec	2949 m/sec	3260 m/sec
Gained energy in the mouth of the nozzle in % of E.	29,3	35,1	42

Flight conditions in d/dm =0.14:

p_m =	0,0729 at	0,1305 at	0,250 at
T_m =	500°K	1041°K	2225°K
c_m =	2760 m/sec	3066 m/sec	3330 m/sec
c =	2820 m/sec	3178 m/sec	3520 m/sec
Gained energy in the mouth of the nozzle in % of E.	35,1	43,4	51

Optimum conditions in case of complete relaxation.

$p_m \rightarrow$	0 at	0 at	0 at
$T_m \rightarrow$	0°K	0°K	0°K
c_m = c_{max} = c =	2970 m/sec	3496 m/sec	4438 m/sec
Gained energy in the mouth of the nozzle in % of E.	40,7	56,5	90,9

Completely lossless conversion of the total input energy E into kinetic energy would give a theoretical exhaust speed

$$c_{th} = \sqrt{2gE/A} = 4655 \text{ m/sec}$$

The concepts of mouth velocity c_m, maximal velocity c max, and effective exhaust speed c (19), require more detailed explanation. In general, for rough calculations, standard adiabatic-flow formulas, using a fictitious average $\varkappa$, whose magnitude and evaluation has been discussed already in presenting the three types of flow. Thus for expansion to a mouth pressure p_m, the mouth velocity is $c_m = \sqrt{\frac{2\varkappa}{\varkappa-1} p_0 v_0 \left[1-\left(\frac{p_m}{p_0}\right)^{\frac{\varkappa-1}{\varkappa}}\right]}$ for expansion to the theoretically possible limiting pressure $p_m = 0$, $c_{max} = \sqrt{\frac{2\varkappa}{\varkappa-1} p_0 v_0}$ and from these two relations:

$$c_m/c_{max} = \sqrt{1-\left(\frac{p_m}{p_0}\right)^{\frac{\varkappa-1}{\varkappa}}} = \sqrt{1-T_m/T_0}$$

If we multiply the velocity c_m by the mass blown out per second dm/dt we obtain the mouth-momentum J_m of the jet.

In experiments with rockets, if the mouth pressure p_m in the jet is equal to the pressure of the surrounding still air p_a this mouth momentum is directly recorded by a dynamometer as the force P*; it depends on the external air pressure, i.e. on the barometer reading, altitude of the testing-place, etc. and must not be confused with the thrust P, as can be seen from a consideration of Fig. 15. There the conditions between resistance and thrust for a flying apparatus and their values measured on the ground are schematized.

By resistance to the driven apparatus in flight we mean the vector sum of all the aerodynamic forces on the accelerated surfaces. Let W be this sum of all the pressures and frictional forces. In a wind tunnel or a tow test on a non-driven device one always measures a smaller resistance $W' = W - p' f_m$, where p' is the absolute air pressure beyond the mouth surface f_m of the jet. It follows therefore that $W = W' + p' f_m$. For the moving body, the air pressure p' behind the

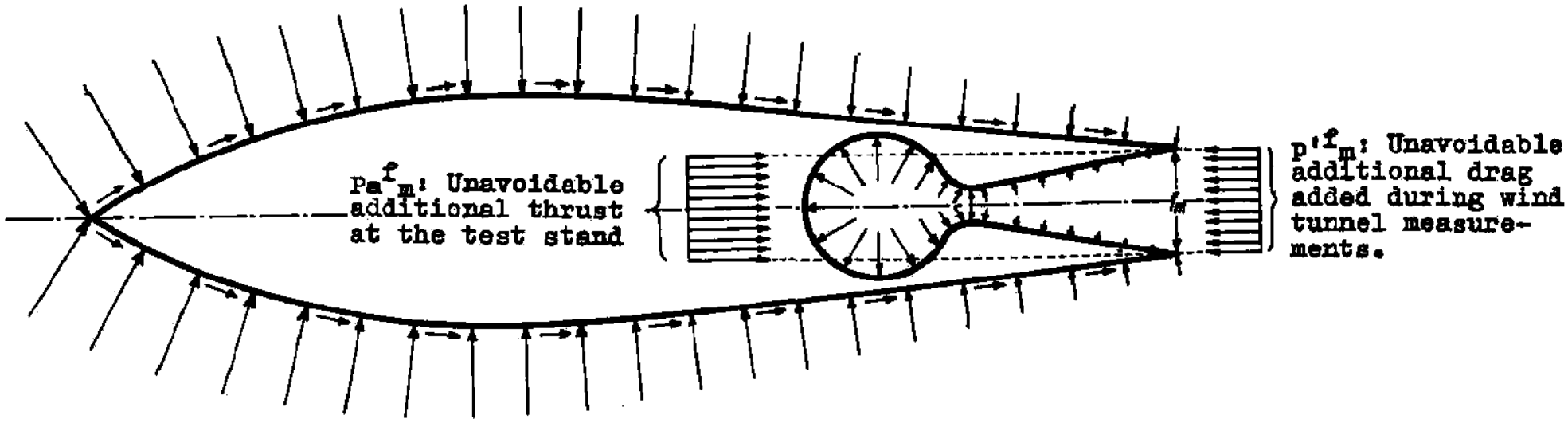

Figure 15; Relationship between thrust and drag in flight compared to sea level test values.

rear surface is always smaller than the pressure p_a of the air at rest; for $v/v_0 > \sqrt{2/(\varkappa-1)} = 2.2$, $p' = 0$. The value p' must always be included in resistance measurements on undriven devices, in order to obtain the true resistance W of the body.

By thrust on an apparatus in flight we mean the vector sum of all the flame pressures on the surface of the rocket in contact with flame (inner walls). In a test one always measures a smaller thrust $P' = P - p_a f_m$ where p_a is again the pressure of still air. The thrust measured in a test depends on the pressure of the surrounding air, and for the effective thrust we obtain $P = P' + p_a f_m$.

The effect of these two unavoidable additional effects in a wind-tunnel or a test can be seen most clearly by calculating the resultant force (thrust-resistance) which accelerates a mass $m = G/g$:

$$m\, dv/dt = P - W = P' - W' + f_m (p_a - p')$$

For measurements on the ground, an unavoidable additional force proportional to f_m is thus included, which is different in measurements of resistance and thrust, and for which special correction must be made. The correction is small at moderate velocities (e.g. in the use of rockets for takeoff) and becomes largest for very high supersonic speeds (e.g. rocket projectile, long distance military rocket aircraft).

In order to calculate the effective thrust P of a rocket motor, one must add to the mouth impulse $J = c_m \frac{dm}{dt}$ the total pressure of the combustion gas on the jet mouth ($p_m f_m$); or one must add to the free dynamometer thrust in the test

$$P' = J_m + f_m (p_m - p_a) = c_m \frac{dm}{dt} + f_m (p_m - p_a)$$

the total thrust of the still air on a surface the size of the jet mouth:

$$P = P' + p_a f_m = J_m + p_m f_m = c_m\, dm/dt + p_m f_m$$

In the initially mentioned, most frequent case $p_a = p_m$, mouth impulse J_m and dynamometer reading P' are identical.

Thus the effective velocity c, which is independent of external air pressure, and which when multiplied by $\frac{dm}{dt}$ gives the effective thrust is:

$$c = c_m + p_m f_m\, dt/dm = c_m + \frac{p_m}{\rho_m c_m}$$

and further

$$c/c_{max} = \sqrt{1 - \left(\frac{p_m}{p_o}\right)^{\frac{\varkappa-1}{\varkappa}}} \left[1 + \frac{\varkappa-1}{2\varkappa} \frac{(p_m/p_o)^{\frac{\varkappa-1}{\varkappa}}}{1 - (p_m/p_o)^{\frac{\varkappa-1}{\varkappa}}}\right]$$

The determination of the effective exhaust speed c has the following peculiar, technically interesting consequence: in the usual engine construction the thermal efficiency is $\eta_{therm} = c^2/c_{max}^2 = 1 - T_m/T_o$. In the rocket motor the quantity which corresponds to this is the jet efficiency:

$$\eta_D = c^2/c_{max}^2 = (1 - T_m/T_o)\left(1 + \frac{\varkappa-1}{2\varkappa} \frac{T_m/T_o}{1 - T_m/T_o}\right)^2$$

(see also (19) p. 6). This expression implies that the higher temperatures and the quantities of heat at those temperatures are more " effective" than lower temperatures and quantities of heat at lower temperatures. This represents no contradiction to the energy theorem, since the effective exhaust speed is not identical with the actual velocity of flow of the combustion gas, but is <u>larger</u> than it. This relation has nevertheless a technical value, because the part of the initial heat content at lower (temp.) ranges can be made available only by special technical procedures (for gases, which soon tend to develop degeneracies, like condensation, it can't be done at all) and non-availability therefore leads to relatively smaller losses than one would expect according to the second law, for the non-available heat content.

Aside from the relations already given, we can, from the well known equation for the rate of gas flow through the jet throat

$$\Delta G = \mu a f' = f' \left(\frac{2}{\varkappa+1}\right)^{\frac{1}{\varkappa-1}} \sqrt{2g \frac{\varkappa}{\varkappa+1} p_o/v_o}$$

and the equation for the effective exhaust speed, obtain a frequently useful relation between P, f' and p_o in the form $P = k p_o f'$ where

$$k = 2\left(\frac{2}{\varkappa+1}\right)^{\frac{1}{\varkappa-1}} \sqrt{\frac{\varkappa^2}{\varkappa^2-1}\left[1 - \left(\frac{p_m}{p_o}\right)^{\frac{\varkappa-1}{\varkappa}}\right]} \left[1 + \frac{\varkappa-1}{2\varkappa} \frac{(p_m/p_o)^{\frac{\varkappa-1}{\varkappa}}}{1 - (p_m/p_o)^{\frac{\varkappa-1}{\varkappa}}}\right]$$

By means of this factor k, by which the effective thrust is greater than the product of furnace pressure and jet-throat surface, one can reduce the otherwise tedious determination of effective thrust of a rocket motor, for sufficiently lengthened jet, to a measurement of the furnace pressure and the outside pressure, which can be easily done with ordinary manometers. This type of thrust measurement is very convenient in trial setups as well as in measurements on aircraft in

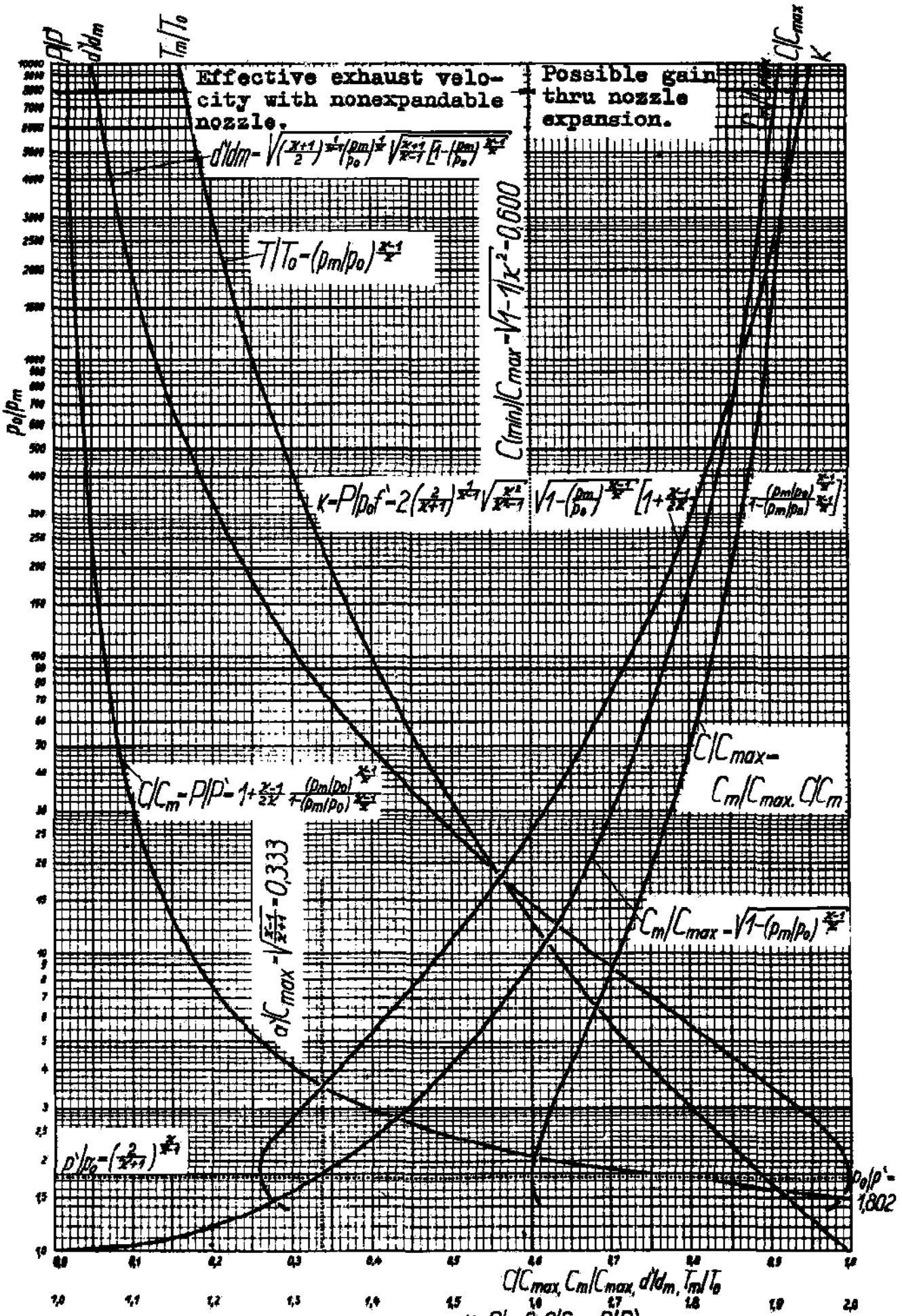

Figure 16; Firegas flow with x=1.25

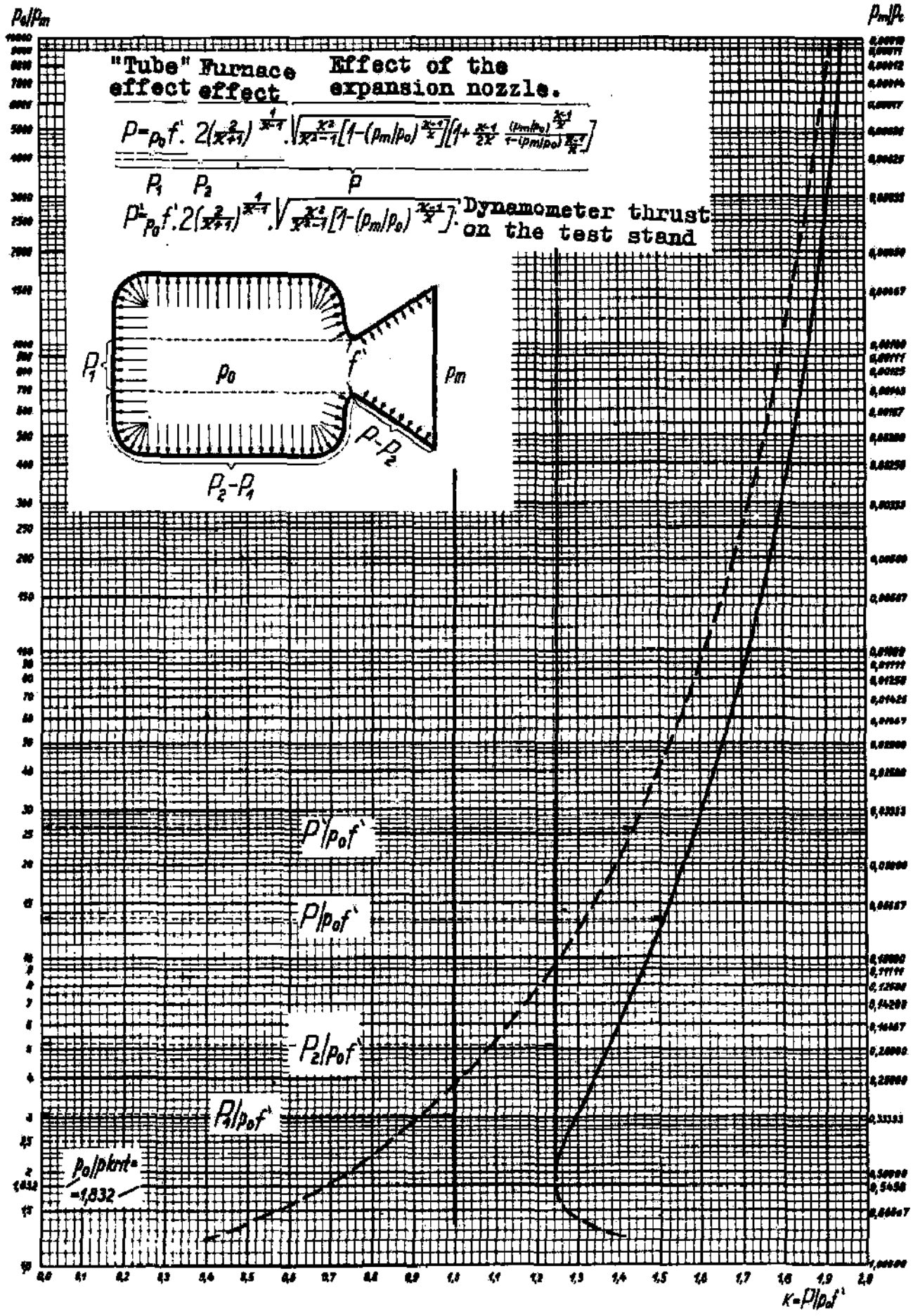

Figure 17; Analysis of effective thrust of rocket motor with x = 1.

flight. Conversely, in a test, if furnace pressure and effective thrust (or dynamometer thrust) are measured, the actually effective $\varkappa$ can be determined.

All these relations: the factor k, the ratios c/c_{max}, c_m/c_{max}, c/c_m, Tm/To and d'/d_m are shown in Fig. 16 as functions of the ratio of furnace pressure to mouth pressure, for a frequently used value of $\varkappa = 1.25$.

As is shown in Fig. 17 for the special case $\varkappa = 1.25$, the individual factors in the expression for k can be interpreted very intuitively; the total thrust P of the rocket motor is made up of the partial thrusts: $P_1 = p_0 f'$, arising from the pressure p_0 of the combustion gas on that spot, f', of the rear wall of the furnace which one sees when looking down the axis of the jet throat. A cylindrical tube, closed at one end, would show this same effect; $P_2 = p_0 f' 2\left(\frac{2}{\varkappa+1}\right)^{\frac{\varkappa}{\varkappa-1}}$, the increase relative to P_1, arises from the non-uniformity of the pressure distribution on the remaining furnace-wall surfaces due to the pressure gradient in the direction of the jet opening;

$$P_3 = P = p_0 f' \varkappa 2\left(\frac{2}{\varkappa+1}\right)^{\frac{1}{\varkappa-1}} \sqrt{\frac{\varkappa^2}{\varkappa^2-1}\left[1-\left(\frac{p_m}{p_0}\right)^{\frac{\varkappa-1}{\varkappa}}\right]}\left[1+\frac{\varkappa-1}{2\varkappa}\,\frac{\left(p_m/p_0\right)^{\frac{\varkappa-1}{\varkappa}}}{1-\left(p_m/p_0\right)^{\frac{\varkappa-1}{\varkappa}}}\right]$$

This increase relative to P_2 is caused by the pressure of the combustion gases against the extended jet.

The free thrust P' of the rocket motor is

$$P' = \Delta\frac{G}{g} c_m = p_0 f' \varkappa 2\left(\frac{2}{\varkappa+1}\right)^{\frac{1}{\varkappa-1}} \sqrt{\frac{\varkappa^2}{\varkappa^2-1}\left[1-\left(p_m/p_0\right)^{\frac{\varkappa-1}{\varkappa}}\right]}$$

and is shown for comparison in Fig. 17 by the dotted curve.

Before these physical considerations on chemico-energetic problems are treated in relation to the effective exhaust speed, we want to discuss briefly their significance in terms of the long-range rocket-bomber project. The familiar relation, that jet and rocket motors produce their energy conversion most effectively when the velocity of flight is (as closely as possible) equal and opposite to the velocity of the jet, might lead us to the false conclusion that the exhaust speed should be adjusted to the instantaneous velocity of flight. Since in the aircraft what matters is not ideal energy conversion per se, but rather the smallest consumption of fuel in terms of weight, fuels with higher energy content, which give larger c-values, are to be preferred, even when this greater energy content per unit weight is not used so effectively. For a given consumption (of fuel) by weight, the energy given to the aircraft becomes greater, the greater the value of c, because the useful part $\eta_a = 2\eta_t(1+\eta_t/2)$ of the driving energy $c^2/2$ from a unit mass of fuel (i.e. $\eta_t = \eta_a/\eta_t c^2$), increases rapidly with exhaust speed. Despite this, the great importance of the exhaust speed may be limited if the fuel having higher exhaust speed has other disadvantages. For example, a 50% aluminium-gasoil suspension and oxygen, having a tank volume per kg. fuel requirement of 0.84 dm, is preferable despite the somewhat lower exhaust speed, to liquid H_2 and O_2, which requires 2.4dm^3 tank space per kg. of fuel, and for which moreover special heavy devices are needed in the tank space because of the low temperature of the liquid H_2. The following general statement can be made concerning the effect of density on the choice of fuel: if the flight path s is approximately proportional to the cube of the maximum flight velocity v, and v is related to the exhaust speed c and weight ratio G/G_0 by the equation of page 207, $v = 0.443c + c \ln G_0/2G$, then $s = \text{const.} \times c^3 \chi (\ln \frac{G_0}{G} - 0.25)^3$. One can therefore obtain equal ranges for different values of c, if G/Go varies properly. By differentiating (keeping s, v, and G_0 constant) we obtain $\frac{\Delta c}{c} = \frac{c}{v}\frac{\Delta G}{G}$. A dependence of the expression $\Delta G/G$ on the small change ΔE_v in the energy density E_v can be estimated as, for example, $\frac{\Delta G}{G} = -0.5\frac{\Delta E_v}{E_v}$. Thus $\frac{\Delta c}{c} = -0.5\frac{c}{v}\cdot\frac{\Delta E_v}{E_v}$, so that in the region of interest, $\eta_v \approx 0.5$, $\frac{\Delta c}{c} \approx -\frac{1}{4}\frac{\Delta E_v}{E_v}$. Variations in exhaust velocity are four times as effective as improvements in density. Furthermore these considerations permit a comparative evaluation of different fuels, by starting from a standard fuel, say a hydrocarbon with liquid oxygen, having values c and E_v. From these and the corresponding c_1 and E_{v1} of the comparison fuel, an evaluation number K can be given in the form;

$$K = \frac{c_1}{c} = \left[\frac{c_1}{c}\cdot\frac{\ln\frac{2}{1+E_1/E_v}\cdot\frac{G_0}{G}-0.25}{\ln\frac{G_0}{G}-0.25}\right]^3, \quad \text{or, for } \frac{G_0}{G}=10 \quad K = \frac{\left[2.746-\ln(1+E_v/E_v)\right]^3}{8.650}\cdot\frac{c_1^3}{c^3}$$

A typical hydrocarbon reaction is the burning of octan in oxygen:

$$C_8H_{18} + 12\tfrac{1}{2}O_2 = 8CO_2 + 9H_2O + 2587\ kcal/kg;\ c_H = 1655\ m/sec\ [11]$$

The value for the upper limit of the heat of mixing is referred to 0°K. From Fig. 18, it is clear that we must subtract from this value the 9.1% loss due to heat required for physical separation (melting, vaporization) and that the pressure dependent losses due to chemical separation (dissociation) amount to 34.4% at 100 atm. furnace pressure, so that under these driving conditions the furnace efficiency is $\eta_o = T_i/E = 0.565$. This graph of octane combustion at

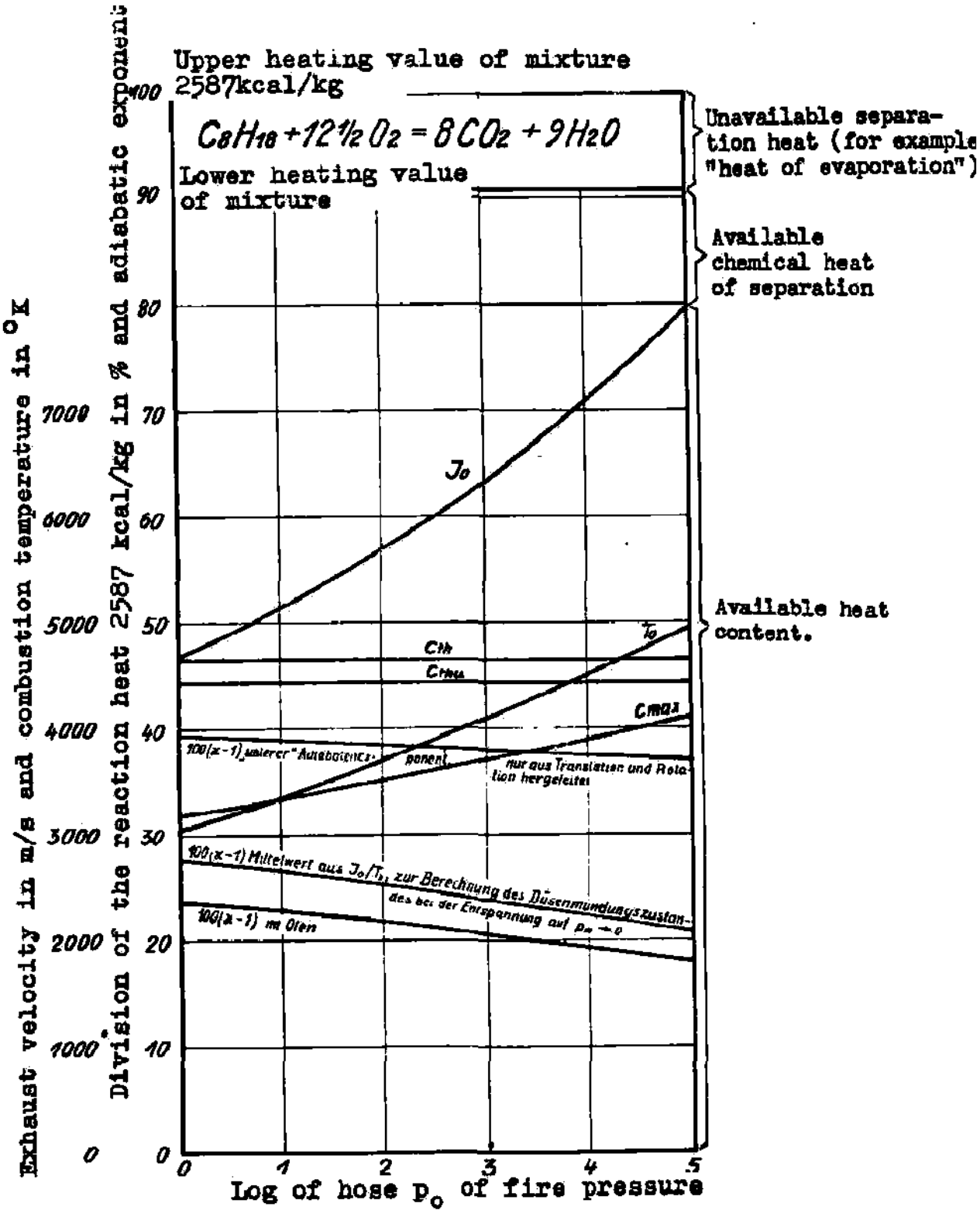

Figure 18; Heat of evaporation, dissociation, enthalpy, firegas temperature, theoretical and maximum exhaust velocity and adiabatic gas exponent of the combustion products in the case of oxygen and octane with static equilibrium.

varying furnace pressures, as well as the later graphs and tables for other fuels, were calculated by M. V. Stein, taking account of all the dissociation products, and assuming that physical and chemical equilibrium are reached in the furnace, and that expansion can be followed, as a flow of the second kind, to an external pressure zero. In addition the lower limit of the heat developed by the mixture ($E-R_{io}$), the heat content J_o, furnace temperature T_o, theoretical and maximum exhaust speeds are plotted, as a function of the log of the furnace pressure, for the proper average $\varkappa$ corresponding to this expansion; also to give some idea of the range of variation of $\varkappa$ for other types of expansion and other jet-mouth pressures, the adiabat exponent corresponding to the instantaneous furnace-state is shown as an upper value, and the value of $\varkappa$ for the calculations of flow-type 1 is shown as an upper limit. In this and the later graphs, which enable only a relative comparison of different fuels, the effective exhaust speed c, which is the determining factor for flight, and whose value for octane combustion has been previously given, is not especially noted. It can be determined from the maximal velocity using the value of jet efficiency: $\eta_D = (c/c_{max})^2$

The expression for the total loss of the rocket motor is

$$\eta_i = \eta_o \cdot \eta_D = \left(\frac{c}{c_{th}}\right)^2 \cdot \left(\frac{c}{c_{max}}\right)^2 = \left(\frac{c}{c_{th}}\right)^2$$

numerically, for octane combustion at 100 atm. furnace pressure, $\eta_i = 0.565 \times 0.825 = 0.465$. The flight is fixed in this and all the later calculations by $d'/d_m = 0.14$, on the basis of the following consideration: in flight, the pressure behind the stern of the rocket bomber drops below 1 atm, so that the pressure gradient p_o/p_m at say 100 atm furnace pressure must go far above 100. The combustion gas will actually spread over the whole 2.50 m^2 surface of the stern of the aircraft; i.e., the ratio of jet mouth surface f_m to the jet throat surface f' will be about 50; throughout the working period of the rocket motor, corresponding to $d'/d_m = \frac{1}{\sqrt{50}} = 0.14$.

In addition to the important and carefully studied hydrocarbon-oxygen mixture, there is a second group of rocket fuels, having the common property that they are elements in the first columns of the periodic table, and which when burnt in O_2 give much higher energy concentrations per unit mass, and also generally per unit volume, than the hydrocarbons.

The following reactions were considered:

Untersucht wurden folgende Reaktionen:

Be	+ 0,5 O_2	= BeO	+ 5930 kcal/kg	bei 0°K;	
2 B	+ 1,5 O_2	= B_2O_3	+ 4930 kcal/kg	" " ;	
2 Li	+ 0,5 O_2	= Li_2O	+ 4750 kcal/kg	" " ;	
2 Al	+ 1,5 O_2	= Al_2O_3	+ 3920 kcal/kg	" " ;	(6, 13, 14)
H_2	+ 0,5 O_2	= H_2O	+ 3900 kcal/kg	" " ;	
Mg	+ 0,5 O_2	= MgO	+ 3330 kcal/kg	" " ;	

Combustion of Al and H_2 are shown in Fig. 19 and 20 in the same form as for octane combustion. The following table gives the most important characteristics for these light-metal-fuels with stochiometric liquid O_2 at 1, 10, and 100 atm. furnace pressure:

Upper value of heat of mixture E [kcal/kg]	BeO	B_2O_3	Li_2O	Al_2O_3	H_2O	MgO
	5930	4930	4750	3920	3900	3330
Heat of Vaporization R_{io} [kcal/kg]	5040	2300	2780	1290	750	3750
Weight of Solid-Liquid Phase in Combustion Gas at 1 atm	13,8	-	-	-	-	43,0
at 10 atm	18,0	-	-	-	-	48,0
at 100 atm	23,2	-	-	-	-	54,5
Heat Content J_o in % of E at 1 atm	20,6	40,5	21,9	21,5	45,8	28,7
at 10 atm	23,8	46,7	24,1	24,4	51,7	35,0
at 100 atm	28,4	51,4	27,0	28,1	59,7	44,1
Boiling Point at 1 atm [°K]	3400	1990	1100	3250	373	3120

	BeO	B_2O_3	Li_2O	Al_2O_3	H_2O	MgO
Furnace Temperature T_o [°K] at 1 atm.	3400	6210	2350	3700	2950	3350
at 10 atm	3920	7010	2730	4070	3200	3970
at 100 atm	4550	7680	3200	4700	3560	4850
κ or $\bar{\kappa}$ at 1 atm	1,24	1,125	1,320	1,280	1,300	1,11
at 10 atm	1,22	1,110	1,315	1,260	1,250	1,10
at 100 atm	1,20	1,100	1,310	1,240	1,220	1,08
c_{th} [m/sec]	7050	6420	6310	5730	5720	5280
c_{max} [m/sec] at 1 atm	3200	4090	2950	2660	3870	2830
at 10 atm	3440	4390	3100	2830	4110	3130
at 100 atm	3760	4610	3280	3030	4420	3510

In this calculation all heats of fusion were neglected relative to heats of vaporization; all possible dissociations of the end products of combustion were taken into account.

B, Li, Al and H_2 do not differ essentially from hydrocarbons in their behavior during combustion, but differ only in the numerical results; for example, Li and Al, despite their higher heat production, reach lower maximal exhaust speeds than for hydrocarbons, because of the vaporization and dissociation losses. Be and Mg are basically different. In the case of Be, the large heat of vaporization of BeO permits only a part of the burning mass to vaporize, while a large part remains in the liquid state (fog) or solid state (dust). These parts can then make use of the upper limit value of the heating value of the mixture, so that despite the large heat of vaporization, high temperatures, and high heat content of the total mass occur, with consequent large values of c_{max}. These liquid and solid masses in the combustion gas have a great effect on the expansion of the total mass, which expresses itself in the form of a very small adiabat-exponent: This $\bar{\kappa}$ of the total mass is calculated from the weight fraction k_g of the gas phase, the weight fraction k_f and specific heat c_f of the liquid-solid phase by the equation:

$$\bar{\kappa} = \frac{k_g c_{pgas} + k_f c_f}{k_g c_{vgas} + k_f c_f}, \quad \text{where } c_{pgas} = J_{gas}/T_o \text{ and } c_{vgas} = J_{gas}/T_o - AR$$

are obtained in the usual way for a flow-type 2, to mouth pressure $p_m = o$. The T_2 curve at the same time represents the boiling point of BeO, since the combustion temperature is determined by the boiling point of the BeO. For Mg, whose lower heat value is actually negative, the large fraction of liquid-solid phase results in very high temperatures and heat content of the total mass and especially low $\bar{\kappa}$ values, so that the burning mass rapidly loses the characteristics of a gas or vapor and approaches the behavior of a hot lava.

From the given values of maximum exhaust speed, the resultant effective exhaust speeds for the individual light-metal fuels at 100 atm. furnace pressure can be computed, if we take account of the jet efficiency corresponding to the κ values for $d'/d_m = 0.14$, using the relation

$$\left(\frac{d'}{d_m}\right)^2 = \frac{c}{c_{max}} \cdot \frac{\left(\frac{\kappa+1}{2}\right)^{\frac{1}{\kappa-1}} \left(\frac{\kappa+1}{\kappa-1}\right)^{\frac{1}{2}} \left(\frac{p_m}{p_o}\right)^{\frac{1}{\kappa}} \left[1 - \left(\frac{p_m}{p_o}\right)^{\frac{\kappa-1}{\kappa}}\right]}{1 - \frac{\kappa+1}{2\kappa}\left(\frac{p_m}{p_o}\right)^{\frac{\kappa-1}{\kappa}}}$$

In first approximation, κ was obtained from the somewhat too large mean value between To and o, instead of between To and T_m; this leads to less favorable values.

BeO :	κ = 1,20;	$\sqrt{\eta_p} = c/c_{max}$ = 0,844;	c = 3170 m/sec;
B_2O_3 :	1,10;	0,690;	3180 ;
Li_2O :	1,31;	0,925;	3030 ;
Al_2O_3 :	1,24;	0,880;	2670 ;
H_2O :	1,22;	0,865;	3820 ;
MgO :	1,08;	0,630;	2210 ;

(The approximate mean value for κ is 1.255 for octane and gives c = 3120 m/sec. For purposes of uniformity, these numbers were used in later comparison calculations).

For application to rockets, in addition to the effective energy concentration in the mass, the effective concentration E_v in the tank volume is important, since it determines the size of the fuel tanks, rate of feed of the injection pumps and the evaluation number k of the fuel.

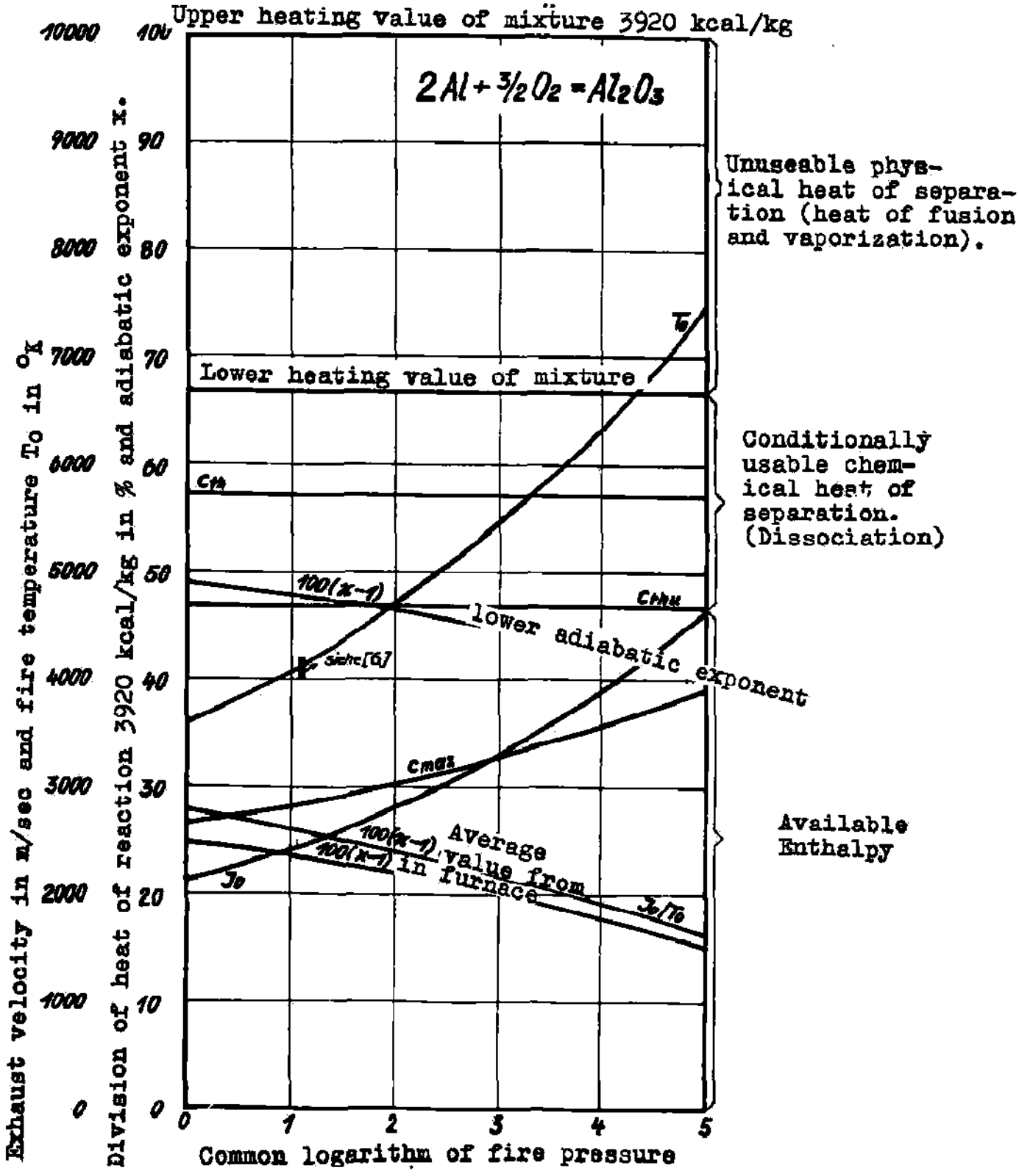

Figure 19; Heat of vaporization, dissociation, heat content, firegas temperature, theoretical and maximum exhaust velocity and adiabatic exponent of firegases for the burning of aluminum in oxygen with static equilibrium.

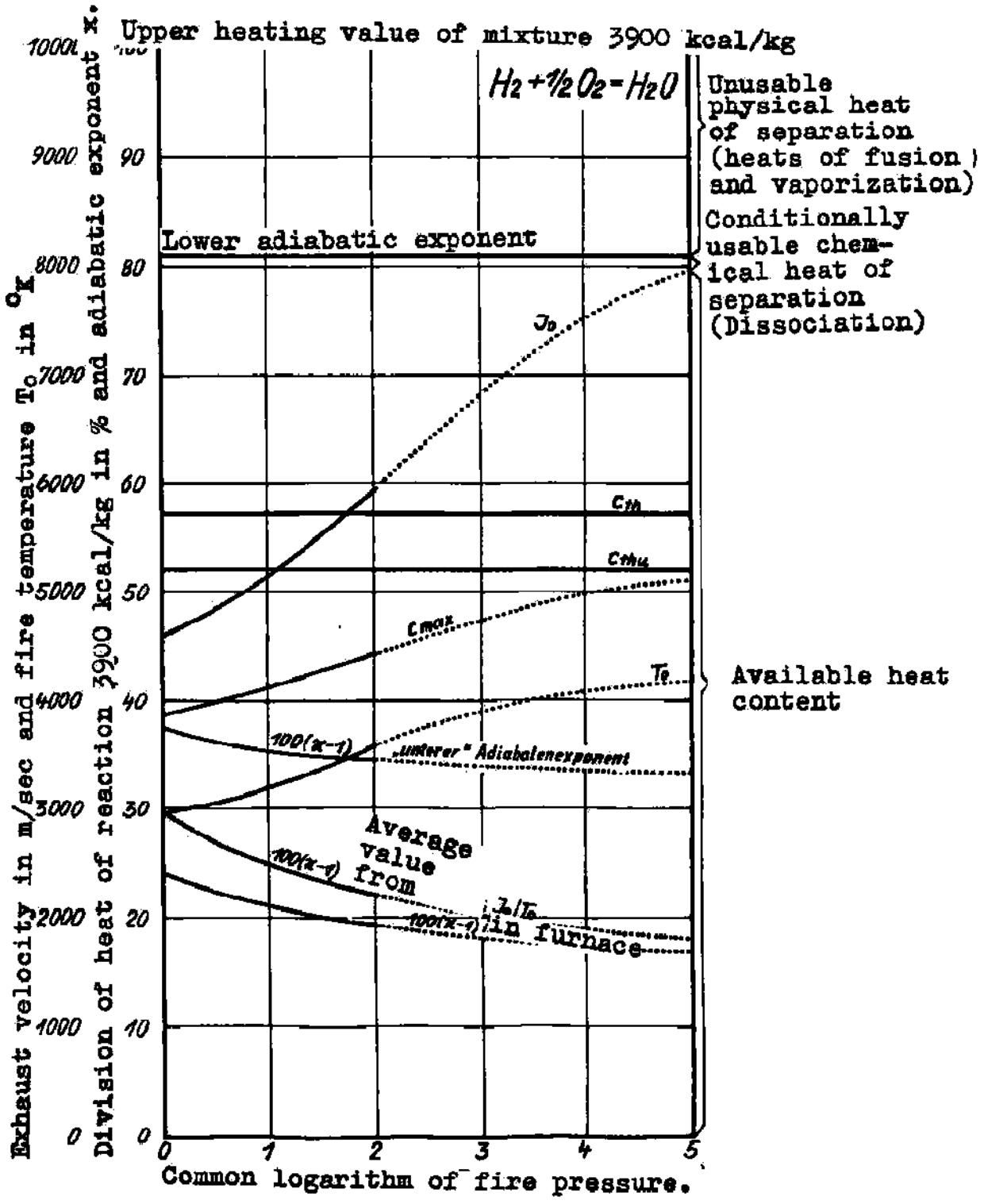

Figure 20; Heat of condensation, dissociation, enthalpy, firegas temperature, theoretical and maximum exhaust velocity and adiabatic exponent of firegases in the burning of H_2 in O_2 with static equilibrium.

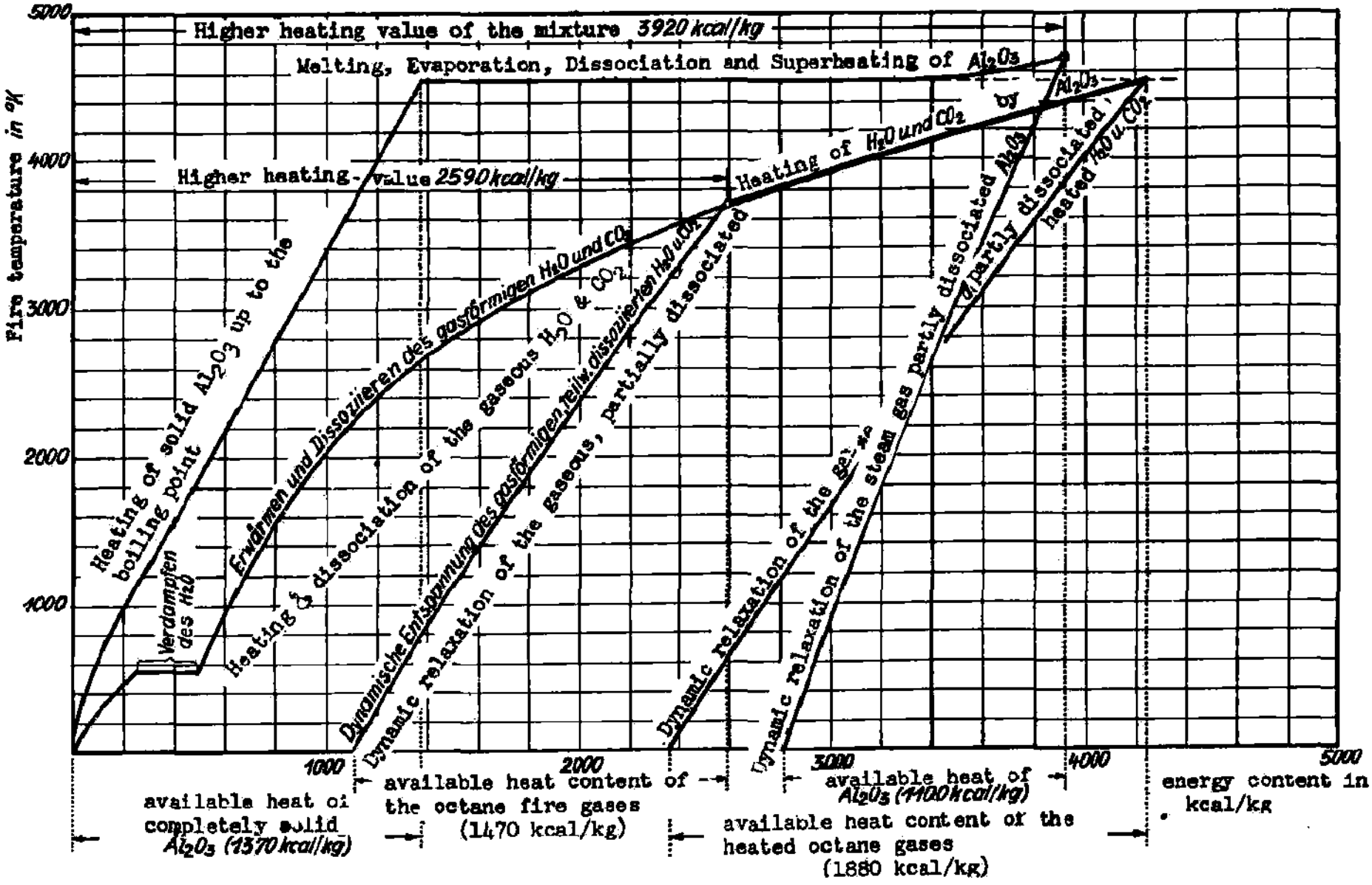

Fig. 21: Energy - Temperature - diagram of aluminum plus hydrocarbon combustion in O_2 at 100 atmospheres chamber pressure and static behavior of the gases.

Beryllium mit Flüssigsauerstoff	E_v = 1580 kcal/dm³	K =	1,23;
Bor mit Flüssigsauerstoff	1640	;	1,27;
Lithium mit Flüssigsauerstoff	820	;	9,64;
Aluminium mit Flüssigsauerstoff	1390	;	0,68;
Flüssigwasserstoff mit Flüssigsauerstoff	780	;	1,22;
Magnesium mit Flüssigsauerstoff	840	;	0,25.

Die Standardwerte fur Oktan (Gasöl) mit Flüssigsauerstoff betrugen E_v = 1240 kcal/dm³; K = 1,00.

Thus we arrive at the result that, among the fuels in the second group only Be, B and liquid H_2 are superior to hydrocarbons. Be and B are immediately eliminated since, under the conditions possible in the tank, they are in the solid state, so that feeding them into the high pressure furnace of the rocket motor is impossible. If one should try to overcome this difficulty by using the material in the form of wire or powder, then the concentration in the tank would be decreased so much that the calculated small superiority would be lost. Use of fuel in the liquid state is eliminated because of the high melting point. So apparently liquid H_2 is the only material in the second group of fuels which can compete with hydrocarbons. Its 22% superiority is endangered by the fact that at the temperature of liquid H_2, condensation of the surrounding air will start on the metal tanks in the aircraft, so that the rate of evaporation of the H_2 will be increased and the aerodynamic forces will be affected, unless special precautions are taken. Nevertheless, liquid H_2, because of its easy procurement and also for reasons to be discussed later, may be considered as a most promising rocket fuel.

Since, with this exception, the light metals are only slightly (if at all) superior to hydrocarbons as fuel, a second possibility should be tested,- a combination of two e.g. in the form of metallic suspensions in mineral oils. Suspensions not only combine good feed characteristics (they are easily pumped) with high energy density (with consequent low requirements on tank volume and feeding speed); in many cases they have the amazing property that their heat content is greater than that of their individual components such as hydrocarbons and light metals. (30) Fig. 21 shows cycles for Al - O_2 and octane - O_2 at 100 atm. flame pressure. A comparison of these shows the interesting fact that the end temperature in the combustion of octane (3700° K) is about 830° lower than the boiling point of Al_2O_3. If one assumes that equal stöchiometric mixtures of octane -O_2 and Al -O_2 are burned together, that relaxion-free heat exchange takes place between all the molecules of both burning gases, and that finally the two burning masses do not interact appreciably chemically, then one sees from the two cycles that energy will flow from the higher temperature level of the Al_2O_3 to the colder octane. This will be heated at the expense of the heats of dissociation and vaporization of the aluminium combustion gas until the boiling point of Al_2O_3 (4530° K) is reached. After this process of temperature equalization has occurred, the useful heat content of the octane will have risen considerably, while the heat content of the Al gas will not have changed appreciably; i.e., the heat content and maximum exhaust speed of this 70% Al-octane suspension are larger than for Al or octane alone. The advantages of the combination are the following:

1. The temperature of the burning gases for the suspension has not taken on a value midway between those of the individual components, but rather the whole combusting mass has reached the boiling point of Al_2O_3. The requisite energy has been obtained at the expense of the otherwise unavailable energy of dissociation and vaporization of the Al_2O_3.

2. As a result of the temperature equalization between the two fuels in the suspension, the relatively slight dissociation of Al_2O_3 has been decreased, while that of the octane has increased markedly. Thus the average specific heat $c_p = Jo/T_0$ of the gas has increased, as one can see from the smaller slope of the expansion curve for the octane. Both these circumstances result in increased heat content $J = c_pT$.

One realizes, moreover, that the random example of a 70% suspension chosen here, which has equal parts by weight of Al - and octane - combustion gases, may not give the best results for c_{max}. The best Al - octane suspension will be one having enough Al to heat the entire mass to the boiling point of Al_2O_3. The upper heat values of the Al will be fully used in this case, since no metallic oxide vaporizes. The extra heat of vaporization and dissociation of Al_2O_3 are used to increase the heat content and dissociation of the octane. The best results are obtained for a 60.5% Al - octane suspension.

The considerations concerning the Al - octane suspension can be extended to the other light metals. Fig. 22 shows for Be, B, Li, Al and Mg suspensions with varying metal content, the chief

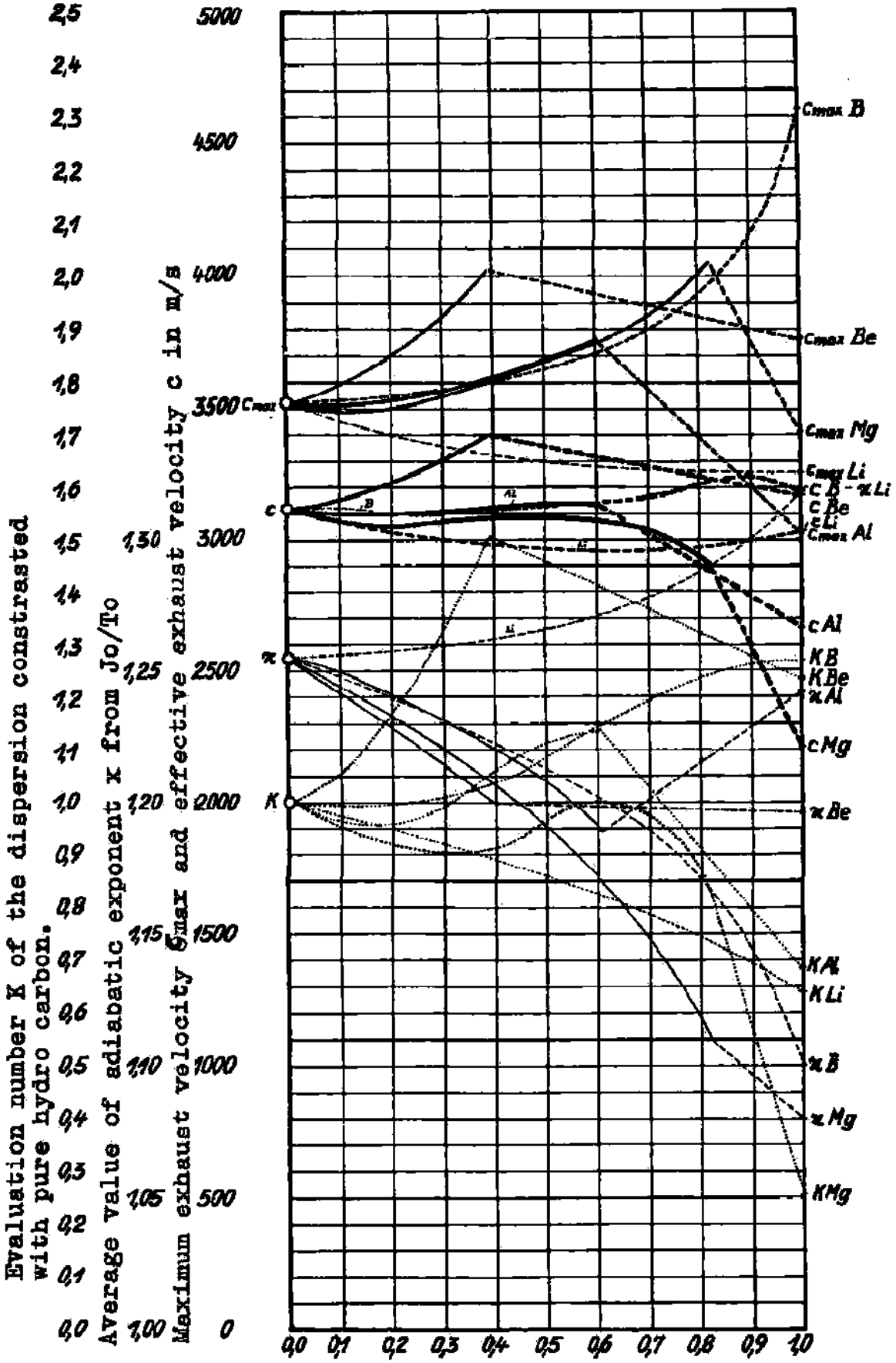

Figure 22; Properties of the metal oil dispersions against metal content at 100 atmos chamber pressure.

characteristics of the combustion at 100 atm furnace pressure: maximum exhaust speed, average adiabat exponent, effective exhaust speed in flight, and evaluation number K. From the graph we see that those fuels, like B and Li, the boiling point of whose oxide is below the end temperature of combustion of octane, do not show the characteristic effect of the dispersion. For them the curves of c_{max}, $\varkappa$, and c, show no maximum; i.e., the suspension is no more favorable than the better of its two components. For the remaining materials, Be, Al, and Mg, the characteristics at optimum composition are:

for Be - *hydrocarbon fuel with* 39% by weight *of metal* $c_{max} = 4100$ m/sec, $\varkappa = 1.20$; $c = 3400$ m/sec; $K = 1.51$; $E = 1557 \frac{kcal}{dm^3}$

for Al - hydrocarbon fuel with 60.5% by weight of metal $c_{max} = 3760$ m/sec; $\varkappa = 1.189$; $c = 3140$ m/sec; $K = 1.14$; $E = 1453 \frac{kcal}{dm^3}$

for Mg - hydrocarbon fuel with 80% by weight of metal $c_{max} = 3725$ m/sec; $\varkappa = 1.171$; $c = 3080$ m/sec; $K = 1.00$; $E = 1330 \frac{kcal}{dm^3}$

Summarizing we can say: Mg dispersed in hydrocarbon has no advantages over pure hydrocarbon. Al and Be show a wide range of suspensions in which they are superior to the pure hydrocarbon by up to 14% and 51% resp. Because they are easily obtained, Al - suspensions have special importance for military rocket-flight technique, while Be - suspensions come into consideration for special uses. All the studies were limited to stöchiometric proportions, so the possibility still exists that other mixture proportions may reach better values of K or c.

The preparation of 60% Al - gas oil suspensions, which are still usable after many weeks if left untouched, and which are easily fed through centrifugal pumps, was done in two ways on the basis of suggestions by H. Troitzsch and E. Husser:

1. Increasing the viscosity of the gasoil by dissolving various materials such as metallic salts of fatty acids, waxes, fats, rubber or various synthetics. Good results were obtained in tests with natural and synthetic rubber, and similar high-polymer hydrocarbons, the oppanols. The oppanols have the further advantage that, being pure hydrocarbons, they require no ballast materials, but burn completely with large heat output.

2. Decrease of particle size of the Al dust while hindering surface oxidation as much as possible, since with decreasing particle size, the sedimentation speed and, in most cases, the viscosity decreases. (?) For these large quantities of metal, pulverizing by using supersonics seemed impractical. So the powder was ground in ball-mills in a nitrogen atmosphere.

In connection with the use of liquid O_2 as a component of all the rocket fuels discussed so far, the problem of storing very large quantities of this material is important. Because its boiling point is - 183° C, it will be continuously boiling as a result of the steady flow of heat from its warmer surroundings, and will liberate the energy absorbed by vaporizing with a heat of vaporization of 51 kcal/kg, so that the residual material can maintain itself at this low temperature. This undesirable vaporization can be decreased by lowering the heat transfer from the surroundings, which occurs mainly through the tank walls which are wet by the liquid. A first method is the decrease of the wetted surface by putting all the material to be stored into a single tank of spherical shape. The heat flow through this smallest surface can be further decreased by the use of various standard heat-insulation procedures, of which heat-stopping materials like loose powder of magnesium carbonate, with a heat conductivity of $\lambda = 0.027$ kcal/mh°, have shown themselves effective, in the form of thick layers. In the existing temperature range of + 20°C to -183°C, 131 kcal per square meter of tank surface will go through a 1 meter thick insulating layer during a 24-hour period; this corresponds to O_2-vaporization at the rate of 2.57 kg per day per sq. meter of surface. With these figures, the daily loss by vaporization is shown in Fig. 23, for various containers up to a million ton capacity, for three thicknesses of the insulating layer 1m, 5m, and 10m, and taking account of the spatial heat flow through the thick walls.

The results of this calculation were confirmed in a trial installation of a liquid O_2 tank with 56 ton capacity and a magnesium carbonate insulating layer of average thickness 2.6m. This tank has been running at the aircraft-testing station at Trau since 1938; the manufacturer is the " Aktiengesellschaft für Industriegasverwertung Berlin - Britz". Although even this tank, (though small as measured by rocket-technical requirements) represents a brand-new development as compared to all previously constructed liquid O_2 containers, and no experience with tanks of such size existed, the tank worked satisfactorily from the first day it was used. Its vaporization is 140 kg/day, which is exactly the theoretically expected value, as can be seen by substituting the

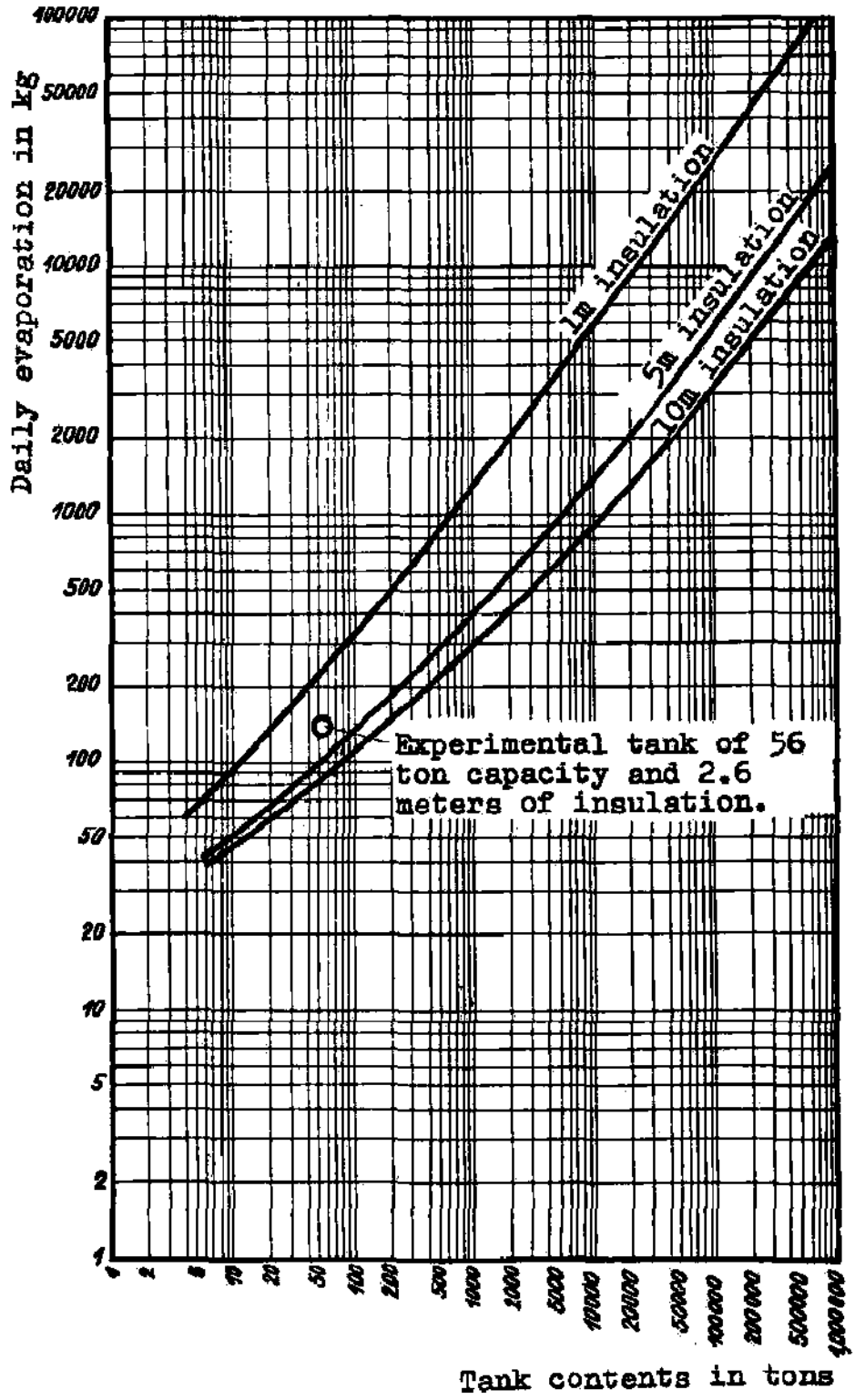

Figure 23; Daily evaporation loss from cylindrical large scale containers for liq. O_2 for various capacities and various thicknesses of inorganic insulating material.

tank-volume, insulation thickness, daily vaporization in Fig. 23. In the photograph, Fig. 24, can be seen the 8 m. high, 8m. diameter outside cover of the tank. Inside this steel cover hangs the actual container for the fluid; it is made of brass and has a capacity of 50 m^3 or 56 tons. The space between the two metal shells averages 2.6 m in width, and is loosely filled with finely powdered magnesium carbonate. The whole tank stands freely in a subterranean space, where it can be approached and examined from all sides. This room has a completely normal cellar climate; no noticeable drop in temperature can be observed. The outer steel cover of the tank is also at normal temperature; moisture in the air does not condense on it. The 140 kg. of O_2 vaporized each day are collected in flasks and are used for operation of the testing station and for welding.

Fig. 25 shows a schematic diagram of a large container for a million tons of liquid, which has a daily evaporation of 13,000 kg. for a 10 m. insulation thickness. This container, when once filled and left alone, will become empty only after 200 years. The amount evaporated daily can be used by simply filling steel flasks and transferring them to the consumer. The cylindrical inner container of Cu-alloy has a diameter of 103.5 meters. and, including the arched base, a height of 119 m. The bottom end is conceived of as a hanging floor which rests on a ring running along the boundary of the outer cylinder. This ring is supported on the ground by poorly conducting pillars placed at intervals. The top cover is hung on the outer steel cover at various points. The insulating layer of loose magnesium carbonate powder is around the inner container, and is 10 m. thick on the sides and cover, 15 m. thick below the floor. This insulating layer is bounded and supported by the steel cover which is rigid and strong. The whole thick-walled container stands on a cylindrical subterranean bunker of reinforced concrete.

The liquid O_2 comes in through the intake at the left and is led through the intake pipe to the floor of the container, in order to excite as little motion of the oxygen during filling as possible. At the top of the tank is the drain pipe for the vaporized gaseous O_2, by means of which normal atmospheric pressure is maintained above the liquid surface. The liquid is removed at the lowest point of the container. At the same level as this point, a pump system stands on the right at the edge of the bunker, and feeds the liquid to the outlet at the top edge of the bunker.

Further details and auxiliary equipment of the tank will not be mentioned here, but the behavior of the liquid O_2 in the large tank requires further consideration. In the liquid pool, which has a depth up to 117 meters, the hydrostatic pressure, as shown in Fig. 25, increases with the depth up to 13.1 atm. The boiling point of O_2 depends on the pressure, and increases with depth in the liquid from -183° C at 1 atm to -144° C at 14.1 atm. In spite of this, the entire contents of the tank will stay at -183° C, the temperature of the surface of the liquid. For if the masses of liquid down below should warm to higher temperatures than the upper layers, their density would decrease and a convection would occur which brings the warmer masses upward to the region of lower hydrostatic pressures, where as a result of the decreased pressure they will begin to boil, give off the heat of vaporization of the liberated gas, and cool to the temperature of their surroundings. Since this process holds for layers at any depth, the lowest temperature at the liquid surface will bring all the lower layers to the same temperature. Thus in practice one will actually find the liquid at the bottom of the tank to be at -183° C. Since the heating occurs mainly through the side walls, the movement of the fluid will be such that the heated boiling masses of liquid rise along the walls, while the cold masses sink in the middle of the tank so that the toroidal streaming shown in Fig. 25 develops.

Liquid O_2, whose combustion properties and storage have been discussed in detail here, need not give, in combination with the previously described fuels, the greatest exhaust speed. Therefore, two further notable candidates will be discussed briefly - fluorine and ozone (or ozone-enriched liquid O_2).

Fluorine would be used only for metallic fuels. The corresponding metal fluorides in some cases have higher heats of formation and lower heats of vaporization than the oxides, give the prospect of higher exhaust speeds, but are not considered further because of the technical difficulties in using liquid fluorine in place of liquid O_2. The use of pure ozone can be easily checked for the case of octane. Since ozone has available a disintegration energy of 710 $\frac{kcal}{kg}$, the heat-output of the mixture increases from 2587 $\frac{kcal}{kg}$ for O_2 to 3140 $\frac{kcal}{kg}$ for ozone, and the theoretical exhaust speed c_{th} = 4655 $m/_{sec}$ increases by 10% to 5120 $m/_{sec}$. The use of pure ozone increases the effective exhaust speed by this same order of magnitude.

To test the applicability of ozone to rockets, H. Schumacher in Frankfurt made tests on a small scale, with the following main results:

Both gaseous and liquid pure ozone are explosive under the working conditions in flight, and are thus not suitable. Gaseous ozone - O_2 mixtures at N.T.P. will react, in pipes or spherical chambers, starting at a 10% weight fraction of ozone, if the reaction is initiated by an

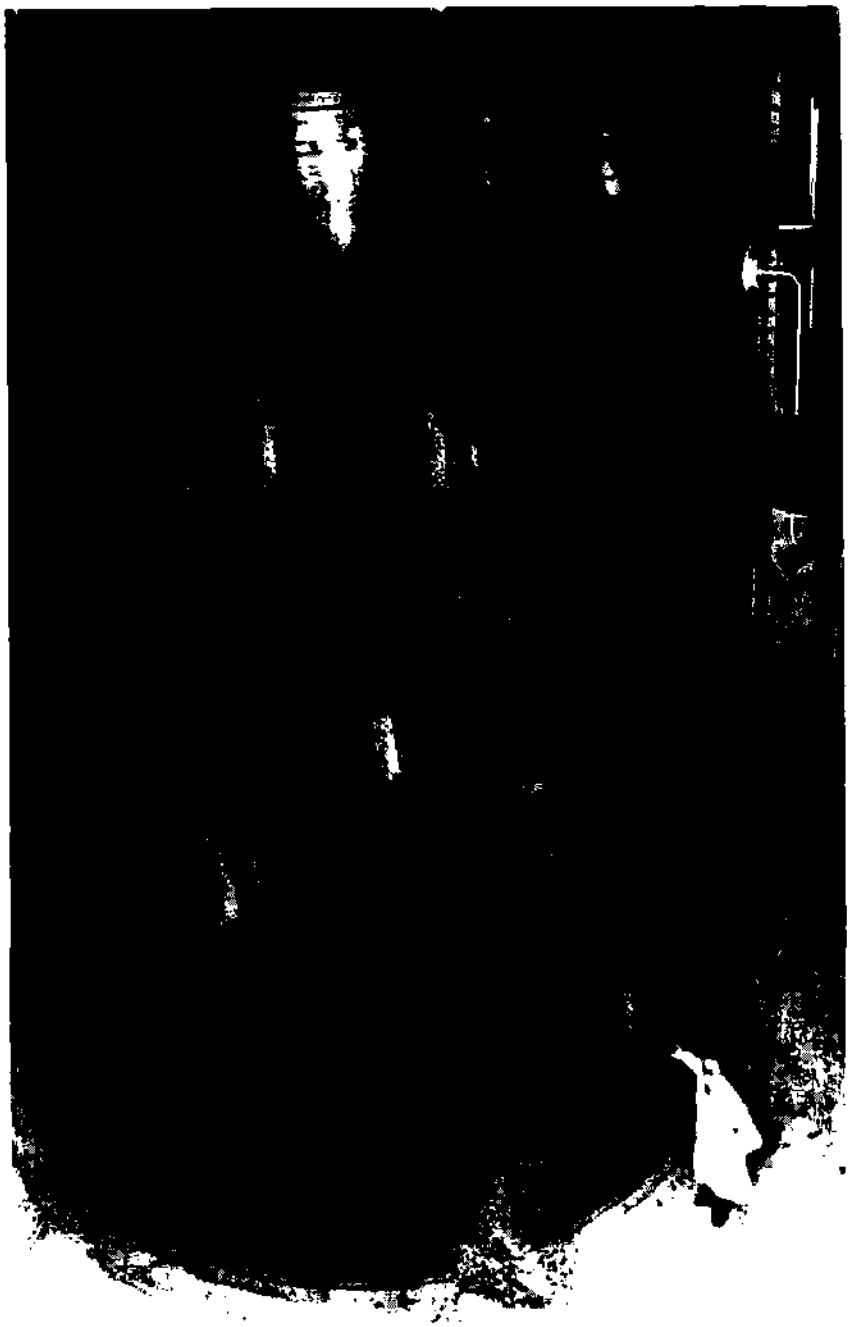

Figure 24; External view of liq. O_2 tank of 56 ton capacity, 2.6 m insulation thickness and 140 kg daily evaporation.

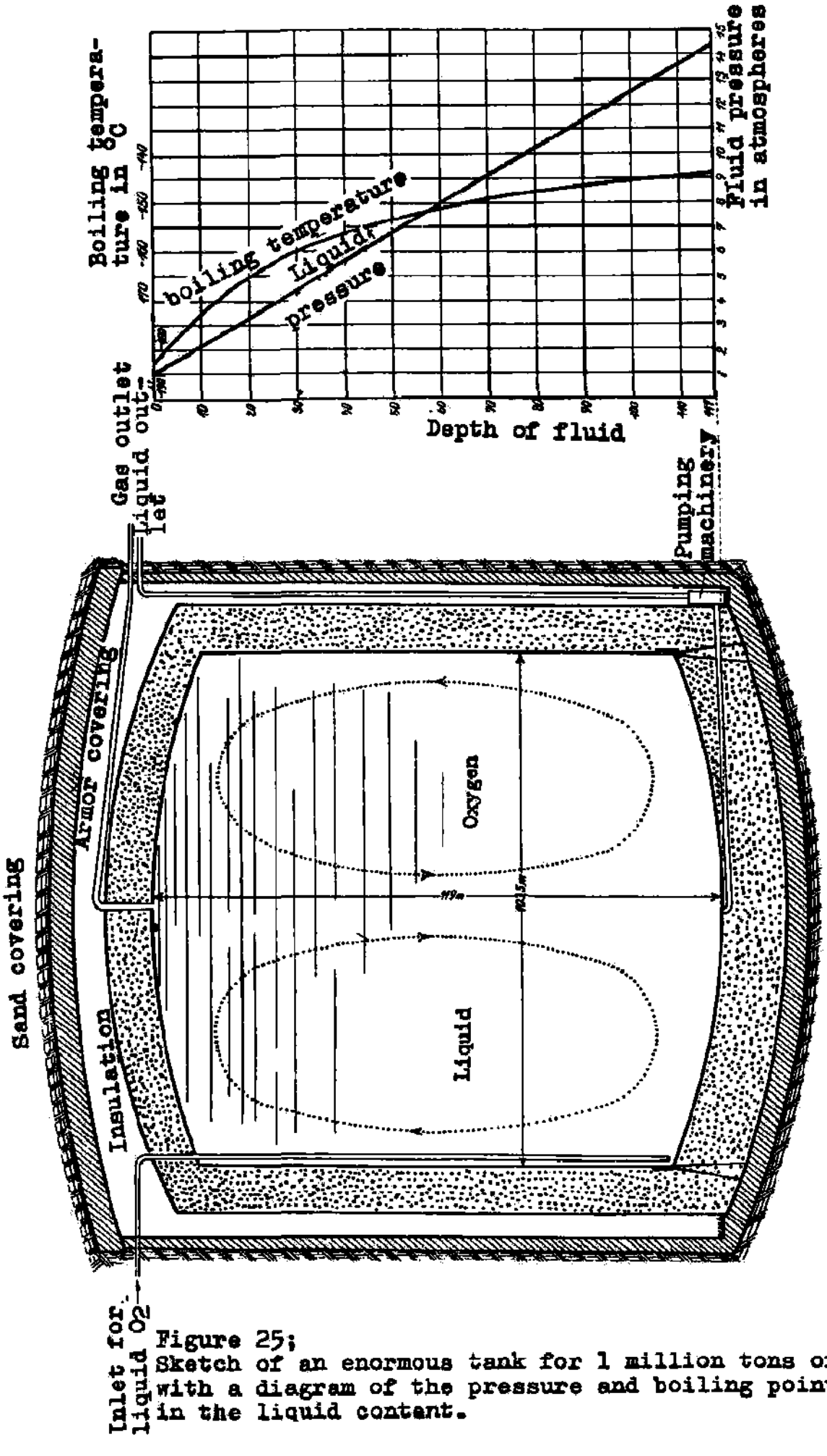

Figure 25;
Sketch of an enormous tank for 1 million tons of liq. O_2 with a diagram of the pressure and boiling point ratio in the liquid content.

incandescent body, but the reaction will not spread to all of the mass until the ozone concentration reaches 17% by weight. Even then the pressures developed in the reaction are so moderate that they might be expected to require motors and armatures.(?) The pressure increases are of the order of 2 atm. A luminosity starts only at ozone concentrations of 40-50% by weight, and the pressure increases reach 6-10 atm.

Liquid ozone-oxygen mixtures at atmospheric pressure and the corresponding boiling point seem to have, for weight % of ozone above 25%, a tendency to explode with great destructive effect, if gaseous ozone above them explodes with emission of light. The miscibility of liquid ozone with liquid O_2 and the boiling point of the mixture are sufficiently understood from the solubility diagram and vaporization curve at atmospheric pressure, that we assume the following regarding the storage of large quantities of the mixture in open containers:

Mixtures up to 25% by weight of ozone are stable, do not separate, and have a temperature of -183° C. Since such mixtures seem to be safe from explosion, they are of importance for technical use. Mixtures between 25 and 55 weight % of ozone are not stable; they split into a heavier, deep violet, ozone-enriched phase (>55% O_3), which sinks to the bottom, and a lighter, light blue, O_2 -enriched phase (>75% O_2), which floats above. The phase which sinks is probably explosive. Mixtures with more than 55% ozone by weight are again stable but in danger of exploding, so they are without immediate technical value.

For increased pressures the critical solubility temperature of -179.5 is quickly passed, and a miscibility gap no longer occurs. Liquid ozone-liquid oxygen mixtures which are stored for long periods become ozone-enriched because of the more rapid boiling off of O_2, so that the resultant explosive tendency of the tank contents must be counteracted by adding O_2. The gas phase above the liquid surface reaches the critical ozone concentration of 40-50 weight -% only for ozone concentrations >90% in the liquid phase, so that the products of vaporization of liquid ozone - O_2 mixtures of up to 25% ozone content are scarcely dangerous even for rapid vaporization on uncooled machine parts. Fig. 26 shows the behavior of liquid ozone-liquid O_2 solutions.

A few other oxidizing agents are mentioned in the first part of this book; two of them, H_2O_2 and HNO_3 have attained some practical value for certain rocket uses.

Aside from the three groups of non-self-acting rocket fuels : combustion of hydrocarbons with O_2 or ozone, burning of light metals in O_2 or fluorine, and the combination of the two groups in the form of light metal-hydrocarbon suspensions, a fourth group of self-acting fuels is possible, which use the heat liberated in formation of molecules from the substance in atomic form: atomic nitrogen (9) (11)

$$2N = N_2 + 6050\ kcal/kg \quad , \quad c_{th} = 7120\ m/sec$$

and atomic hydrogen

$$2H = H_2 + 51400\ kcal/kg\ (11,32), \quad c_{th} = 20,800\ m/sec$$

Since the life times of these unstable materials is very short (the life time of active hydrogen is given as at most 10 sec [9, page 253], research in this branch of rocket fuel development must first take the following lines: 1. Finding a basic method for prolonging the life of active nitrogen or hydrogen. 2. Determination of the dependence of lifetime on temperature and pressure, especially in the direction of very low temperature. 3. If necessary, development of a method for enriching liquid or solid material with the monatomic modification.

Though the difficulties of such research may be great, and the prospects of technically valuable results are small, it should be noted that, because of the 10-20 times greater energy concentration of H as compared to presently available fuels, the more favorable specific heat, the higher α values - i.e., greater jet efficiency, the higher reaction velocity - i.e., greater furnace efficiency for smaller furnace volume, and the highly diathermic behavior - i.e., slight thermal stress on the furnace walls; even partial successes, say a 10% enrichment of H in H_2 by perhaps dissolving gaseous H in liquid H_2, would be of extraordinary technical importance. For the limiting case of 100% N or H concentration as starting fuel for combustion, the following characteristic quantities were calculated for a furnace pressure of 100 atm:

$$N_2: \ T_e = 8260° \ ; \alpha = 1.49; \ \sqrt{\eta_D} = 0.97; \ c = 4690\ m/sec$$

$$H_2: \ T_e = 5500° \ ; \alpha = 1.49; \ \sqrt{\eta_D} = 0.97; \ c = 14100\ m/sec$$

For atomic hydrogen these values are plotted in Fig. 27 for various flame pressures. This diagram shows clearly the extraordinary properties of active hydrogen; i.e., that the probability of regaining large portions of the dissociation energy by after-burning in the jet is very large.

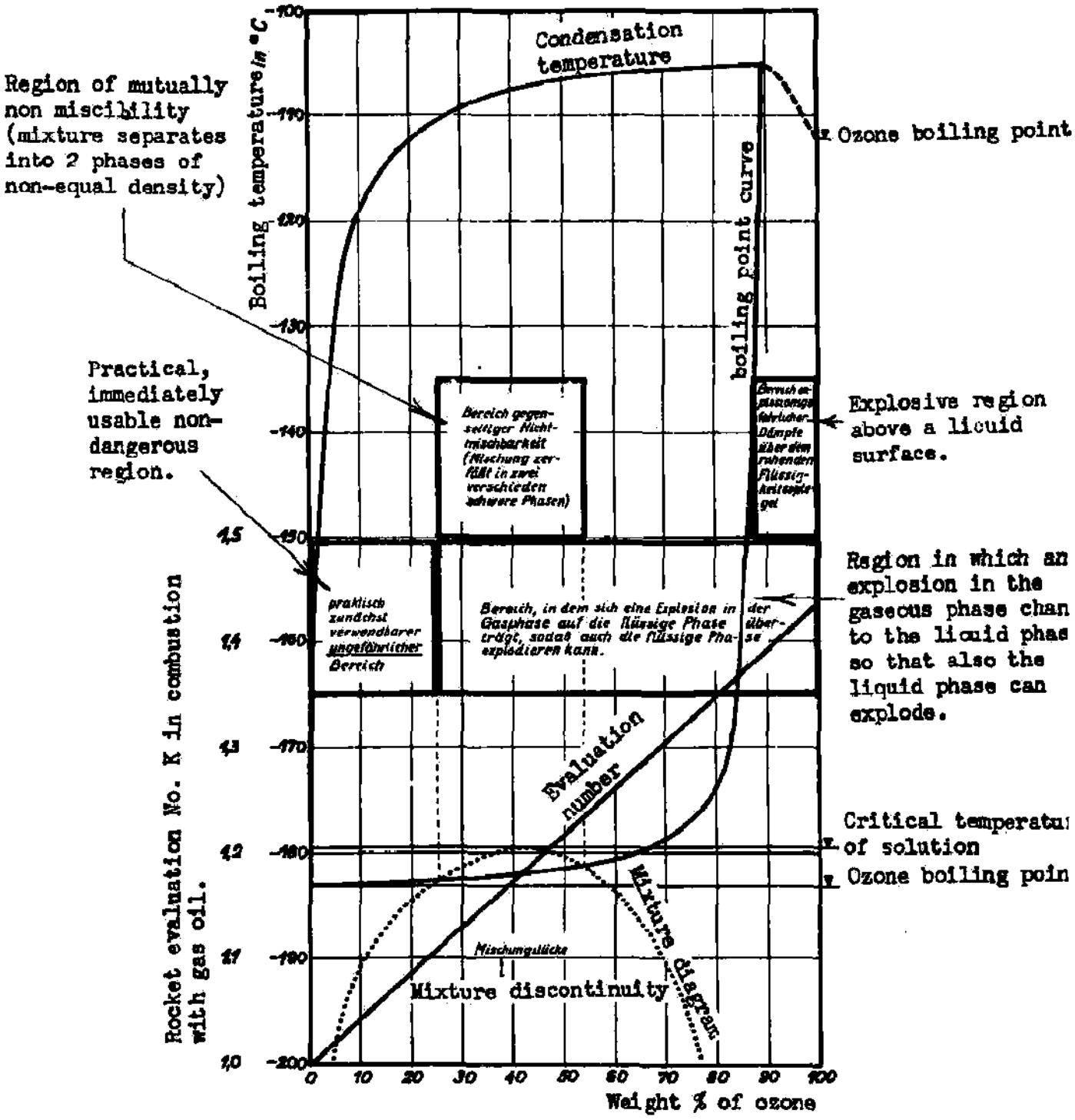

Fig. 26: Behavior of mixture of liquid ozone and liquid oxygen at 760 mm pressure according to Schumacher-Frankfurt.

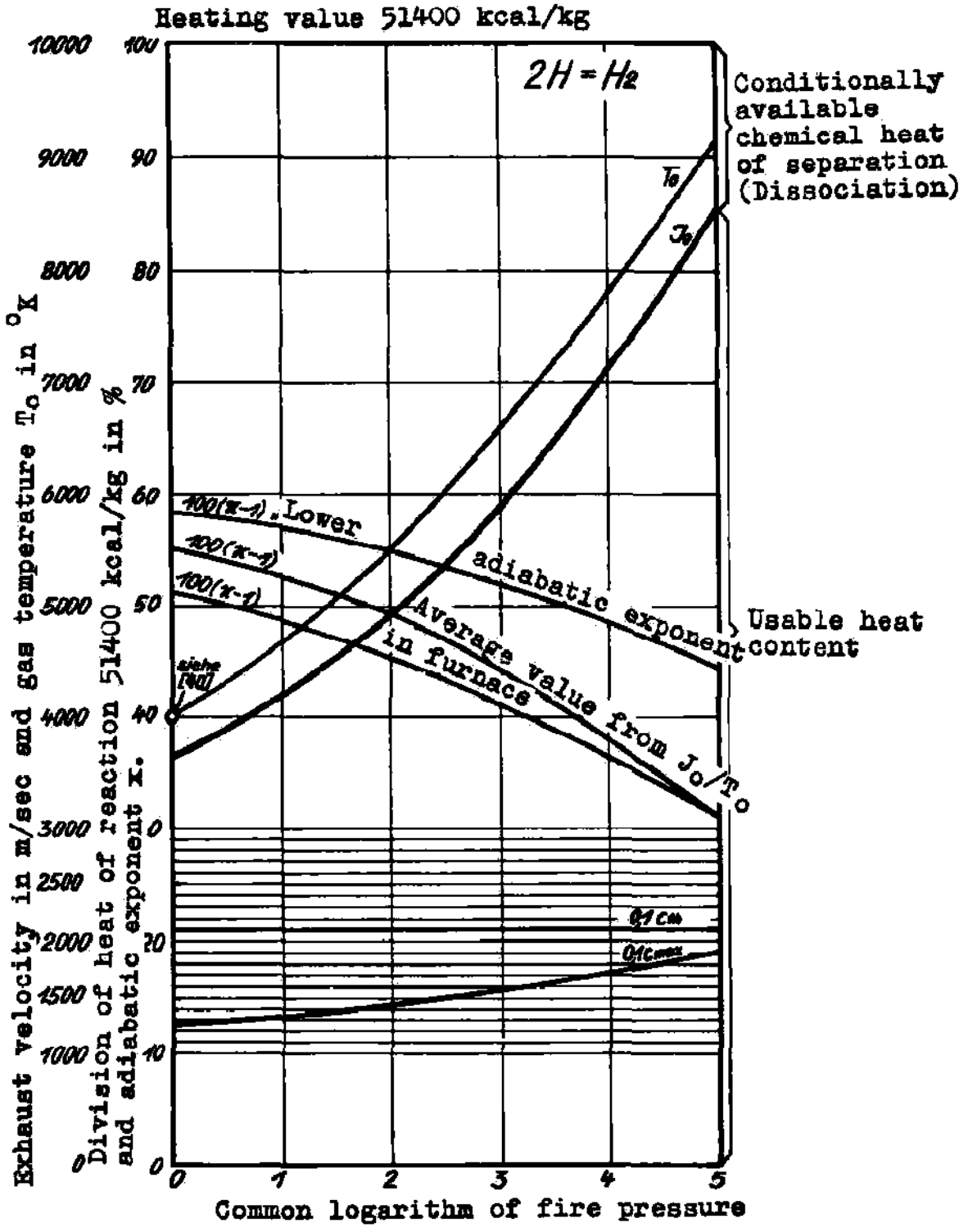

Figure 27; Dissociation, heat content, combustion temperature, theoretical and maximum exhaust velocity and adiabatic exponents for fire gases in the case of association of active H_2 to molecular H_2 with static equilibrium.

Finally another group of fuels is worthy of note: These fuels based on nuclear reactions can result in exhaust speeds of 10^6-10^8 $m/_{sec}$, and have recently, because of the reactions in uranium fission, moved into the domain of technical interest. (3).

Summarizing the numerical results of this section concerning the problem of exhaust speeds, we may say that by means of stöchiometric combustion of hydrocarbons in O_2 in rocket motors at 100 atm. furnace pressure, exhaust speeds above $c = 3100$ $m/_{sec}$ are possible. For excess fuel, 5% higher values are obtained. By enriching the O_2 with ozone, a further increase of exhaust speed to $c = 3400$ $m/_{sec}$ may be possible with stochiometric mixtures. The use of Al - hydrocarbon suspensions with liquid O_2 gives similar exhaust speeds, but more favorable proportions by weight on the aircraft, because of the higher fuel density. We may expect exhaust speeds, of rocket motors in flight, over 3800 $m/_{sec}$ for liquid H_2 with liquid O_2, and over 4000 $m/_{sec}$ if ozone is included, while the addition of atomic hydrogen would give even higher values. For calculations of flight - and military performance of the rocket bomber we shall use the values $c = 3000$ $m/_{sec}$ and $c = 4000$ $m/_{sec}$. To see the effects of higher exhaust speeds we shall calculate with $c = 5000$ $m/_{sec}$ for comparison.

3. Properties of the Air-Frame

The external appearance of the rocket bomber is shown in Figs. 28-31 and discussed theoretically in the next section. The bow of the aircraft's fuselage consists of an "ogival" with 9.6 caliber radius of curvature, which is cut by a plane through its long axis so that a flat underside results for the fuselage. Between the wings the semi-ogive goes over into a roomy chamber with perpendicular side walls, while the fuselage gradually tapers toward the stern with a steady decrease in cross-section. The large blunt end surface at the stern of the fuselage is necessitated by the size of the mouth of the jet of the rocket motor. The relatively small wing stumps serve mainly for stabilization in flight, and for landing; the wing cross-section is the well-known triangular wedge profile with a maximum thickness of 1/20 of the depth at 2/3 of the wing depth. (18, p. 170). To this peculiar aircraft shape there correspond the laws of flow for very high Mach numbers. An angle of incidence between fuselage and wings is unnecessary, so that for the low-wing arrangement chosen, the lifting flat surfaces of the fuselage and wings go over into each other without a break, as can be seen most clearly in Fig. 31. For the tail surfaces, a symmetrical quadrangular cross-section was chosen, which also has a greatest thickness of 1/20 of its depth in the last third of its depth. The whole arrangement of the tail surfaces is independent of the streaming from the rocket jet, since use of the rocket motor and flight below sound velocity never occur together.

The size of the rocket bomber was chosen as a compromise between a series of contradictory requirements. The idea of making the aircraft as large as possible is suggested by the fact that then the ratio of additional load to weight when empty is generally more favorable, that the construction of larger rocket motors is simpler, that with increased size of aircraft the military strength of a rocket bomber group increases while the number of capable pilots required per unit of load transported decreases. If one computes a few comparison designs in the range of 10-100 tons starting-weight, one finds that with increasing weight of the aircraft, the aerodynamical lifting power contributed by the fuselage represents (for geometrical reasons) a smaller part of the total weight, so that the wings have to be relatively larger; finally the weight of the wings predominates, without giving any noticeable improvement in gliding angle in the region of high Mach numbers. Such considerations lead to an apparently favorable takeoff weight of 100 tons, to which corresponds an empty-weight on landing of 10 tons. Thus a limit of 90 tons of fuel with about 76 m^3 tank space must be included, which leads to the fuselage dimensions shown in Fig. 28.

The wing dimensions are determined by the permissible wing loading of the bomber. The starting procedure by rocket catapult, which has already been described briefly, permits practically high wing-loading; thus even though before landing the consumption of all fuel and removal of all ballast reduces the weight to 1/10 the takeoff weight, the landing speed determines the wing size. Though landing speeds of over 200 km/hr can be used in special cases, a permissible limit of 150 km/hr was first chosen because the landing of the rocket bomber is to be considered a glide-landing, and because one cannot count on the availability of experienced test pilots. The corresponding stagnation pressure is $q = 110$ kg/m^2. From Fig. 34, the very thin and slightly curved wing profile leads one to expect a maximum lift coefficient of only $C_{a\ max} = 1.25$ even with landing aids, so that the wing-loading before landing is limited to $q\ C_{a\ max} = 137.5$ kg/m^2. Aside from this figure, the wing size is determined by the fact that the fuselage plays an important role in the lifting power of the whole aircraft. According to the investigations of the next section, for large Mach numbers 2/3 of the total weight is carried by the fuselage, and 1/3 by the wings. At landing speed, the lift coefficient of the fuselage, at the angle of attack for maximum lift, is $C_a = 0.45$; with the already fixed fuselage supporting surface $F_r = 80.8$ m^2 the total lifting power is $F_r \cdot C_a \cdot q = 4000$ kg, while the residual landing weight of 6000 kg goes

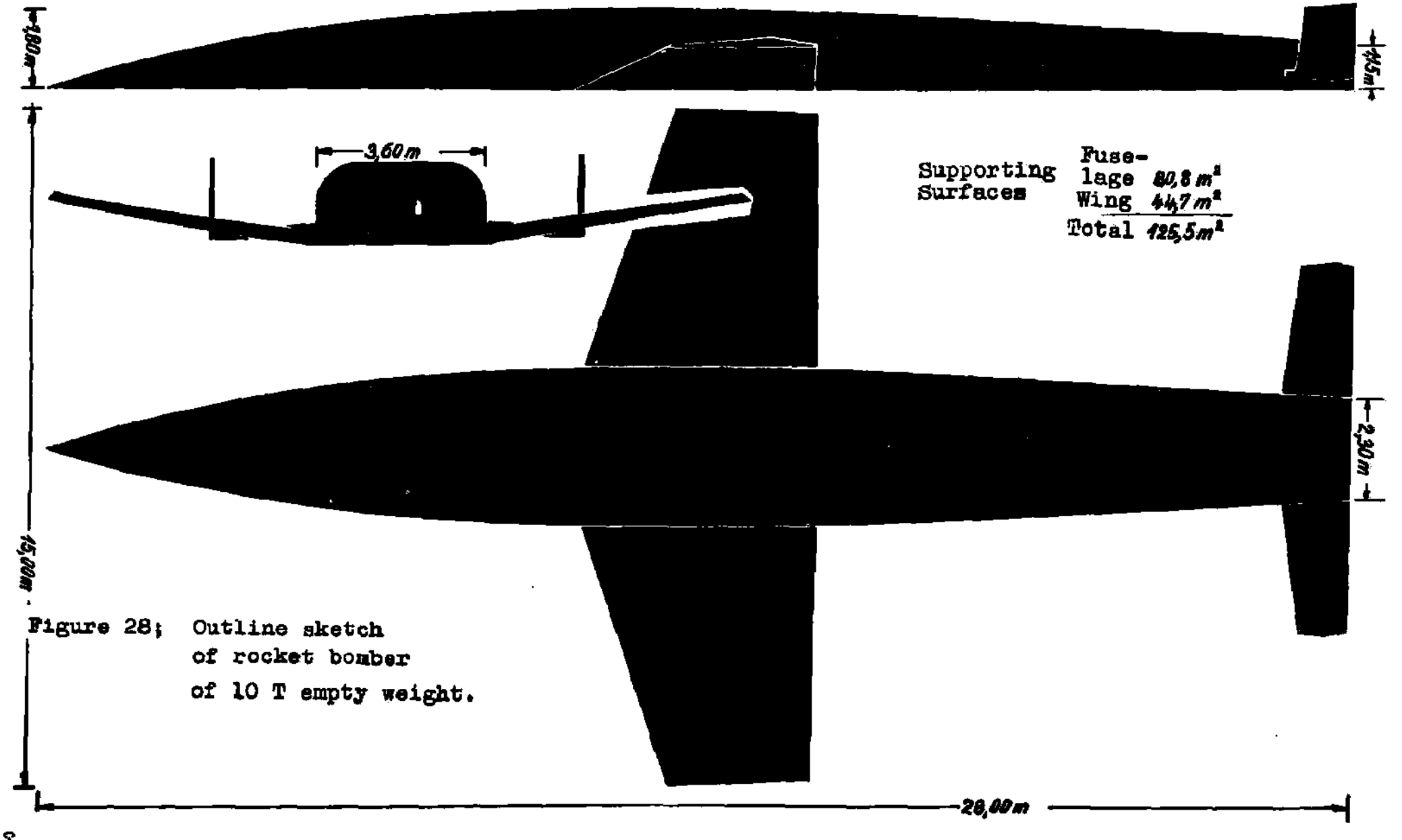

Figure 28; Outline sketch of rocket bomber of 10 T empty weight.

Fig. 29: Top view of rocket bomber of 10 ton empty weight.

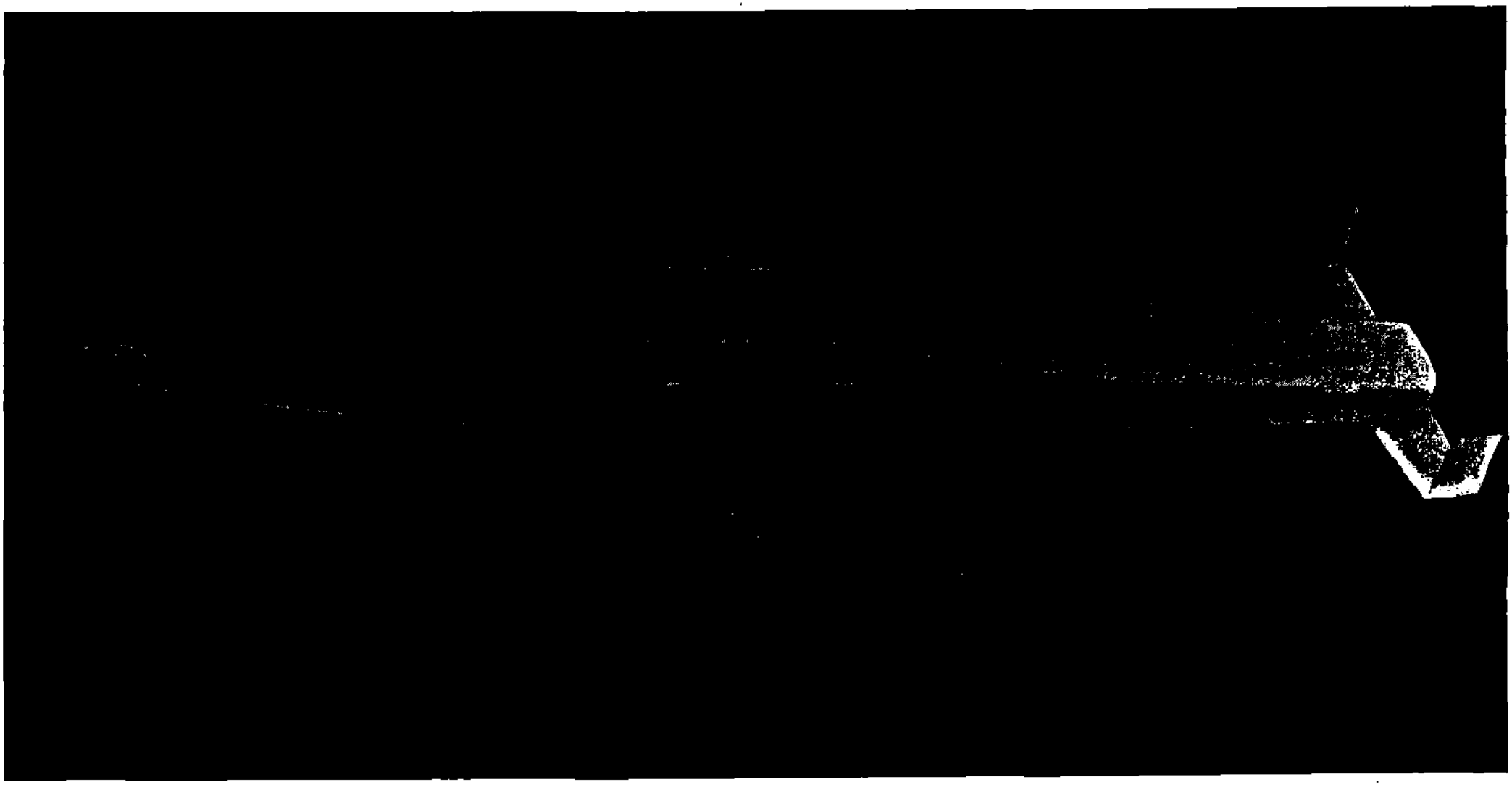

Fig. 30: Outer form of Rocket Bomber of 10 tons empty weight, perspective view from front-above.

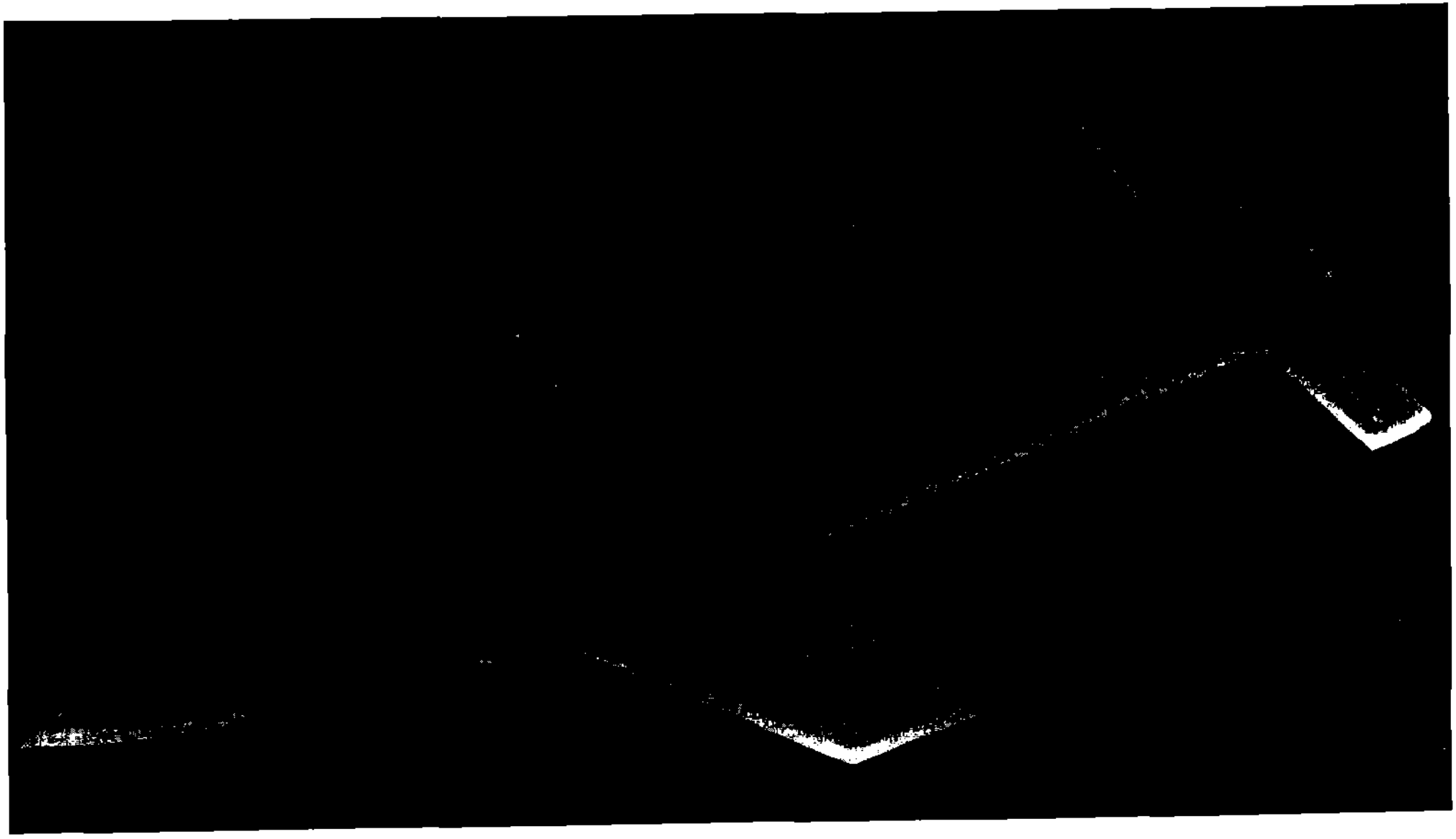

Fig. 31: Perspective view from "backwards below" of 10 ton empty weight Rocket bomber.

to the wings. Thus the required wing size is about 44 m^2; according to Fig. 28, the total supporting surface is 125.5 m^2; the mean wing-loading is 10,000/125.5 = 79.7 kg/m^2 and the lift coefficient for landing is $C_a = A/qF = 0.74$, in agreement with Fig. 34.

At take off, the mean wing-loading is ten times as high, i.e., 797 kg/m^2; for the assumed climbing speed of 500 $m/_{sec}$ the stagnation pressure at takeoff is 15930 kg/m^2 and the total lift coefficient C_a is 0.05, corresponding to an angle of attack $\alpha = 3°$, while the lift coefficient at optimum gliding angle is $C_a = 0.173$ for $v/_a = 1.5$. At a 3° angle of attack, 38% of the total weight of 10^5 kg falls on the fuselage, and 62% on the wings; the wing loading is thus 1390 kg/m^2. After the aircraft rises to the optimum angle of attack of 8°, C_a becomes 0.173; thus the lift for hauling the craft at $V/_a = 1.5$ is 346000 kg, of which 48% rests on the wings with $C_aF = 0.083$, corresponding to a wing loading of 3720 kg/m^2 in this state of flight which determines the wing stress.

Other cases of loading are important for various parts of the rocket bomber; e.g., for the fuel tanks it is the acceleration at takeoff; for fuselage and pilot it is the acceleration at the end of the climb; for fuselage and landing gear it is the landing which is important.

In estimating the ratio of empty-weight G, after consumption of all fuel and dropping of the useful load, to the flight weight G_o immediately after rising from the ground, we started from the known weight distribution for overloaded long range aircraft: airframe 18%, power plant 13%, auxiliaries 3%, additional load 66%, so $G/G_o = 0.34$. The main parts of the rocket bomber were estimated as: cabin - 500 kg, rocket motor - 2500 kg, wings - 2500 kg, a total of 56 kg/m^2; fuselage 3250 kg, tail, landing gear, bomb-bay, etc., altogether 1250 kg; thus the total weight of the aircraft is 7000 kg, whereas flight weights for ordinary bombers of similar size are about 3000 kg. The reason that the rocket bomber with its 10 times greater takeoff weight is only 2.3 times as heavy as an ordinary bomber of the same size is mainly because the supporting surfaces, especially the wings, carry not 10 times but only 3-4 times the weight, while the remainder is directly supported by the air without any intermediary structure; moreover because of the definite way of starting and climbing the factor of safety for the rocket bomber need be only a small fraction of that for an ordinary bomber. Thus the total weight distribution f the rocket bomber is airframe 7%, power plant 2.5%, auxiliaries 0.5%, additional load 90%, so $G/G_o = 0.1$. All these considerations are valid for scaled-up weights. One thus obtains directly the correct performance figures, if the bomb load is diminished by the excess weight, above 10 tons, of the aircraft.

Figs. 32 and 33 show an overall schematic of the rocket bomber.

The front view of the craft does not show the retractable front wheel, which operates in conjunction with a retractable tail skid and the landing gear which is retractable into the fuselage between the wings. The front wheel serves to prevent dangerous contact with the ground of the bow end during the bouncing motion of the aircraft during landing, and to slow down (with the aid of the landing gear) as quickly as possible the aircraft which comes on to the ground at 150 km/hr and has practically no wind resistance then because of the small wings. Behind the bow is the pressure-tight cabin, in which the single pilot sits. It is tight for inside pressures of 0.4-0.5 atm. with vacuum outside, and should permit rapid exit of the pilot in case of danger (e.g. after takeoff). Because of the smooth external shape, visibility from the cabin is very poor. In free flight at high velocity, side view slits and optical aids are sufficient. For landing a kind of detachable windshield can be used, since than the pressurization of the cabin and maintenance of the bullet-shape are unimportant. A further essential arrangement for the cabin is that the pilot's seat be so arranged that the pilot can take up the high accelerations along the aircraft axis in the best possible position, so that not only body and head, but also feet and arms have good supporting surfaces, and at the same position can be shifted. The remaining equipment of the pilot's cabin - instruments, D/F and radio equipment, ventilation, etc. is not considered further. At the back of the pressurized cabin are the tank installations, which consist of two large tubes 20.5 m. long and with maximum diameter 1.8 m; these constitute the main part of the fuselage. The upper fourth of the tubes' circumference forms the skin of the aircraft, while the lower half and the space between the tubes is covered so that the required shape is obtained. For constructional reasons the tank tubes are subdivided into the actual containers by means of cross-walls. The purpose of the cross-walls is first to have separate containers of correct capacity one behind the other for fuel and liquid O_2 and that each fuel shall lie symmetrically with respect to the axis of the aircraft, so that thermal stresses and twists are not developed due to asymmetries; second, as a result of the subdivision, to lower the liquid pressure on the rear end of the tank during acceleration and to prevent the aircraft from becoming tail-heavy as the tanks are emptied; finally the cross walls give the thin-walled fuselage the stiffness necessary for taking up the torques at the roots of the wing-spars. It is advisable to put the oxygen tanks in the front end of the fuselage so that the force driving the O_2 to the

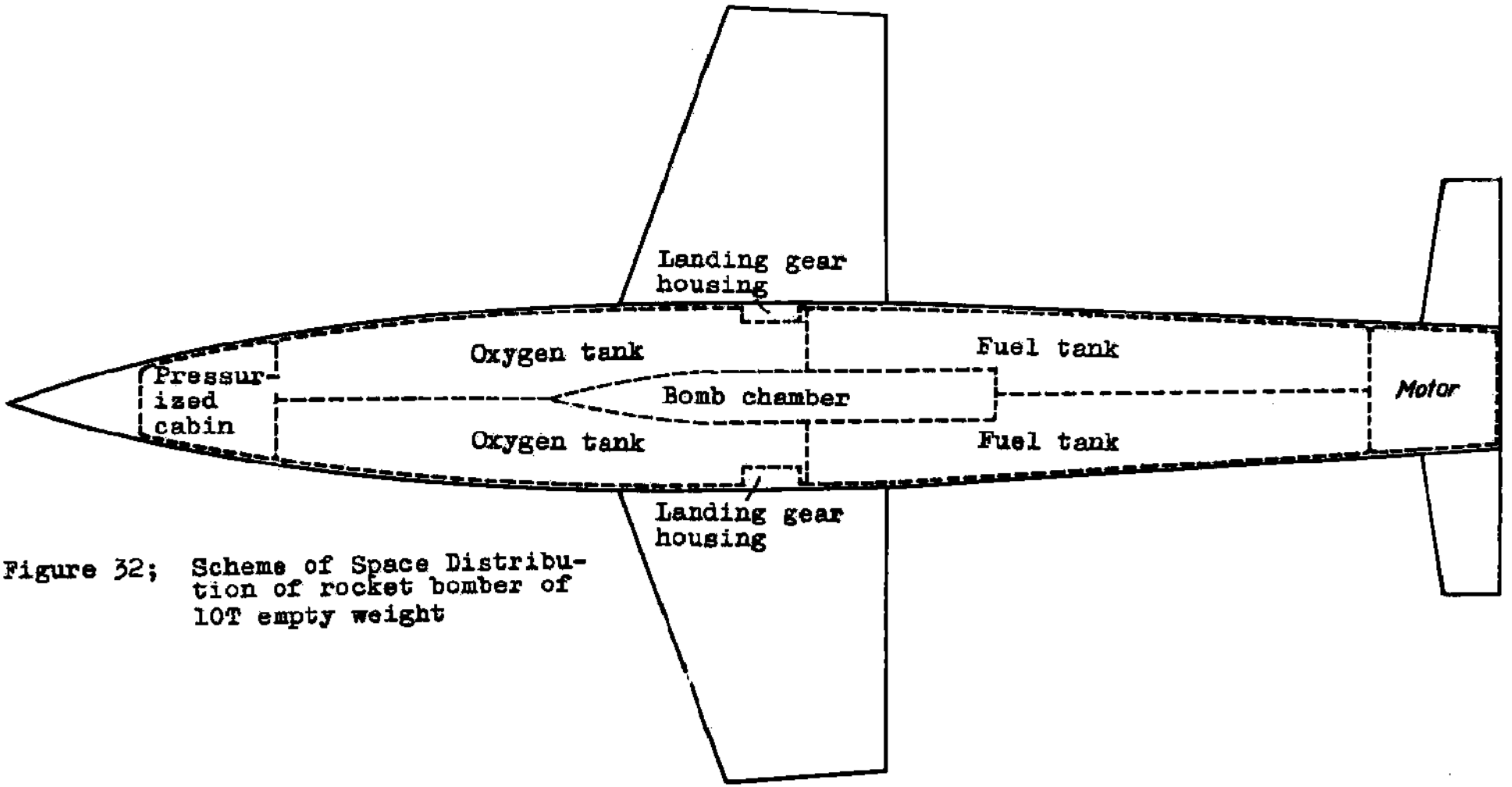

Figure 32; Scheme of Space Distribution of rocket bomber of 10T empty weight

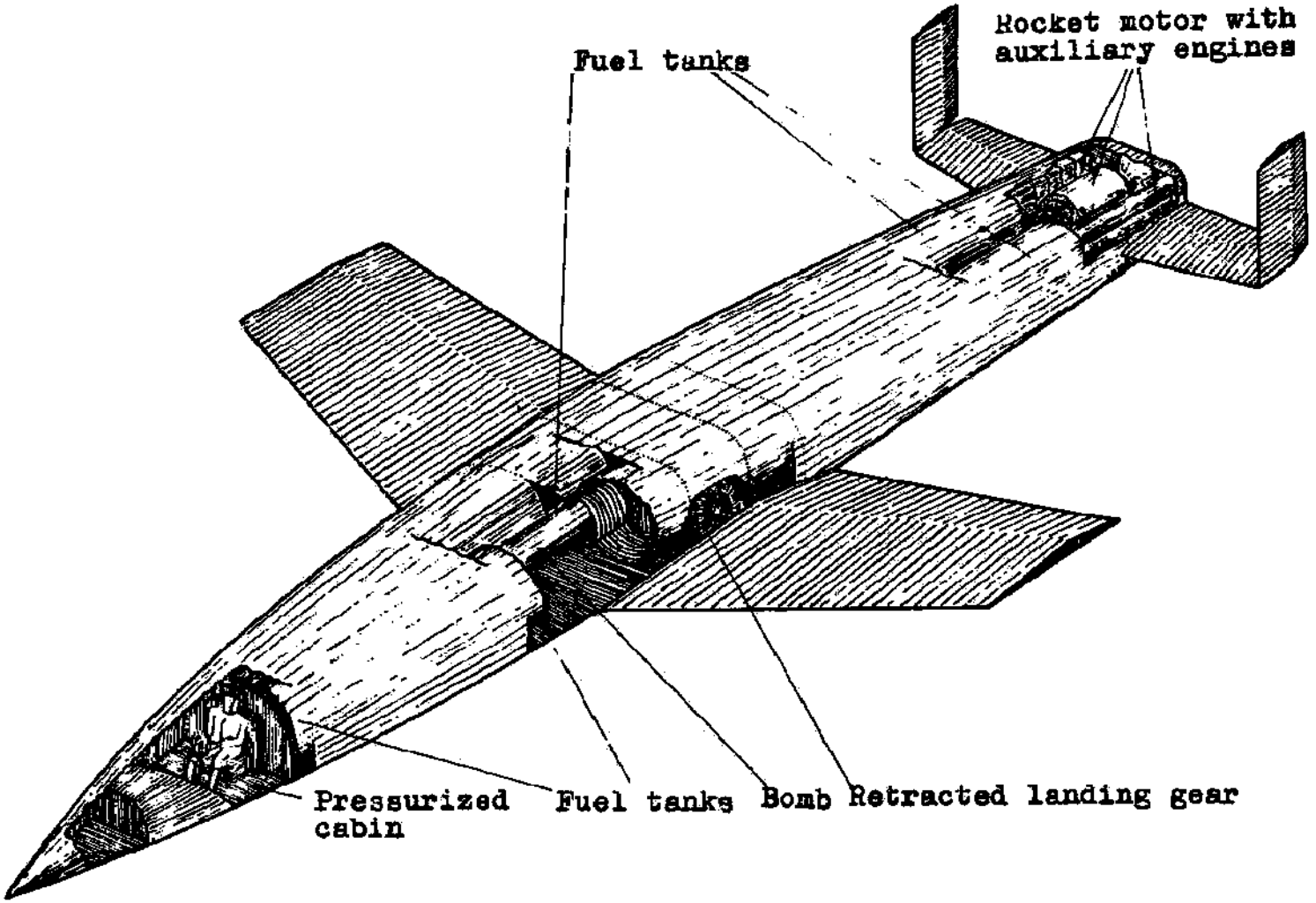

Figure 33; Total view of 10 ton Rocker Bomber

pumps will be as large as possible. Between the wings and the tanks is the bomb bay, suitable for projectiles up to 30 tons in weight. When the bombs are released, the floor of the bomb bay must be opened completely for a short time so that the axis of the bomb is parallel to that of the aircraft, since in the perpendicular position premature detonation may occur. Just before the main spar meets the fuselage there are chambers for the extendable landing wheels; these chambers are partly on the vertical sidewalls of the fuselage and partly recessed into the tank cylinders.

Finally, Fig. 33 shows the rocket motor at the end of the fuselage.

4. The Glide-Number of the Air-Frame

During its flight the rocket bomber goes through velocity ranges with entirely different flow characteristics, e.g., the ordinary subsonic range, the supersonic range up to three times the velocity of sound, the domain of large Mach numbers V/a, in which Newton's law of air resistance is valid - i.e., the aerodynamic forces vary with the square of the velocity and the angle of attack; and finally the range of gas-kinetic streaming with very long free paths of the air molecules and thus special laws of air resistance which are still similar to Newton's.

In all these regions the aircraft must have sufficient stability characteristics, whereas the glide-angle is important chiefly in the Newtonian region for both density types, for if the rocket bomber at the beginning of its glide had Mach number 30, then 99% of its kinetic energy, would be consumed in the Newtonian region, and only 1% below a Mach number of 3.

In the region of higher densities the glide angle can be estimated at only a few special points on the Mach scale, say $V/_a = 0.1$; 1.5; 3 and ∞, whereas for rarefied air closed gas-kinetic formulae can be given.

For a landing speed of 150 km/hr, i.e., $V/_a = 0.12$, polars of the bomber and the wings were determined by wind tunnel tests on a 1:20 scale model; the results are shown in Fig. 34. The best reciprocal glide number is $1/\varepsilon = 7.75$ for angle of attack $\alpha = 5°$; the best lift coefficient is $C_{a\ max} = 0.575$ for $\alpha = 16.5°$.

For $V/_a$ between 1 and 3 the difference in pressure compared to the pressure of still air is, for two-dimensional flow at small angles of attack,

$$\Delta p/q = \pm 2\alpha/\sqrt{V^2/a^2 - 1},$$

according to Ackeret and Busemann; for spatial flow around the rotation-symmetric end of a cone

$$\Delta p/q = 2\alpha^2 \ln[(2 \operatorname{tg} \operatorname{arc\,sin} 1/M)/\alpha]$$

according to Busemann and V. Kármán, and the tangential friction stresses are $\tau/_q = 0.072 \left(\frac{1}{Re}\right)^{0.2}$ according to V. Kármán. With the aid of these relations the values given in Fig. 35 and 36, for polars of the wings, fuselage and complete frame of the rocket bomber at $V/_a = 1.5$ and 3, can be computed. From the Figs. we read off the best reciprocal glide number $1/\varepsilon = 3.94$ for $V/_a = 1.5$ and $\alpha \triangleq 8°$ and $1/\varepsilon = 3.83$ for $V/_a = 3$ and $\alpha \triangleq 7°$. Wind tunnel measurements of the polars, which are feasible in this domain, could not be carried out. In the calculation a total vacuum was assumed behind the stubby stern-surfaces. Actually these surfaces, in this velocity range where the motor is off and they are not in contact with the flame, can be acted on by oticeable pressures which make the wind resistance appear to be less than when the motor is going; this must also be noted for wind-tunnel measurements.

For $V/_a \to \infty$ the thermal velocities of the air molecules and the pressure of the undisturbed air are respectively negligible compared to the flight speed and the dynamic pressure on the surfaces struck by the air stream. The part of this normal pressure p_1 which arises from molecules bouncing into the wall can be taken directly from Newton's law for inelastic collisions: $p_1/q = 2\sin^2\alpha$ Whether there is a further contribution to the pressure depends on how these molecules leave the surface. For dense air this must take place along the surface of the plate. If the wall were flat and the density of the gas layer which streams away were infinite, then the air molecules coming off would receive no acceleration perpendicular to the plate and there would be no further pressure contribution. According to V. Karman the ratio of density increase $\Delta\rho$ to density ρ before collision is $\Delta\rho/\rho = 2/(\varkappa - 1)$ when the corresponding air pressure ratio is $\Delta p/p = \infty$; so this case can occur only for $\varkappa = 1$. For $\varkappa = 1.4$, $\Delta\rho/\rho = 5$, the air density at the plate is 6 times as large as for still air, the layer has a finite thickness, the angle of impact of the air is greater than the angle of attack, and the air pressure p is greater than p'; according to Busemann $p/q = (\varkappa + 1)\sin^2\alpha$. As far as the value of $\varkappa$ is concerned, the molecular collisions in the flow of the condensations are sufficient in number to fully excite all molecular rotations; i.e., $\varkappa = 1.4$. If the high stagnation temperatures necessary for

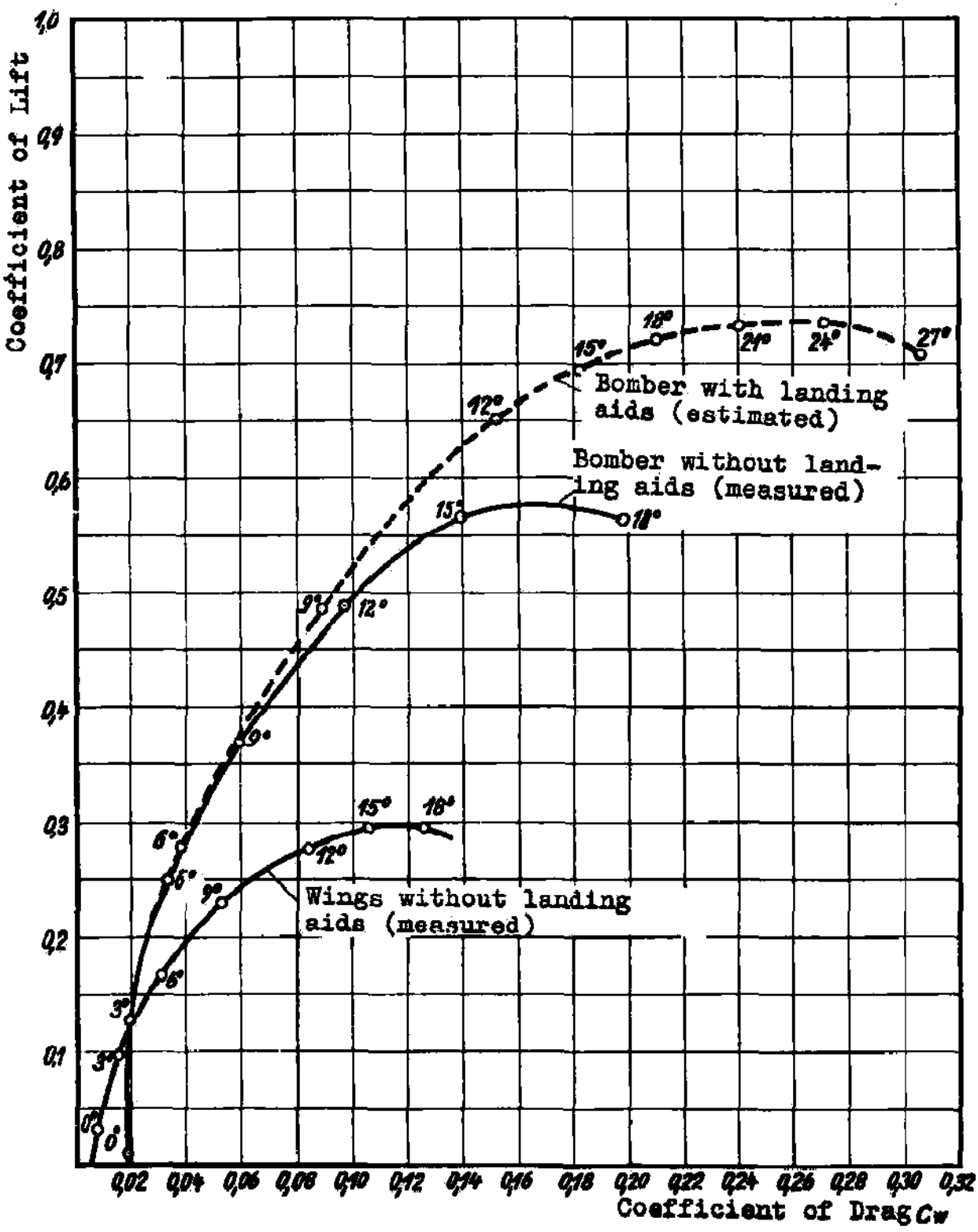

Figure 34; Wind tunnel measurements at Reynolds' Number 4×10^6 and Mach number corresponding to the landing speed. (The aerodynamic coefficients are based on the area of the supporting surfaces.)

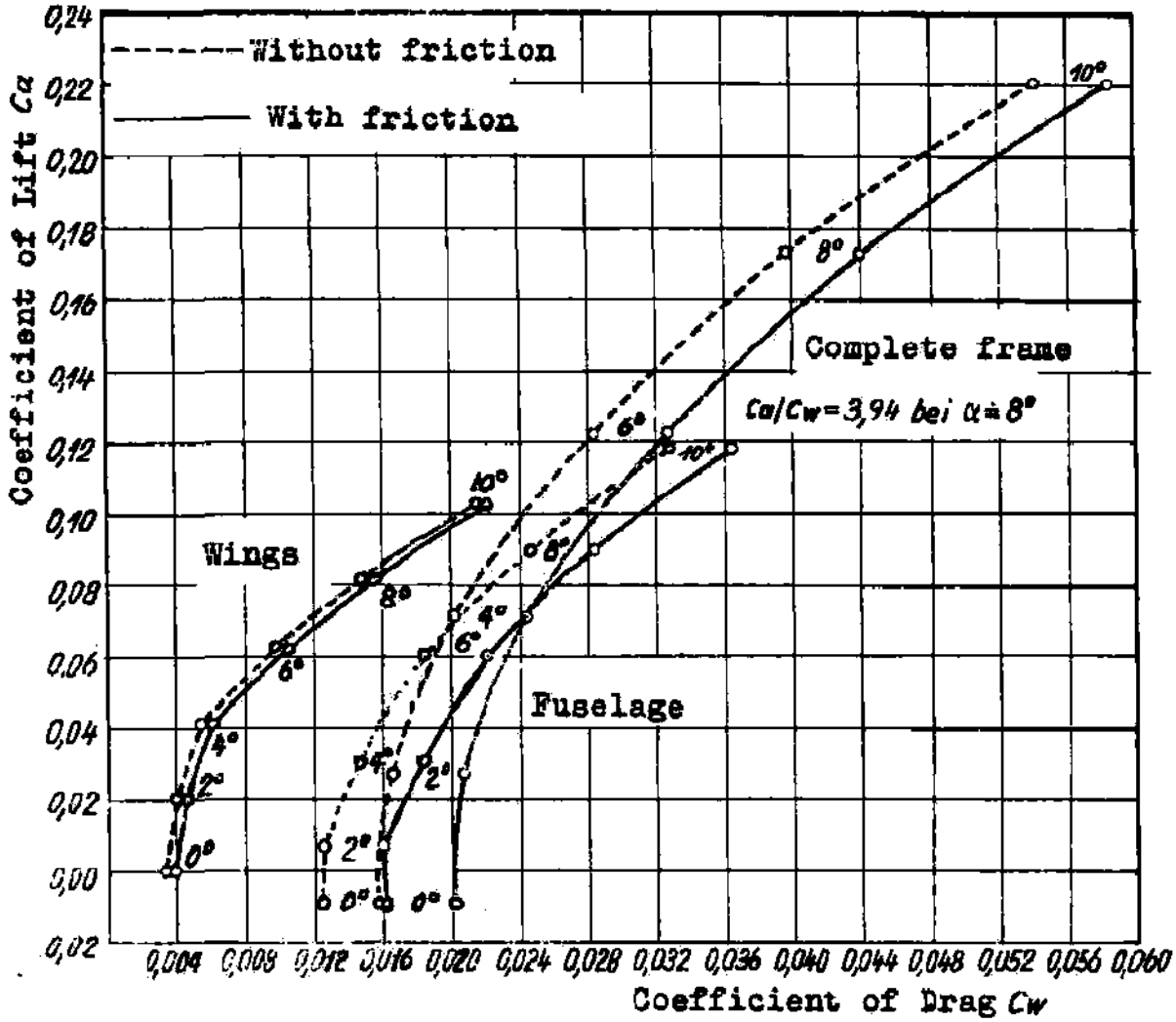

Figure 35; Calculated polars of wings, fuselage, and of the entire frame of the Rocket Bomber in the gas dynamic region and M = 1.5. These aerodynamic values are based on the area of the supporting surfaces.

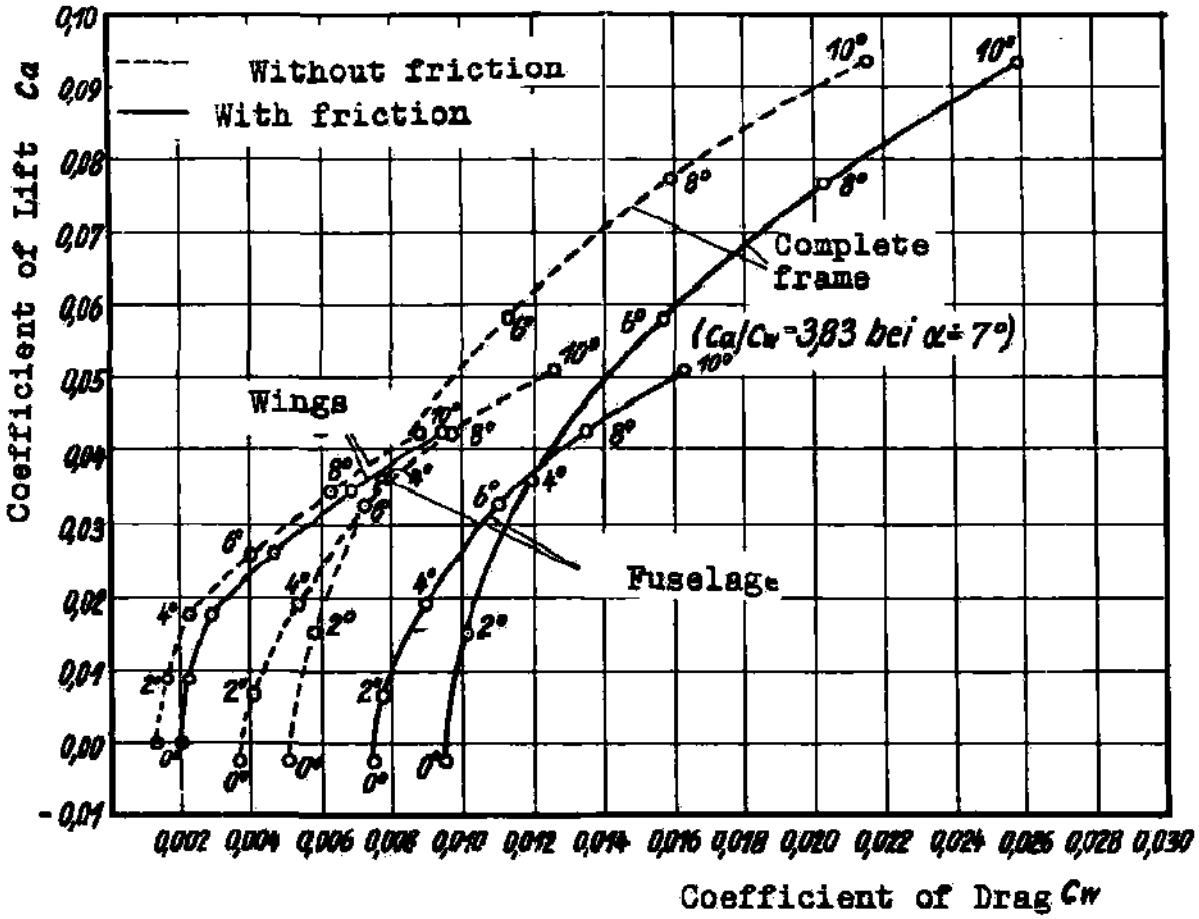

Figure 36; Computed polars of the wing, the fuselage, and of the entire frame of the Rocket Bomber at M = 3. (The aerodynamic coefficients are based on the area of the lifting surfaces.)

excitation of molecular vibrations are reached, then considerable oscillation can occur in the available streaming time, i.e., $\varkappa$ approaches 1.29. For $\varkappa = 1.4$ the pressure on a flat surface is $p/q = 2.4 \sin^2\alpha$. The corresponding pressure in the case of a cone with stream along its axis is, according to Busemann and Guderley, $p/q = 2.1 \sin^2\alpha$. If the wall surface is curved in the direction of the streaming, the layer streaming off along the wall must follow this curvature and undergoes acceleration perpendicular to the plate, so that for convex curvature a negative additional pressure p_2 results. For $\varkappa = 1$, these were calculated by Busemann for general curvatures. For the important case of constant radius of curvature the equations can be integrated and give for the lens profile $-p_2/q = \sin^2\alpha_s - \sin^2\alpha$ and for the ogive-shape, $-p_2/q = \frac{2}{3}\sin^2\alpha_s + \frac{1}{3}(1 - \cos\alpha_s \cos\alpha) - \frac{2}{3}\sin^2\alpha$ where α_s is the angle of attack for the first surface element. Thus the air pressure drops very rapidly as we move back from the end of the object, and vanishes, in the case of the lens profile, at the point for which the angle of attack is $\alpha_s/\sqrt{3}$; for the bullet shape it vanishes somewhat later, at $\alpha_s/\sqrt{8}$, so that the average pressure on the curved surfaces is far less than for plane surfaces. For $\varkappa > 1$ the centrifugal effects, according to Busemann and Guderley, are somewhat larger, so that the pressures for $\varkappa = 1.4$ are 7% smaller than for $\varkappa = 1$, in the case of the lens profile.

As regards the frictional stresses parallel to the wall between the fixed surface and the air, for dense air, momentum parallel to the wall is transferred to the wall only by a thin boundary-layer of molecules near the wall, so that the usual friction laws are valid. One is led, in the case of high supersonic velocities, to give main importance to laminar frictional effects, so that the friction is determined by V. Karmans formula $\tau/q = 1.3/\sqrt{Re}$. In the valleys of the flight path of the aircraft, which determine the energy consumption, we may use a value of $Re = 10^8$, which gives $\tau/q = 0.00013$ for flat, untilted surfaces. At finite angles of attack, the density, friction and temperature change on the leeward side (negative angle of attack) become zero, while for the windward side they are 6 times as great as for free air; at the same time the viscosity of the air increases with the stagnation temperature $v^2 \sin^2\alpha/2000$ according to the relation

$$\eta = 1.753 \times 10^{-6} \left[(273 + v^2 \sin^2\alpha/2000)/273\right]^{0.76}$$

The frictional forces on the surfaces to windward are approximately

$$\tau/q = 6 \times 1.3/\sqrt{6 Re \left[(273 + v^2 \sin^2\alpha/2000)/273\right]^{0.76}}$$

With the aid of these equations we can calculate the aerodynamic forces on an arbitrary body for $V/a \to \infty$. Fig. 37 shows the polars first for the infinitely thin flat plate which is known to be theoretically the best wing for flight above the velocity of sound, second for the wedge profile with flat sides and a thickness 1/2 of the wing depth in the second third of the profile (8, p. 170) and finally for the symmetric double-convex lens profile composed of two equal circular arcs, also with thickness 1/20 of the depth. In the region of $V/a = 1$ to 3, where the linear dependence of the aerodynamic forces on the angle of attack is valid, and where the excess pressures on the windward surfaces and the subnormal pressures on the leeward surfaces are of the same order of magnitude, the biconvex lens profile gives the best glide-numbers; in the Newtonian region, where the air pressure varies quadratically with the angle of attack, and where the air pressure vanishes in the shadow region, the flat-surfaced wedge profile is definitely superior. In the region of angles of attack which are greater than the front bevel angle of the wedge, it is as good as the infinitely thin flat plate. In addition it has the remarkable property, in this velocity range, that the ordinarily strict requirement of minimum profile thickness is weakened, in the sense that even the limiting profile can be so thick that the whole wing surface is in the shadow. The inferiority of the lens profile to the wedge profile in this velocity region arises from the fact that larger angles of attack give poorer glide-numbers; since the pressure depends quadratically on the angle of attack, the large angles for the front parts of the surface outweigh the effect of the small angles at the back parts so that altogether a poorer glide-number results than for the flat underside of the wedge profile. A further reason for the inferiority of the lens profile is that the curved surface, because of the centrifugal action, is acted upon by smaller normal pressures and about the same frictional stresses as for the wedge profile; thus to obtain the same lift, larger surfaces must be used, which involves not only greater weights but also greater frictional forces. Since the rocket bomber needs the best possible glide number at high velocities, it should be designed with wings having a wedge profile.

These considerations can in principle be extended to spatial flow. Fig. 38 shows the polars for 3-dimensional flow around three surfaces with equal projected area and the same height which might be considered for the bow shape - a circular cone with height four times the diameter of the base, a bullet with the same height and base diameter (16.25 caliber radius), and finally a half-bullet with the same height and a semicircular base of the same size as that of the two surfaces of revolution, i.e, with 8.25 caliber radius. The aerodynamic coefficients are all for

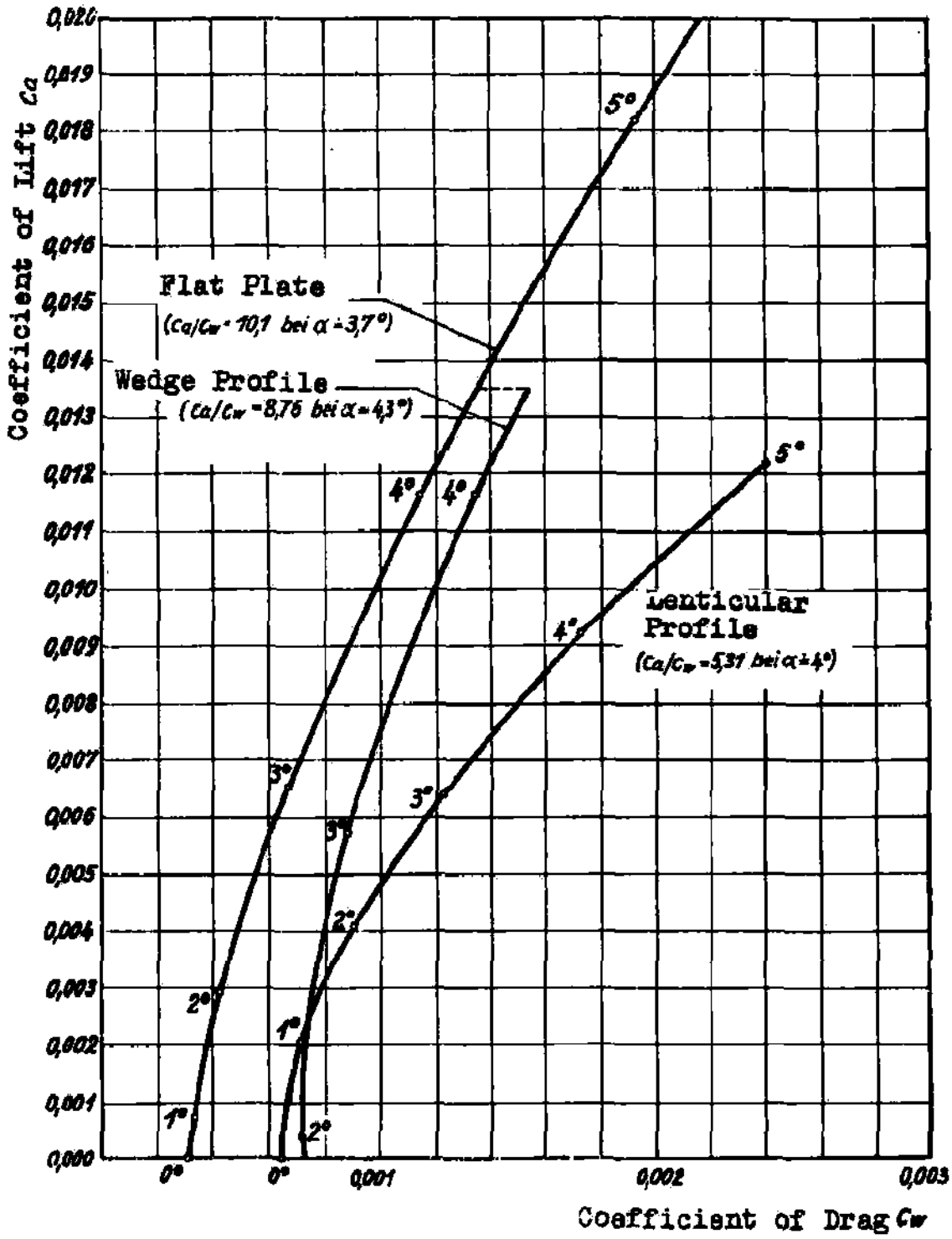

Figure 37; Polars of a plane curface, a wedge profile and a lenticular profile at M=3 (The aerodynamic coefficients are based on the area of the lifting surfaces)

the same projected area. While the cone and bullet differ little in glide-number, the half-bullet with flat surface to the front, is far superior, having a glide-number with $1/\varepsilon = 4.12$. This is of decisive importance for the shape of the fuselage of the rocket bomber. While in the region V/a = 1 to 3, the bullet has the optimum glide-number, the laws determining the shape of a body under 3-dimensional flow change for high Mach numbers in the same way as for the wing sections; on the under side of the surface, which mainly determines the magnitude and direction of the net aerodynamic force, the air pressure should be as large, and the resistance components as small, as possible. The underside should consist solely of surfaces tilted toward the course wind. For a given average angle of attack of the undersurface, and for quadratic dependence of pressure on angle of attack, one obtains the best ratio of drag to lift on the underside if it is curved as little as possible in the direction of flow. On the upper side of the body, which with proper shape is unimportant for determining the total aerodynamic force, the pressures should be as small as possible. Therefore, the upper side should preferably consist only of surfaces tilted to leeward. If this is not possible, the parts of the upper surface which are to windward should have the smallest possible angle of attack, and be curved convex to the direction of flow, to keep the streaming pressure low by taking advantage of the centrifugal effect of the airmass streaming off the curved surface. Summarizing, for large Mach numbers, bodies should be so streamlined with a point or dihedral at the front, that the lifting undersurface is not curved in the direction of stemming, and that the upper surface should consist as far as possible of surfaces to leeward; the unavoidable windward sections of the upper surface should have a convex curvature in the direction of flow. (29)

The fuselage of the rocket bomber was shaped in accordance with this recipe; its polars for $\lambda_0 \to \infty$ are shown in Fig. 39. From the figure we see that the optimum angle of attack for wings and fuselage are $\alpha = 4°20'$ and $\alpha = 8°30'$ resp. Since the wing surface is smaller than the fuselage surface, the more favorable glide-number for the wings has little effect compared to that of the fuselage, and one finds a theoretically most favorable angle between wings and fuselage of -2° for which the optimum reciprocal glide number $1/\varepsilon = 6.51$ is obtained for angle of attack $\alpha = 5°30'$ for the wings and $\alpha = 7°30'$ for the fuselage. For constructional reasons, and also to have simple streaming conditions at the wing roots, the angle of incidence was chosen as 0°; the polar for this case is shown in Fig. 36, which shows a best $1/\varepsilon = 6.4$ for $\alpha = 7°$. This value of glide-number, which can be attained by proper shaping of the fuselage and wings, is surprisingly favorable for high supersonic speeds, and is scarcely different from that of present aircraft below the velocity of sound. We may safely assume, for the velocity range $\frac{V}{a} = 30$ to 10, that the results derived for $\lambda_0 \to \infty$ still apply, and that below this range the characteristics for $\frac{V}{a} = 1$ to 3 gradually appear.

On the basis of the previous investigation the variation of glide number of the rocket bomber for various angles of attack can be represented as in Fig. 40 for the whole range of velocities in dense air. The very favorable glide-number below sound-velocity, $\varepsilon = \frac{1}{7.75}$ at $\alpha = 5°$, drops very rapidly as we approach the velocity of sound, then takes on the value $\varepsilon = \frac{1}{3.6}$ at $\alpha = 8°$ for velocities slightly above the velocity of sound. Above $\frac{V}{a} = 3$, the glide-number improves and then rapidly approaches its favorable behavior for high Mach numbers, with

$$\varepsilon = \frac{1}{6.4} \quad at \quad \alpha = 7°$$

In all the previous considerations on the aerodynamic forces, the air was considered as a continuous medium. As the later sections show, the path of the rocket bomber reaches heights of over 1000 km. There the density of the air becomes so very small that on the one hand the stagnation pressures for even extreme velocities no longer result in aerodynamic forces at all comparable with the other external forces on the aircraft, and also the laws for calculating the aerodynamic forces are no longer those derived for a continuous medium. Fig. 41 is a plot of the air density ρ as a function of the height H for values up to 20,000 m from the well known formula for a homogeneous isothermal atmosphere; for heights between 11 and 22 thousand m, the relation is $\rho/\rho_0 = 1.6839\, e^{-H/6341}$ (see also "Dinorm 5450" or (33)). This expression for density at great heights is used in the later (note: original has error; 'uses ρ instead of $\rho_{(T,K)}$) calculations. It is frequently assumed that the composition of the atmosphere at high altitudes is the same as on the ground - i.e., mostly N_2 and H_2, but that these materials are more or less dissociated into atoms. Therefore two dotted curves in Fig. 41 are used to show the density if all molecules are dissociated into atoms (left curve), and if only a partial dissociation occurred, as assumed by Godfrey (middle curve). The molecular free path for constant composition varies with the density according to the relation $l_{[m]} \doteq 10^{-7}\, \rho_0/\rho$. This relation also holds approximately for the dotted curves for the dissociated atmosphere, since the effect of dissociation on the free path is of the same order as the error in determination of the free path. At heights of 40 km, the free path is already greater than the thickness of the laminar boundary layers (10^{-4}–10^{-5} m), reaches the size of the aircraft dimensions at a height of 120 km., and rises to over 1000 km. at a height of 200 km. The stagnation pressure corresponding to the "velocity of escape" V = 12000 m/sec is less than 1 kg/m2 at 100 km. altitude; i.e., at 100 km. altitude the aerodynamic forces have practically disappeared, and the motion of the rocket bomber is along practically a pure inertial path. The expressions derived for the aerodynamic forces on the assumption of a continuous medium are already invalid at heights over 40 km. since the distances

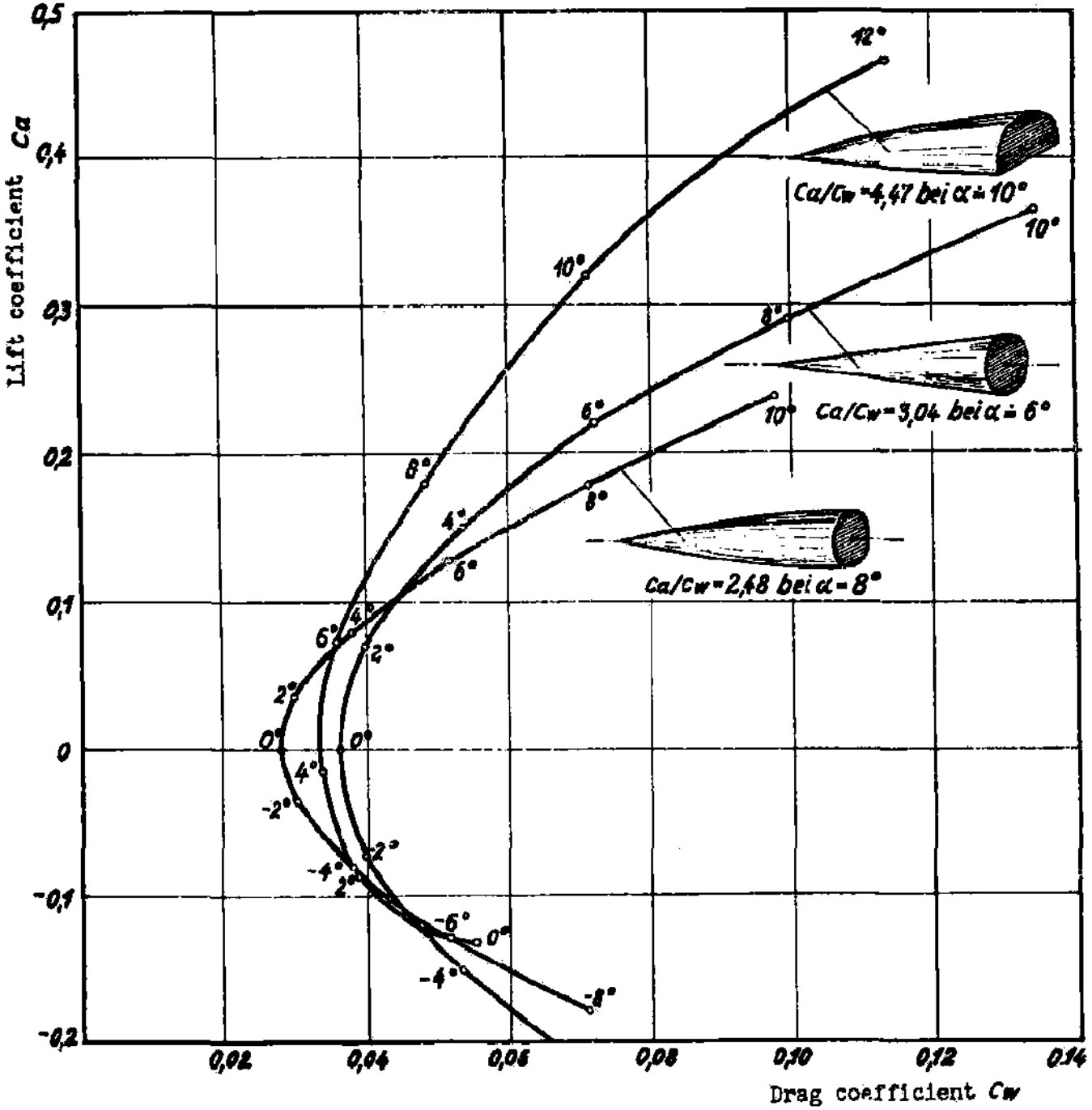

Fig. 38: Polars for three bodies having equal height and equal base cross-sectional area.

1. A right circular cone
2. An ogival shape
3. A half ogival shape

Aerodynamic coefficients are based on the base area. Mach number infinite. Gas dynamic region.

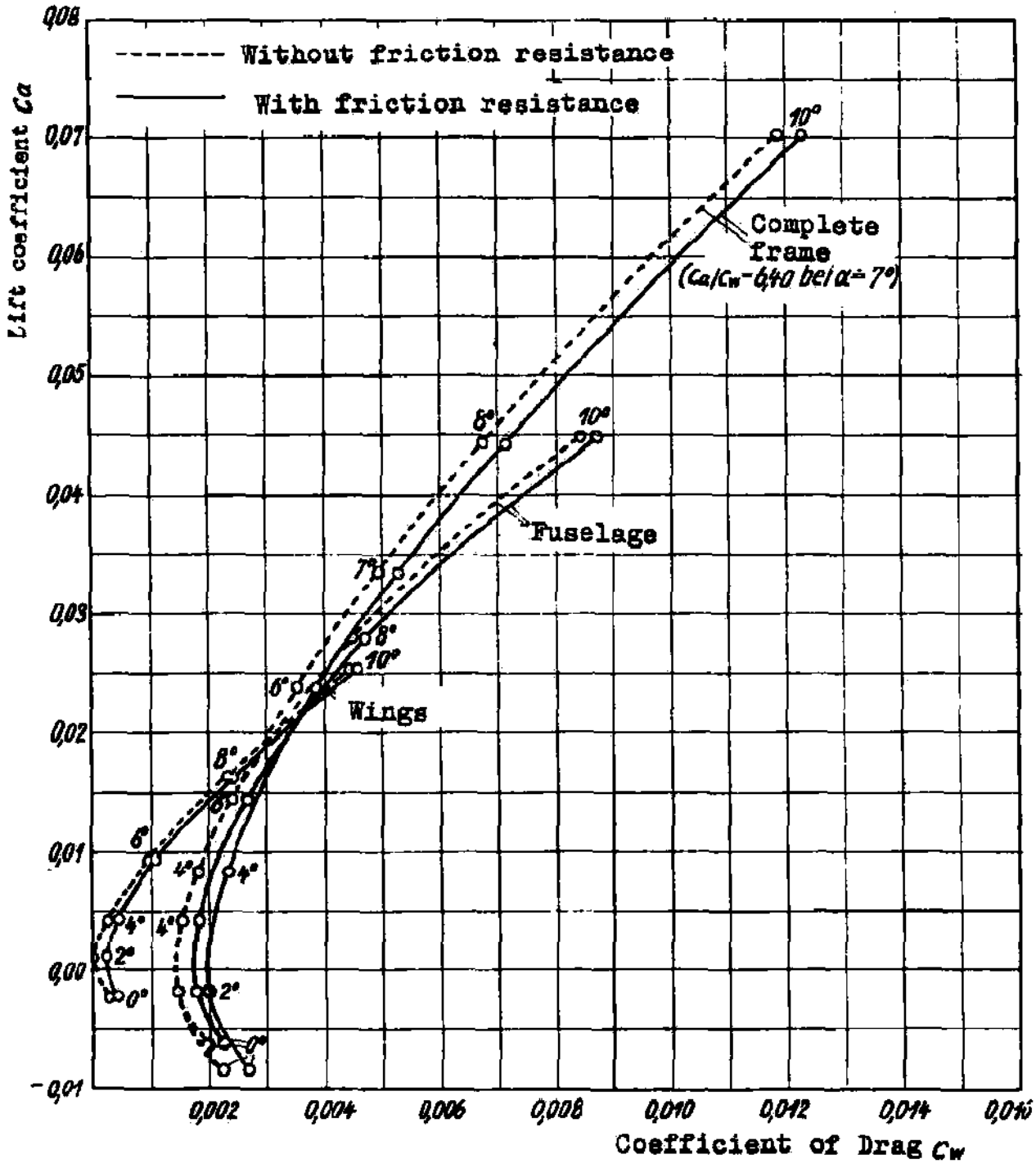

Figure 39; Computed polars of the wings, the fuselage, and the entire frame of the Rocket Bomber at M=3 (The aerodynamic coefficients are based on the area of the lifting surfaces).

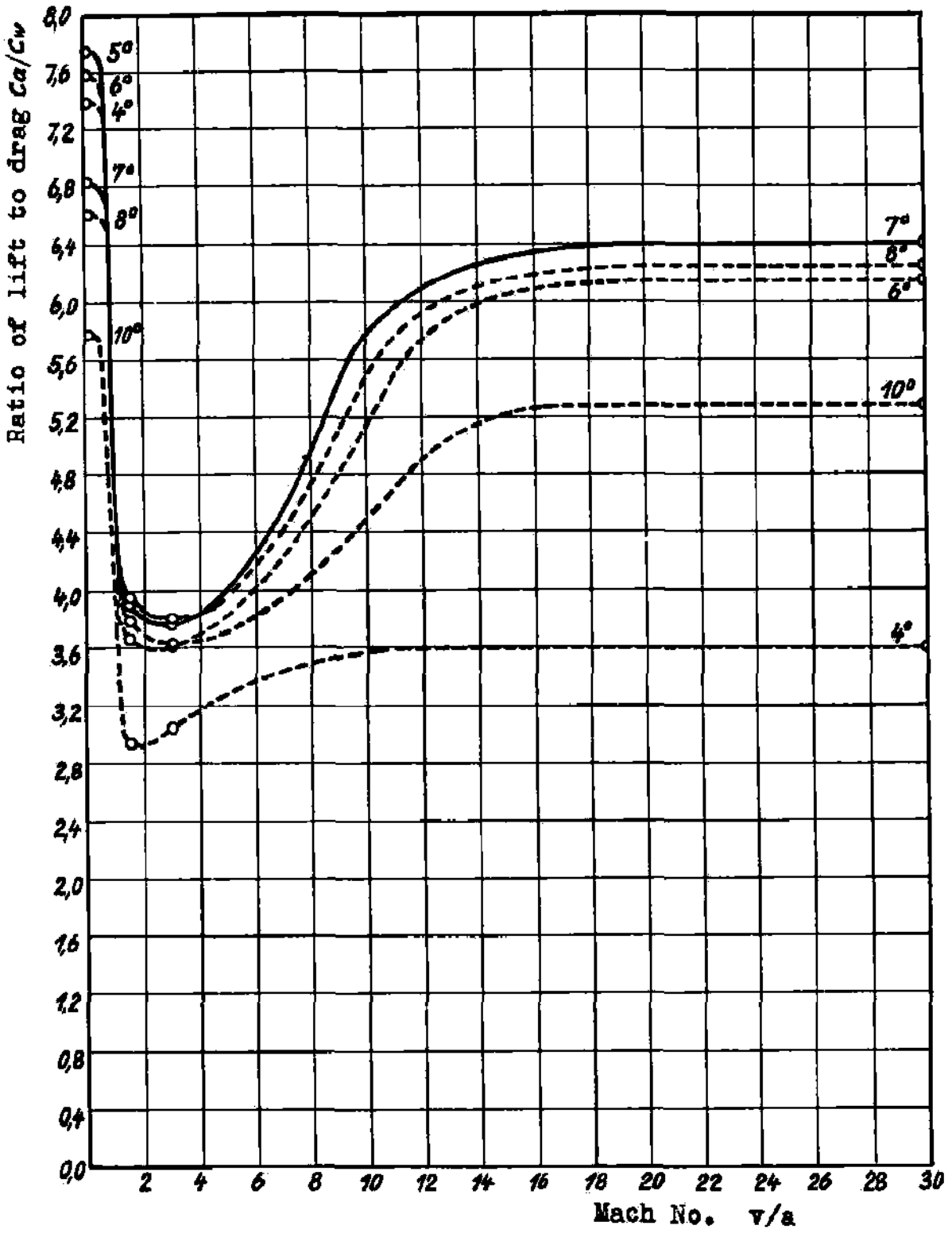

Figure 40; Probable behavior of lift-to-drag ratio and best angle of attack of Rocket Bomber at $0.1 \leq M \leq 30$.

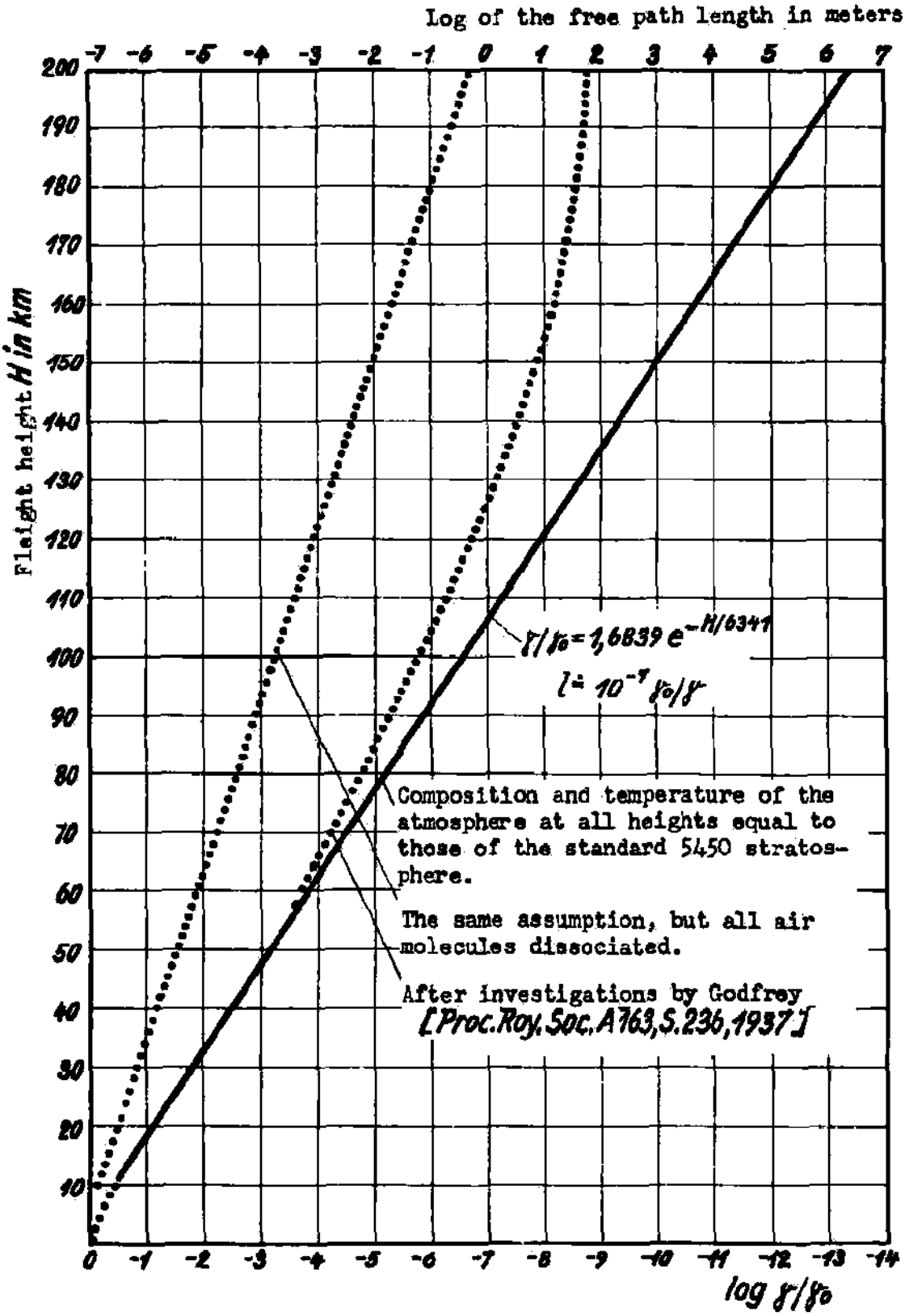

Fig. 41: Variation of the specific weight of the atmosphere, and the free path length with the flight height H.

between air molecules are already larger than the dimensions of the streams assumed in the calculation, e.g., the thickness of the boundary layer. For such rarefied air, no procedure for calculating aerodynamic forces is known. Only when, for altitudes above 100 km, the free paths approach the dimensions of the moving body, do the relations simplify sufficiently to enable a fairly exact estimate of the aerodynamic forces. (28)

In this region of gaskinetic streaming the following equations are valid for the aerodynamic forces on a body moving at arbitrary velocity V at altitudes above 100 km, where the upper (lower) sign refers to negative (positive) angles of attack:

$$p/q = (i_{pH} + i_{pR})/q$$

$$i_{pH}/q = \mp \sin\alpha \cdot \frac{C_H}{V} \cdot \frac{e^{-\frac{V^2}{C_H^2}\sin^2\alpha}}{\sqrt{\pi}} + \left(\sin^2\alpha + \frac{1}{2}\frac{C_H^2}{V^2}\right)\left(1 \mp \frac{2}{\sqrt{\pi}} \int_{x=0}^{\frac{V}{C_H}\sin\alpha} e^{-x^2} dx\right)$$

$$i_{pR}/q = +\frac{\sqrt{\pi}}{2} \cdot \frac{C_R}{V} \cdot \frac{C_H}{V} \cdot \frac{e^{-\frac{V^2}{C_H^2}\sin^2\alpha}}{\sqrt{\pi}} \mp \frac{\sqrt{\pi}}{2} \cdot \frac{C_R}{V} \sin\alpha \left(1 \mp \frac{2}{\sqrt{\pi}} \int_{x=0}^{\frac{V}{C_H}\sin\alpha} e^{-x^2} dx\right)$$

$$i_{\tau}/q = +\cos\alpha \cdot \frac{C_H}{V} \cdot \frac{e^{-\frac{V^2}{C_H^2}\sin^2\alpha}}{\sqrt{\pi}} \mp \sin\alpha\cos\alpha \left(1 \mp \frac{2}{\sqrt{\pi}} \int_{x=0}^{\frac{V}{C_H}\sin\alpha} e^{-x^2} dx\right)$$

where V is the speed of flight, $C_H = \sqrt{2gRT_0}$ is the most probable velocity of the gas molecules before collision with the wall, $C_R = \sqrt{2gRT_w}$ is the most probable diffuse recoil velocity of the molecules after contact with a wall at T_w °K. For very large V, i_{pH}/q approaches $2\sin^2\alpha$ (since $\int_0^\infty e^{-x^2}dx = \frac{1}{2}\sqrt{\pi}$) and i_{pR}/q approaches zero, i e. we approach the Newtonian formula $p/q = 2\sin^2\alpha$. A presentation of these aerodynamic forces in closed form as a function of Mach number is not possible; though a simple relation between C_H and a is known $C_H = a\sqrt{2/\varkappa}$, there is no corresponding relation between C_R and a.

All the equations refer to diatomic gases or gas mixtures. Also they require the knowledge of the characteristic temperature Θ, and thus involve more special assumptions than do the gas-dynamic equations which require only a knowledge of the no. of atoms per molecule and the sound-velocity, since they involve only $\varkappa$ and a.

The equations for the momentum i_{pH} of the molecules colliding with the wall, and for the tangential momentum i_τ given to the wall on recoil are taken from (28). The recoil momentum must be considered in more detail.

Before an expression for the recoil momentum can be set up, one must have a clear picture of the recoil of the molecules, which have a random thermal velocity c and a relative velocity V making an angle α with the plate. One must decide whether a bundle of molecules, striking the plate with a perpendicular velocity component $V\sin\alpha + c_x\cos\varphi$ leave the plate by specular reflection or under some other definite or random angles; further, whether the collision velocities are conserved for each individual molecule or have a definite relation to the recoil velocities, or whether they are completely random so that we can derive relations only for the average or most probable speeds, on the basis of energy considerations. One should investigate whether, during the collision, the velocities C_x as well as V are conserved, or whether they interchange their kinetic energy in whole or in part, or whether the internal degrees of freedom of the air molecules or wall molecules take part in this exchange. These questions were answered on the basis of a paper of Frenkel on "Theory of Adsorption and Related Phenomena" (4), whose opinion we give verbatim: "No matter how small the time of adherence, gas molecules colliding with a wall do not simply bounce off, but are emitted again with velocities which need not have any definite relation to the original velocity, either in magnitude or direction. The usual picture of elastic reflections of molecules, from which the kinetic theory of gases starts in deriving the pressure on the walls of the container, is false in principle. If one arrives at correct results in this case, it is because the solid body and the gas are considered to be at the same temperature and at rest relative to each other. Under these conditions, the velocity distribution of the emitted molecules is the same as if they were actually reflected from the wall surface. Actually a quite different picture would result if one bombarded the surface in a definite direction with a molecular beam." Summarizing these considerations we find that, in setting up a formula for the recoil momentum, we must consider a gas whose probable recoil velocity C_R is derivable by purely energetic considerations from the probable velocity C_H before collision, from the systematic velocity V and the wall temperature T_w. The mass of gas striking the wall per second is:

$$\overline{\rho} = \frac{\rho}{2\sqrt{\pi}} \cdot C_H \left[e^{-\frac{V^2}{C_H^2}\sin^2\alpha} + \frac{V}{C_H}\sin\alpha \left(2\int_{x=0}^{\frac{V}{C_H}\sin\alpha} e^{-x^2} dx \pm \sqrt{\pi}\right)\right] = \frac{\rho}{2\sqrt{\pi}} C_H \cdot k$$

In the normal gas-kinetic case ($V = o$ and $C_R = C_H$) the process of emission of the molecules can be considered as quasi-specular, with recoil momentum $\tau_{pR} = \rho C_H/4 \cdot C_H$ for a mass colliding per second of $\bar{\rho} = \frac{\rho}{2\sqrt{\pi}} \cdot C_H$. For the moving plate ($V \neq o$), K times as many molecules collide each second as for the plate at rest, and just as many must come off per second if none sticks permanently to the wall. Since according to the research cited, the process of recoil is completely independent of the process of collision, and is of the same type as for recoil at $V = o$, the only possible difference can consist in a change of the factor K for the colliding molecules $\tau_{pR} = \frac{\rho}{4} C_H \cdot K C_H$ as long as $C_R = C_H$. For the same reasons, the difference between recoil and collision temperatures can produce no change in the structure of the formula for the recoil momentum; one gets for $C_R \neq C_H$, $\tau_{pR} = \frac{\rho}{4} C_H K \cdot C_R$. The probable translational recoil speed C_R must be considered further. According to the theorem of Conservation of Energy, for the assumed closed system the sum of the energy E_R taken away by the recoiling molecules plus the energy E_W remaining at the wall must equal the energy E_A of the impinging molecules: $E_A = E_W + E_R$

$$E_A = E_{A\,trans} + E_{A\,rot} + E_{A\,osc} = A\bar{p}\left[\frac{V^2}{2} + \frac{C_H^2}{2}\left(\frac{3}{2} + \frac{2}{2} + \frac{\Theta}{T_G(e^{\Theta/T_G} - 1)}\right)\right]$$

$$E_W = E_{W\,trans} + E_{W\,rot} + E_{W\,osc} = A\bar{p}\left[\frac{3}{4} C_{W\,trans}^2 + \frac{1}{2} C_{W\,rot}^2 + \frac{1}{2} \frac{\Theta}{T_{W\,osc}(e^{\Theta/T_W} - 1)} C_{W\,osc}^2\right],$$

$$E_R = E_{R\,trans} + E_{R\,rot} + E_{R\,osc} = A\bar{p}\left[\frac{3}{4} C_{R\,trans}^2 + \frac{1}{2} C_{R\,rot}^2 + \frac{1}{2} \frac{\Theta}{T_{R\,osc}(e^{\Theta/T_W} - 1)} \cdot C_{R\,osc}^2\right],$$

where the values C_{rot} and C_{osc} have only a computational significance and are therefore not used in what follows.

Usually the ratio of the energy loss of the impinging molecules to the excess of their initial energy over the temperature level of the wall after collision is called the accommodation coefficient α; e.g. the average accommodation coefficient for the whole process has the value $\bar{\alpha} = (E_A - E_R)/(E_A - E_W)$. The accommodation coefficients for the individual degrees of freedom can be written as:

$$\alpha_{trans} = (E_{A\,trans} - E_{R\,trans})/(E_{A\,trans} - E_{W\,trans}) = \left(V^2 + \tfrac{3}{2} C_H^2 - \tfrac{3}{2} C_{R\,trans}^2\right)/\left(V^2 + \tfrac{3}{2} C_H^2 - \tfrac{3}{2} C_{W\,trans}^2\right)$$

$$\alpha_{rot} = (E_{A\,rot} - E_{R\,trans})/(E_{A\,rot} - E_{W\,rot}), \quad \alpha_{osc} = (E_{A\,osc} - E_{R\,osc})/(E_{A\,osc} - E_{W\,osc})$$

The average accommodation coefficient $\bar{\alpha}$ is built up from the coefficients for the separate degrees of freedom as follows:

$$\bar{\alpha} = \alpha_{trans}(E_{A\,trans} - E_{W\,trans})/(E_A - E_W) + \alpha_{rot}(E_{A\,rot} - E_{W\,rot})/(E_A - E_W) + \alpha_{osc}(E_{A\,osc} - E_{W\,osc})/(E_A - E_W)$$

Considerations on accommodation coefficients in the physical literature state in essence that the external degrees of freedom take part immediately and completely in the energy exchange during molecular processes, whereas the exchange of internal molecular energy, especially that of vibration, is slowed down considerably and is effective only after long relaxation times, so that the accommodation coefficients for translation are 1 and also α_{rot} may be assumed to be ≈ 1, while the deviations of the total accommodation coefficient $\bar{\alpha}$ from 1, observed in practice, are to be ascribed to the slowness of changes in vibration. From $\alpha_{trans} = 1$ it follows that $C_{R\,trans} = C_{W\,trans} = \sqrt{2gRT_W}$ where $C_{R\,trans}$ is thus the desired most probable recoil velocity of the molecules leaving the wall diffusely; T_W is the wall temperature in °K.

Before calculating the aerodynamic forces one must estimate the wall temperature T_W. This is done by equating the energy radiated by the wall per cm^2 per sec, $E_S = \varepsilon_a \frac{4.96}{3600}\left(\frac{T_W}{100}\right)^4$ to the energy E_W transferred by the air molecules to the same surface in the same time. If one introduces the previously established assumptions $\alpha_{trans} = 1$, $\alpha_{rot} = 1$, $\alpha_{osc} = 0$, one obtains $E_W = A\bar{p}\left[\frac{V^2}{2} + \frac{5}{2} gR(T_G - T_W)\right]$ where $\bar{p}$ is the mass of the molecules striking unit area of the plate per unit time. These expressions were used in constructing Fig. 42, where the following numerical values were assumed; temperature of still air $T_G = 320$ °K, density of still air $\rho = 10^{-7}$ kg sec^2/m^4, (corresponding to H ≈ 90 km.) composition of the air 14% O_2 + 86% N_2. Ionization and dissociation were not considered; also the atmosphere was assumed to be at rest on the earth's surface. The optical absorption of the wall was assumed to be $\varepsilon_a = 0.80$. Radiation of heat to the wall from the outside (sun), from the air space or the earth's surface was neglected, as well as from the interior of the aircraft to the wall. Fig. 42 shows that the equilibrium temperature of the plate at rest is 136° K and that this equilibrium temperature of the surface of the aircraft increases with increasing velocity and angle of attack, as long as the latter is positive so that the surface is tilted toward the course wind. For surfaces to leeward the equilibrium temperature drops to absolute zero, since the heat supply vanishes with the number of impinging molecules. Altogether the temperatures remain within reasonable limits for all angles of attack and velocities occurring in practice. At greater heights even lower temperatures may be expected; at lower heights a transition occurs to temperatures calculable by kinetic theory.

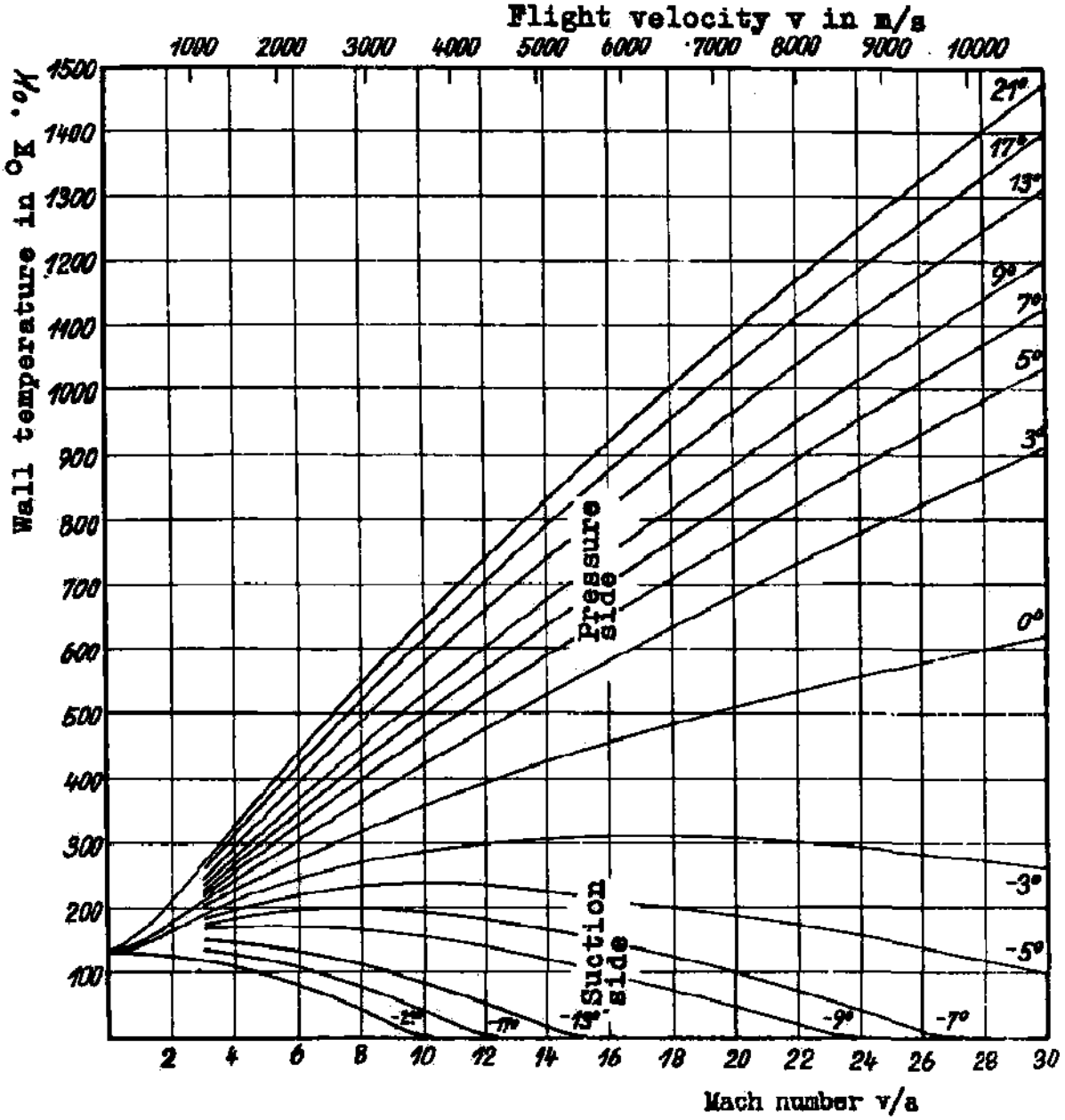

Fig. 42: Surface temperature of a flat plate in an atmosphere of 86% N_2 and 14% O_2 and with density $\rho = 10^{-7}$ kg sec^2/m^4 (in molecular flow region) for various flight velocities v/a and various angles of attack α

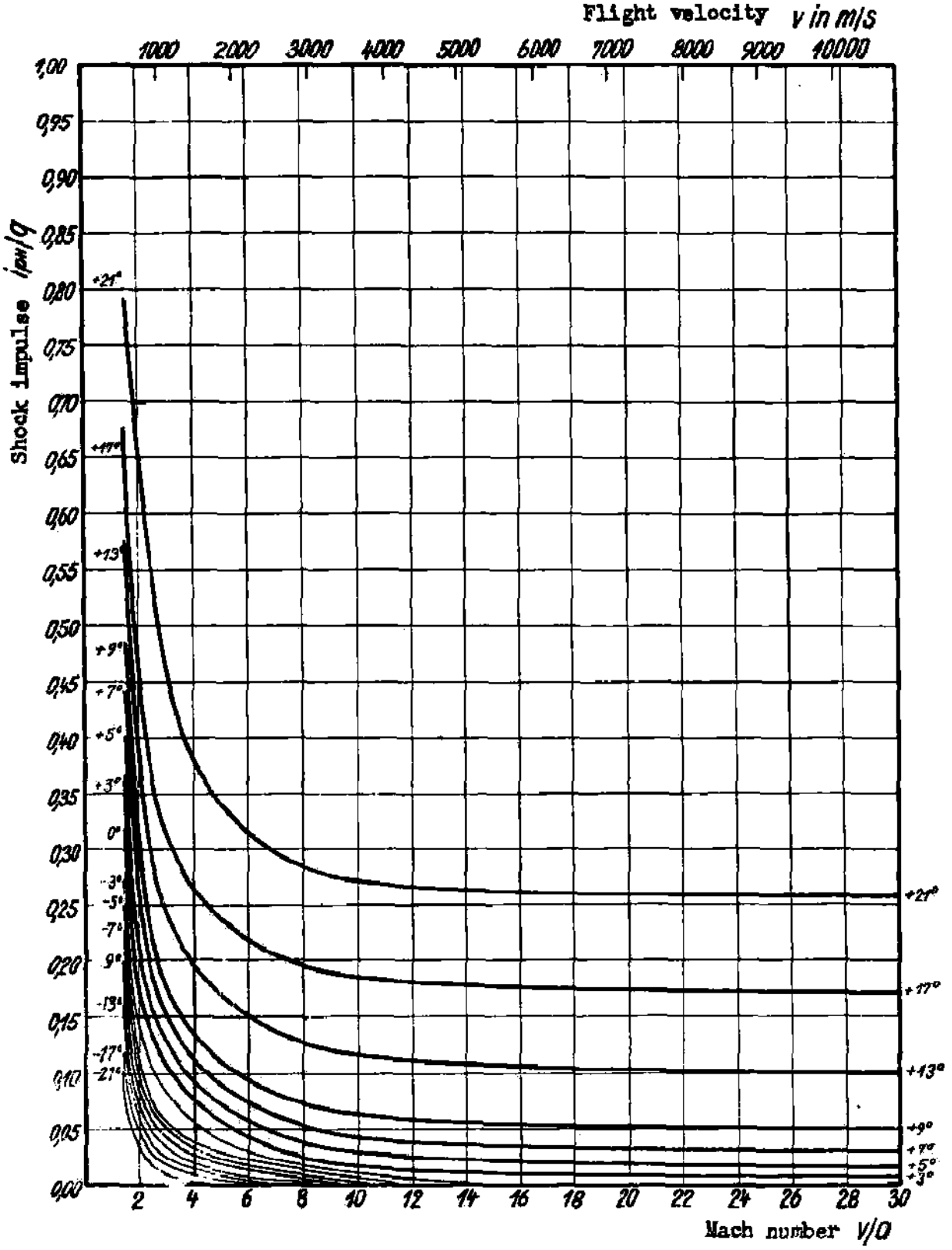

Fig. 43: Coefficients iph/q of a shock impulse perpendicular to a flat plate for various flight velocities v and angles of attack α in an atmosphere of 86% N_2 and 14% O_2 and density $\rho = 10^{-7}$ kg sec^2/m^4 (molecular flow region).

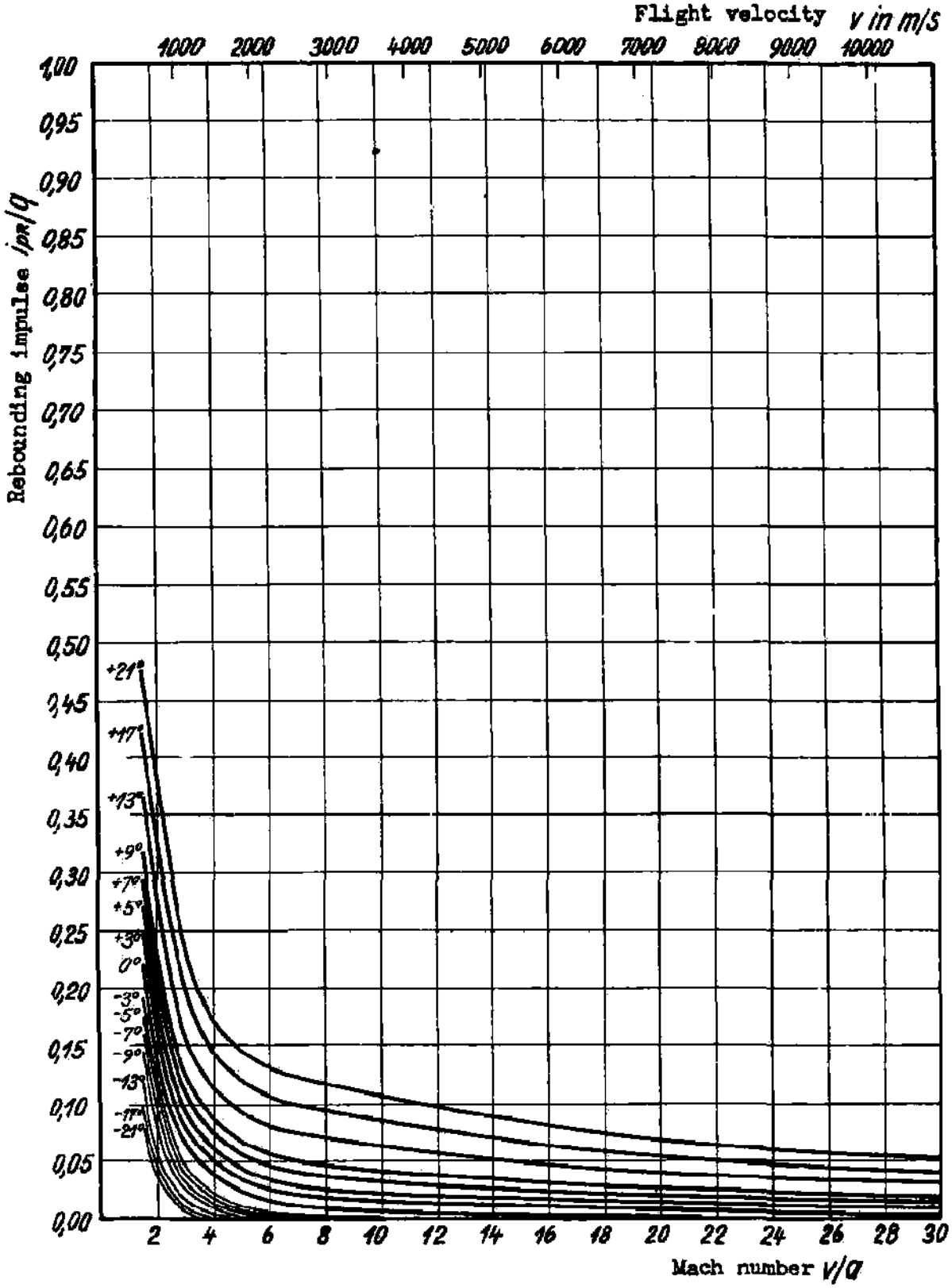

Fig. 44: Coefficient ipR/q of restitution (rebounding impulse) on a flat plate for various flight velocities v and angles of attack α in an atmosphere of 86% N_2 and 14% O_2 and density $\rho = 10^{-7}$ (molecular flow region).

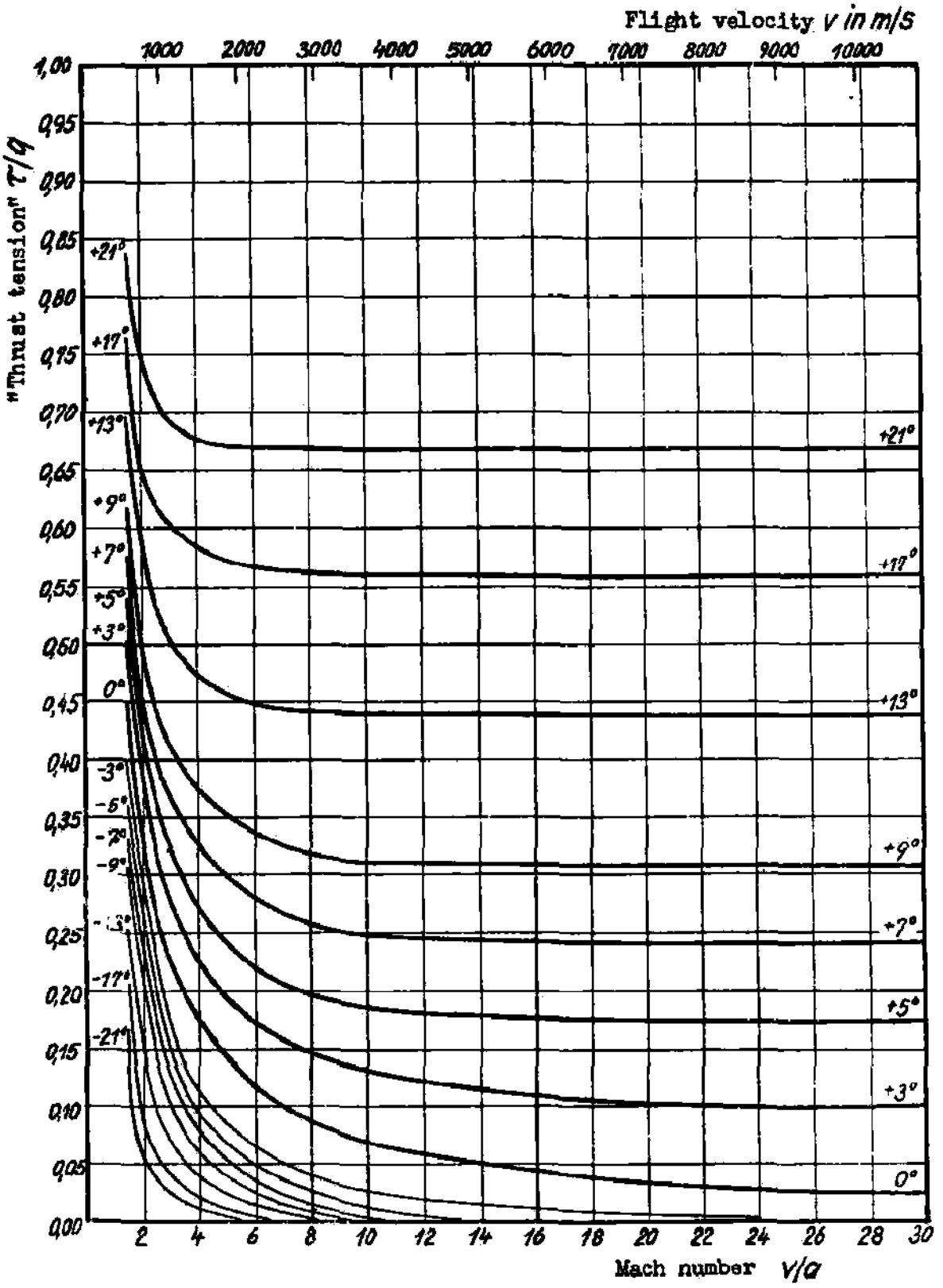

Fig. 45: Coefficient τ/q of the thrust tension between air and plane plates for various flight velocities v and various angles of attack α in an atmosphere of 86% N_2 and 14% O_2 and density $\rho = 10^{-7}$ kg sec^2/m^4 (molecular flow region).

With the aid of the equations the aerodynamic forces were calculated for an assumed atmosphere with temperature 320° K, density 10^{-7} kg sec^2/m^4 and composition 14% O_2 + 86% N_2. The momentum $i_\rho H$ of the air impinging on the plate is plotted in Fig. 43 for various angles of attack and velocities of flight; the corresponding recoil momentum $i_\rho R$ is shown in Fig. 44, and the tangential momentum in Fig. 45. Since $i_T = T$, Fig. 45 also represents the coefficient of friction τ/q between the air and the wall, for all angles of attack and for the same range of flight velocities. In this figure, the extraordinarily large coefficient of friction in the domain of gas-kinetic streaming is noteworthy. While values of $\tau/q = 0.001$ to 0.003 are customary in aerodynamics, we have in this case values of the friction 300 to 1000 times as large, and these are not accompanied by corresponding increases in the values of the perpendicular components of the aerodynamic forces. The reason for this astonishingly high friction is the fact that in the domain of gas-kinetic streaming the protective boundary layer at the surface of the moving body no longer exists, so that all the molecules which have the chance to transfer perpendicular momentum to the wall, at the same time transfer their tangential momentum completely on the average, whereas this latter momentum transfer is limited to the few molecules inside the boundary layer, in the case of aerodynamic streaming. This very unfavorable behavior of the aerodynamic forces in the rare upper atmosphere would completely prevent flight at these heights, if the stagnation pressures and consequently the forces did not decrease rapidly and finally vanish. Obviously the shaping of the aircraft to fit the streaming conditions loses some of its significance of these heights. Nevertheless, the Newtonian character of the air pressures (i.e. their quadratic dependence on flight velocity and angle of attack), and the rapid disappearance of forces on leeward surfaces, is very apparent at higher velocities of flight. Thus in the gas-kinetic domain all the requirements are fulfilled for the use of streamlined bodies, whose underside is curved as little as possible in the direction of streaming, and whose upper side consists, as far as possible, of leeward or convex surfaces, while the thickness of the body is of no importance. Reciprocal streamline-numbers and polars were derived for the flat plate, from Figs. 43-45, and plotted in Figs. 46 and 47. These graphs of the behavior of the aerodynamic forces on a flat, infinitely thin plate, have direct practical importance, because any wing profile of finite thickness, with a flat under-side and upper-side to leeward, undergoes exactly these same aerodynamic forces at high flight velocities, regardless of the shape of the upper side and the thickness of the profile.

Figs. 48 and 49, which show the aerodynamic forces on the rocket bomber in the range of gas-kinetic streaming, were also derived from Figs. 43-45. In the same way as for the gas-dynamic calculations, the actually curved surface of the aircraft was split up into a number of small flat surfaces, and the air forces calculated for each of these component surfaces.

Finally Fig. 50 shows a plot of the dependence of the air forces on height and velocity of flight for the domains of gas-dynamic and gas-kinetic streaming. This plot of ρ/q against height, for the flat plate, for various Mach numbers and with the fixed angle of attack of 7° (which is the optimum for the gas-kinetic case), shows that the air-force-coefficients decrease with height in this region. This phenomenon is caused by the decrease of temperature of the plate with height, so that ceteris paribus the recoil velocity and recoil momentum also decrease. The forces in the range of heights from 40-90 km (which cannot be calculated exactly) were interpolated approximately in the form of the dotted curve.

Fig. 51 shows the final result of this whole section, i.e. the dependence of the rocket bomber's glide number (or its reciprocal) on the velocity and altitude of flight. With this we close the investigations on glide-number of the rocket bomber.

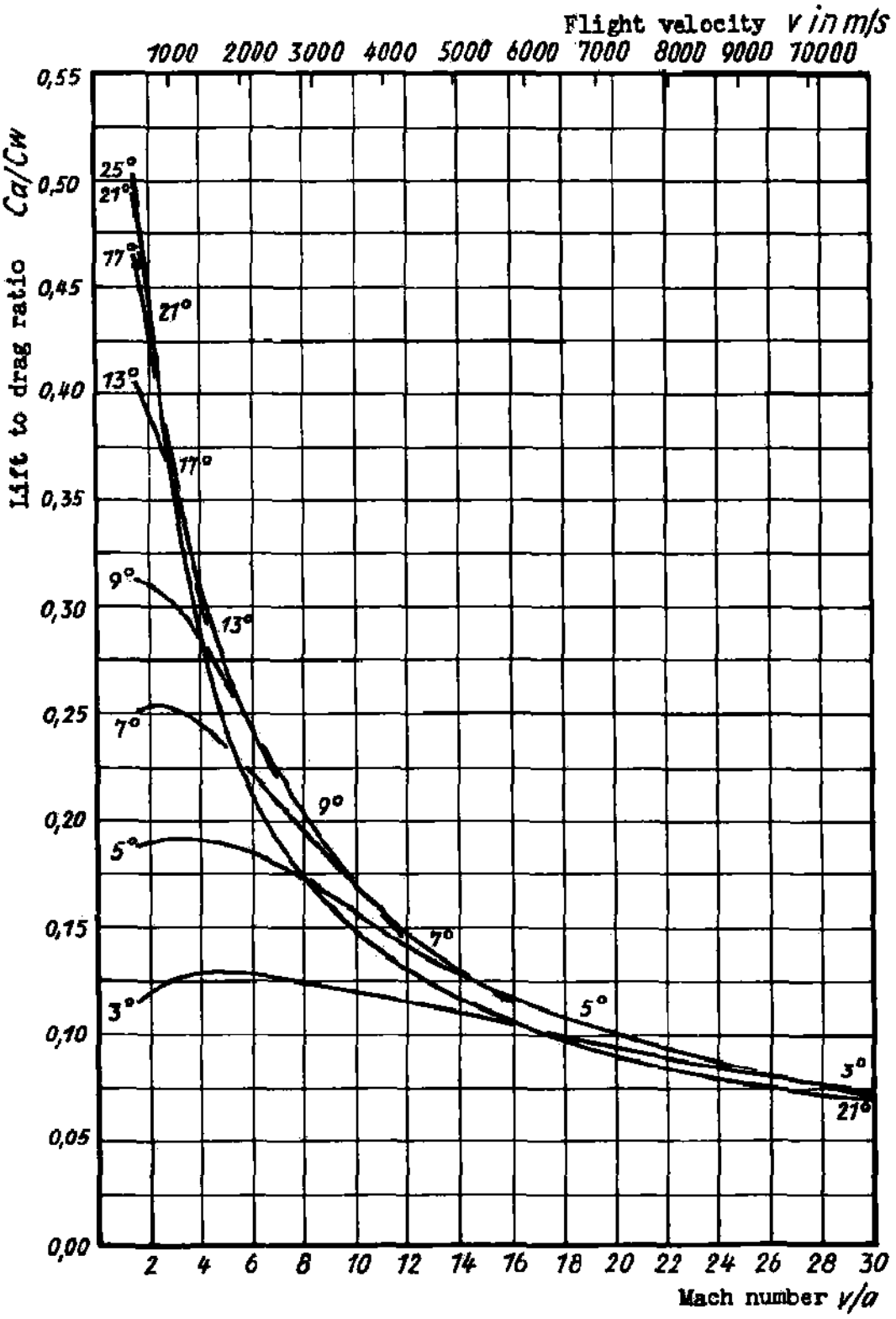

Fig. 46: Lift to drag ratio of a flat infinitely thin plate in molecular flow region.

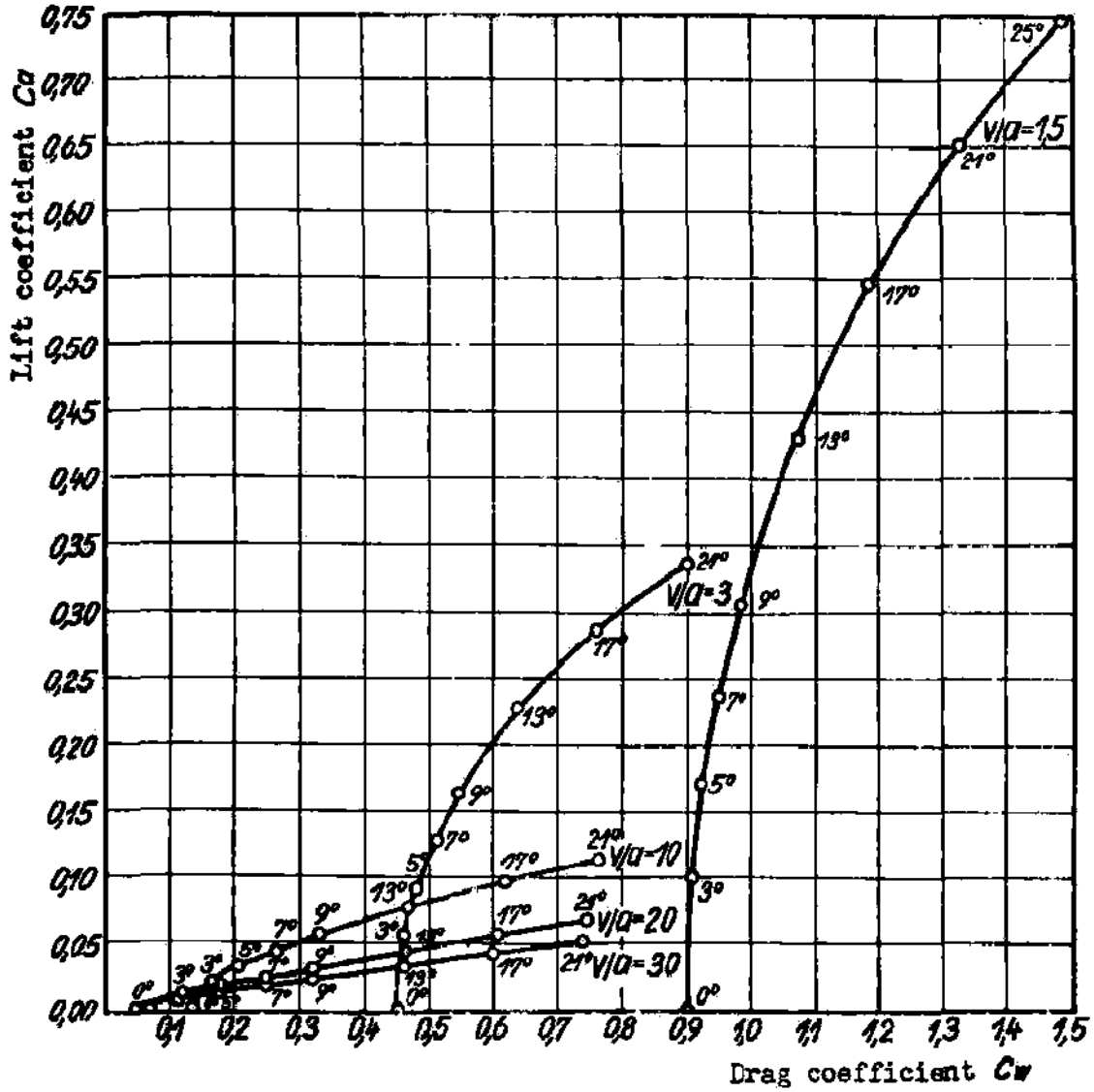

Fig. 47: Polars of a flat, infinitely thin plate in molecular flow region for various flight speeds.

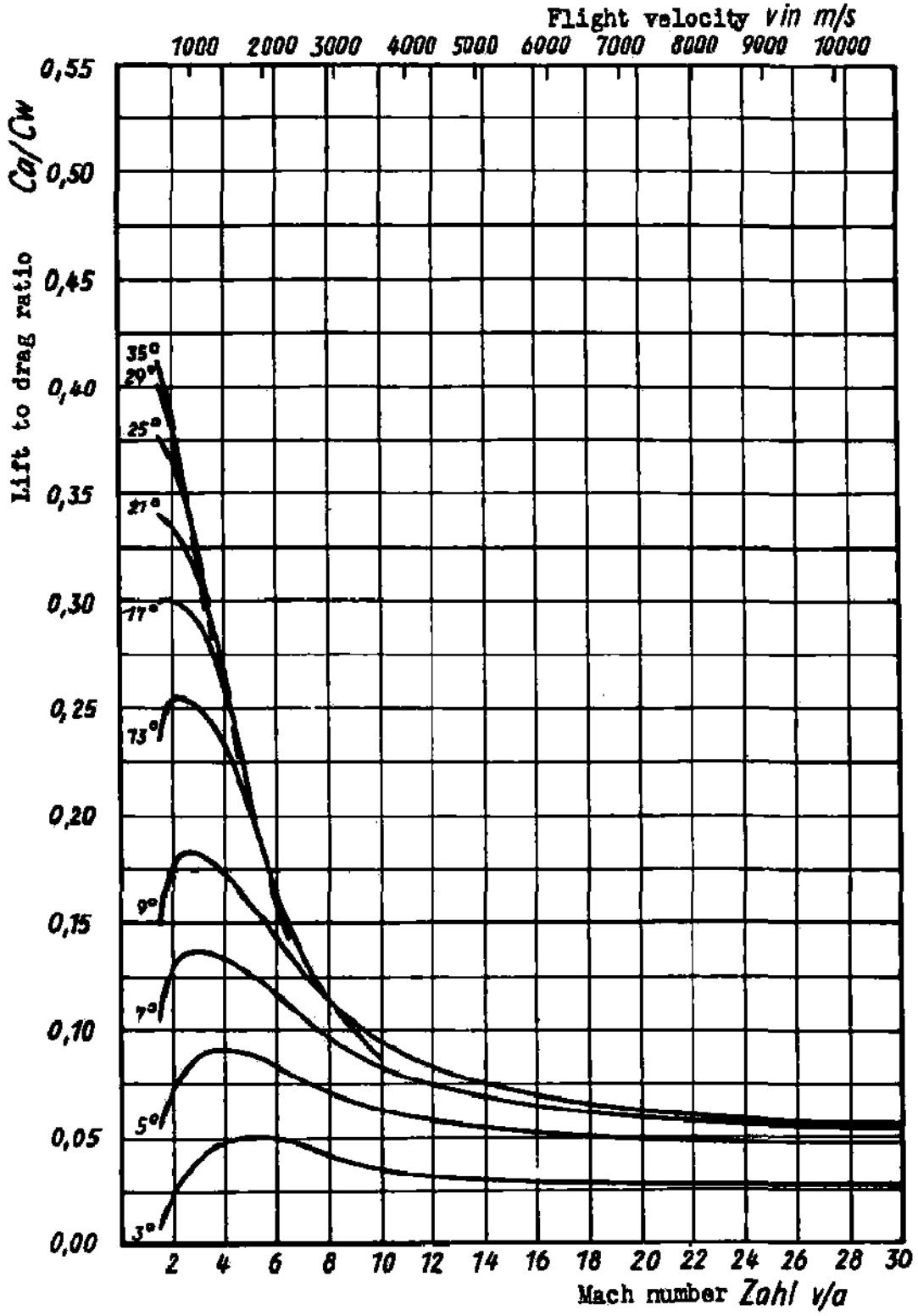

Fig. 48: Lift to drag ratio of the Rocket Bomber in molecular flow region.

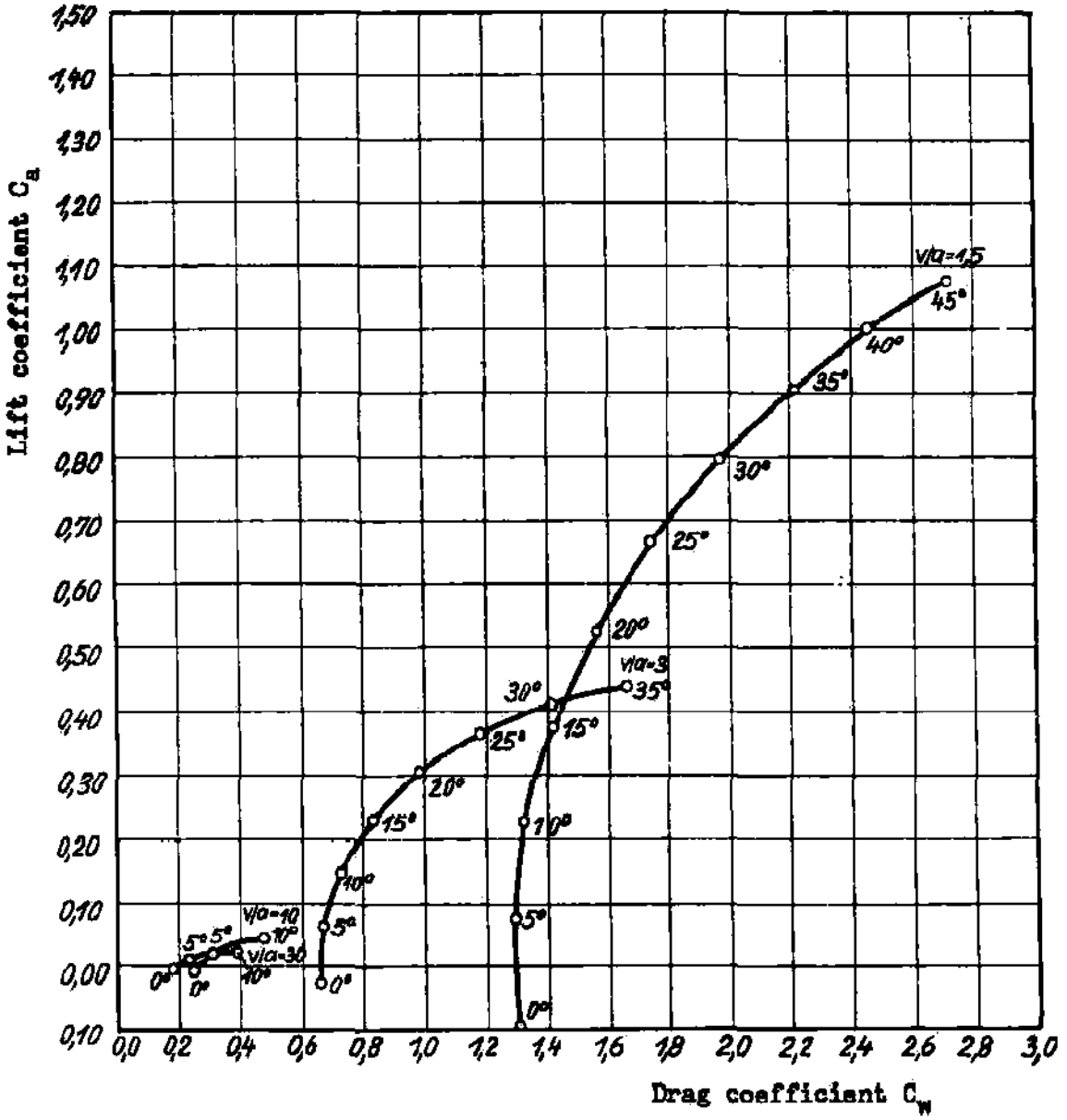

Fig. 49

Polars of the Rocket Bomber in the molecular flow region for various flight velocities.

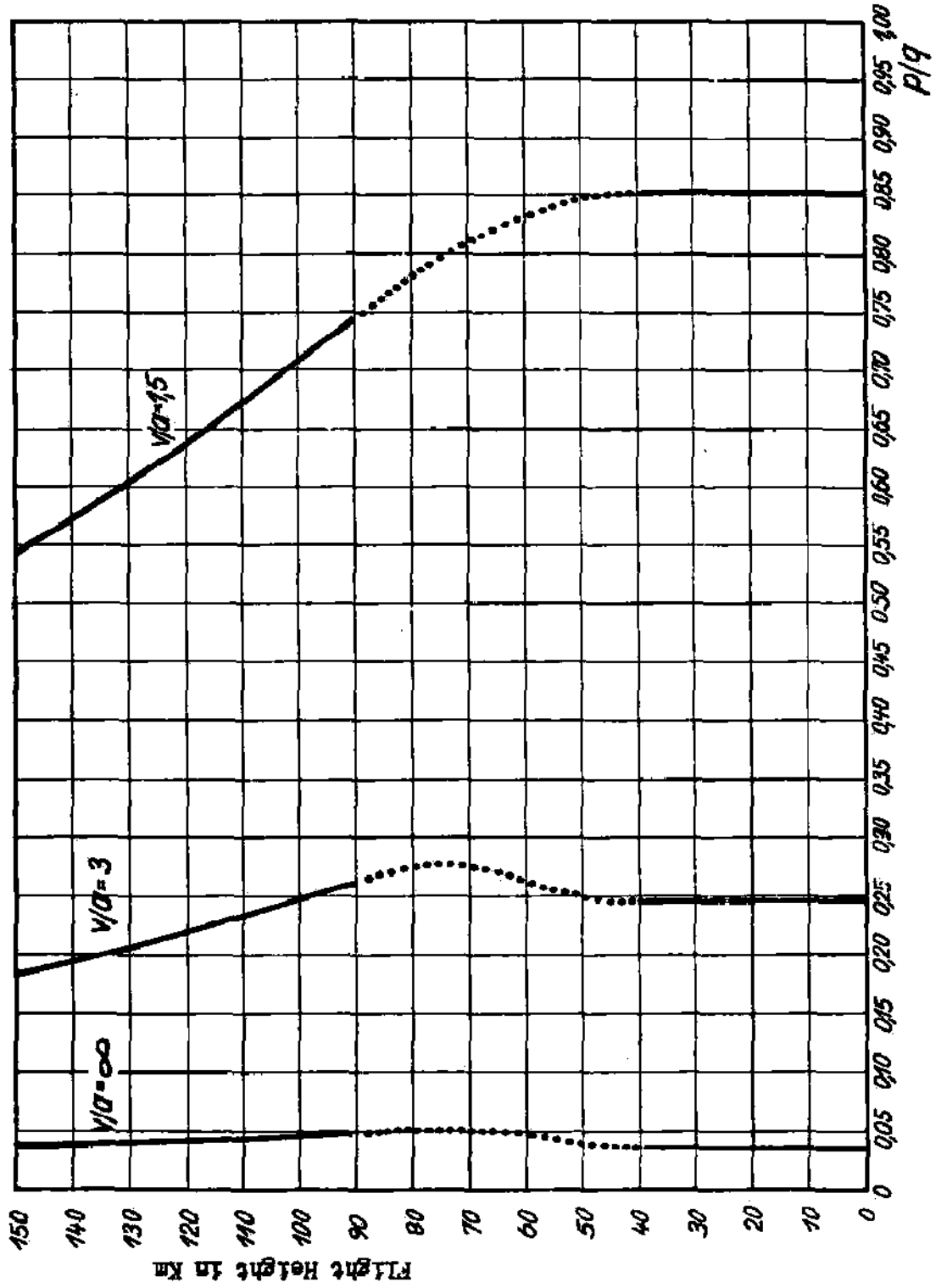

Fig. 50; Behavior of the coefficient p/q of the air pressure perpendicular to a flat plate when angle of attack $\alpha = 7^{\circ}$ as a function of flight velocity and flight altitude (conventional fluid mechanics, molecular flow, and transition region).

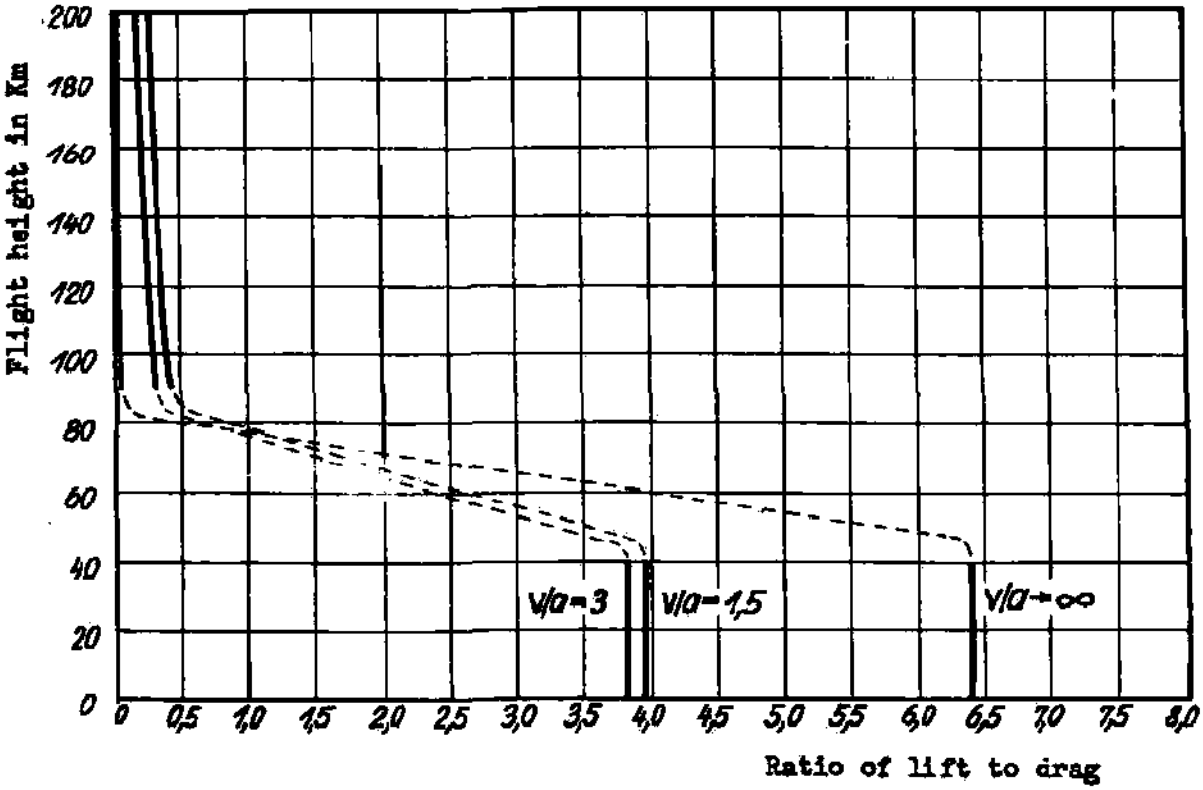

Fig. 51;

Behavior of the best lift to drag ratio of the Rocket Bomber plotted against the flight altitude and flight velocity (conventional fluid mechanics, molecular flow, and transition region).

III. LAUNCHING AND CLIMB

1. Acceleration of the Aircraft

The launching and climb of the rocket bomber have the purpose of giving it, with a minimum of fuel consumption, the high velocity necessary to carry it through its long glide path; they are in the nature of an impulse which lasts only for a few minutes. Despite this, there are various possibilities for the variation of this external force during this short time; we wish to find the most favorable, i. e., the one with the least possible fuel consumption for a given final velocity.

In Fig. 52, the effective exhaust speed c is again taken as a measure of the useful energy content per unit mass of fuel and the attainable velocity increase V is measured in units of c; the fuel consumption $G_0 - G$ is measured in units of the starting weight G_0 or the weight of the accelerated mass G. If one could completely transfer to the accelerating body the energy available from the combustion gases $(G_0 - G)c^2/2g$, which is theoretically possible in firing from a tube, then $V/c = \sqrt{G_0/G - 1}$. This relation for ideal fire is shown as curve 1 in Fig. 52. In the case of rocket drive, the acceleration process, if it was opposed only by the inertial forces of the bomber and not by air resistance, gravity, etc., would after integration of the equations expressing the Conservation of the Center of Mass ($c\,dm + m\,dv = 0$), be represented by the fundamental rocket equation $V/c = \ln G_0/G$. Curve 2 for ideal rocket acceleration thus gives much smaller final speeds for the same fuel consumption. The energy lost to the acceleration process is that of the motion of the combustion gases relative to the place of launching; this is often called the external efficiency of the rocket drive. This fundamental curve for ideal rocket drive gives no indication of the actual accelerations. Actually the acceleration of the bomber occurs against air resistance and at least a component of the weight and these resistances become more important for the smaller accelerations. For example, if one assumes that the air resistance and the component of weight along the path together represent a fixed fraction, say 1/5, of the instaneous weight and that the acceleration is constant during the climb, then one can denote by k the ratio of the rocket thrust reduced by the resisting forces to the effective thrust; from the equation $k c\,dm + m\,dv = 0$, one then derives a modified rocket equation $V/c = k \ln G_0/G$. If one takes the rocket thrust to be equal to the instaneous weight, then $k = (1 - 0.2)/1 = 0.8$ and the curve for this type of drive has the equation $G/G_0 = e^{V/0.8c}$ or $V/c = 0.8 \ln G_0/G$. This curve for K = 0.8 is shown as number 3 in Fig. 52. In practice one does not obtain this curve if the aircraft starts with customary small speed at the ground, because for the assumed accelerations the aerodynamic forces would increase much too quickly for subsonic velocities. Curve 4 shows the climbing process for a commercial rocket plane with high requirements of safety and convenience, i.e., small takeoff and landing speeds, and small, practically constant accelerations along the path of climb; these are taken from a previous detailed calculation of the path. (18) The long, tedious, uneconomical climb until the velocity of sound is reached is shown clearly; we see how costly low velocities at the ground and the accompanying small accelerations are for rocket flight. Curve 5 shows a possible acceleration process under the following assumptions: the rocket thrust is a times the initial weight G_0 and stays constant over the whole path of climb; thus the acceleration increases with the decreasing mass of the rocket up to a value determined by the weight of the crew and the aircraft, and the rocket motor is used fully. Thus the weight loss per second is constant and equal to $a G_0 \cdot g/c$ so that the weight at time t is: $G = G_0(1 - a g t/c)$. By equating the inertial and friction forces (the latter with the same assumptions as for curve 3) to the rocket thrust, it follows that $V/c = \ln G_0/G - a(1 - G/G_0)/a$. This calculation is shown in Fig. 52 for three values of $a = P/G_0 = 0.25$, 1.0 and 10. In the curve for $P/G_0 = 0.25$ the acceleration increases from 0.5 m/sec^2. to 25 m/sec^2. Because of the small acceleration the curve deviates noticeably from that for ideal rocket drive. For the case $P/G_0 = 1.0$, in which thrust and initial weight are equal, the accelerations vary between 10 m/sec^2 and 100 m/sec^2, and the curve approaches most closely that for ideal rocket drive. Finally for $P/G_0 = 10$, the thrust is ten times the initial weight, the accelerations lie between 100 m/sec^2 and 1000 m/sec^2, which is certainly way beyond humanly bearable limits. Thus the very great effect of the acceleration process on the final velocity attainable with a given G/G_0 is clear.

The curves for $P/G_0 = 1$ and 10 are based on such reasonable assumptions that noticeably more favorable types of launching could hardly be found; thus more detailed study of the processes of takeoff and climb under these assumptions is advisable. The two curves differ only in the accelerations during the climb. The usable accelerations are limited only by the strength of the aircraft and by human resistance. From our present knowledge of the physiological behavior of the man under high accelerations one must admit that an unmanned rocket aircraft can be driven at somewhat higher accelerations than a manned craft; nevertheless, the unmanned craft also soon reaches the point where greater accelerations are compensated for by the greater construction weight necessary for craft capable of undergoing large accelerations. In addition the rocket

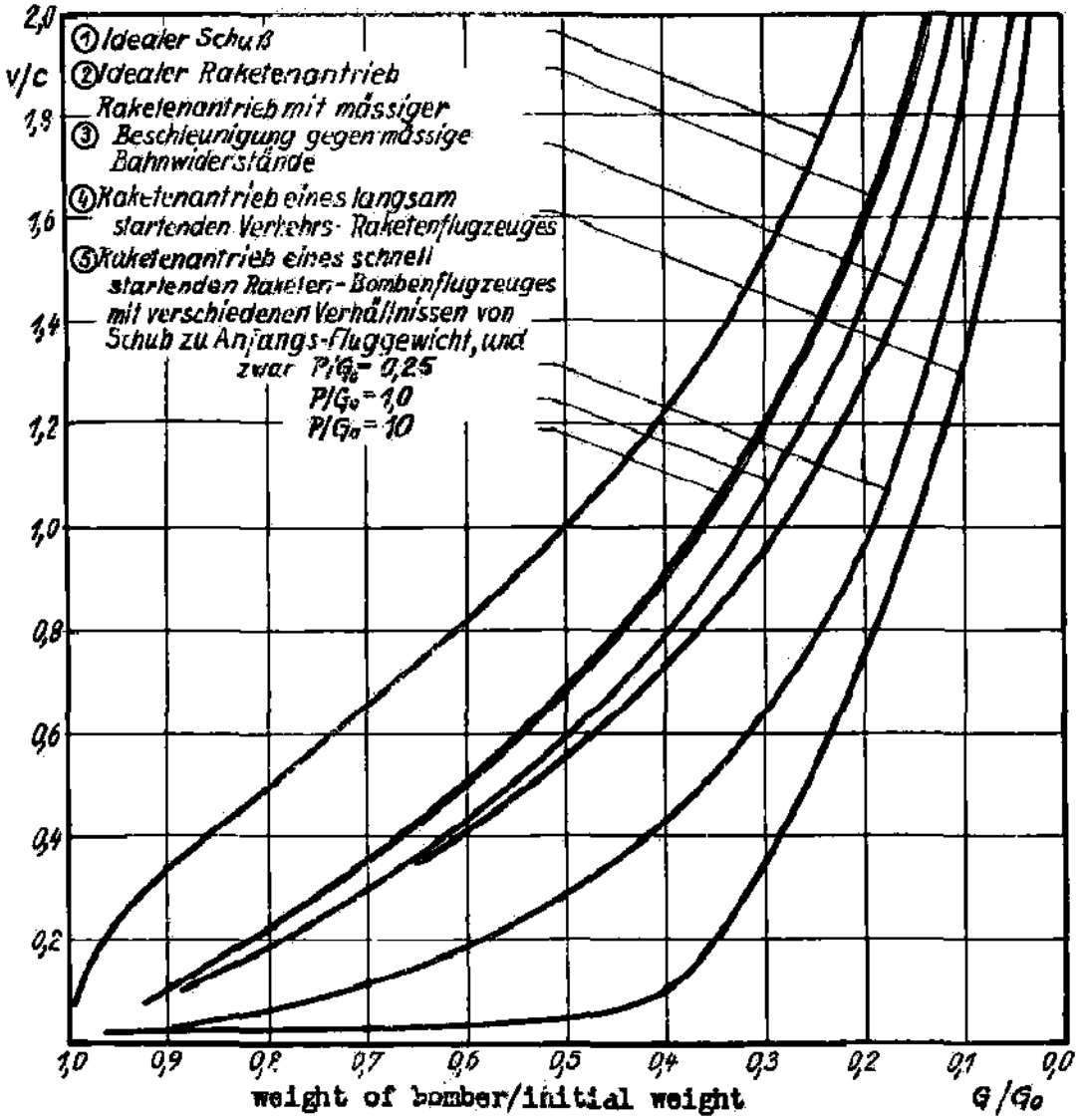

Fig. 52; Reference curves for the Rocket take-off.

(1) Ideal trajectory "shot"
(2) Ideal rocket take-off
(3) Rocket take-off with moderate acceleration against moderate path resistance
(4) Rocket take-off of a slowly starting commercial rocket plane
(5) Rocket take-off of a rapid starting rocket bomber with various ratios of thrust to initial weight

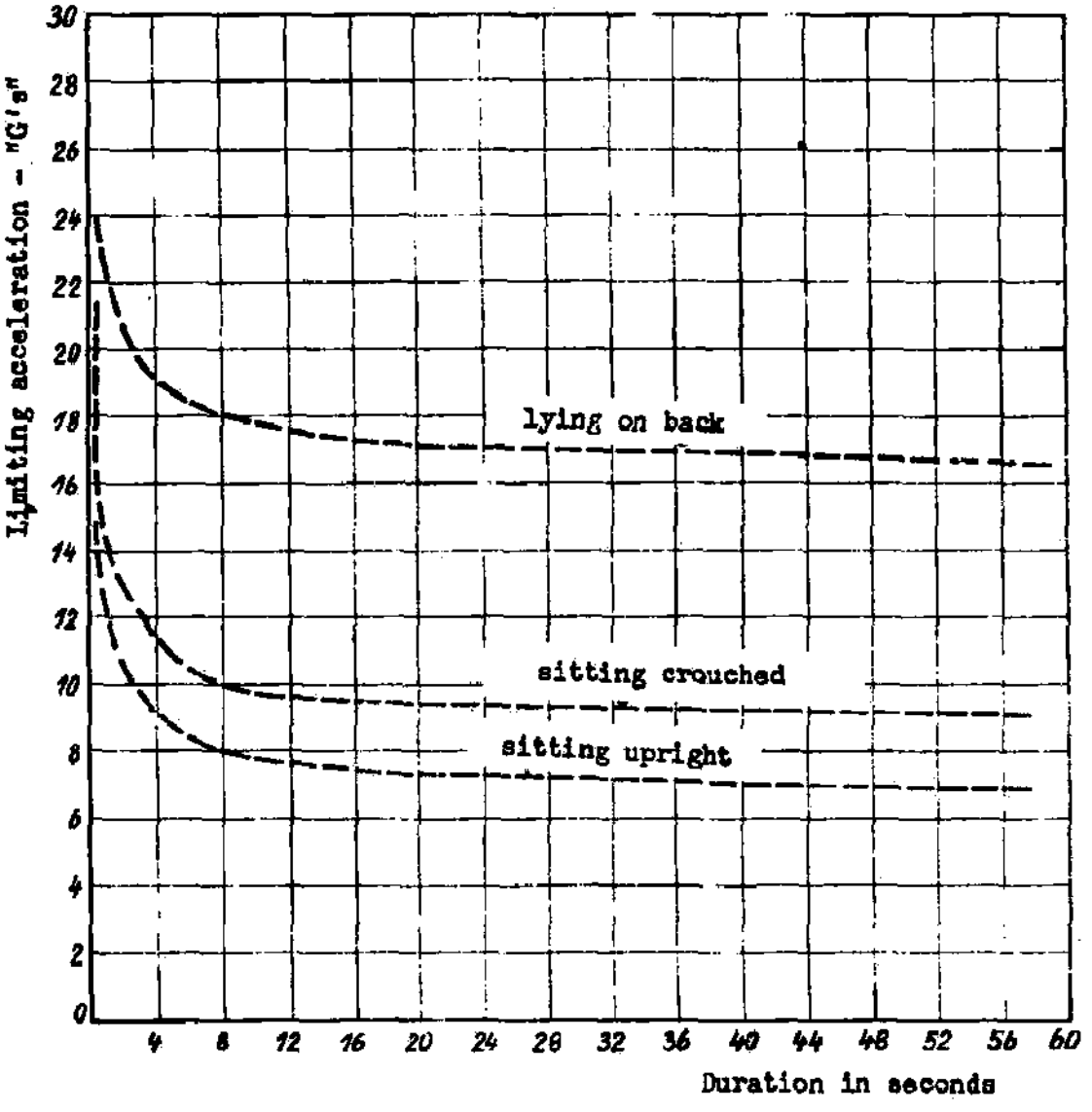

Fig. 53;

Limits of accelerations withstood by trained pilots in terms of "G's" as a function of time of duration

bomber, because of its long range and the accurate navigation necessary for the bomb release, cannot do without a pilot on board. Thus the permissible accelerations are limited to values that can be withstood by trained flyers.

In Fig. 53 are shown the results of most recent studies (2, 12, 15, 31) on the highest accelerations that are bearable by a man in different body positions, as a function of the length of the acceleration time. Whereas in the sitting position the limit is determined by disturbanc of the circulatory system especially caused by loss of blood from the brain or heart due to differences in hydrostatic level inside the circulatory system, this danger decreases in the lying position, and the limit then seems to be set by difficulties in breathing as a result of greatly increased weight of the thorax. This more favorable lying position is directly achieved in the seating arrangement sketched in Fig. 33, since the accelerations due to the engine are taken up by the pilot in directions perpendicular to the axis of his body. In the lying position in caroussel tests accelerations of 20 g for more than a minute have been withstood by drugged apes, and accelerations of 17 g for more than 180 sec. by men.

During the takeoff and climb of a rocket bomber there are two phases during which the accelerations can reach critical values: the catapult takeoff and the end of the climbing path. The catapult process at takeoff lasts several seconds; the accelerations can be chosen freely, the acceleration starts rather suddenly, keeps its top value for about 11 sec. and then stops again suddenly. Adjustment of the circulatory system is thus scarcely possible. Because of this impulse and rather long action, one cannot go beyond an acceleration at takeoff of more than 5 g, even for the favorable perpendicular position. Also higher takeoff accelerations, though they result in economizing on starting-rockets by decreasing the run on the ground, are unfavorable as regards flight performance, since they necessitate stronger construction of the tank assembly. Conditions are quite different at the end of the climb. During the climb the accelerations increase in the ratio G_o/G as the result of decreasing mass of the aircraft for constant motor thrust. Even if the aircraft flies without payload, this ratio will end up at 10. This climbing process lasts several minutes, with the greatest acceleration occuring in the last second. The body has plenty of time to adjust itself to the high accelerations, and the highest accelerations last for only a short time. The conditions are thus very favorable, and the effect of the high acceleration on flight performance is also favorable. One can, therefore, go closer to the limits of resistance and, in view of the perpendicular position of the pilot, permit accelerations of 10 g.

For the assumed $G/G_o = 1$, this means that the factor g equals 1, i.e., the motor thrust equals the initial weight. The limiting acceleration of 10 g is of course not reached if the bomber varries cargo. E.g., if it has only 5 tons of bombs on board, then $G/G_o = 0.15$ and the limiting acceleration is 6.67 g. For $P = G_o$, the acceleration at the start of the climb is 1 g, and increases in say $t = c/g \cdot (1 - G/G_o) = 340$ or 360 sec. to 6.67 g or 10 g respectively if we use the relation $b = g/(1-gt/c)$ which neglects frictional forces. The last increase from 6.67 g to 10 g thus occurs in the very short time of 20 seconds. Only during these last 20 sec. is the pilot subjected to the critical accelerations, after he has become accustomed to the high acceleration gradually and uniformly during the previous 340 sec.; furthermore, this holds only for the practically unimportant case where he takes off without bombs. With this the assumptions concerning permissible accelerations during climb seem justified.

2. Catapult Takeoff

The rocket bomber is to be brought to a takeoff speed of 500 m/sec by means of equipment on the ground, in order to increase as much as possible the final velocity attainable with the fuel on board, to minimize the difficulties associated with the initial wing loading of 800 kg/m^2, and to eliminate the uncertain flight characteristics of the airframe in passing the velocity of sound. For this purpose a catapult-like, perfectly straight, horizontal starting-track several kilometers in length is needed; on this sits a sled, which carries the aircraft, and which is driven by rocket apparatus having a large thrust but moderate exhaust speed. Fig. 54 shows a schematic of the sling arrangement. The downward forces acting along the takeoff path are the weight of the bomber with sled and starting rockets, about 150 tons; in addition there are large forces acting vertically upwards or in the direction of the path due to driving and retarding actions respectively. These forces and the necessity for very precise installation of the slide-rails suggest the construction of the roadbed out of reinforced concrete, whose cross-section for the single-track arrangement chosen has the isosceles triangle shape shown in Fig. 54; the base of the triangle serves to fix the structure in the ground, while the sled carrying the aircraft rides on the apex of the triangle. The upper construction of the rail arrangement consists of the main rail lying on top of the wall, which has to take up the perpendicular forces and also transmits the very large horizontal retarding forces, and of two lead-rails halfway up the wall, which support only occasional small forces, and which prevent rotations of the whole system of aircraft plus sled around its longitudinal axis. Lubricants of the proper viscosity are used on the main-

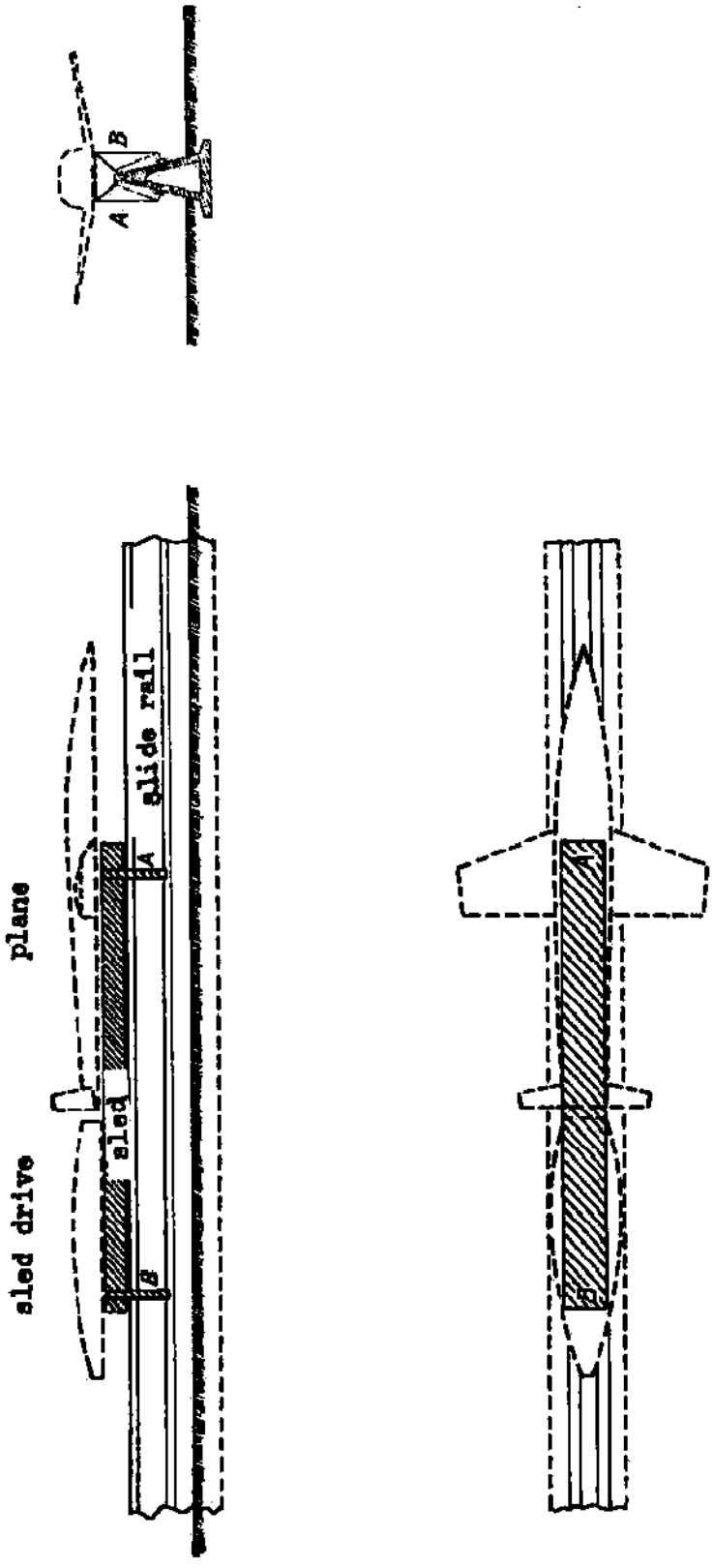

Fig. 54; Starting sled of the Rocket Bombers

and lead- rails, so that the sliding faces of the sled can glide on them with little friction. The sled itself is mounted on the sliding faces at A and B and also has a pair of fittings to prevent overturning. The aircraft to be catapulted sits up front on the main body of the sled, the sled's power plant is at the back, behind the aircraft. The high takeoff thrusts are transmitted to the aircraft through the main body of the sled. Very high thrusts of 610 tons for 11 seconds and the utmost safety in operation are required of the starting rockets, while their exhaust speed can be moderate since they do not affect the flight performance of the bomber. In the use of 40 tons of fuel for starting, one will not, for reasons of safety and cost, use the selfacting fuels like powder or H_2O_2, which are customary for moderate exhaust speeds, but rather the fuels consisting of two materials, say liquid O_2 and gasoil-water emulsion, are preferable. For the calculation of the catapult process, we shall take, as exhaust speed of the ground-based starting rockets, C = 1500 m/sec, so that the fuel consumption per second is P/c = 4000 kg/sec. The weight of the whole apparatus, for constant starting thrust P is $G_s = G_{os} - Pt/c$ at any instant. The air resistance of the whole catapult system is estimated to be 75,000 kg for $\frac{V}{a} = 1.5$, and increases during the takeoff according to the equation $W = 0.3\,V^2$. The sliding friction of the sled on the takeoff rail is completely negligible compared to the two forces mentioned. Using the second law of motion we can write for the acceleration at any moment during takeoff: $dv/dt = g(P - 0.3v^2)/(G_{os} - Pt/c)$

If we require that the acceleration at the end of the takeoff shall not exceed 50 m/sec^2, then we obtain for the constant starting thrust P value of 610,000 kg if the final weight of the take-off mass is 105,000 kg. By integrating once, we obtain a relation between time elapsed and velocity attained $t = G_{os}/3990\left[1 - \left(\frac{428 - 0.3v}{428 + 0.3v}\right)^{2.48}\right]$

For V = 500 m/sec we obtain for the time of takeoff: $t_1 = 7.37 \times 10^{-5} G_{os}$; the law of consumption of the takeoff rocket yields a second relation: $G_s = 105000 = G_{os} - Pt_1/c$ from which t_1 = 10.96 sec and G_{os} = 148700 kg. The total path length can be obtained most simply by numerical integration. Summarizing, these relations concerning the takeoff process give the results that: the takeoff rockets develop a thrust P = 610 tons for 11 sec, use up 43.7 tons of fuel with c = 1500 m/sec if the system to be catapulted weighs 105 tons, the length of the tow path is 2750 m; and that the accelerations during towing increase from an initial value of 40.2 m/sec^2 to the permissible limit of 50 m/sec^2 at the end of the takeoff; thus for approximate estimates one may use an average acceleration b = 45 m/sec^2 and calculate all the other quantities; e.g. $t = v/b = \frac{500}{45} \doteq 11$ sec and $s = \frac{1}{2} b t^2 \doteq 2750$ m.

Fig. 55 shows the dependence on length of path of the velocity V attained and the residual weight G; also given are some of the data concerning the sliding jaws of the takeoff-sled. The two sliding jaws at A and B can be assumed to be of bronze or hard steel and have a square jaw-surface of 0.25 x 0.25 m; they are a sort of self-adjusting bearing-plate in Michell bearings, and are movable about a hinged edge; the flat undersurface of the jaw is bent up at the front end to assure the flow of lubricant to the edge. From Gumbel - Everling (7, P. 150/151) one obtains, for a square sliding jaw of side length t, if the point of application of the force corresponds to the safest thickness of lubricating layer ($\chi_1 = 0.8$), some fundamental equations; e.g., the coefficient of friction is $\mu = 2.37\sqrt{\eta v/pt}$, where p is the average pressure P/t^2 on the jaw; the minimum thickness of lubricating layer is $h_0 = 0.30\,t\sqrt{\eta v/pt}$, and the angle of tilt is $\alpha = 0.37\sqrt{\eta v/pt}$.

From these, $\mu = 7.97\,h_0/t$ i.e., the minimum gap h_0 between the sliding jaw and the rail surface, which make an angle α with each other, should be kept as small as possible to permit large loads P to slide with little frictional resistance. In the desired state of pure liquid friction, h_0 is limited by the roughness of the sliding surfaces; for the long sliding surfaces of the takeoff track which is subject to rough handling and all kinds of weather, we may expect values of 10^{-4}-10^{-3} m. Thus the minimum gap-height h_0 to assure dynamical buoyancy of the jaws is $h_0 = 10^{-4}$ m, with $\mu = 0.00316$. The largest section-loading ever experienced by the jaws is p = 75000/625 = 120 kg/cm^2; during takeoff this drops to 4 kg/cm^2. From the previous equations we see that minimum thickness h_0 (and the minimum μ) can always be maintained, if the viscosity η of the lubricant, decreases in the same manner as V/p increases; i.e., if $\eta v/p$ is constant. At the start of the motion of the sled, the sliding speeds are so small that there is no η sufficiently large to keep the product constant. In this case, the flat surface of the jaw will lie flat on the surface of the rail and will rise to the angle α only as the velocity increases. Fig. 55 shows the residual part G-A of the weight G which rests on the jaws at any moment; it is assumed that the buoyance A varies quadratically with V from A = 0 for V = 0 to A = 100 tons for V = 500 m/sec. Thus $P = \frac{G-A}{2}$ and the required lubricant viscosity at any position on the track is $\eta' \doteq 11.1\,P h_0^2/v t^3$. η' is the viscosity of the hot oil in the film for minimum thickness h_0. The rise in temperature ΔT of the oil film can be estimated by assuming that all the work against friction goes to heat the oil. Because of the very brief duration of this heating process, the heat conduction from the oil will be extremely small. From $APfv = th_0 v\gamma c_s \Delta T$ it follows that the heating is independent of the velocity; taking values of

$\gamma = 900$ kg/m^3, $c_s = 0.5$ kcal/kg°, ΔT is $0.000834\,P$

so that as P decreases it drops from 60° to about 2° C at the end of the catapult process, as shown in Fig. 55. If we assume an external temperature of + 15° C, then at the end of the tow path a lubricant is required which has a viscosity of $\eta = 0.00002$ at +17° C; e.g., benzine, water, petroleum; three meters from the beginning of the takeoff we need a lubricant with $\eta = 0.1$ at 75° C; this requirement is satisfied by pitch. In between there is a whole range of possible lubricants. In the first three meters of the slide, pure liquid lubrication will not be possible; one will have to use graphite-pitch mixtures. The equations given are valid only for moderate sliding speeds; actually the velocity of motion reaches a final value of 500 m/sec which is 1/3 the velocity of sound in the lubricant; because of this we may expect a great increase in the coefficient of friction, but no physically different friction phenomena, especially since the high velocities are accompanied by small pressure on the sliding jaws. The proper lubrication of the 3 km long surface should be maintained and protected by a special lubricant carriage which runs the full length of the track, along the rails. The brake arrangement at point B can be modelled on that of a railroad; i.e., cast-iron jaws are pressed onto the braking surfaces of the rail; after the aircraft rises the forces are released and the empty sled is brought back to rest as quickly as possible.

To test the basic feasibility of sliding at high speeds, R.Schmid has made tests on the sliding of projectiles along curved metal walls lubricated with vaseline. The experimental arrangement consisted of a drawn-steel tube of 10 mm inner diameter, which was slit along its axis to produce a U-shaped groove. This channel was bent into a closed circle 8 m. in radius, so that the surface of the channel was toward the outside; then the projectile sliding in the channel is kept there by centrifugal force. Through a branch tube which was tangent to this circle, an sS projectile was fired from a German 98 K, and into the circular path. The bullet ran through the circular path several times till it was brought to rest; after the test it was found lying completely unharmed in the channel (Figs. 56, 57, 58)*. The thin copper plating of the steel was, in most tests, rubbed off at the position of the maximum diameter; the steel surface showed isolated scratches apparently caused by filings and burrs along the slide-path. Immediately after finding it, the bullet was still warm to the touch. Also it was compressed in cross-section; this is probably caused by the fact that the spinning of the bullet stops after a short time and then the centrifugal force, which is initially 100 kg, causes the lead core to flow. After cessation of rotation and slight deformation, the initial point contact with the wall is increased to a surface of about 1 cm^2, so that the 100 kg/cm^2 pressure between the surfaces, which is caused by the centrifugal force, corresponds approximately to that of the sliding jaws of the takeoff sled. Since the sS -bullet is made of lead with a thin soft steel cover, and in the course of its 150 m. sliding path goes through all velocities from 800 m/sec down to zero without being harmed, this experiment may be considered as a proof of the feasibility of construction of sliding jaws for velocities of 500 m/sec; provided the slide-rails are properly constructed and lubricated.

If the accelerations of the aircraft during its launching are to remain within permissible limits for both aircraft and pilot, a launching path of about 3 km. is required, so that it is not possible to use a movable construction which would point the craft toward its target at takeoff. One will therefore install a takeoff track, usable in both directions, so that it points in the most probable directions for attack, say east-to-west; the more precise correction of the direction of flight can be left to the pilot during the very first part of the climb path, where the velocity and acceleration are still sufficiently small to permit such changes of path.

If the bomber rises off the takeoff-sled at 500 m/sec, then its lift coefficient is $c_a = 0.05$, whereas the best glide-number occurs at much larger angles of attack and a lift coefficient $c_a = 0.173$. If one limits the normal acceleration during the first driveless part of the climb-path to 20 m/sec^2, then the initial radius of the turning-path, which goes from the horizontal takeoff direction to the direction of climb at $\varphi = 30°$, is 12500 m. This curved path of turn, which begins at the end of the takeoff is 6540 m. long and ends at an altitude of 1700 m., with the required path inclination of 30° As a result of air resistance and gain in altitude, the velocity at this point has dropped to 370 m/sec, the lift coefficient is $c_a = 0.093$ - still much smaller than the one for optimum glide-number. The bomber then climbs further at an angle of 30°, at the expense of its flying speed until, after a linear climb of 4000 m. to a height of 3675 m. and a velocity V = 284 m/sec, the angle of attack for optimum glide-number is reached; at this moment the rocket drive for the actual climb can begin. During this 25-second-long, undriven motion after takeoff, the path of the aircraft can be turned in the direction of the target. At the same time, this procedure helps increase the range of the bomber over its value if one took off at V = 250 m/sec with optimum glide-number and started the engine immediately after takeoff, because we have gained a slight excess velocity and a few kilometers for the climb.

*These Figs. omitted

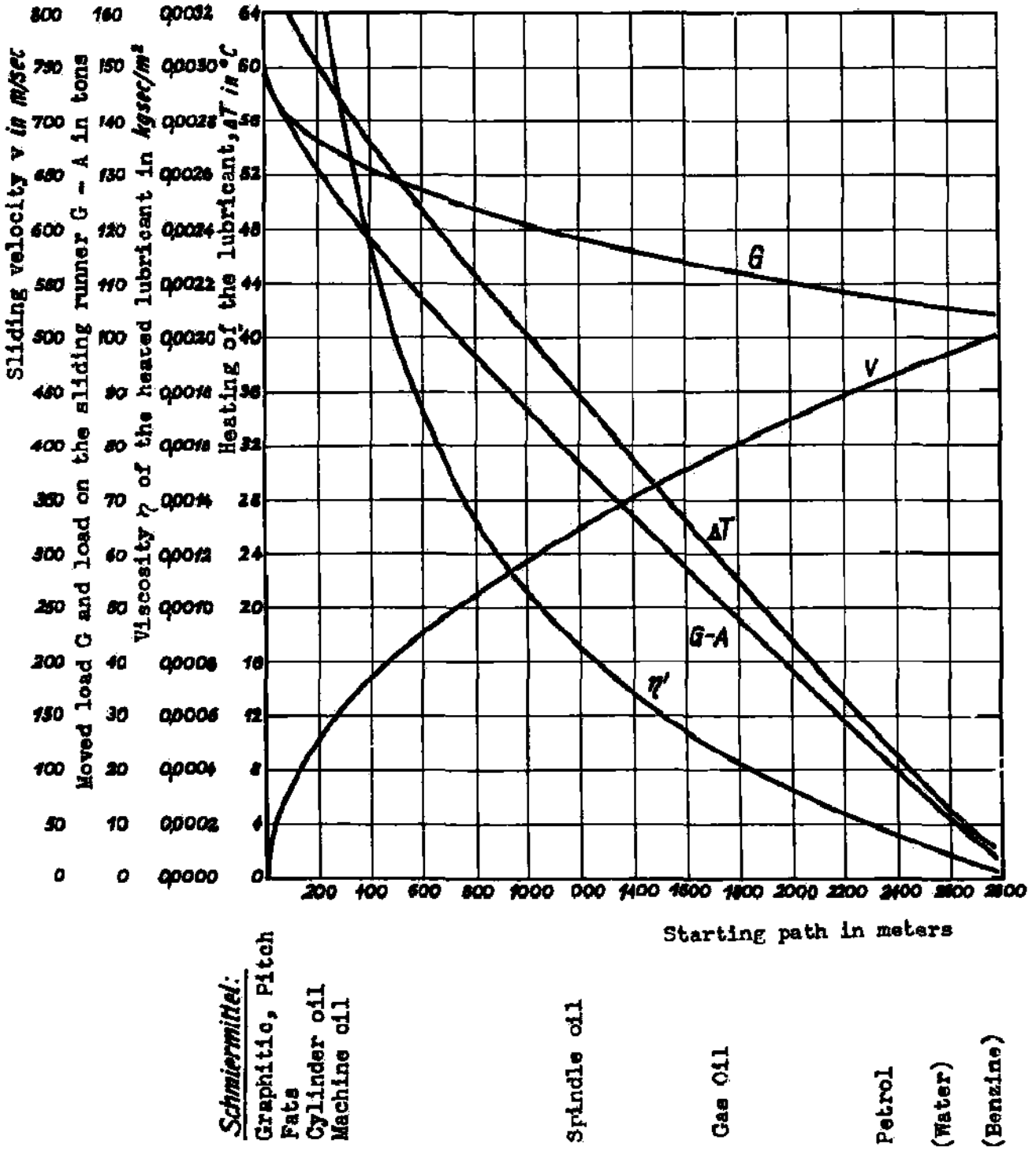

Fig. 55; Gliding velocity v, moved load G, loading on the runners G - A, heating of the lubricating film ΔT, viscosity η of the heated lubricating agent, and practical manner of lubricating for various points along the starting path.

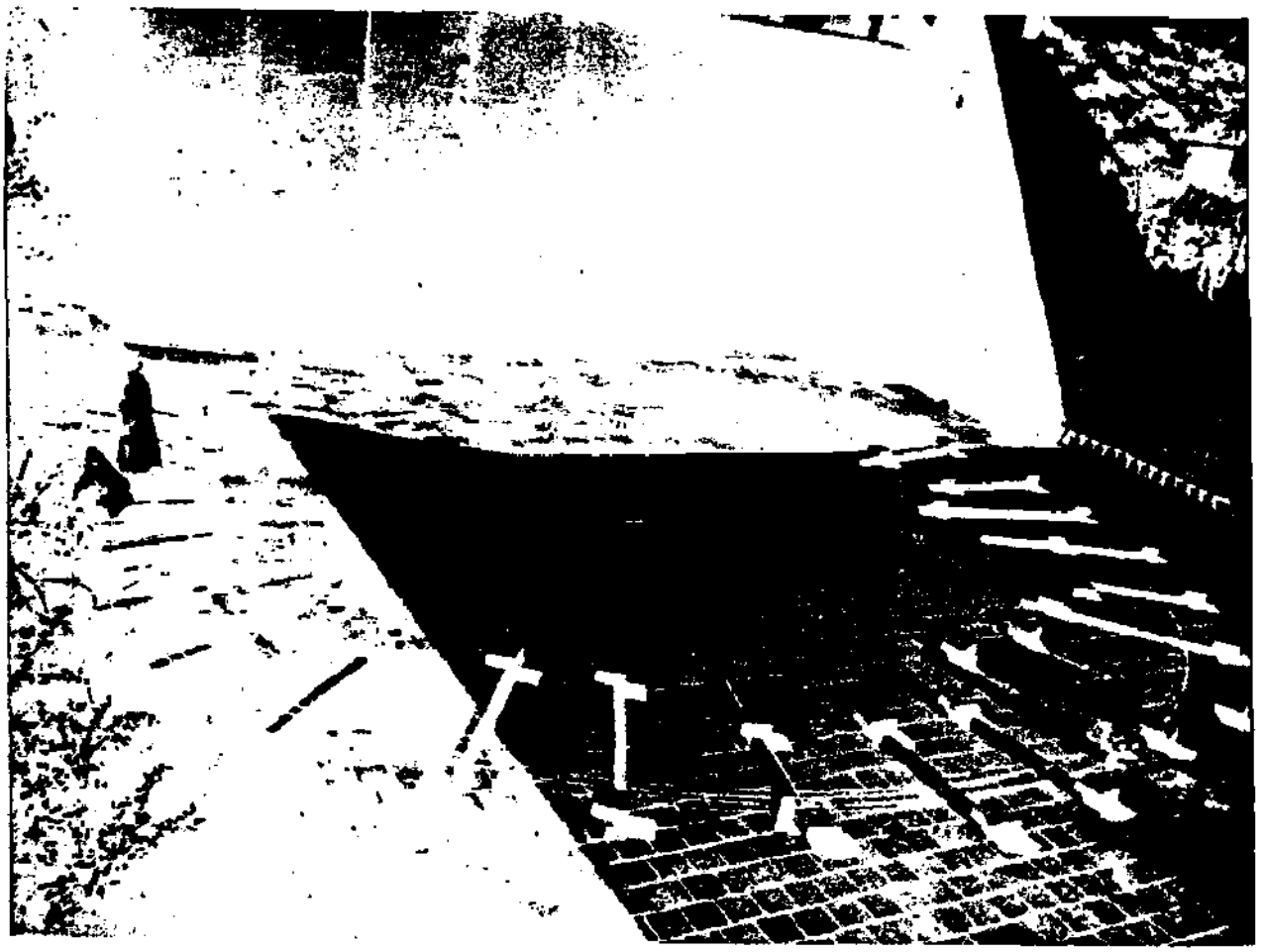

Abb. 56; Versuchanlage für Gleitreibungsversuche bei sehr hohen Gleitgeschwindigkeiten, bestehend aus einem Militarkarabiner 98K und einer mit 5 m Radius gekrummten, geschmierten und geschlossen-kreisformigen Gleitbahn für das sS-Geschoss.

3. Climb Path

The climb path of the rocket bomber is determined by the forces acting on its center mass. If one momentarily neglects the rotation of the earth, these are:

The weight of the aircraft-magnitude $G = (G_0 - P_g t/c)[R/(R+H)]^2$ direction toward the center of the earth.

The aerodynamic lift-magnitude $A = c_a F \rho v^2/2$, direction perpendicular to the tangent to the path and in a plane through the center of the earth;

The air resistance-magnitude $W = \varepsilon A$ in the direction of the tangent to the path;

The thrust of the motor-magnitude P = 100 tons, tilted from the tangent to the path by angle of attack, lying in the plane through the center of the earth and the tangent to the path.

The d'Alembertian inertial force T, equal and opposite to the resultant of the other forces, having a tangential component $m\frac{dv}{dt}$ and a normal component $= Va^2/\rho$.

These five forces all lie in a plane, so that the path is also in a plane.

The rotation of the earth makes the situation more complicated. If the earth's atmosphere were fixed in space, so that it did not rotate along with the earth, then the path relative to the earth's surface could be calculated as if a sixth force, the Coriolis force, having arbitrary direction and magnitude $C = 2[\vec{w} \cdot \vec{v}](G_0/g - F\rho_c)$ acted on the center of mass of the aircraft. Because of its arbitrary direction in space, this force makes the orbit, relative to an observer on the earth, appear to be no longer in a plane. The atmosphere, which actually rotates with the earth, produces dragging forces on the bomber which cause its absolute path also to be twisted, so that the bomber is pulled like a weather vane by the apparent wind developed by the rotation of the atmosphere, and will tend to turn except when it is flying in the west-east direction, as can be seen by considering a flight starting from the pole. This interfering weathervane action will have to be countered by the pilot's steering; i.e., by a seventh force perpendicular to the tangent, if the absolute path prescribed by celestial navigation is to be maintained. In the calculation, it is assumed that the transverse aerodynamic forces excited by the elimination of the weather-vane action do not noticeably alter the glide-number. Since these transverse forces are always perpendicular to the plane of the orbit and only prevent a shift of the aircraft out of the plane, they need no longer be considered in the calculation of the orbit. To illustrate the *the relation between the forces acting on the center of mass, Fig. 59 shows two views of the air*craft during the climb; the line of sight is along the horizon at the level of the aircraft. If all the dependences were available in analytic form, one could introduce suitable space coordinates, resolve the forces along these directions, apply the dynamical equation to each direction and thus obtain three differential equations for the three coordinates of the climb path; the integration would almost certainly be impossible, since the far simpler equations of ordinary exterior ballistics are not. The determination of the relative orbit is much simpler; one proceeds in two steps; first the absolute path is calculated neglecting the Coriolis force (i.e., using the five forces previously listed). Then one calculates separately the turning of the earth's surface below the aircraft. Finally, the two components are combined on the sphere to give the twisted relative path in space. The plane absolute orbit is determined by a step-by-step method which is familiar in Ballistics. (1, Vol. 1, p. 207) As in Fig. 60, the continuously curved path is broken up into a polygon, whose sides are sufficiently short that they can replace the arc of which they are the chord. All the forces acting on the aircraft are combined at the vertices, A, B, C, etc., and along with the inclination φ of the orbit are assumed constant along $\Delta s = \overline{AB}, \overline{BC}$, etc. By setting the resultant force in the tangential direction equal to zero, we obtain $b_1 = g(P\cos\alpha - \varepsilon A_A - G_A \sin\varphi_A)/G_A$

so that the velocity increases in first approximation from V_A to $V_{B1} = \sqrt{V_A^2 + 2b_1 \Delta s}$ in the time $\Delta t_1 = V_B - V_A/b_1$. By setting the resultant normal force equal to zero we obtain $\rho_{A1} = G_A V_{Aa}^2/(G_A \cos\varphi_A - P\sin(\alpha - \lambda_A)g$. The absolute velocity Va_A at the point A can be determined with sufficient accuracy from the velocity of flight V_A and the angular velocity of the point of takeoff. Thus the arc $\overset{\frown}{AB}$ can be drawn, and B, is determined in first approximation. Now that the average value of the inclination and the average force between A and B, are known, one can locate B in second approximation in the same manner. One repeats the procedure at B, often enough so that the orbit is given in analytical or graphical form. The calculations of the orbit by this method were done numerically by A Woyczechowski; the initial conditions were height 3675 m. above sea level, relative velocity of flight 284 m/sec, and inclination of orbit 30°, and the path was studied out to $G/G_0 = 0.1$. The orbit was also calculated for $c = 3000, 4000$ and 5000 m/sec and finally neglecting the earth's rotation, and then with maximum effect of the

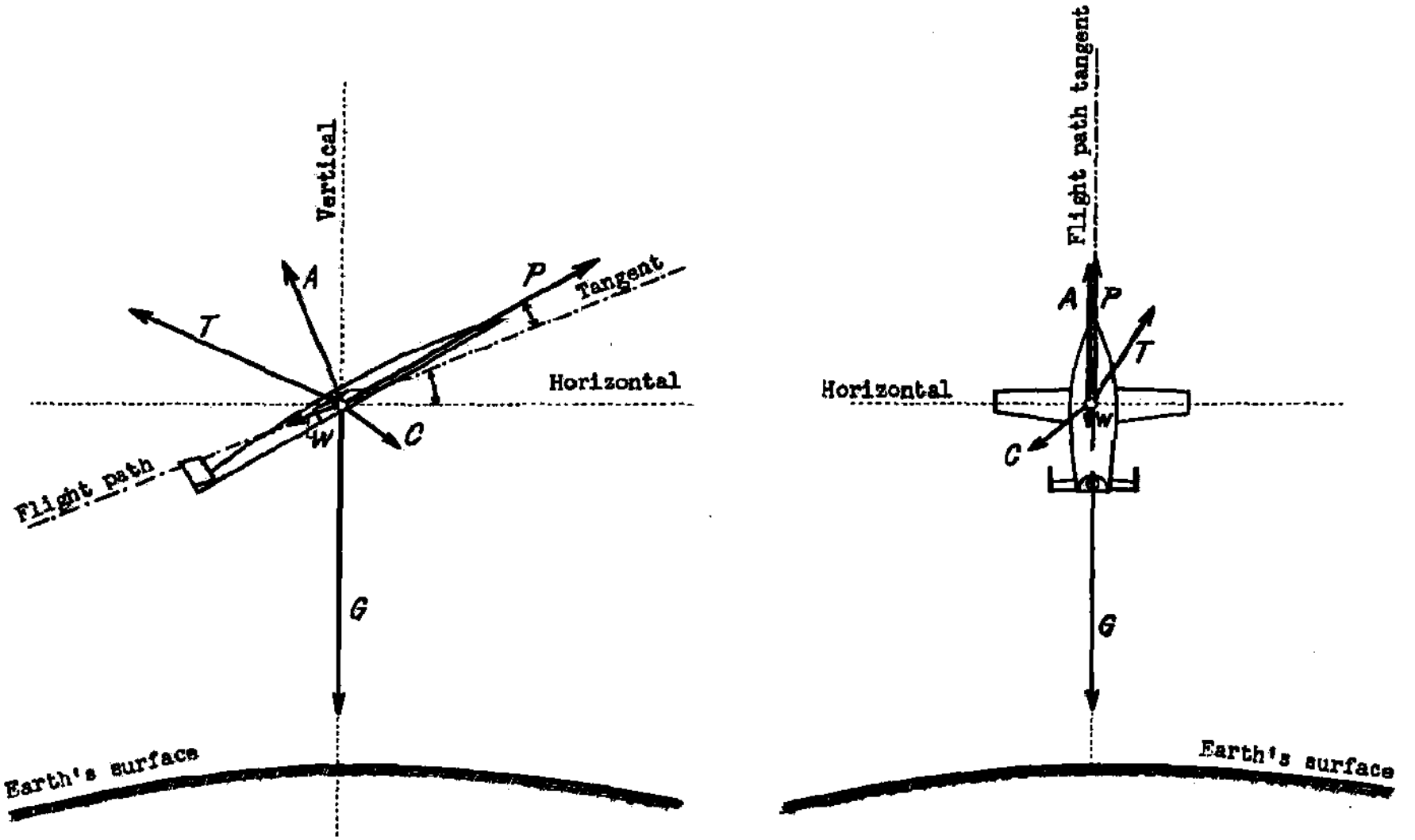

Fig. 59; External forces on the Rocket Bomber in climbing.

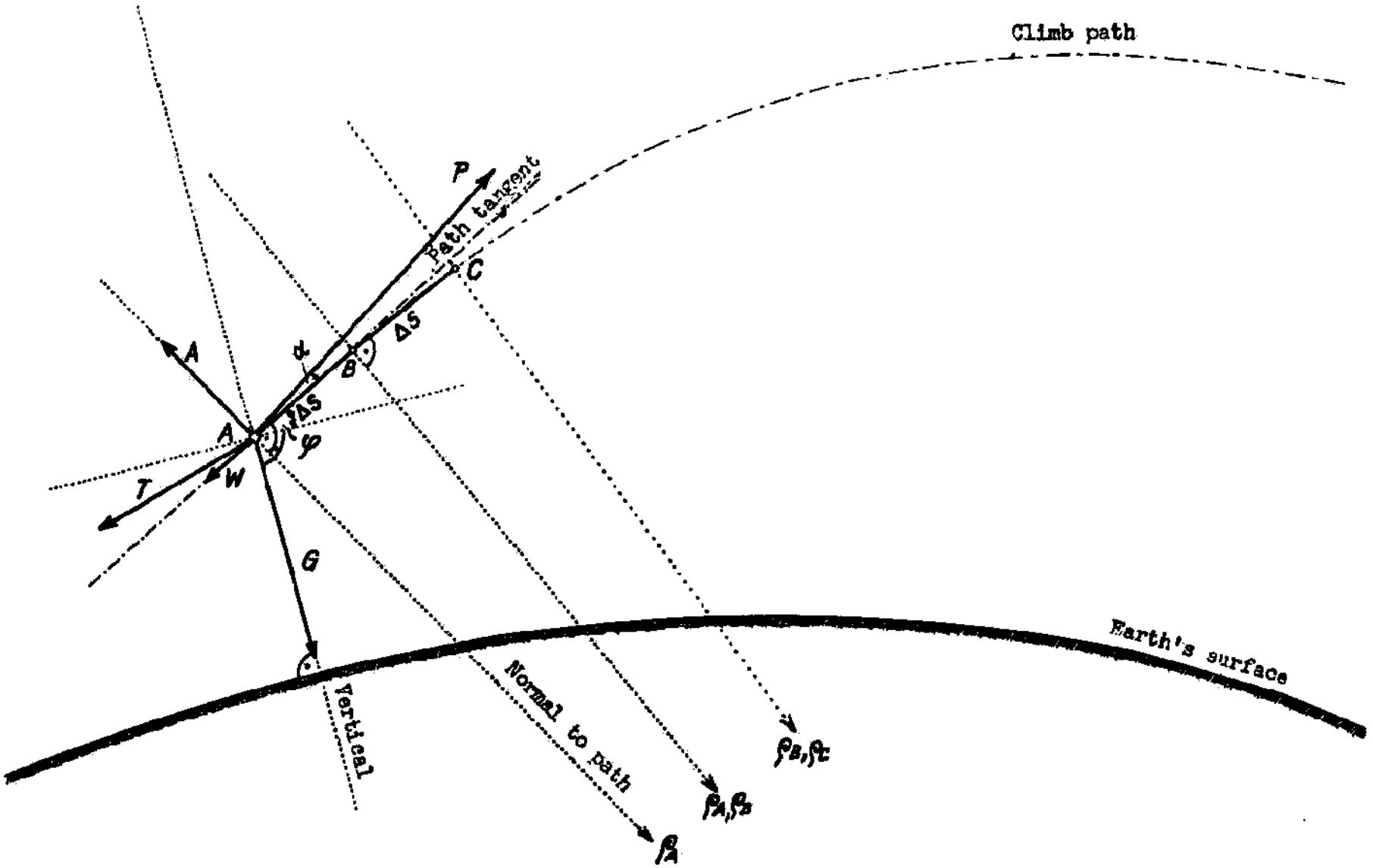

Fig. 60; Approximate graphical solution for the climb path

Exhaust velocity in m/sec	Flight Velocity v m/sec	Instantaneous wt / Initial wt.	Bomb load in tons	Altitude in Km	Horizontal projection of the climb path in Km	Angle in degrees between horizon and the terminal tangent	Axial acceleration m/sec^2	Normal acceleration $in\ m/sec^2$	Elapsed time in seconds
c=3000m/sec	1000	0,60	50,0	37,0	55	+15,5	12,8	-6,8	124
	2000	0,42	31,8	46,5	135	+ 0,4	22,0	-6,7	178
	3000	0,30	20,0	41,5	230	- 4,1	30,4	-4,8	214
	4000	0,22	11,5	36	320	- 3,7	41,0	+3,7	240
	5000	0,15	4,8	34,5	405	+ 1,2	55,8	+37,0	261
	6000	0,10	0,3	40	485	+ 7,3	77,3	+39,1	274
c=4000m/sec	1000	0,69	58,7	33,5	60	+ 8,2	12,1	- 7,1	124
	2000	0,53	43,3	31	150	- 8,1	19,1	- 5,5	189
	3000	0,40	30,5	44,5	280	+7,6	18,3	+26,8	243
	4000	0,30	20,0	47	425	+9,5	28,3	- 2,4	283
	5000	0,23	13,3	68,5	560	+8,1	37,7	- 4,0	313
	6000	0,18	8,0	84	675	+7,4	47,5	- 3,0	333
	7000	0,14	3,8	98,2	785	+7,3	61,3	- 0,8	350
	8000	0,11	1,0	109	860	+7,6	81,6	+ 1,6	362
c=5000m/sec	1000	0,75	65,0	31	60	+3,1	11,5	-7,3	128
	2000	0,62	51,7	18,5	155	-10,6	16,3	+5,0	196
	3000	0,48	37,5	43,5	335	+11,9	16,7	-3,9	267
	4000	0,38	28,1	71	505	+7,3	22,3	-6,3	315
	5000	0,30	20,1	87,5	665	+4,4	28,8	-5,8	351
	6000	0,25	15,0	98,5	830	+2,9	34,8	-5,1	380
	7000	0,20	10,5	106	975	+2,6	41,0	-4,1	404
	8000	0,17	6,5	112,3	1135	+1,8	49,5	-2,9	424
	9000	0,14	3,5	117	1275	+2,0	60,3	-1,3	440
	10000	0,11	1,0	121,5	1400	+2,3	73,3	0,4	452

Numerical characteristics for three various climbing paths of the Rocket Bomber.

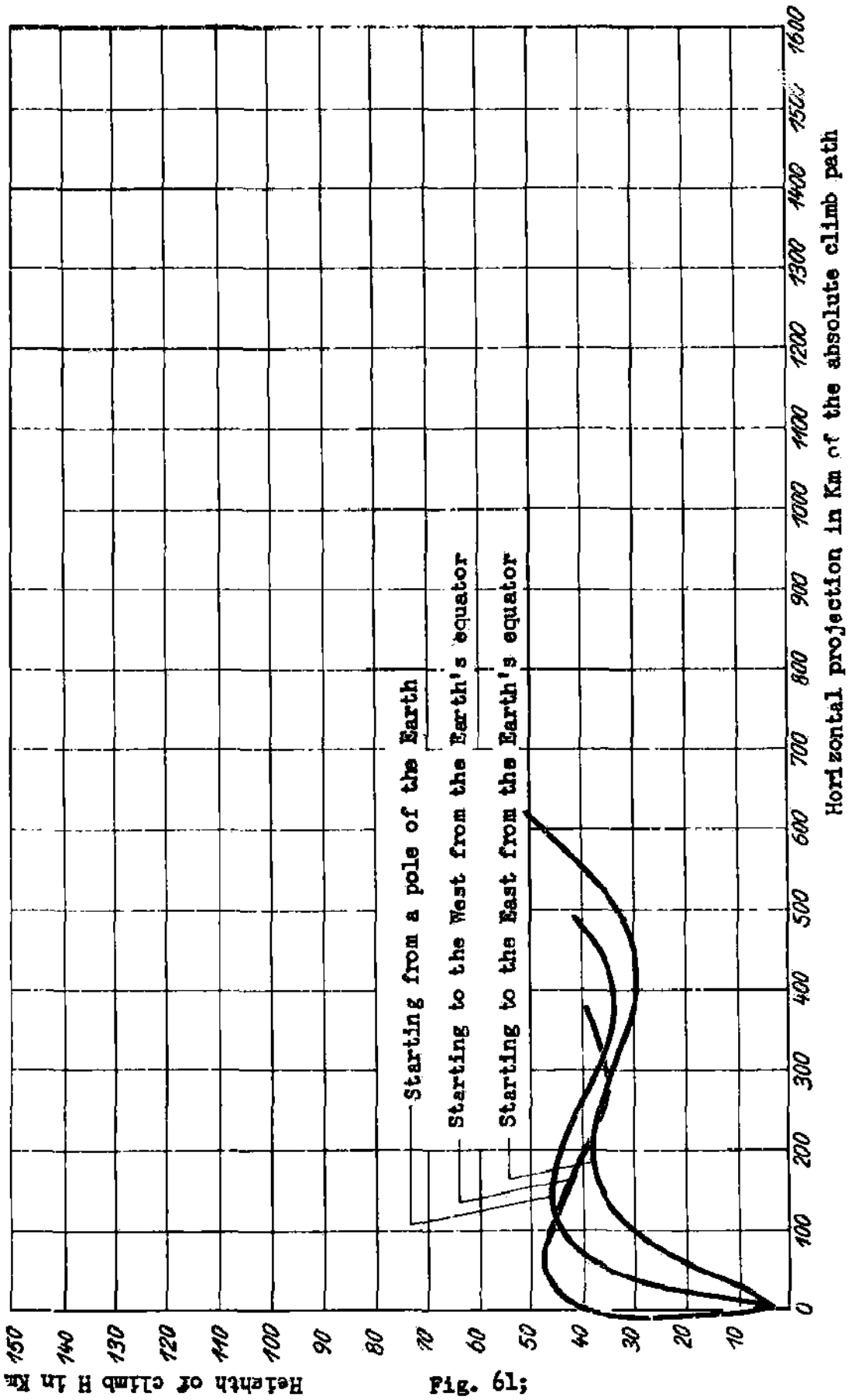

Fig. 61;

Absolute climbing path of the Rocket Bomber with c = 3000 m/sec, without consideration of the Earth's rotation, but with consideration of rotation velocity of a point on Earth's equator, launch to East and launch to West.

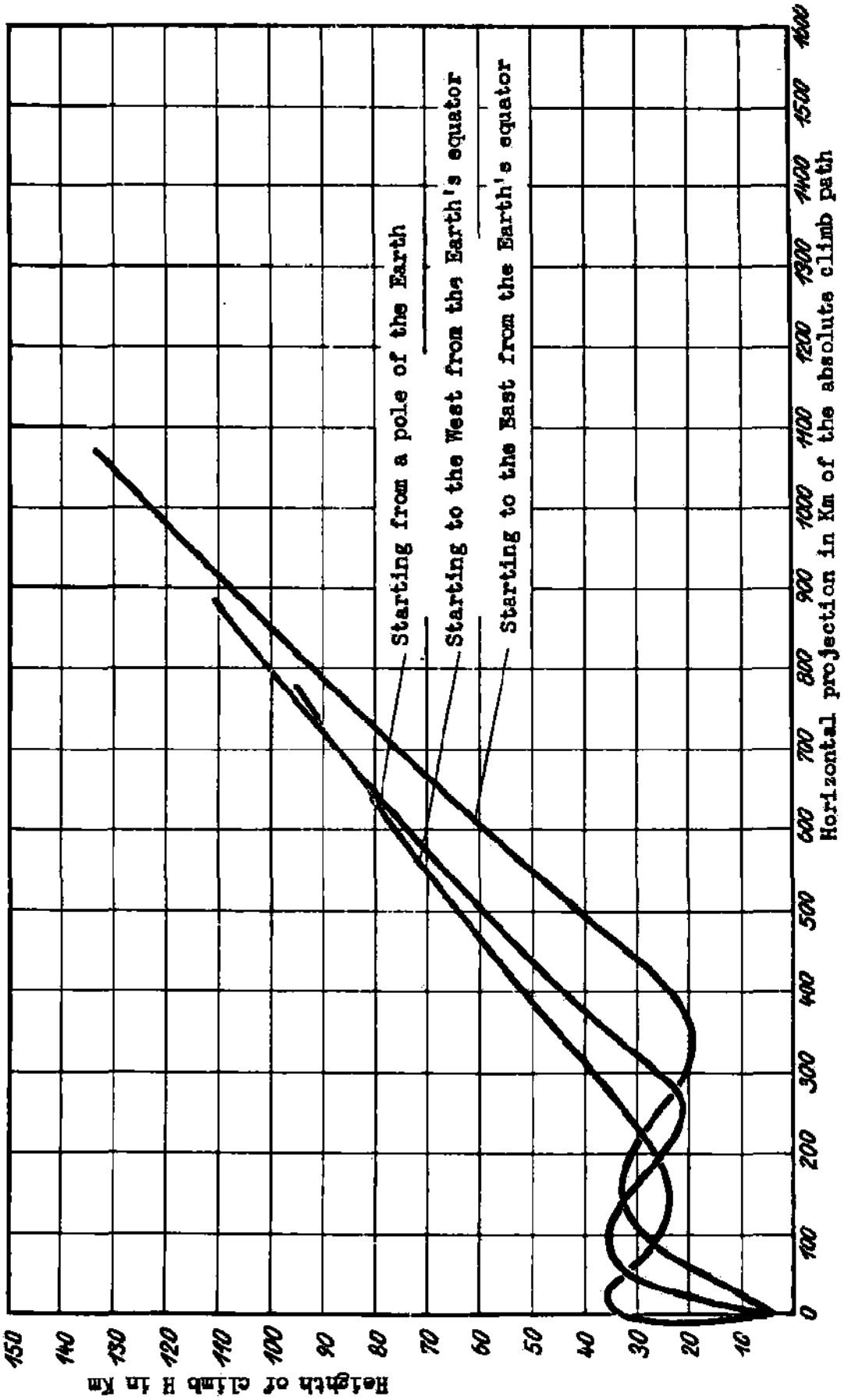

Fig. 62: Absolute climbing path of the Rocket Bomber with c = 4000 m/sec, without consideration of the Earth's rotation, but with consideration of rotation velocity, of a point on Earth's equator, launch to East and launch to West.

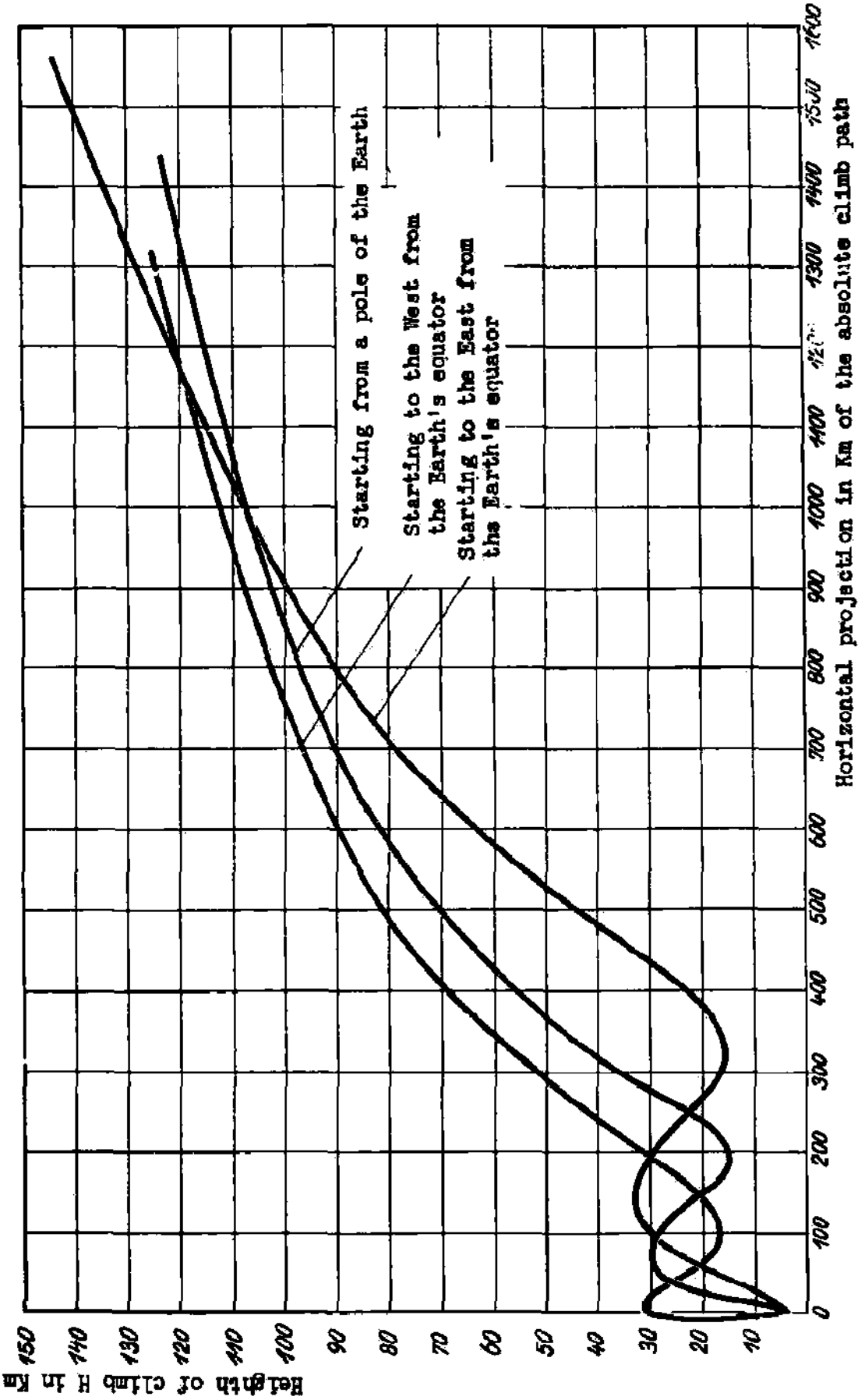

Fig. 63: Absolute climbing path of the Rocket Bomber with c = 5000 m/sec, without consideration of the Earth's rotation, but with consideration of rotation velocity, of a point on Earth's equator, launch to East and launch to West.

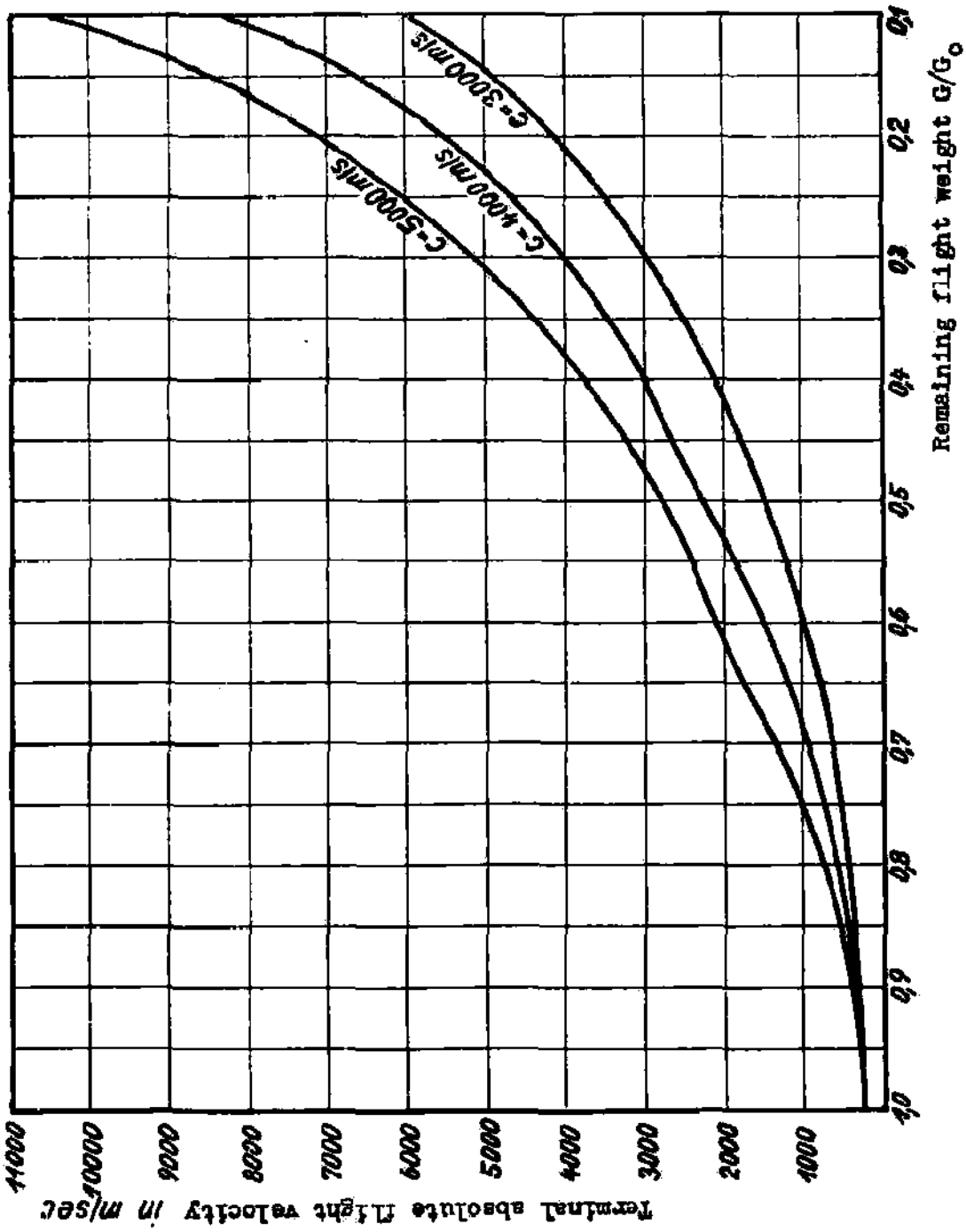

Fig. 64: The absolute flight velocity of the Rocket Bomber attained during climb with c = 3000, 4000, and 5000 m/sec as a function of G/G_o, and without consideration of Earth's rotation.

rotation - i.e., takeoff from the equator in an easterly or westerly direction. The following figures show some examples of the results; Fig. 61-63 show the shape of the absolute orbit, Fig. 64 shows the velocities reached. Table III gives a summary of the most important results for all the orbits, neglecting the earth's rotation.

A fairly accurate estimate of the final velocity, which is the most important datum for the climb path, can be obtained without doing the exact calculation of the orbit, by using the equation $V/C = \ln G_o/G - q(1 - G/G_o)$ This is especially so if one fits the actual conditions by setting q (ratio of total air resistance plus weight component along the path to instantaneous weight) equal to 0.5 in the range $G/G_o = 1.0$ to 0.5, and $q = 0$ for $G/G_o = 0.5$ to 0.1. If one carries out this rough calculation for the bomber with 100 ton takeoff-weight and 10 tons empt, weight, for various exhaust speeds C, assuming initial velocity 284 m/sec, one finds that for C = 4000 m/sec the bomber reaches the velocity of a long-range projectile even with a 50-ton bomb load, so that it can compete with long-range artillery; without payload it exceeds the velocity V = 7900 m/sec. Between these two extremes lie all sorts of velocities and bomb loads. An interesting result which is easily obtained, is that in the range of bomb loads suitable for military use, i.e. 5-40 tons, the exhaust speed has little effect on the final speed. This means that the development of a rocket bomber does not have to wait for availability of rocket motors with C = 4000 m/sec; with C = 3000 m/sec one can already construct a very dangerous weapon.

Figs. 65 and 66 compare this rough calculation to exact orbit calculation and to the curve for ideal rocket propulsion; the initial velocity after takeoff is included. One sees that the rough estimate gives the actual behavior with sufficient accuracy, especially for large values of C; also the final velocities actually attained, especially with large bomb loads, are far below those for ideal rocket propulsion, because the weight component in the direction of propulsion is comparable to the thrust for the initial steep climb, and because of the rather high air resistance during the climb. The propulsion curve could thus be improved by lessening the resistance or increasing the propulsive forces. A lowering of the initial angle of climb φ would decrease the harmful weight component, but would result in great increase in air resistance in regions of dense air - we can expect no success from this procedure. Another possibility might be a great increase in the thrust during the initial part of the path, so that, say, the tangential acceleration is constant in the range of the permissible limit 10 g, and the resisting forces are half the instantaneous weight initially and then drop to zero below $G/G_o = 0.5$. The rocket motor would have to start with a thrust of 1000 tons, and then be throttled gradually to 100 tons at the end of the climb. Taking $V = 284 + 0.95C \ln G_o/G$ for $1.0 > G/G_o > 0.5$ and $V = 284 + 0.659C + C \ln G_o/26$ for $0.5 > G/G_o > 0.1$ we get the results shown in Fig. 67. While the 100-ton rocket motor weighs 2500 kg, one must assume a weight five times as great (i.e., 12500 kg) for a well-regulated motor with 10 times greater maximum thrust. If, despite the more powerful motor, all other weights of the bomber remain the same, then the empty weight would be 20000 kg. instead of 10000 kg; i.e., the most favorable G/G_o would be 0.2, and the bomb load would already have dropped to zero at $G_o/G = 5$. The propulsion curve shown in Fig. 67 for 10-ton empty weight would, for the now necessary 20-tons, move considerably to the right; despite the increased difficulties with the regulable 1000-ton motor one would achieve only a slight improvement for short distances of attack, while the 100-ton motor would still be superior for long range attacks. Thus the second method for improving the propulsion curve also fails in practice, and the curves of climb shown in Figs. 65 and 66 represent the best solution of the problem.

The rocket bomber, at each moment of its flight, tends toward that part of the atmosphere where the buoyant forces are equal to its weight. If this equilibrium position is such that the altitude stays constant for a few seconds, it will be said to be stationary. Such a stationary equilibrium occurs, for example, if the aerodynamic driving force A of the bomber, increased by the centrifugal force F, which for flight at constant altitude is a consequence of the earth's curvature, is equal to the instantaneous weight G of the bomber.

During the climb the thrust component $P \sin\alpha$ also acts as a buoyant force. For example, starting with a weight in flight, $G_o = 100$ tons, at altitude $H_o = 3500$ m, and $C_{a_o} = 0.2$, by equating the weight to the propulsive force, we can obtain for the horizontal velocity a value $V_o = \sqrt{2gG_o/c_{a_o}\delta F} = 300$ m/sec. At any other altitude, if we set the weight equal to the buoyant force $c_a \rho v^2 F/2g + Gv^2/gr = G$ we get a one-to-one relation between altitude and velocity. This relation is shown in Fig. 68, for C = 4000 m/sec. We see that these stationary altitudes are low, below 60 km for velocities up to 7000 m/sec. If we include the vertical component, $P \sin\alpha$ of the motor thrust of 13920 kg, we get the upper curve. It is interesting to note that for V = 4700 m/sec., the curve becomes vertical; i.e., no stationary equilibrium is possible at finite altitude as soon as V = 4700 m/sec. In the first curve the stationary equilibrium is no longer attainable above V=7900 m/sec. These assumed stationary states probably do not exist in flight. In particular, the center of curvature of the path is seldom at the center of the earth so that the altitude would remain constant - most of the time it is near the earth's surface, and at times it is even above the aircraft; also the radius of curvature is usually much less than the radius of the earth. As a result strong transverse dynamical forces are developed, which permit "dynamical" equilibrium of the bomber at heights far above the stationary ones.

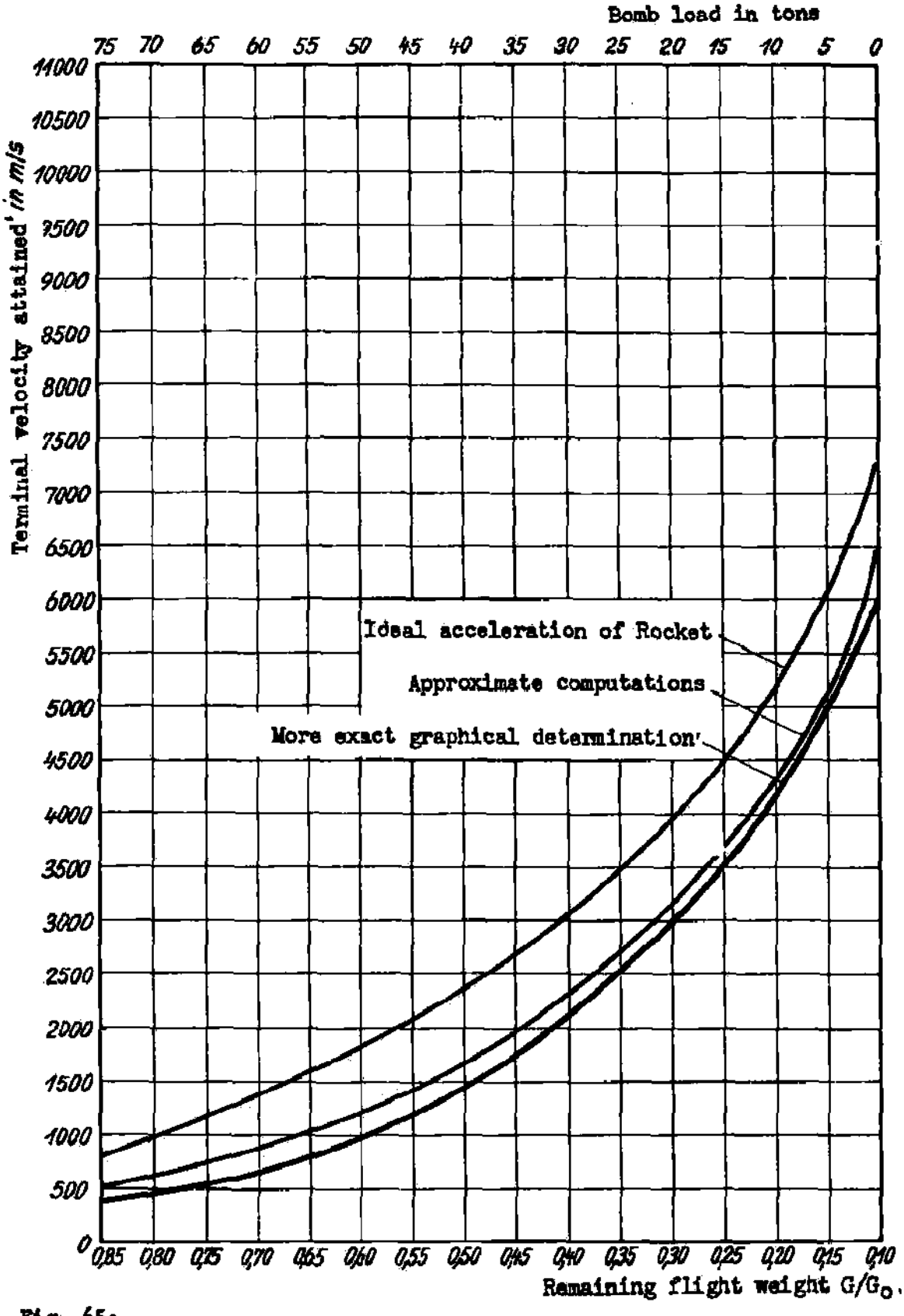

Fig. 65:

More exact determination of the relationship between bomb load, terminal velocity of the Rocket Bomber attained for v = 3000 m/sec and v_0 = 284 m/sec by means of the graphical determination of the course. For comparison are plotted the approximate calculations and the curve for ideal Rocket acceleration.

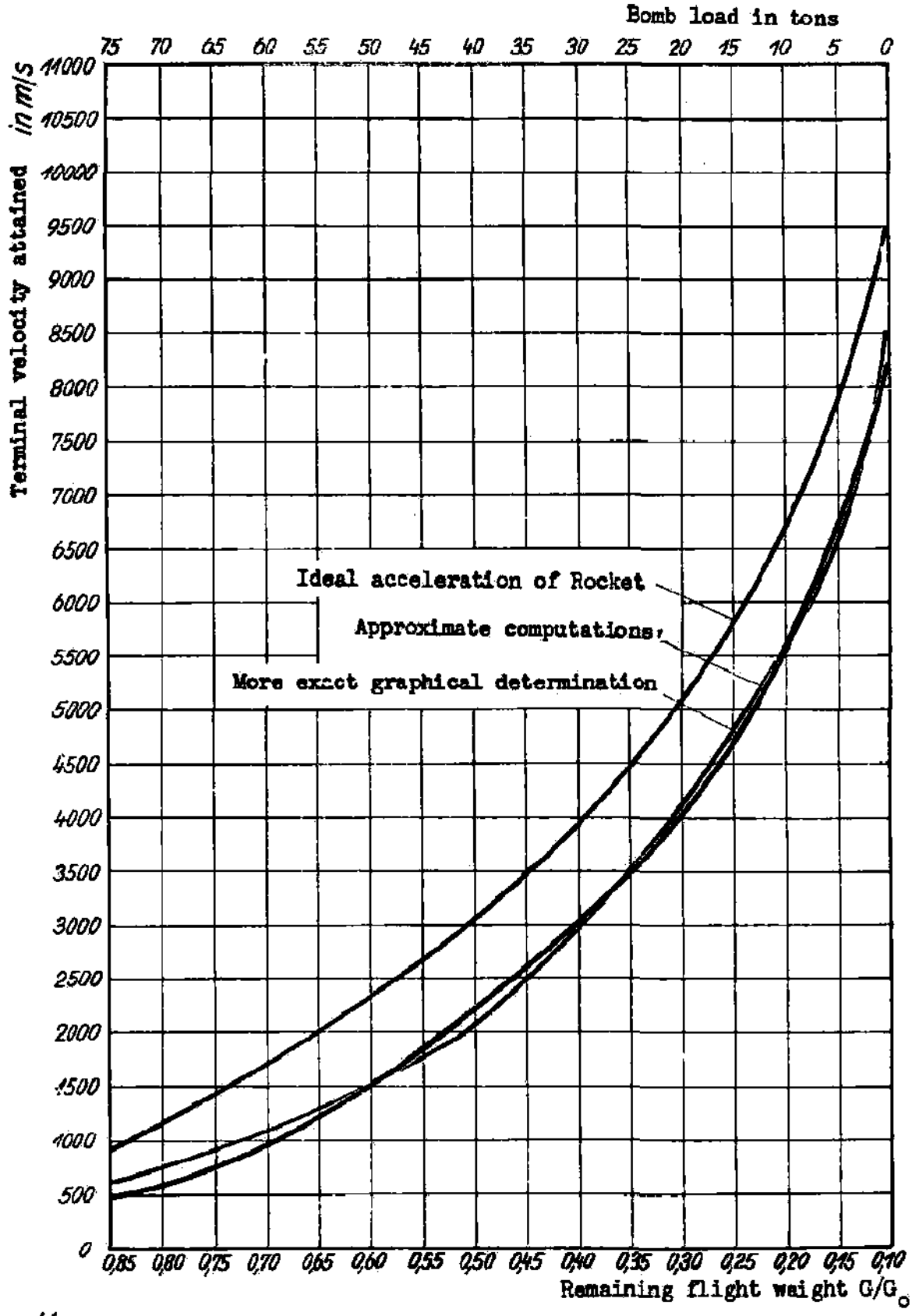

Fig. 66:

More exact determination of the relationship between bomb load, terminal velocity of the Rocket Bomber attained for v = 4000 m/sec and v_o = 284 m/sec by means of the graphical determination of the course. For comparison are plotted the approximate calculations and the curve for ideal Rocket acceleration.

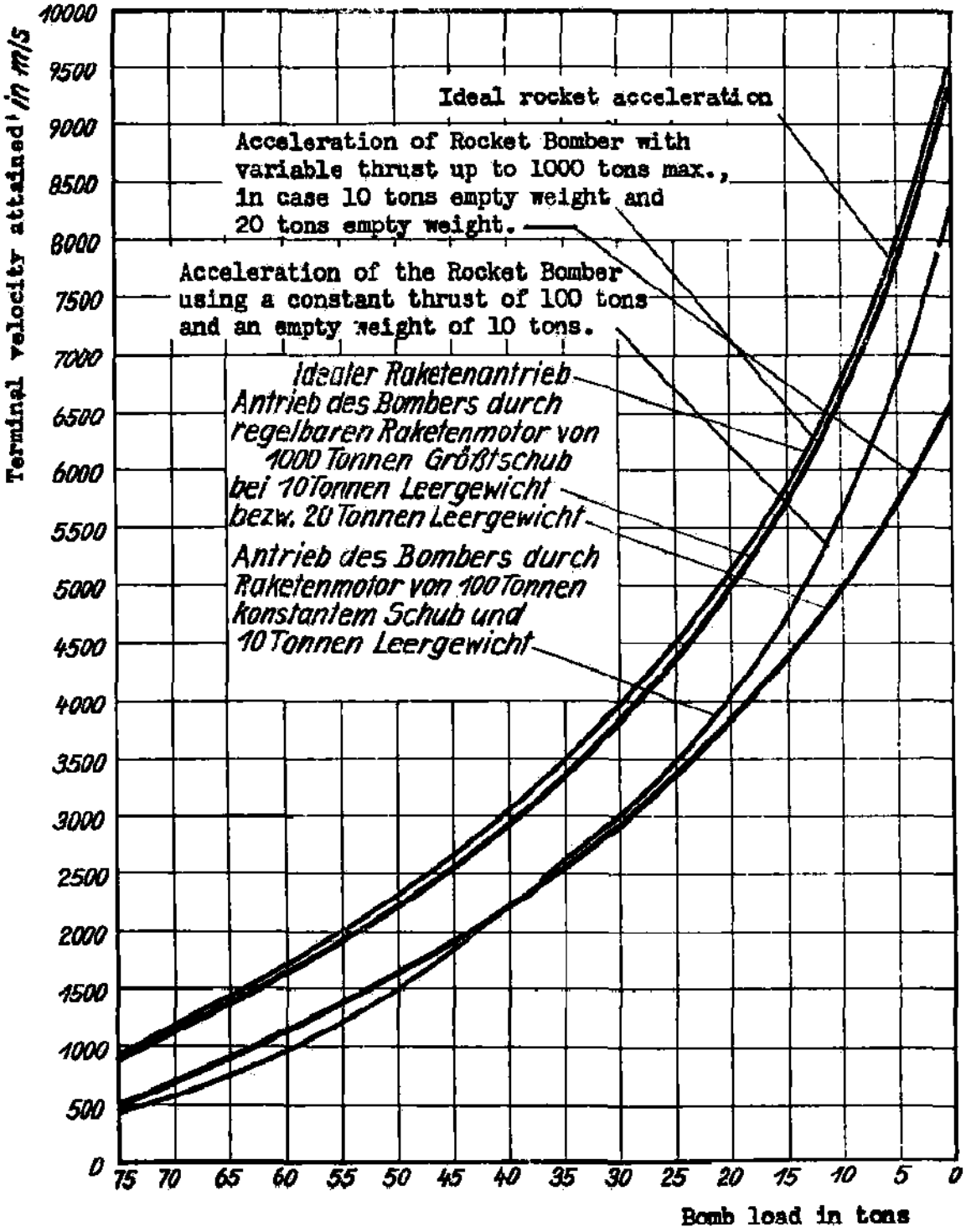

Fig. 67:

Climb of a Rocket Bomber whose thrust is adjustable between 100 and 1000 tons, i.e. high almost constant acceleration with c = 4000 m/sec exhaust velocity.

The actual heights oscillate about the stationary ones, with very large amplitude, while the additional dynamical forces tend to bring the aircraft back to the position of stationary equilibrium; i.e., they are restoring forces pointing toward the stationary position and increasing with distance of the aircraft from it, like spring-forces. The number of oscillations; for the example shown in Fig. 68, is not quite 2 for the whole climb; this is shown by the following consideration.

At first, the stationary altitude is greatly exceeded. This results from the fact that initially the air density decreases more slowly than the increase in velocity, so that the aircraft takes on a very steep position at angles $\varphi = 45°$ or more. Already at fairly high velocities, the aircraft must now be turned through more than 45° from this position to that of horizontal flight. Because of the small radius of curvature available, this results in powerful centrifugal forces, which drive the aircraft up above the stationary equilibrium heights of 40-60 km, to heights over 100 km. One might now expect that the aircraft would immediately drop down again from these extreme altitudes, since the path is approaching parallelism with the earth's surface, and the radius of curvature is approaching the value of the earth's radius. This drop from the heights initially attained occurs only in slight degree, if at all, because in the meantime the velocity has increased very rapidly, and is already near the value $V = 4700$ m/sec for which the altitude of stationary equilibrium of the bomber becomes infinite. At this speed, the bomber is in stationary equilibrium at every altitude, so that it does not have to fall. If it exceeds $V = 4700$ m/sec, then it suddenly finds itself below the altitude of stationary equilibrium, so that it has an excess of buoyant force, and begins to climb again so long as the propulsion continues. This actual curve of climb is obtained from the exact calculation of the orbit, and is shown in Fig. 68. The whole climb may be considered as dynamic flight only in a limited sense. For the most part it follows an inertial path, like that of a projectile or a heavenly body, at heights which are practically in empty space, since one can no longer speak of an atmosphere in the sense of aerodynamics when the molecular free paths are greater than several hundred meters. Fig. 69, obtained from exact orbit calculations, shows the actual dynamical altitudes attained during the climb of the rocket bomber.

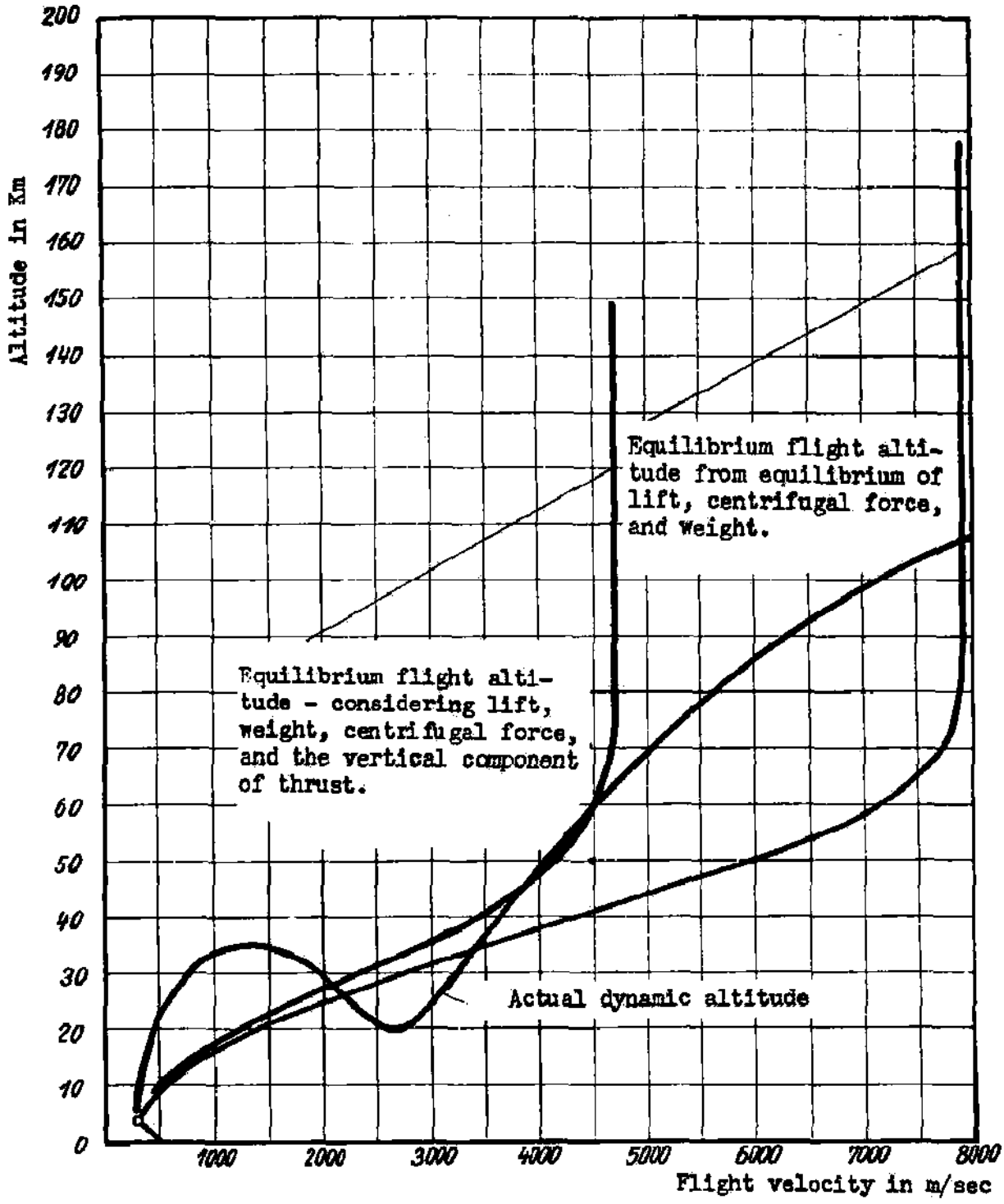

Fig. 68:

Comparison of stationary (i.e. instantaneous equilibrium) and actual, dynamic flight altitude when the Rocket Bomber is climbing with c = 4000 m/sec.

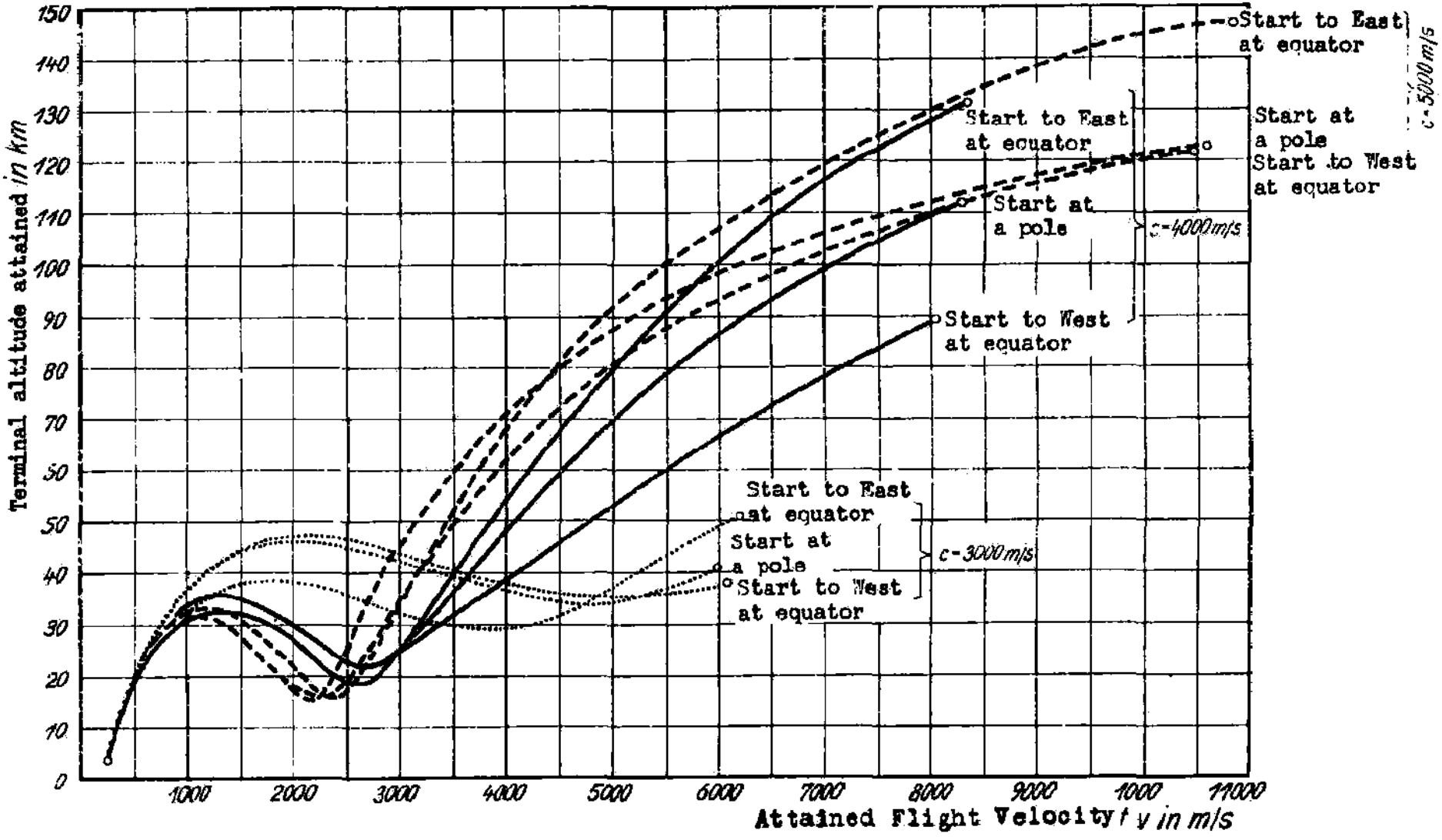

Fig. 69: Absolute climbing path of the Rocket Bomber with c = 3000, 4000 and 5000 m/sec, without consideration of the Earth's rotation, but with consideration of rotation velocity, of a point on Earth's equator, launch to East and launch to West.

IV. GLIDING FLIGHT AND LANDING

1. Supersonic Path of Gliding Flight

The supersonic path of gliding flight of the rocket bomber is determined by the forces acting on its center of mass, in the same manner as for the climb path. These external forces are: the weight of the aircraft, $G = mg_0 (R/R+H)^2$, the aerodynamic lift $A = c_a F \rho v^2/2$, the air resistance $W = \varepsilon A$, and the d'Alembertian inertial force T. The same results apply to the rotation of the earth and the atmosphere as in Sec. III 3; in particular, the supersonic gliding path is to be considered as occurring in a plane, for an observer out in space; the deviating effect due to atmospheric rotation, which is especially effective in the lower layers of the atmosphere, must be eliminated by steering. Only in special cases will the Coriolis force be eliminated by steering, so that the orbit relative to the earth is plane; this will occur if the bomber is to go all around the earth on one hop, and land at its starting point. To do this in a perfectly plane absolute orbit is possible only if the takeoff field is at the pole, or if it is at the equator and the plane of the orbit coincides with the equatorial plane. Otherwise the procedure of circumnavigation will go as follows: until the bomb release an absolute plane orbit will be flown for purposes of precise celestial navigation; only the weather-vane action will be eliminated. After the bomb release a suitable relatively plane orbit will be flown, i.e., both weather-vane and Coriolis effects will be eliminated by steering. The arrangement of forces used in calculating the path are shown in Fig. 70 for gliding flight in two aspects, both viewed along the horizontal at the level of the aircraft. The procedure of calculation corresponds exactly to the stepwise method used in determining the climb path; first the absolute orbit is determined neglecting the Coriolis force and then the separately computed rotation of the earth is combined with the absolute orbit to give the desired relative orbit. The initial conditions for the decending path are given by the endpoint of the climb path. Since the climb path can be broken off at any point, there is a singly infinite manifold of possible paths of descent for each ascending path. Actually we started from the previously calculated ascending paths with c = 3, 4 and 5000 m/sec. and each of these was broken off at V_0 = 1, 2, 3 up to 8000 m/sec, provided that all these velocities were actually reached. They represent the initial velocities for the descending path. Each descending path is followed until the velocity has dropped to 300 m/sec. In Figs. 71 and 72 two paths are shown; one for c = 3000 m/sec, V_0 = 4000 m/sec; the other for c = 3000 m/sec, V_0=6000 m/sec at 6.36 times the altitude. In the figures, the strong oscillations of the paths, especially in the first portion, are notable. Because of the considerable tilt of the orbit resulting from the climb, the bomber overshoots its stationary altitude of flight, then approaches it from above, passes through it because of inertia, then is driven upward again by the greatly increased aerodynamic forces, until after several such oscillations the amplitude has decreased so much that the aircraft levels off at the stationary altitude and continues its flight at that altitude. This ricocheting generally has a favorable effect on the range of the bomber. It has the advantage that the thermal stresses of the external surfaces of the aircraft which face the course wind vary in time at high velocities of flight. The oscillation of the path will be hindered by steering, only if flight at the stationary altitude is needed for some special reason, say aiming before the bomb release.

Figs. 73 and 74 show the main elements of the two orbits in greater detail. In Fig. 74, one can easily see the following connections: the orbit shown in Fig. 72 is now represented by plotting the altitude H against the log of the distance S. One can easily locate the peaks and valleys of the orbit for both curves. The climb path ends after t = 300 sec. at an altitude H = 41.2 km, with inclination $\varphi = 6.2^\circ$. At this moment the velocity V_0 reaches 6000 m/sec. When the rocket motor is turned off the tangential acceleration drops from $b_t = +75.5\ m/sec^2$ to -5.5 m/sec^2, so the aircraft is greatly retarded, considering the flat ascending path. At the same time the normal acceleration acting at the cockpit drops from $b_n = +44\ m/sec^2$, after the normal component of the engine thrust has ceased, to $b_n = +18\ m/sec^2$. This positive residue results from the instantaneous center of curvature being above the aircraft. In the first part of its motorless supersonic glide path, the bomber climbs to H = 143.8 km, while the inclination of the path goes through a maximum $\varphi = +2.5^\circ$ also the tangential acceleration gradually increases to $b_t = 0$ at the crest of the wave, while the normal acceleration increases up to $b_n = -10\ m/sec^2$, so that over a long period of time objects in the aircraft will appear to be weightless. At the same time the velocity drops to a minimum of V = 5800 m/sec at the crest of the wave. At the position, S = 1700 km, of the first crest in the orbit, the curves for φ and also practically for b_t (because of the low air-density) must go to zero, while b_n and V pass through a minimum. Then follows the first flight into a valley, with a height loss of 108.8 km. in 250 sec. During this the velocity again rises to 6000 m/sec, the largest inclination is -8°, the largest tangential acceleration is $b_t = +1\ m/sec^2$. In the trough the height is H = 35 km, and the largest normal acceleration acting at the cockpit is $b_n = +58\ m/sec^2$

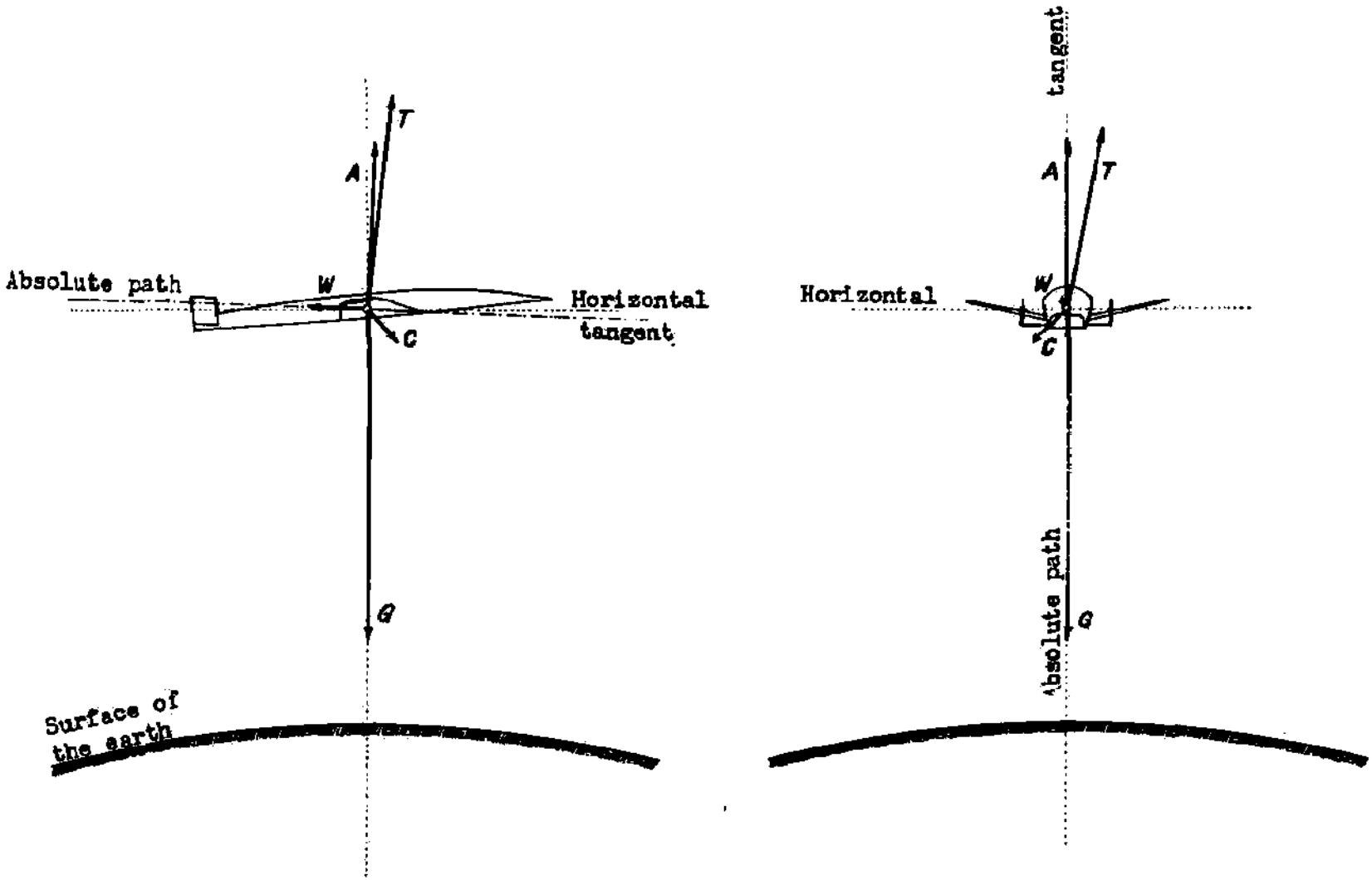

Fig. 70: External forces on the Rocket Bomber in the case of supersonic gliding.

Fig. 71: Flight path of the Rocket Bomber with c = 3000 m/sec, v_o = 4000 m/sec and a bomb load of 11.5 tons.

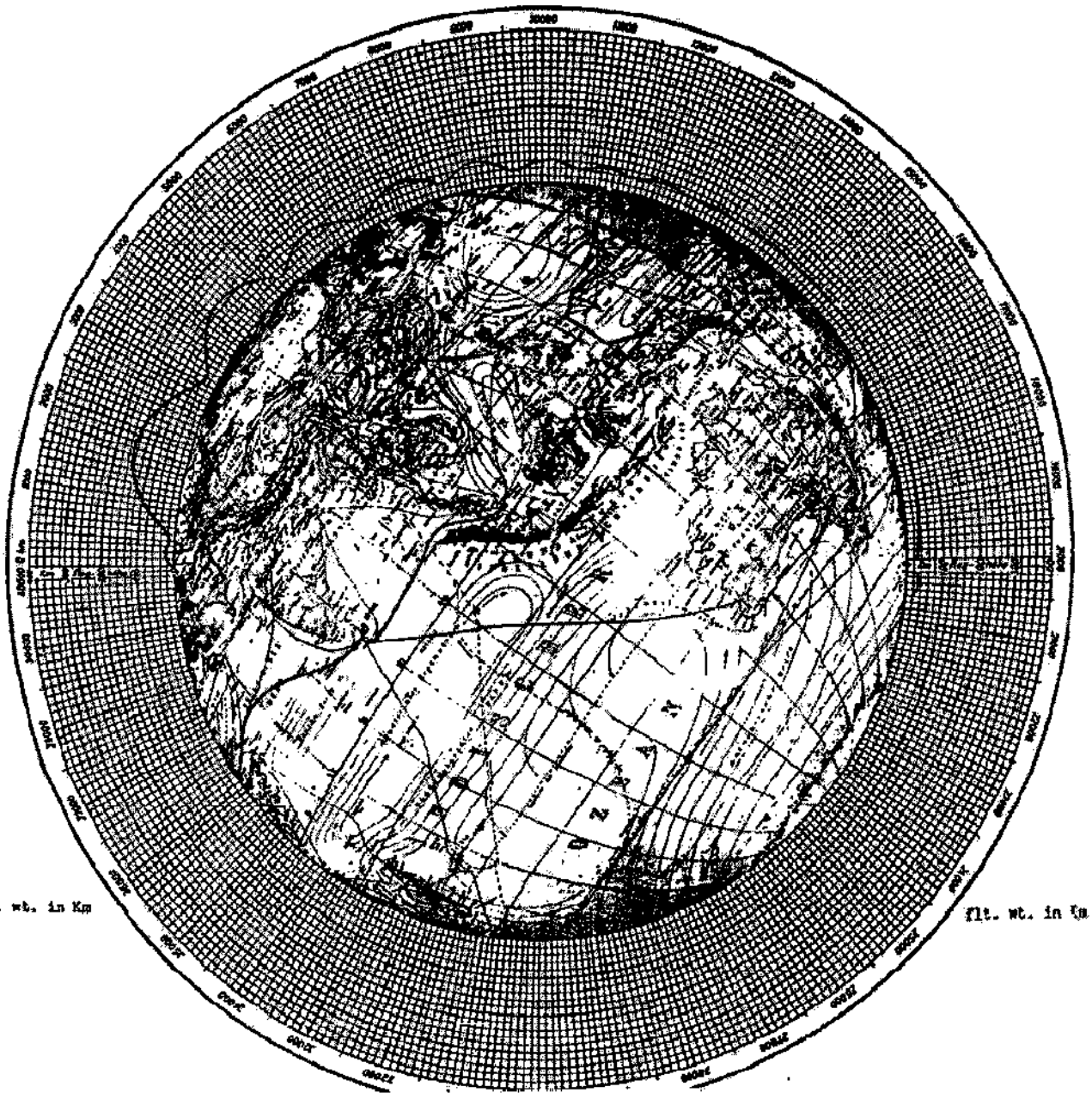

. wt. in Km

flt. wt. in Km

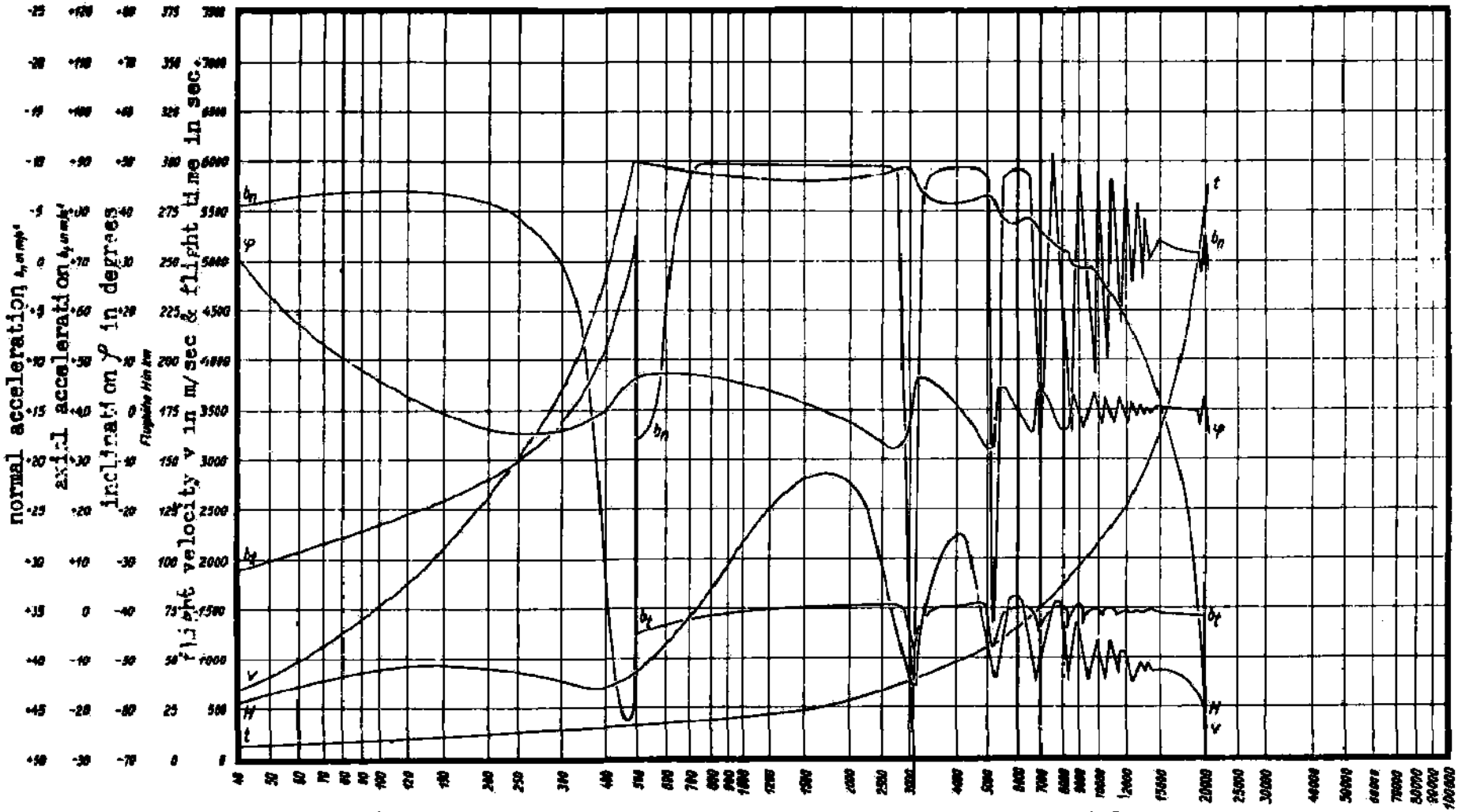

Fig. 74: Flight velocity v, altitude H, path inclination φ, tangential acceleration b_t, normal acceleration b_n and elapsed time t of the flight path of the Rocket Bomber with c = 3000 m/sec, v_o = 6000 m/sec and a bomb load of 0.3 tons.

C	V_0 in m/sec	Bomb load in tons	Flight path length in Km	Time of flight in seconds	Maximum flight height in Km	Maximum positive normal acceleration in m/sec.
3000m/sec	1000	50,0	303	490	40	38,5
	2000	31,8	1528	1300	46	21,7
	3000	20,0	3639	2180	45	17,4
	4000	11,5	6692	2620	47	10,5
	5000	4,8	12171	4330	76	34,9
	6000	0,3	20371	5800	143	46,5
4000m/sec	1000	58,7	295	530	34	28,7
	2000	43,3	1367	1160	37	15,2
	3000	30,5	3477	2100	49	26,0
	4000	20,0	6959	3040	80	35,6
	5000	13,3	12592	4400	104	45,3
	6000	8,0	21139	5820	160	48,8
	7000	3,8	39363	8840	283	50,3
	8000	1,0	91870	16015	1296	58,7
5000m/sec	1000	65,0	291	455	30	22,8
	2000	51,7	1254	1120	31	19,2
	3000	37,5	3847	2225	68	37,3
	4000	28,1	7454	3200	87	37,0
	5000	20,1	12180	4290	102	46,5
	6000	15,0	21531	5990	111	35,9
	7000	10,5	42091	9120	128	36,3
	8000	6,5	293720	41600	778	2,5

Numerical characteristics of 22 various descent paths of the Rocket Bomber.

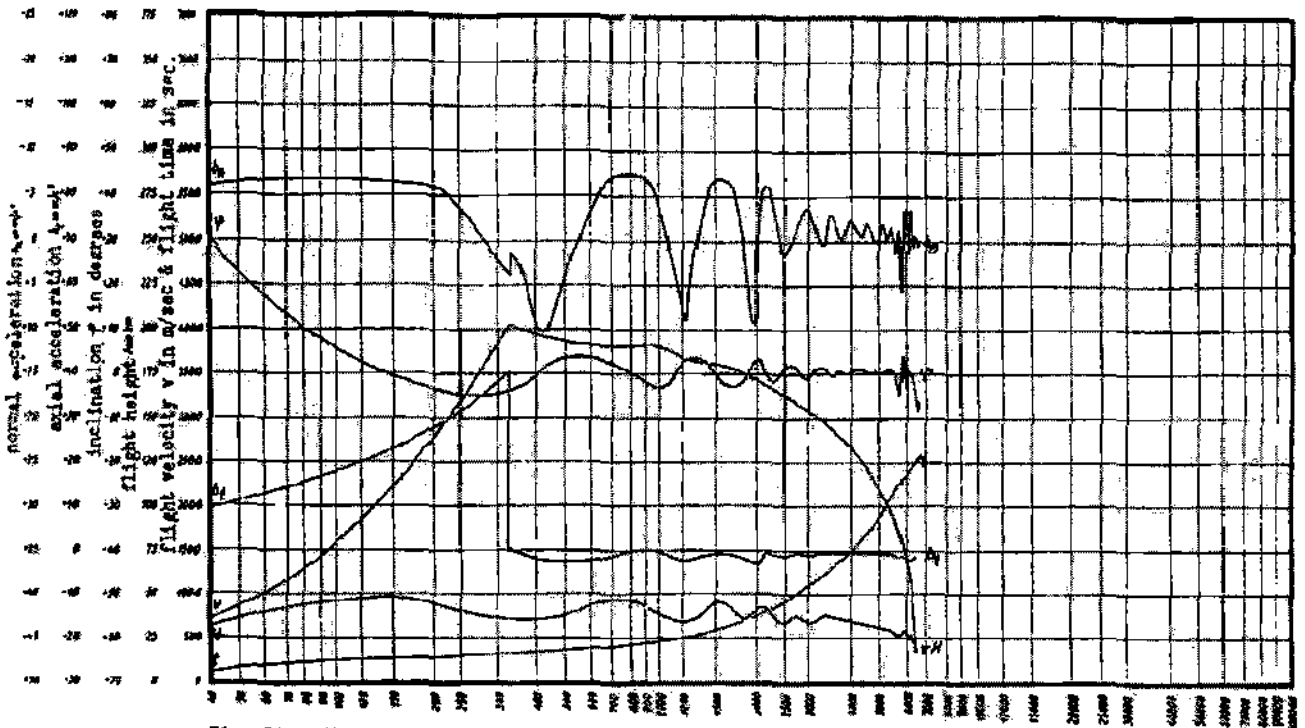

Fig. 73: Flight velocity v, altitude H, path inclination γ, tangential acceleration b_t, normal acceleration b_n and elapsed time t of the flight path of the Rocket Bomber with c = 3000 m/sec, v_o = 4000 m/sec and a bomb load of 11.5 tons.

:t height in km

flight height in kr

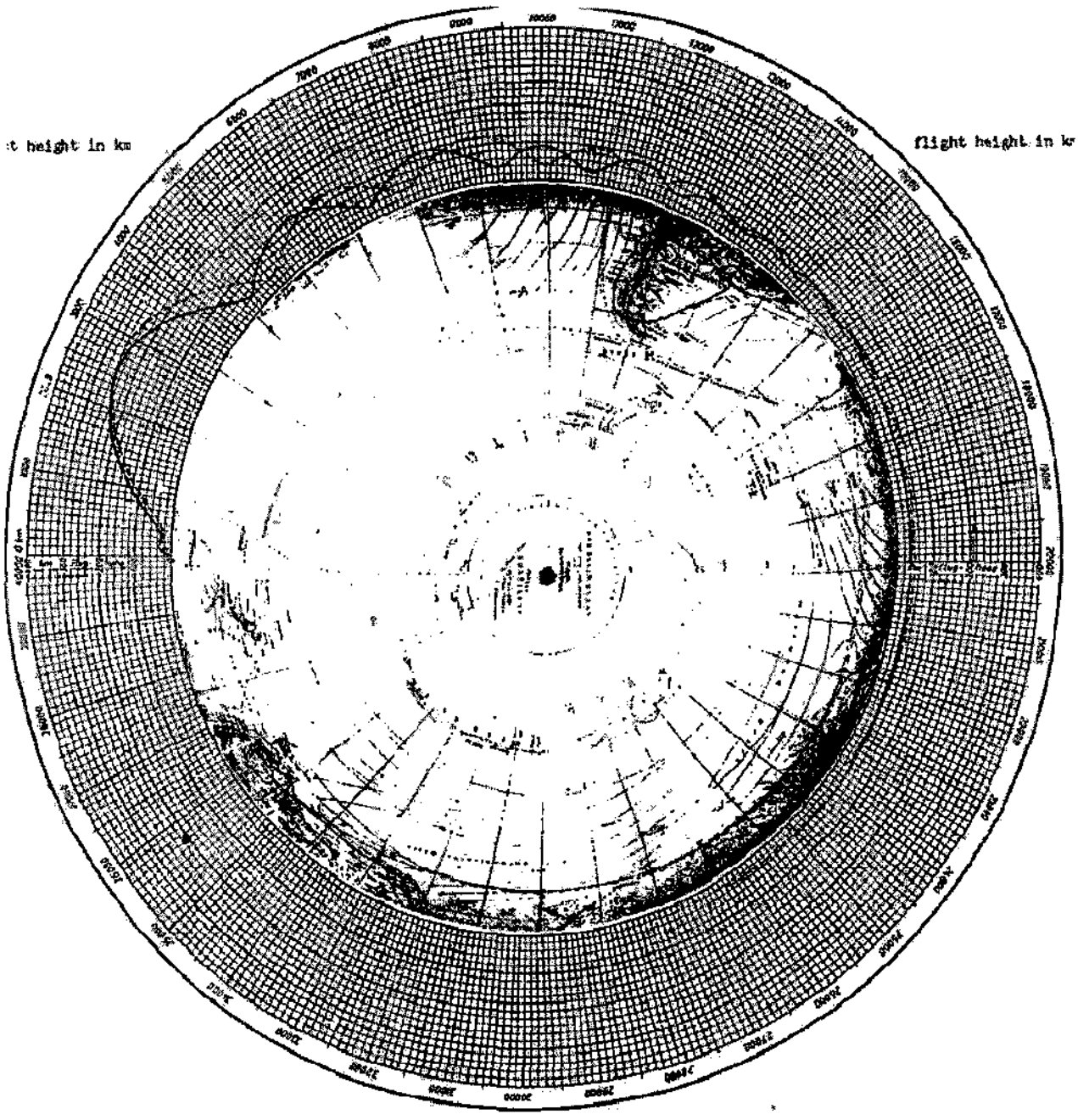

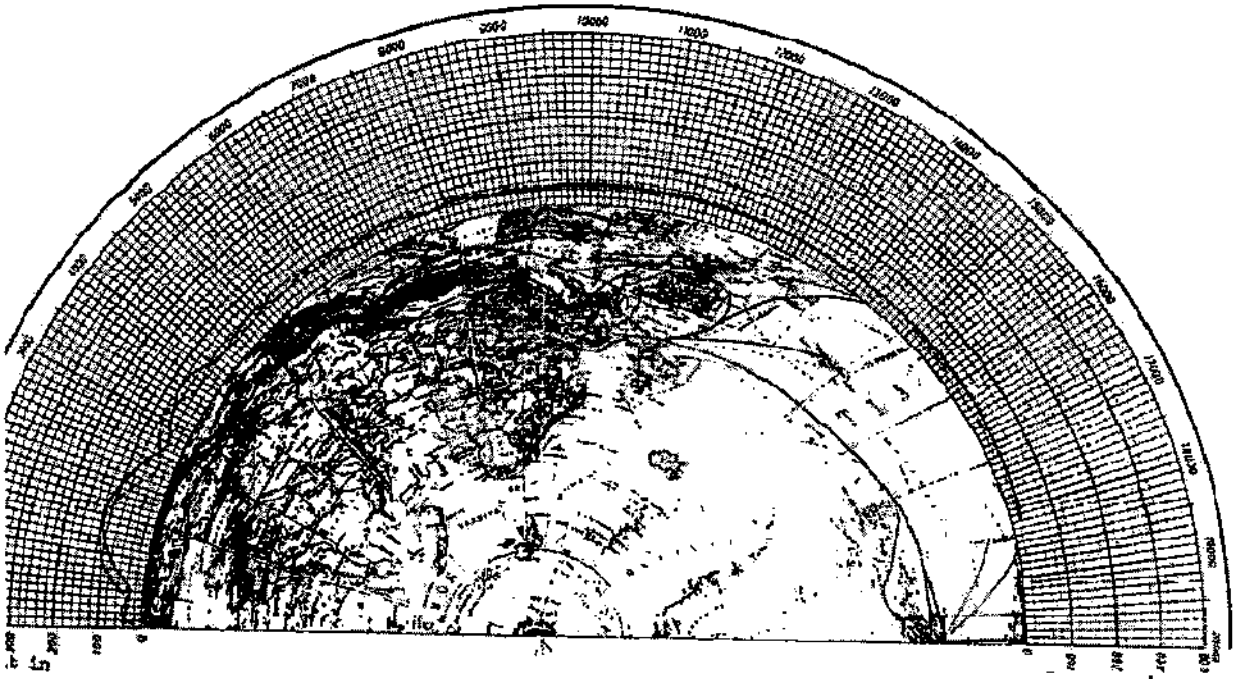

Fig. 76: Absolute (dashed line) and relative (solid line) flight path of the Rocket Bomber with c= 3000 m/sec, v_0 = 6000 m/sec and a bomb load of 0.3 tons, in the case of a start toward the west from a point on the equator and including the effect of the Earth's rotation.

flight height in km

—— - south pole

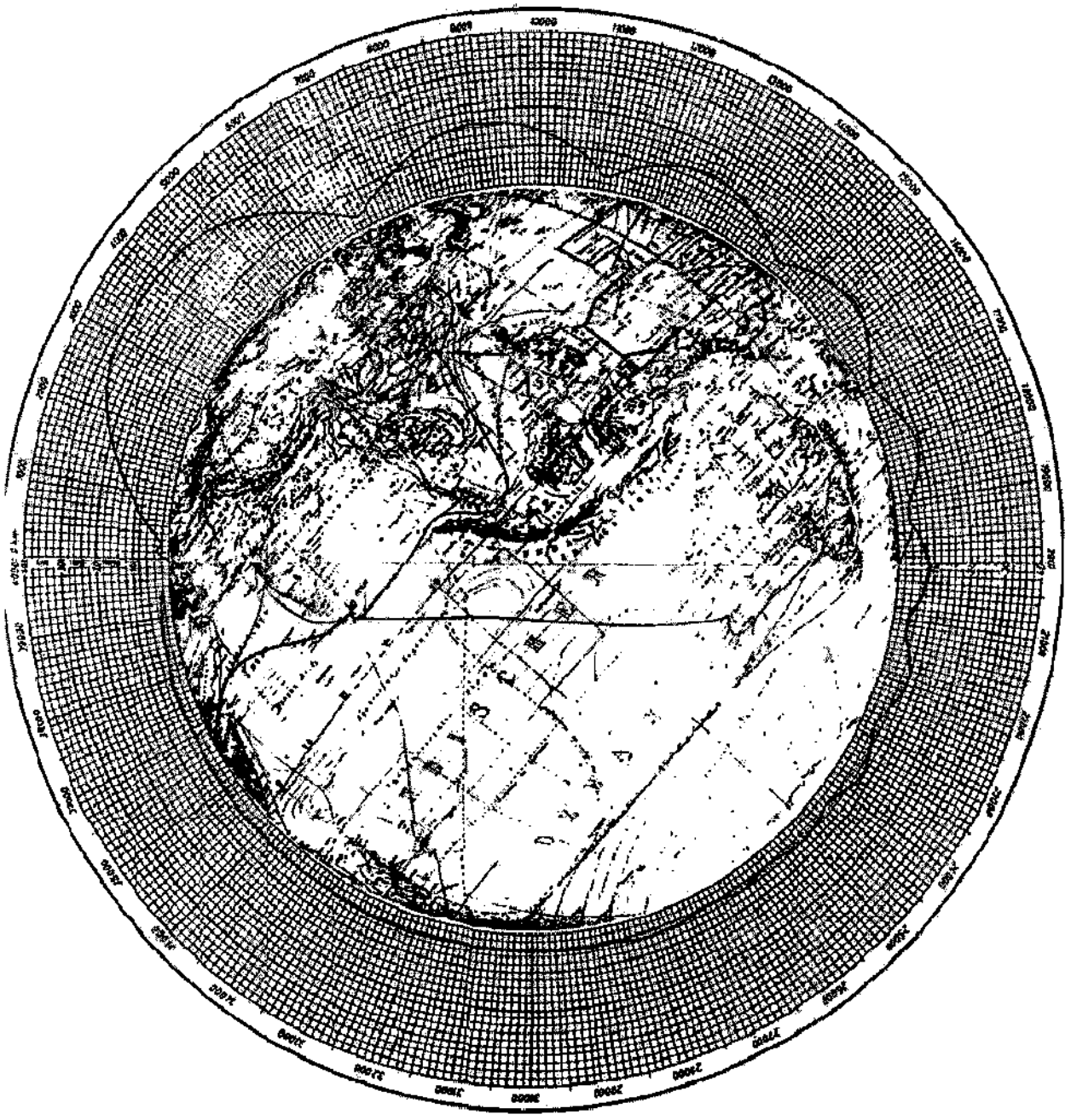

Fig. 77: Influence of the release of a 3.8 ton bomb from a height of 40 km and the velocity of 6060 m/sec on the flight path of the Rocket Bomber with c = 4000 m/sec, v_o = 7000 m/sec.

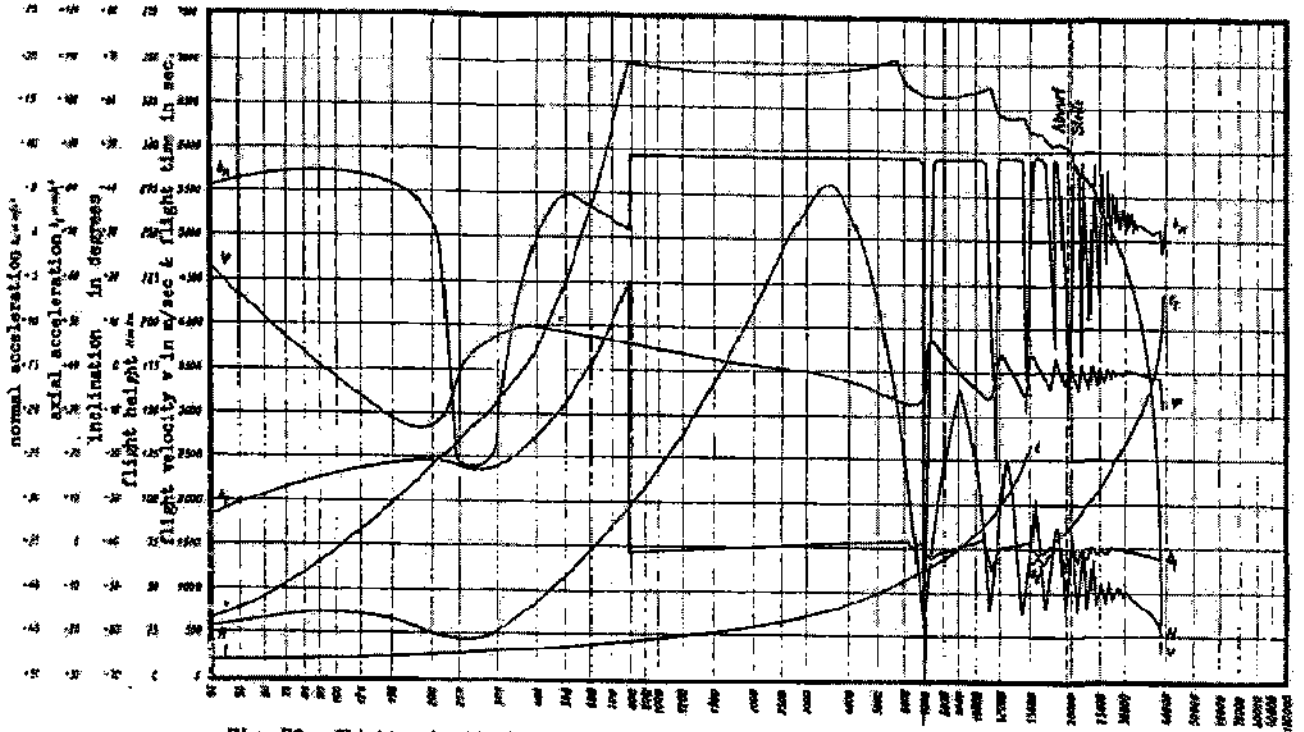

Fig. 78: Flight velocity v, altitude H, path inclination , tangential acceleration b_t, normal acceleration b_n and elapsed time t of the flight path of the Rocket Bomber and dropping of the bomb load B = 3.6 tons at 40 km height; also at 6060 m/sec flight velocity and 19 200 km distance from the starting point.

C-84294

This procedure is repeated at each jump which the rocket bomber makes toward its target, while the extreme values gradually die down and the flight becomes more and more smooth in the neighborhood of the stationary altitude. The total length of the projection of the glide path on the earth's surface is 20371 km, the duration of the flight is 5830 sec. In this manner various orbits were calculated; Table II gives the most important data - length of the orbit, glide-number, maximum altitude attained, and maximum positive normal acceleration.

All these orbit investigations were carried out neglecting the earth's rotation. For this reason Figs. 75 and 76 show the relative and absolute orbits for supersonic flight of the rocket bomber for $c = 3000$ m/sec and with the velocity at the end of the climb path $V_o = 6000$ m/sec, if the aircraft takes off in an exact easterly or westerly direction from a point on the equator. In the case of an eastward takeoff, the velocity of rotation of the takeoff point relative to the earth's center adds to the velocity of the aircraft relative to the takeoff point, so the centrifugal force increases. Because of this influence of the earth's rotation, the range $S = 20370$ km. in Fig. 72 is increased to $S = 23470$ km, more than 13%. This supersonic path relative to the earth's surface is shown in Fig. 75. The most interesting features are the much greater heights of the orbit peaks and the longer distance between peaks, compared to Fig. 72. The absolute path of the aircraft, as seen by an observer out in space, is shown dotted in Fig. 75; naturally the absolute path length is much greater ($S = 26410$ km.). In the case of takeoff to westward, the rotational velocity of the takeoff point is subtracted from the velocity of flight, the centrifugal force decreases and the range drops from 20370 km to 18200 km, i.e., more than 10%. At the same time the heights of, and intervals between, the first waves of the orbit decrease. These results are shown in Fig. 76; the absolute orbit is shown dotted for comparison. The effect of the earth's rotation on the range and height of the supersonic orbit becomes even greater if the maximum velocity of flight approaches the velocity due to the earth's rotation; on the other hand it decreases rapidly if the start is made from the equator in an intermediate, rather than in an easterly or westerly direction, or if the takeoff point moves from the equator toward the poles. For example, the ranges for $c = 4000$ m/sec and $V_o = 7000$ m/sec are 32430 km. for westward takeoff from the equator, 50440 km for eastward takeoff from the equator, and 39363 km for takeoff from the pole; the corresponding ranges for $c = 5000$ m/sec, $V_o = 7000$ m/sec are 32660 km, 58880 km and 42091 km.

When the bomb load is dropped during the supersonic gliding flight, the weight suddenly decreases by 10 tons from the value G, and the stationary altitude increases by $\Delta H = 6341 \cdot G/G_0$. This decrease and the diminished ballistic loading of the aircraft produce an effect on the oscillating orbit, as shown in Fig. 77 for a definite case. It was assumed that, along the orbit for $c = 4000$ m/sec, $V_o = 7000$ m/sec, a 3.8 ton bomb was released horizontally at 40 km altitude and 6060 m/sec velocity, so that it struck the point on the earth opposite to the takeoff point. For a bomb throw of 850 km, the release must occur after 19150 km. At this point the plot of the orbit splits into three curves; the path of the falling bomb, the dotted path which the bomber would have followed if no bombs were released, and the solid line showing the orbit after the bomb release. In the last case the waves in the orbit are higher and broader, so that after several oscillations a definite phase shift is observable, the stationary part of the path lies 1670 m. higher, and the final velocity of 300 m/sec is reached a few dozen kilometers sooner. The difference in range is so slight that one need not make a special investigation of the orbit after the bomb release, but can use the approximate orbit calculated for full bomb load. Fig. 78 shows the elements of this orbit; it is interesting to note that at the point of release the normal acceleration jumps discontinuously from + 7 m/sec^2 to +19.5 m/sec^2, because the aircraft was in a trough and before the bomb release (when it weighed 13.8 tons) it was in dynamical equilibrium with the buoyant forces of the air.

The range of the rocket bomber is largely determined by the length of the supersonic glide path. This important quantity can be estimated to a first approximation, without doing the exact orbit calculation, by setting the inertial force equal to the air resistance, $G/g \cdot dv/dt = -GE$ from which

$$v = v_o - \varepsilon g t \quad \text{and} \quad s = (v_o^2 - v^2)/2\varepsilon g$$

This simple calculation is satisfactory up to $V_c = 2000$ m/sec. Above this, the centrifugal force due to the curvature of the bomber's orbit around the earth can no longer be neglected. In second approximation we may set $G/g \cdot dv/dt = -(G - Gv^2/Rg)E$, from which (18):

$$v = \sqrt{Rg}\,\frac{\frac{\sqrt{Rg}+V_o}{\sqrt{Rg}-V_o} - e^{2\varepsilon t\sqrt{g/R}}}{\frac{\sqrt{Rg}+V_o}{\sqrt{Rg}-V} + e^{2\varepsilon t\sqrt{g/R}}};$$

$$S = t\sqrt{Rg} + \frac{R}{\varepsilon}\ln\frac{1+(\sqrt{Rg}+V_o)/(\sqrt{Rg}-V_o)}{e^{2\varepsilon t\sqrt{g/R}}+(\sqrt{Rg}+V_o)/(\sqrt{Rg}-V_o)}$$

$$t = \frac{R}{2\varepsilon\sqrt{Rg}}\ln\frac{(\sqrt{Rg}+V_o)(\sqrt{Rg}-V)}{(\sqrt{Rg}-V_o)(\sqrt{Rg}+V)};$$

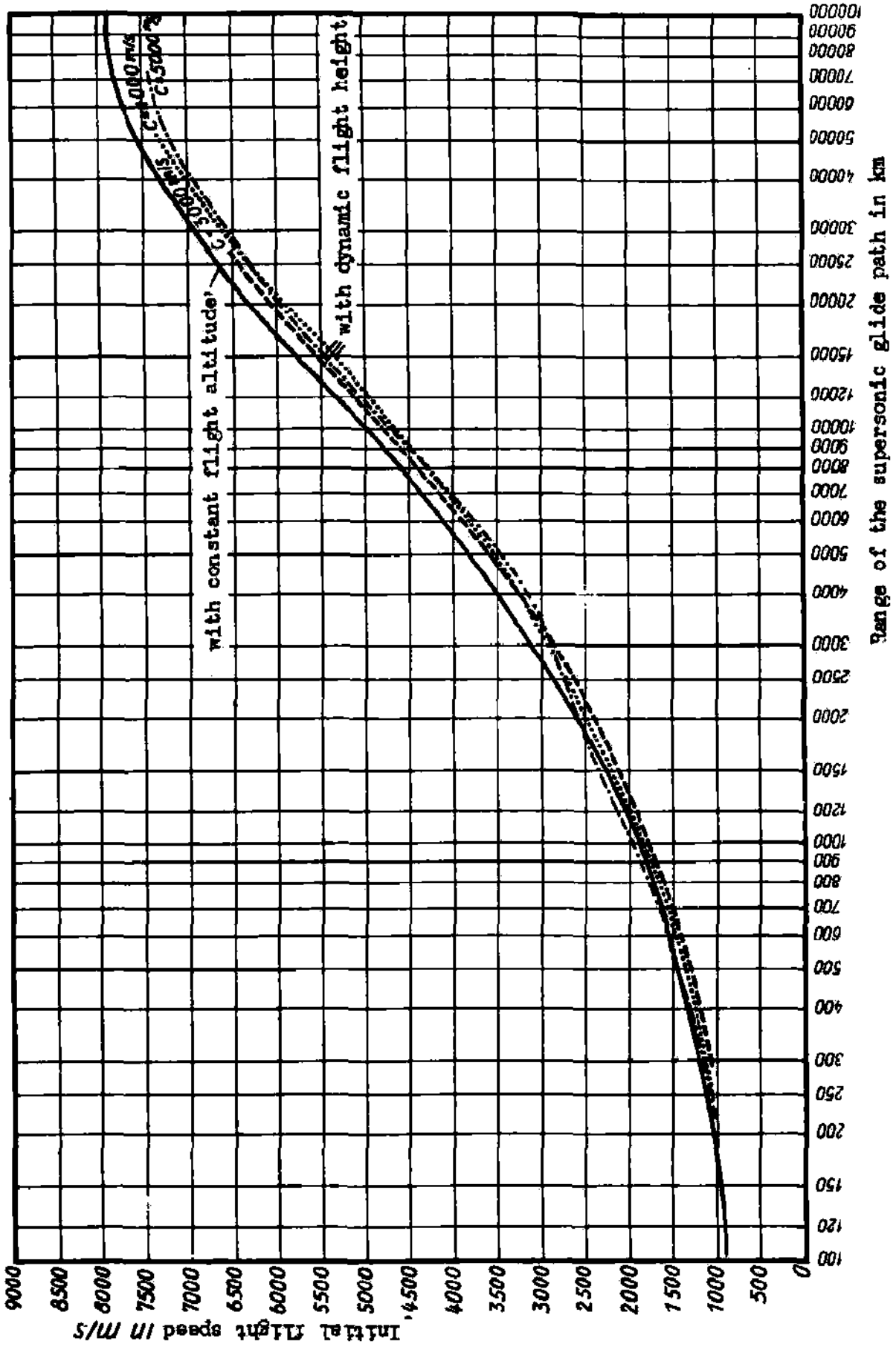

Fig. 79: Comparison of the ranges of the supersonic descent path for equal initial velocities computed by
a) Constant flight altitude
b) Graphical determined flight altitude with c = 3000, 4000 and 5000 m/sec.

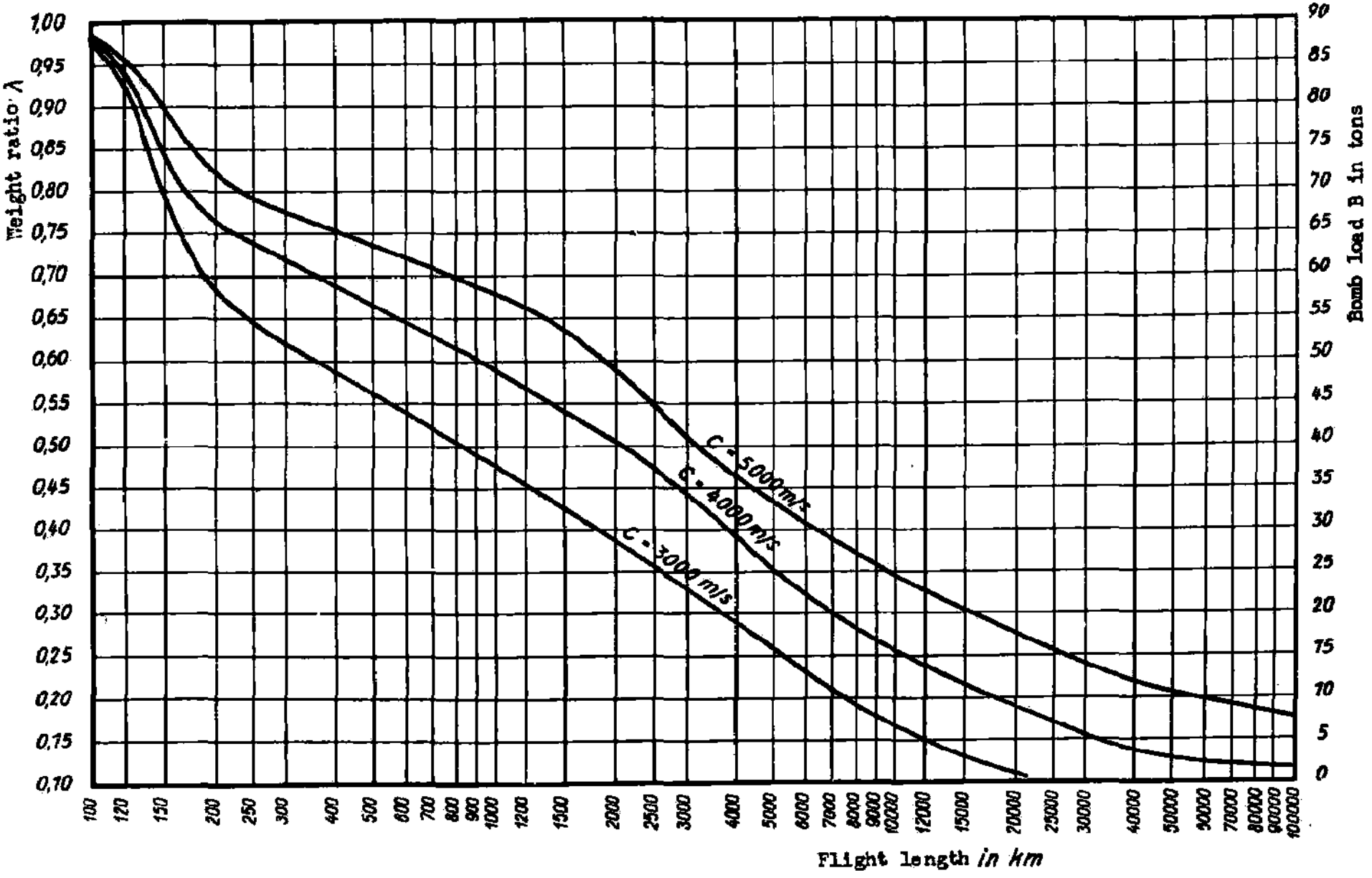

Fig. 80: Relationship between load ratio $\lambda = G/G_o$, bomb load B, and range of the Rocket Bomber for a "straight ahead path" and for exhaust velocities of c = 3000, 4000 and 5000 m/sec.

These equations give good results for the stationary flight paths until we approach the velocity of points on the earth's surface. With the aid of these equations we can also include the effect of the earth's rotation, and obtain values of V_a, t, and S_a for the absolute orbit, if in place of the relative velocity V_o we use the absolute velocity V_{ao} of the takeoff point, which is calculated from its velocity V_e and the compass angle φ of the initial velocity V_o by the equation $V_{ao}^2 = V_o^2 + V_e^2 + 2V_oV_e \sin\varphi$ The effect of the earth's rotation on the path length is greater than 1% in the most unfavorable case for $V_o = 2500$ m/sec, but decreases considerably when we change from absolute to relative path length. The path lengths calculated in this way can be compared to the ranges of fire for the same muzzle velocity V_o; up to $V_o = 6000$ m/sec and for the glide number $1/\epsilon = 6.4$ used here, they are better by a factor 3.2, and as we approach the velocity of points on the earth's surface the factor increases rapidly; i.e., for the same initial velocity one can fly much farther than one can shoot.

Fig. 79 shows a comparison of the results of this second approximation with the stepwise calculation of the oscillating dynamical path. The reason why the dynamical paths are considerably longer than the stationary for the same initial speed is mainly that whereas in the stationary gliding flight the energy consumption is distributed uniformly over the whole path, it is concentrated in the troughs of the dynamical path; the first (and also the longest) jump, which constitutes 15-30% of the total range, has a trough only at its end, and only loses there half of the energy which would be lost at the stationary altitude (this energy represents 15-30% of the total energy store). Other reasons for the greater range of the dynamical paths are that the regions of greatest energy consumption occur at low altitudes where favorable gas-dynamic glide-numbers at high Reynolds numbers exist, while the higher parts of the path, in which unfavorable gas-kinetic glide-numbers and low Reynolds numbers exist, occur in regions of rarefied air or practically empty space; finally, the process of turning out of the climb path, in the case of the stationary orbit, has to occur under unfavorable angles of attack, resulting in increased energy consumption for the same length of path. Even more clear is the plotting of the supersonic range of flight against bomb load or weight ratio, as in Fig. 80. The last two figures do not include the effect of the earth's rotation.

Also important for the use of the rocket bomber is the situation where, after release of bombs, the aircraft starts toward its home base. If the antipodes of the home base or other parts of the opposite hemisphere are being attacked, the bomber will return simply by continuing along its glide path after the bomb release and flying all around the earth. For nearer targets, there is the possibility of return by shifting course after the bomb release. Three possibilities are considered. First, instead of having the path be a great circle, after the initial propulsion, let it be a circle, lying on the earth's surface, with diameter $2r$ equal to the distance between takeoff point and target. For flight along this circular cap, the air resistance for a given velocity increases in the ratio $\sqrt{\cos^2[r/R_\oplus(1-2v^2/Rg)] + v^4/R^2g^2}/\cos[r/R_\oplus(1-v^2/Rg)]$ because of the oblique centrifugal forces, while the circular cap is shorter than the great circle only in the ratio r/R Flight along the circular cap will be more favorable than flight along the great circle only for velocities below 5600 m/sec, so this method of turning seems suitable for shorter distances of attack. However, in this range there is in most cases another favorable turning procedure - to reach the target along a great circle, to turn the aircraft at the target as sharply as possible, and return home along another great circle. If the bomber turns through a small angle $d\sigma$, then the ratio of the work done on the element of turn path of length $r\,d\sigma$ to the kinetic energy of the bomber at the beginning of this element is $2\epsilon\,d\sigma/(1-\gamma^2/b^2)$ which can drop to $b = v^2/r$ because of large centrifugal acceleration which can approach the permissible limit. The turning path then becomes a spiral along which the tangential and radial accelerations are constant. It is not integrable and must be computed step by step. From the equation, the relative loss of weight during the turn is independent of the velocity at the start of the turn, so it can be computed once and for all for all the spirals. It is shown in Fig. 81 for turn-spirals with tangential deceleration 1.75 m/sec^2 and centripetal acceleration 50 m/sec^2. After a 90° turn only 60% of the initial energy is left, after a 180° turn only 37% is left; i.e., the sharp turn still costs a great deal of energy. There are intermediate procedures for turning, which are a combination of narrow turn with non-great circles; these are characterized by less energy consumption than the last limiting case which only permits the use of oscillating flight paths.

A third turning method consists in the aircraft using only enough energy in the climb, to enable it to reach the target; there it turns at its small residual speed, and with the aid of a fuel store on board, gets another push to give it the energy for the return home. This method of using two driving periods has the feature that the aircraft travels slowly over the target at low altitude. So on the one hand the bombs can be dropped with great accuracy on the other hand, the fire power is less than for long range attack, and finally the bomber gets into the enemy zone of defense at the target. Fig. 82 shows the ranges of the rocket bomber when it is turned by the last two methods.

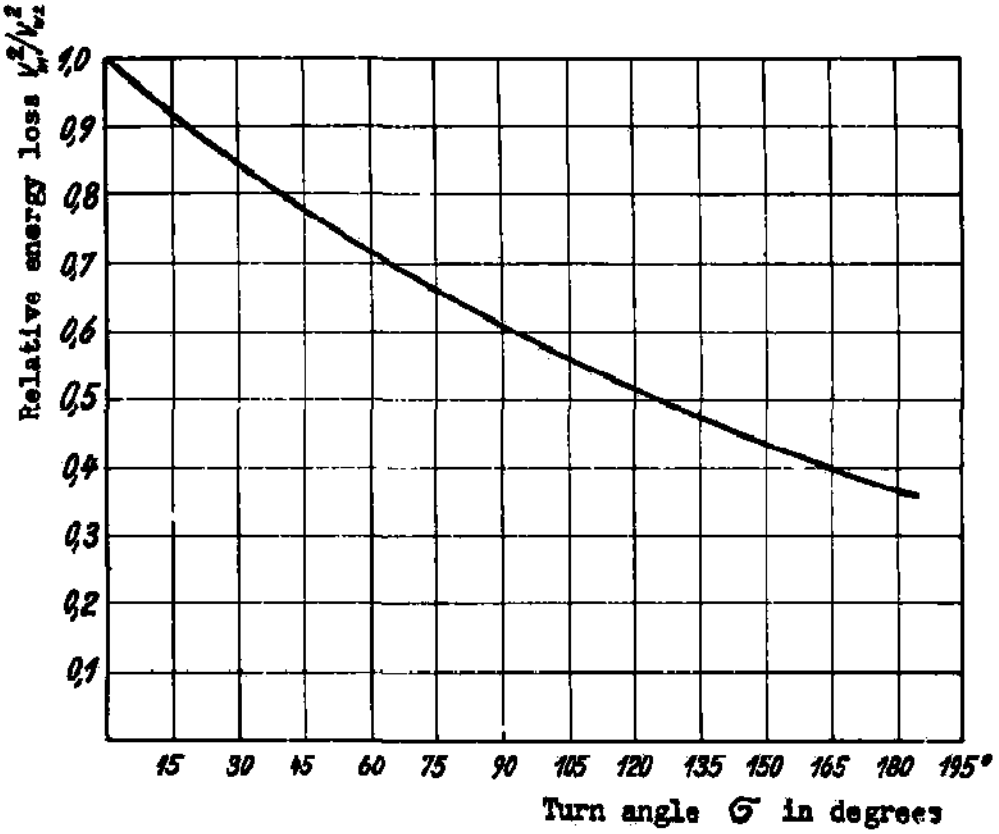

Fig. 81: Loss in kenetic energy during the turning through an angle along the spiral turn. (see p. 122)

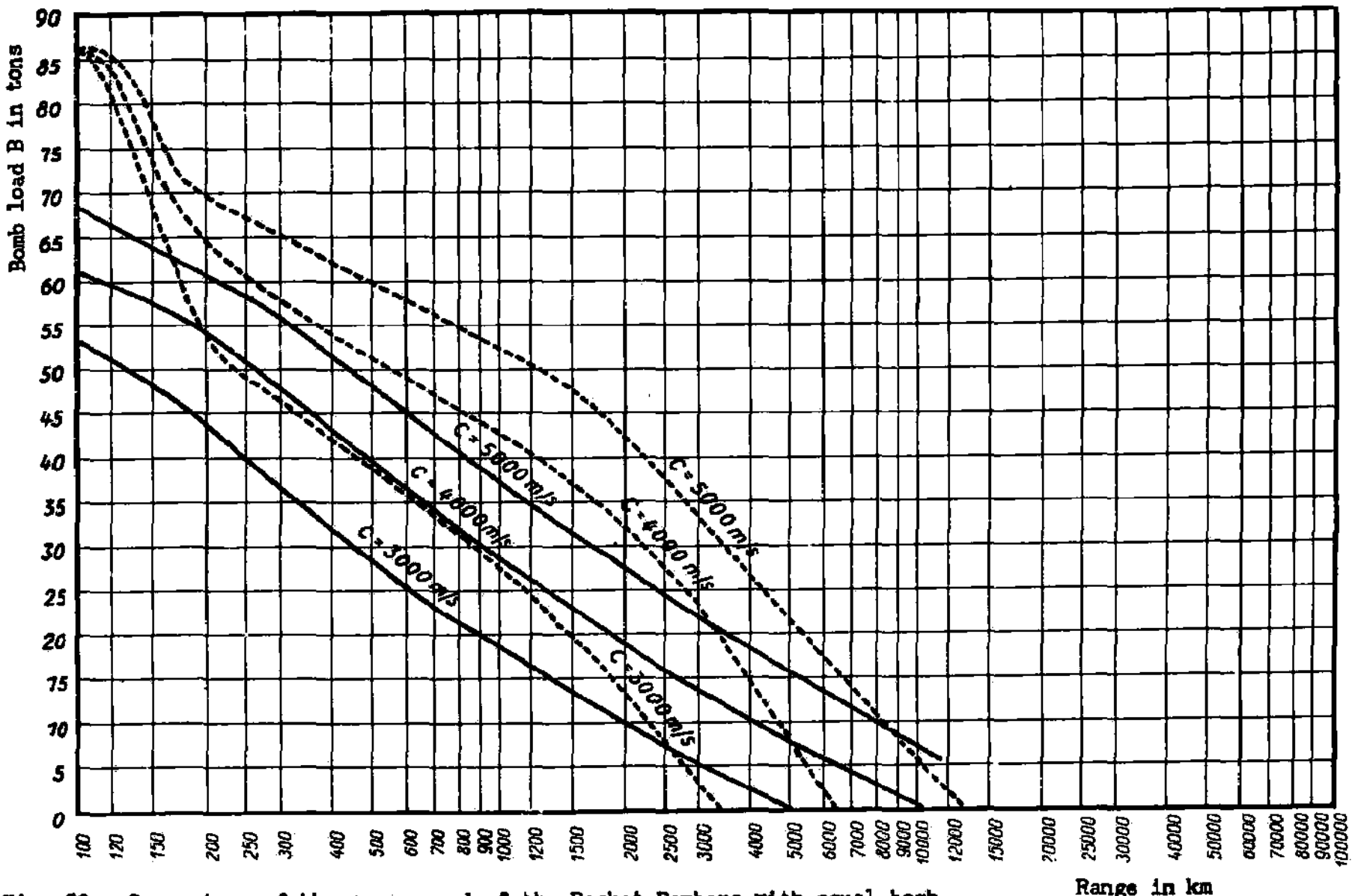

Fig. 82: Comparison of the ranges and of the Rocket Bombers with equal bomb loads for c = 3000, 4000 and 5000 m/sec. if the return to the launching point is effected by a full speed gliding turn (solid lines), or *second*, if there is a slower gliding turn, followed by a second rocket acceleration (dotted lines).

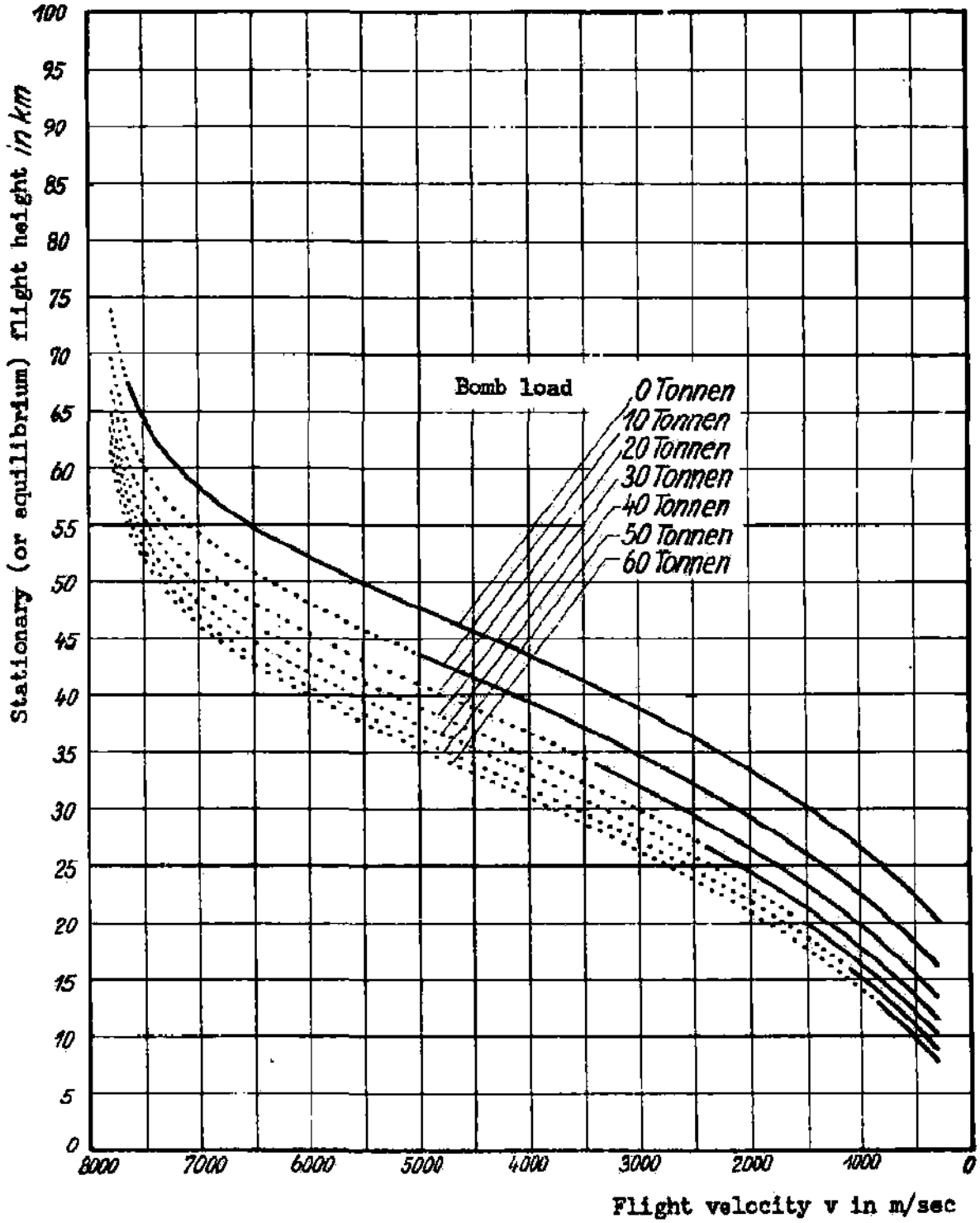

Fig. 83: Stationary flight altitudes of the Rocket Bomber during the supersonic glide with various bomb loads.

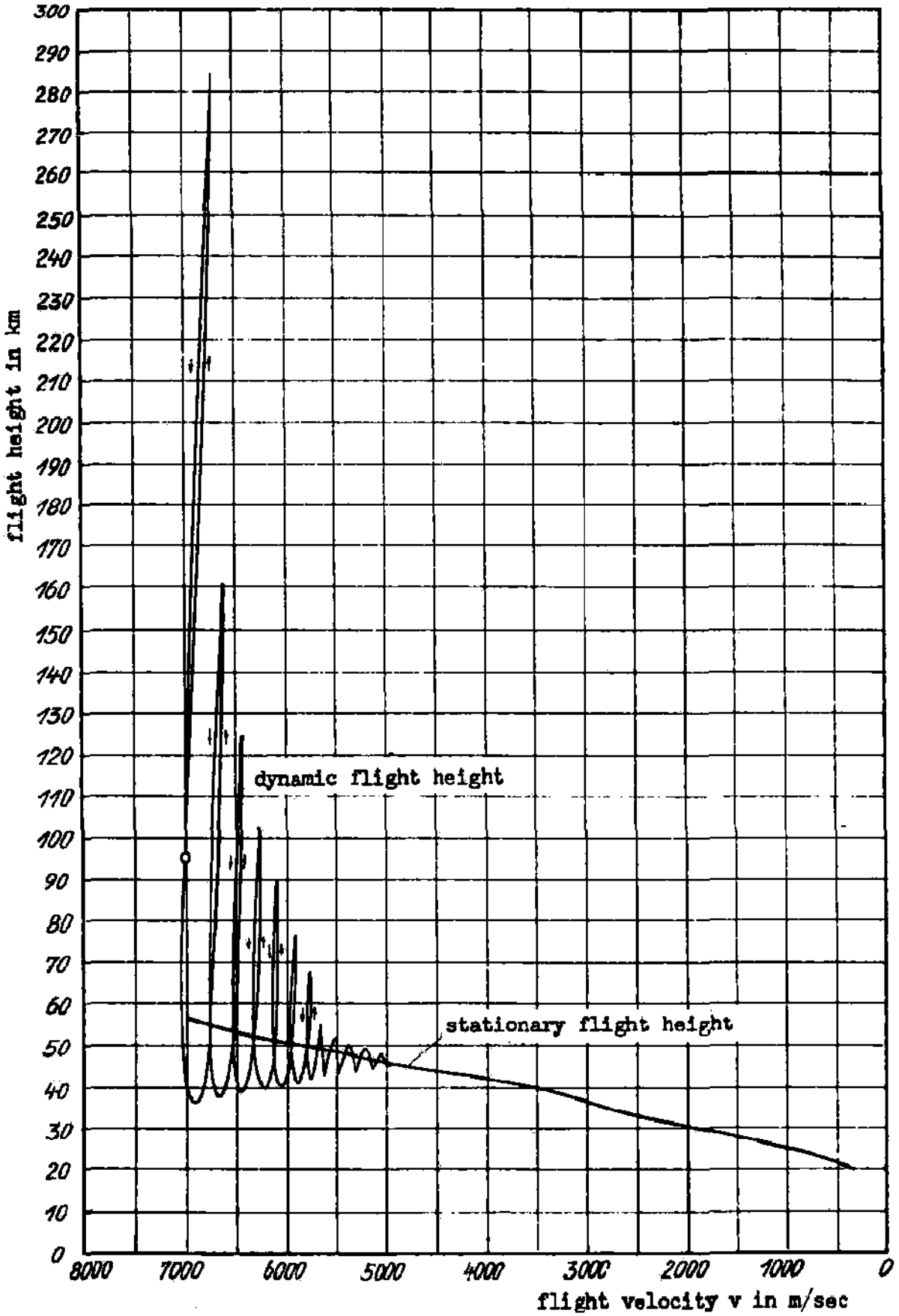

Fig. 84: Comparison of the actual and stationary flight altitudes of the Rocket Bomber during a supersonic glide path. (c = 4000 m/sec, v_o = 7000 m/sec.)

The same considerations apply to the altitudes of supersonic gliding flight as to the climb, especially as regards " stationary " and " dynamic " altitudes. The stationary altitudes, determined by the equilibrium between the constant flight-weight and the propulsive plus centrifugal forces (just as they were used for the second approximation to the length of the supersonic path), are shown in Fig. 83, where the curves are drawn solid out to the point actually attainable with the given bomb load and c = 4000 m/sec. The dynamical altitudes of flight, which result from the varying initial conditions for the dynamical orbit of supersonic glide flight, tend to approach the stationary altitudes of flight, as shown in Fig. 84 which shows the dynamical and stationary paths for c = 4000 m/sec and V_o = 7000 m/sec.

2. Path of Subsonic Gliding Flight and Landing

The subsonic gliding flight, by its definition, begins at V = 300 m/sec with G = 10 tons. The lift coefficient for a favorable glide position is then about C_a = 0.2 and the corresponding height is H = 20 km. The supply of potential and kinetic energy is still 24580 kg m/kg, with which a distance of 24580/ε = 98200 m. can be travelled for an average subsonic glide-number ε = 4. One can follow the descent in small velocity-steps V_1, V_2, V_3 . . . by using the result that the decrease in kinetic energy $(V_1^2 - V_2^2)/2g$ plus that of the potential energy $(H_1 - H_2)$ must always equal the work against air resistance $\Delta s.\varepsilon$; in the stratosphere we get

$\Delta s = (V_1^2 - V_2^2)/2\varepsilon g + 6341/\varepsilon \ln V_1^2/V_2^2$ or $\Delta H = 6341 \ln V_1^2/V_2^2$ in the troposphere

$\Delta s = (V_1^2 - V_2^2)/2\varepsilon g + (H_1 - 44250)/\varepsilon [1 - (V_1/V_2)^{0.47}]$ or $\Delta H = (H_1 - 44250)[1 - (V_1/V_2)^{0.47}]$

The subsonic glide path obtained from these equations is shown in Fig. 85. We see that the subsonic descent lasts 11 minutes, and ends near the surface of the earth at a velocity of 288 km/hr, whereupon the landing can occur. The actual variability of the subsonic glide-number can affect his path of descent.

The landing process begins at V = 288 km/h with C_a = 0.2. The behavior of the aerodynamic forces is given by the upper polar of Fig. 34, so that the velocity of the bomber can be lowered, by using landing-aids, to $288\sqrt{0.2/0.74}$ = 150 km/hr which is required for military glide-landings. With these polars we can determine the air resistance and the required angle of attack α for all velocities between 288 and 150 km/hr, for G = 10 tons, so the landing procedure can be followed by using the dynamical equations. It is shown in Fig. 86.

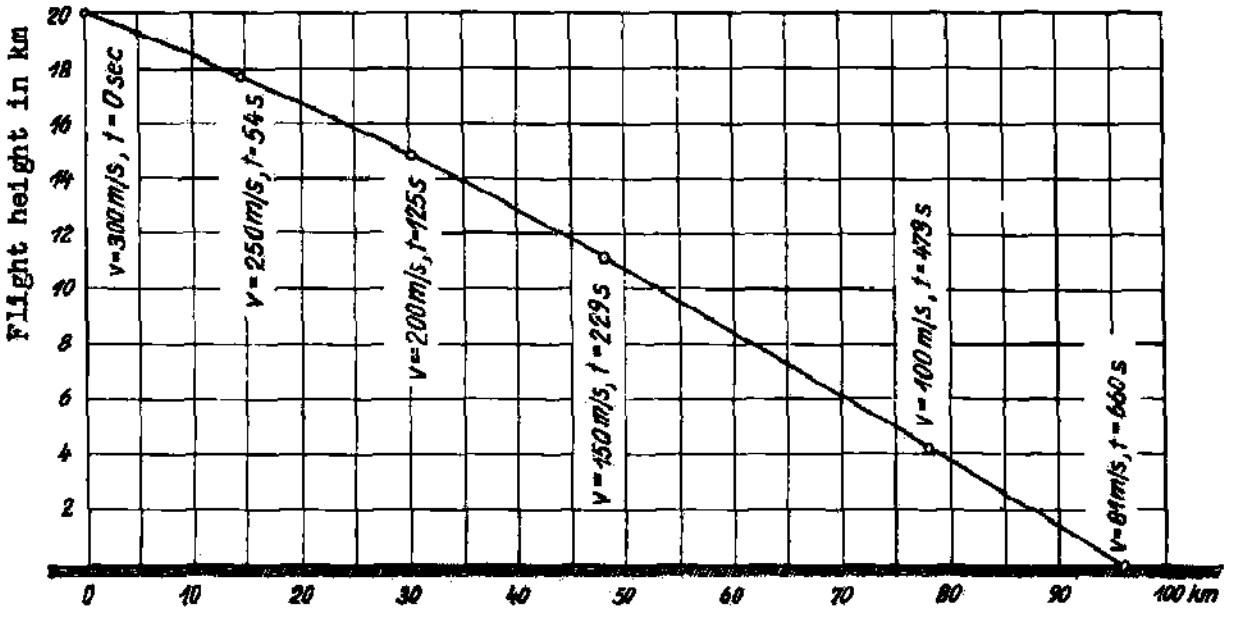

Fig. 85: Subsonic descent path of the empty Rocket Bomber assuming a constant average L/D of 4

Fig. 86: The landing of the Rocket Bomber

V. PROJECTION OF THE BOMBS

1. Types of Projection

The rocket bomber has two different methods of attack: point attack and areal attack. The two procedures differ mainly in the manner and accuracy of the bomb release.

In the procedure of attack on a point, the bomb will be aimed precisely toward a "point"-shaped individual target, and released at moderate altitude and velocity under the same conditions as for ordinary bombers. In practice the same sub-types of bomb release are available to the rocket bomber as for other bombing aircraft, e g. bomb release during horizontal flight, dive bomb attack, bomb release during climb, low-altitude bombing, etc. The well-known conditions and difficulties of these types of release apply practically unaltered to the rocket bomber, especially as regards the accuracy attainable and the need for adequate visibility at the target, so nothing new can be said about these types.

Things are quite different for attack on an area. Here the bomb is thrown from great altitudes (50-150 km) and at very high velocities of flight (up to 8000 m/sec), i.e. under conditions far beyond those of long-range artillery fire. Since the target, for the distances involved, will not be visible, the release on an area will be aimed indirectly, e.g. by celestial navigation. Thus it is independent of weather and visibility at the target. Because of this, it does not reach the accuracy of release on a point, and we must expect spreads of several kilometers. So with areal bombing one cannot hit particular points, but rather a correspondingly large area, with sufficient probability. To achieve an anticipated effect on this whole surface, a single drop will not suffice, rather we will have to project several bombs toward the same target; these will distribute themselves over the surrounding surface according to the laws of chance. The distribution of hits inside the area will not be uniform; the bombs will strike more frequently in the neighborhood of the target than far away; there will also be unavoidable bomb-hits far outside the area being attacked. However, on the basis of laws of probability, the bomb distribution can be predicted well enough so that the goal of the attack can be achieved with the same or even greater accuracy than for point attack.

2. Flight Path of the Bomb

In order to make calculations concerning the bombs thrown from rocket aircraft, we must make some assumptions about the external shape of the projectile. Best suited to the existing conditions is a bullet-shape, with flat base, with a cylindrical tapered portion at the rear, with largest possible ratio of height h to caliber d. With say $\frac{h}{d} = 8$ we get, from the well-known gas-dynamic laws for very high Mach numbers, a resistance coefficient of $C_w = 0.014 + 1.43\ A^2/\gamma 2$; where in the friction contribution $C_{wr} = 0.004$ we neglect the stabilizing surfaces, since they probably can only manage to set the projectile spinning about its axis in the initial part of the flight, before their thin walls are destroyed due to the temperatures developed by friction.

If one assumes that the explosive constitutes 50% of the bomb's weight, then bombs weighing 30 (or 5 or 1) tons have lengths of 11.20 (or 6.16 or 3.60) m., and cross-section loadings of 19.5 (or 10.7, or 6.2) tons/m^2. In a practical situation any bomb load could be made up out of these three sizes. The considerable space required for the projectiles will require an adjustment of the bomb-load-and tank-space to the purpose at hand, in the sense that larger fuel loads will be accompanied by decreased bomb loads and vice versa; i.e., the aircraft described earlier is best suited to the first case.

In estimating the path of flight of the bomb we can proceed in the same way as in determination of the ascending or descending path of the aircraft itself. The force picture differs from that for the climbing aircraft, since we have assumed that no aerodynamic lift forces act on the bomb and that the bomb can no longer be kept in a definite orbit plane by a pilot, so that it follows the tendencies to sideways motion due to atmospheric rotation (weather-vane action) and earth rotation (Coriolis-force), and describes a twisted orbit in space. As shown previously, the weather-vane action is caused by the fact that the bomb, as it flies over places of different latitude, continually moves through layers of air of different absolute speed (depending on latitude), and thus is acted on by a cross-wind, which produces horizontal transverse forces; these do not act at the center of mass of the projectile, but behind it, at least if the projectile has fins. This force as well as the Coriolis force was assumed, in the case of the aircraft, to be eliminated by transverse steering which develops forces equal and opposite to them. In the case of the bomb there are no controls; as a result of the weather-vane action it will not only drift to the side, but also as a consequence of the resultant torque, it will start to rotate about a vertical axis through the center of mass. The flight path of the bomb

is thus determined by five external forces, of which four act at the center of mass and the fifth acts behind it: weight of the bomb, air resistance, transverse air force, Coriolis force, and d'Alembertian inertial force.

The transverse force is perpendicular to the tangent to the path, points the way the transverse wind is blowing, is proportional to the air resistance and the square of the angle under which the unperturbed air stream meets the symmetry plane of the aircraft. This angle in turn is determined by the strength of the cross-wind, i.e. by the course of the bomb and its velocity relative to the ground, by the magnitude of the moment of the crosswind about the center of mass of the bomb, and finally by the slowness with which the bomb responds to the cross-wind and its torque, in turning its apex toward the crosswind. This inertia should be as large as possible, since the tendency to turn always exists except when the bomb is in the plane of a latitude circle. We can get an idea of the magnitude of this effect by considering the 300 km. long path of fall for a point of release over a pole of the earth. The difference in cross-wind between the point of release and the point of impact is, in this case, the absolute velocity of rotation 22 m/sec of the point of impact. Thus the angle of the cross-wind blowing against the projectile is 1/2 degree for a mean forward speed of 3000 m/sec. For such angles of incidence, in the Newtonian velocity region, the transverse force would be equal in magnitude to the resistance of the projectile; the projectile will thus carry out the deflection rapidly despite its large moment of inertia, so that the transverse force cannot increase to such magnitude.

The remaining forces, the Coriolis force and the d'Alembertian inertial force, can be given from our previous analysis. In doing this we should note that the system of forces acting on the bomb is generally a spatial system, i.e. it cannot be balanced by a single inertial force, but rather by a "screw".

If finally the bomb starts to rotate about its axis of symmetry, then gyroscopic, Magnus-, and Poisson- effects start, which affect the course of the bomb.

In order to obtain the path of the bomb, the force components along the principal directions of the compass and along the vertical must be determined and the equations of motion for the three directions in space must be written down. Integration of these would give an exact description of the twisted path in space. This extensive generalization of the well-known 'Fundamental Problem of Exterior Ballistics' is not directly soluble.

To get a preliminary picture of the path of projection, the range, final velocity of the bomb, time of fall, angle of impact, etc., we can use the well-known simple procedure of Poncelet and Didion for stepwise graphical construction of the path of fall. This procedure takes account of the earth curvature, convergence of verticals, and variation of air density and gravity with altitude, and is therefore the best suited of the usual ballistic procedures for the rocket bomb. In the actual calculation of the bomb path by this procedure, it turns out that the effect of air resistance on the path is extremely small, first because of the low air density along most of the path, second because of the small coefficient of air resistance for the slender bullet-shaped body. The paths can therefore be very accurately described as Kepler ellipses, and then the range and angle of impact can be determined from these. The actual velocity of impact of the bombs with the earth will be decreased by a few percent because of the air resistance.

The range of the bomb thrown horizontally and falling along a Kepler ellipse is given by $W = R\varepsilon \arccos\left[\frac{1}{\varepsilon}\left[1-\frac{(R+H)}{R}(1-\varepsilon)\right]\right]$ where $\varepsilon = 1 - \frac{V_0^2}{gR^2}(R+H)$ is the eccentricity of the ellipse. From these equations, the relation between the height at release H, the velocity at release V_0, and the range W, is plotted in Fig. 87. The duration of fall can be determined by integrating the path lengths or by a step-by-step calculation of the orbit, and gives values corresponding to those shown in Fig. 88. For large velocities of release, the earth rotation has a noticeable effect on the range. Since the release point is outside the earth's surface, one can insert for the velocity of release the absolute velocity of the bomb at the point of release, and then obtain the absolute length of the range from Fig. 88; the relative range on the earth can then be calculated in the usual manner.

One thing to be checked is how warm the bomb becomes in falling through the lower layers of air. In the case of the bomber, which has its high speeds in regions of rarefied air, so that it flies at moderate stagnation pressures, it was assumed that equilibrium between heat intake and radiation can be maintained by having a strongly radiating skin for sufficiently low wall temperatures, or that critical thermal stresses can be withstood in the troughs of the path by having a skin with sufficient heat capacity. During the fall of the bomb through more dense layers of air, the heat transfer per unit area of the bomb surface will increase greatly, but the bomb's fall lasts a much shorter time, so that one may compute using the heat capacity of the shell of the bomb. The stagnation- and also approximately the friction-, temperature can be

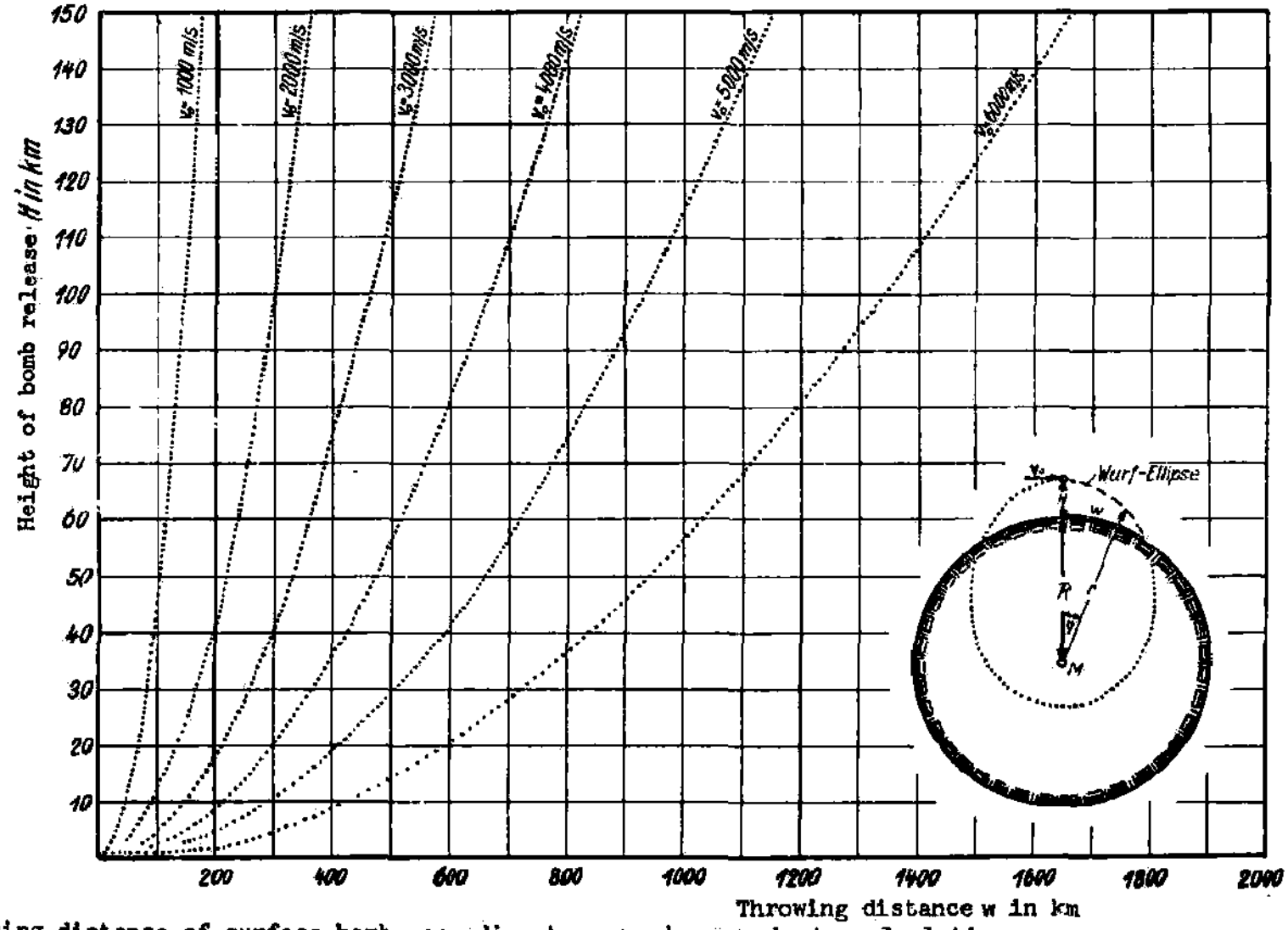

Fig. 87: Throwing distance of surface bomb according to second approximate calculation. (Path as a Keppler ellipse, taking into consideration the Earth's curvature, and also the approximate air resistance) See p. 130.

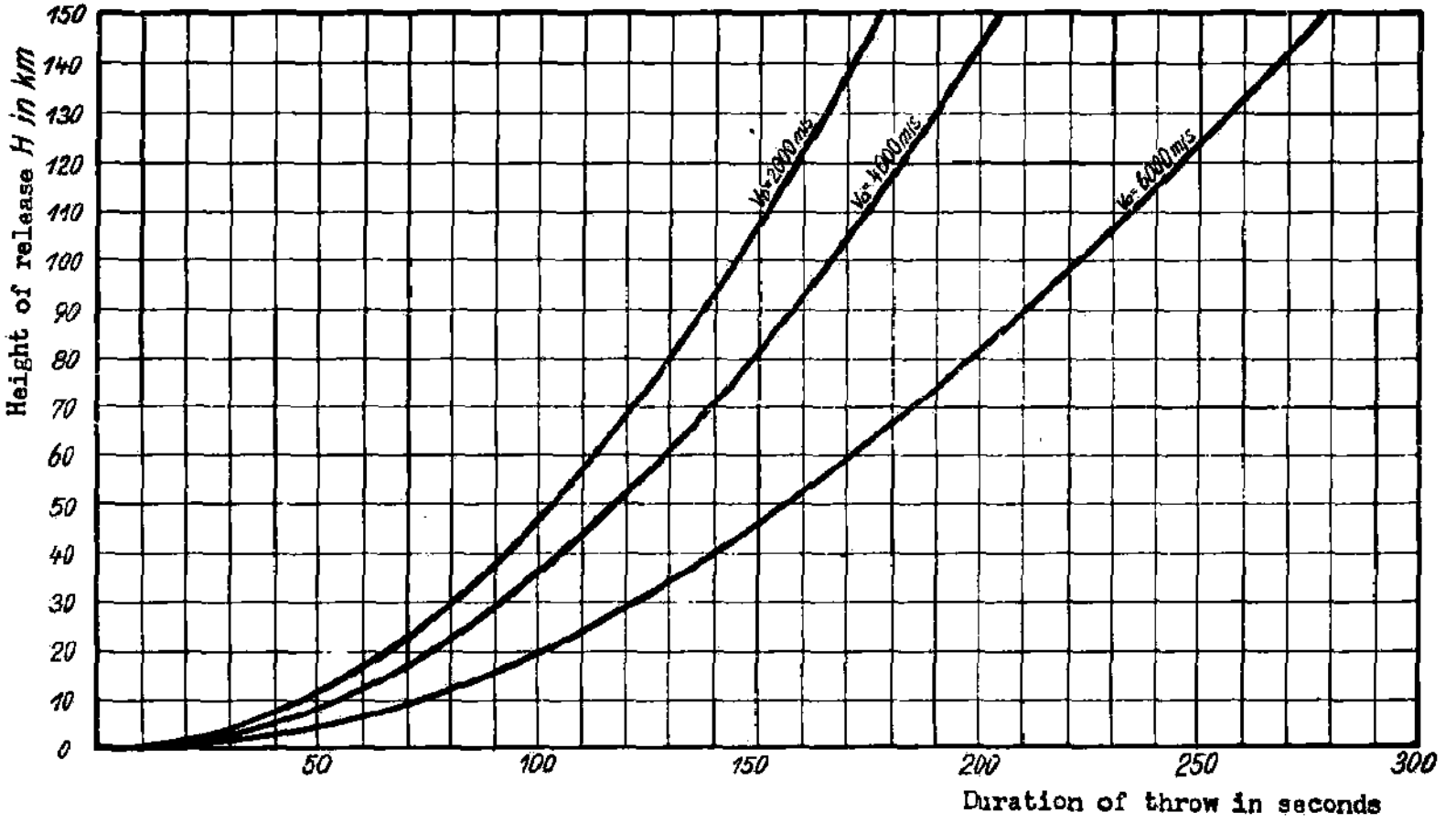

Fig. 88: Dependence of duration of throw as a function of initial altitude and velocity.

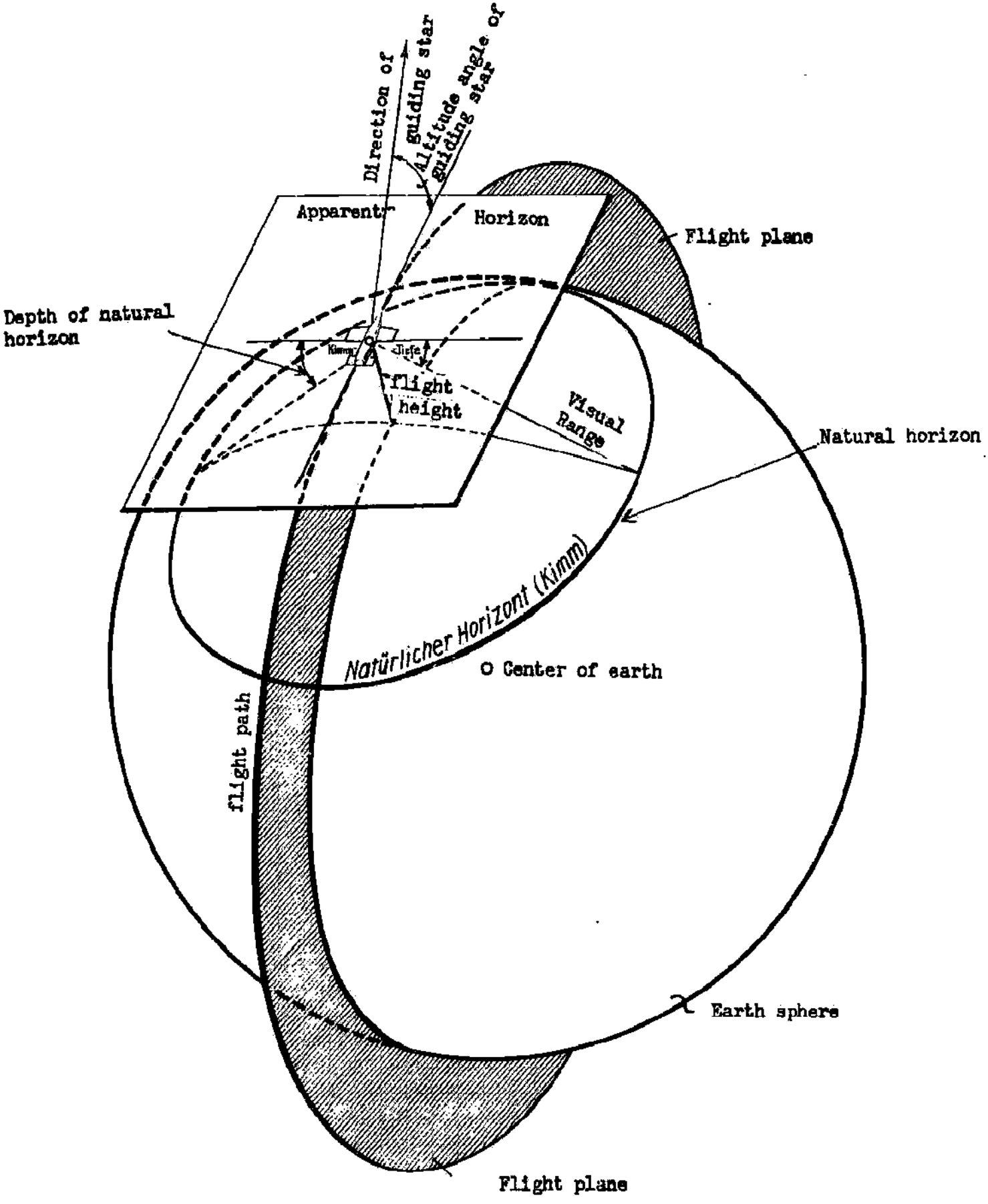

Fig. 89: The third aiming phase of bomb release (see p. 134).

estimated from the gas-dynamic energy equation to be $\Delta T = V^2/2600$ if one assumes that for high temperatures of the boundary layer, the vibrational degrees of freedom of the air molecules are completely excited, but that no dissociation occurs in the boundary layer. The laws governing the transfer of heat from the heated regions of the boundary layer to the rigid wall are unknown, but one can set up a rough energy balance by using the estimated coefficient of laminar friction of the boundary layer $C_f = 0.0003$ to calculate the work of friction per unit surface per sec. as $\tau V = c_f \cdot \varrho \cdot V = 0.5 c_f \rho V^3$ for V = 6000 m/sec at the earth's surface, this gives 5.4 hp/cm^2. If one assumes that a third of this heat goes to the wall, then one obtains the conditions of the jet throat of a powder rocket mentioned on page 8; i.e. an iron jacket only 2 cm. thick would only begin to melt after 10 sec. as a result of this heating. From more recent measurements of heat transfer at high Mach numbers, it appears to increase more slowly than the rate of frictional work, i.e. it goes like $\rho^{0.5} v^{2.5}$ this indicates that the bomb can go through the critical lower atmosphere even without the use of strongly radiating refractory protective layers for the outer covering.

Finally some general considerations are necessary concerning the accuracy of hitting for bomb release from great altitudes at high speed. In gunnery one assumes a diameter of the 50% circle equal to the range of fire. For the rocket bomber, the range of fire in this sense is the length of the path of fall of the bomb. For a mean length of say 600 km, the probable scatter would be 6 km, if one could release from the bomber with the same accuracy as one can fire from a cannon. The actual error will be the resultant of errors in release, which are determined by position-, velocity-, and direction- errors at the point of release, and of deviations during the fall, which are caused mainly by fluctuations in the density and flow of the air. The navigation of the rocket bomber to the release point is divided into three aiming procedures. The first phase consists in having the catapult apparatus lie in the direction of the target, if possible; because of its fixed installation deviations up to 90° may occur. The correction of this error occurs in the second phase right after takeoff, during the motorless flight or right at the start of the propulsion period, when the direction to the target can be set by means of the compass to within a few minutes of arc. During the glide, the aircraft must be steered very accurately, since systematic effects - rotation of the earth and atmosphere, and accidental influences, such as small asymmetries, errors in steering, fluctuations of air density, and movements of the air, continually tend to bring the aircraft out of its orbit. During the glide above the troposphere, the third phase, on which the accuracy of the bomb hits depends, is completed. In this one can think of using astronomical methods for pointing; this will be independent of the influence of the weather or the enemy; in the interference-free stationary glide path before release, it permits determination of position to an accuracy of a few seconds of arc, corresponding to position errors of little over 100 m. To determine the apparent horizon under the excellent visibility conditions available, one can sight on three points of the natural horizon; from the depth of the horizon the altitude can be determined. When the apparent horizon has been fixed, the maintenance of the prescribed orbit in space can be assured by choosing one or several stars in the plane perpendicular to the horizon through the position of the target, and following their apparent motion with a theodolite. If the guiding star, during the dynamic flight, stays in the plane of the orbit (i.e. on the vertical cross-hair) the pilot knows that he is in the prescribed orbit-plane. On the stationary flight path he can determine his absolute velocity from the apparent motion of the star along the vertical cross-hair, and his position and that of the bomb release from the altitude of the star. Whether the target is visible at the instant of bomb release is unimportant. The determination of the point of release involves only the small error in angle measurement, which corresponds to a few hundred meters. Fig. 89 is a pictorial presentation of the conditions during this third aiming phase. The errors arising during the fall of the bomb are more significant. If among the factors affecting the spread of projectiles: differences in propulsive charge, vibrations of the barrel, meteorological fluctuations, differences in the projectiles and errors in direction, only the last two are considered and each is given equal weight, then the spread would be about 2/5 of 1%, i.e. .6% (??), which for a range of projection of 600 km, gives a diameter of 3.6 km for the 50% circle. To this is added the error in navigation of the aircraft itself, so that one obtains for the probable deviation from the target of a single release, $W_{\perp} = 3$ km, with which we can make approximate calculations.

3. Ballistics of Impacts

The process of impact for point release and area release differ fundamentally in having very different velocities and angles of impact. The processes in point bombing are similar to those for ordinary bombing or heavy mortar fire, so that the necessary results can be written down; e.g. in dive bomb attack by the rocket bomber with 30, 5, or 1 ton bombs, for a final diving speed of 500, 300, or 260 m/sec, the penetrating power of bombs through the earth's crust is 100, 30, or 12 m., for reinforced concrete the values are 10% of the above; the corresponding penetrations through armor plate are 200 cm. (1.43 caliber), 60 cm (0.86 caliber) or 25 cm.

(9.55 caliber), in other words greater than the strength of all known ship's armor.

Entirely new conditions occur for the area bomb, which has a velocity of impact 10 times as great. The energy of impact is much greater than the energy content of the explosives in the bomb. The strength of the material of the bomb itself will permit it to penetrate a structure, or even to go through a city with numerous buildings, because of the small angle of impact; it will not permit penetration into the earth. The effect will thus be similar to that of a mine. The range of the explosion of a definite amount G [kg] of explosive can be estimated as $r = \sqrt{kG}$ under the assumption that the surface destroyed is proportional to the explosive charge; here r is the radius of destruction in meters, and k is a constant which gives the degree of destruction; for air pressures of about 20000 kg/m^2 which produce the worst effects on buildings and smash any except specially reinforced one, k is 3; for pressures of 5000 kg/m^2, k is 12, for which value slight damage to structures occurs, walls are overturned, and gables are destroyed; for k = 25 the safe distance of ordinary buildings from explosive storehouses is reached, and k = 200 gives the circle at which window panes and, partly, window frames are broken.

These effects are distributed uniformly in all directions from the point of impact of a very thin-walled bomb, and the result of impact of the rigid body of the shock wave moving with greater than sound velocity through the still air. The development of such shock waves in front of blunt projectiles flying at supersonic speeds is well known. The phenomenon of an explosion wave is quite similar, except that here the excitation comes only to a small extent from the bomb fragments thrown out of the bomb cover, and mostly from the combustion gases of the explosive, which for adiabatic expansion from the pressure and temperature of the explosion to a normal pressure reach radial velocities of $\sqrt{2gE}_A = 3400\ m/_{sec}$ for $E = 1400\ kcal/_{kg}$ while individual portions of the gas can reach even greater velocities at the expense of other portions. If the explosive energy is also shared with the cover of the bomb (representing say 50% the total mass), then the velocity of the radial explosion wave drops to 2400 m/sec, a figure which checks well with actually measured velocities of fragments. The exploding material of the bomb collides with the surrounding still air at this velocity, and starts the powerful and far-reaching explosion wave in it.

From the mechanics of the explosion process we can get a clear picture of the effect of high impact velocity of an areal bomb on the explosive effect. In the following consideration we shall assume an impact velocity of 8000 m/sec, which we would get if the aircraft descended to the earth's surface at 8000 m/sec and released the projectile at short range. After detonation of the areal bomb on or above the earth's surface the mass of the resultant ball of fire has not only a radial velocity of 2400 m/sec, but also the convected forward speed of 8000 m/sec. The two velocities superpose as shown in Fig. 90 to produce a velocity relative to the surrounding still air. The front face of the explosion sphere collides with the air at a velocity of 2400 + 8000 = 10400 m/sec, and excites a shock wave as if the explosive had $(10400/2400)^2 = 18.7$ times as much energy content. The intensity of the explosion wave there is 18 times as great as for a bomb exploding at rest. The intensity drops rapidly for the sideward directions, and disappears completely at the rear.

Since the area of destruction by an explosive charge is proportional to the weight of the explosive, or more precisely to the energy available for the explosion wave, the area of destruction of an areal bomb is increased in the ratio of the sum of impact energy and explosive energy to the latter alone, i.e. in the ratio $(2400^2 + 8000^2)\ 2400^{-2} = 12.1$. At the same time the destroyed area loses its circular shape, and becomes a drop-like area along the direction of release whose outline can be calculated from the square of the resultant of impact- and explosive shock-velocities. The ratio of destroyed areas for the same bomb for point release and area release is shown in Fig. 90 for an impact velocity of 8000 m/sec. The destructive action of a bomb landing after areal release is much greater than that of an equal-sized normally-dropped bomb, is fan-shaped and points in the direction of release. Thus the effect of the bomb no longer depends only on the energy content of the explosive; the kinetic energy of the bomb also produces its full effect. The effect of the fragmentation of the bursting bomb-shell increases and distributes itself in the same manner as the intensity of the explosion wave. We get the instructive conclusion for the rocket bomber that, because of the additional energy of impact, the desired degree of destruction of a given surface can be accomplished by area bombing with much smaller bomb loads than for point bombing.

VI. Types of Attack

1. Basic Types of Attack

The type of attack procedure to be used by the rocket bomber in any specific case is determined by the nature of the target and its distance from the home base.

The extraordinary variety of targets is discussed in Section VI-9. There we discuss in greater detail the basic difference between point and area targets, according to which the types of attack can be subdivided into *point-attack and area-attack procedures.*

The individual types of point attack follow from the requirement that the bomber fly as slowly as possible over the target, so that it may have rather small residual energy there. If in spite of this, the bomber is to return to its takeoff field without a stop-over, then after dropping its bombs, over the target it must be propelled by its own rocket motor until it has acquired a sufficient speed to get home on the corresponding energy. Thus we arrive at a procedure for point attack involving two propulsions and return home, which consists essentially in having the bomber, after being catapulted at the home base, accelerated only till it acquires enough energy to bring it over the target. There it releases and turns at the lowest possible speed, then starts its motor with the residual store of fuel, to get up enough energy for the home trip, and lands back at its home base. Very large quantities of fuel are required for this double propulsion, so that this procedure can be used only for limited ranges of attack (up to 6000 km) and limited bomb loads. Point attacks over greater distances or with larger bomb loads than in this first procedure are possible if the bomber can land not too far from the target, and take on new fuel.

For the point-attack procedure with two driving periods, partial turning and auxiliary point, the bomber is again accelerated after catapult from the home base, until the acquired energy carries it just to the target. Then it releases, turns through the required angle at least possible flight speed, starts its motor with a small residue of fuel on board, to get the small amount of energy which carries it to the auxiliary field not far from the target; it lands there and takes on new fuel. With this, it takes off again in normal fashion and returns to the home base; it has the possibility of making further bombing attacks on the way home.

If a point attack is to be carried out over a larger distance or with very great bomb load and there is no possible auxiliary landing place fairly near the target, then rocket-technique, as seen at the present time, gives no possibility of retrieving the bomber and bringing it back to its home field. If attack on the target seems more important than the bomber itself (which has only a relatively small material value), then there is the possibility of sacrificing the bomber after the attack. This procedure of point attack with a single propulsion period and sacrifice of the bomber is, in principle, applicable to all points on the earth's surface. It is, naturally, to be applied to attacks and targets of very special significance, as for example the surprise destruction of a government building and the governing group assembled there, to the killing of a single, specially important enemy person, to sinking large enemy transports or warships, blocking of important avenues of commerce (say canals or straits), and to similar special cases; this is less because of the loss of the aircraft than for the more valuable pilot.

For procedures of attack on an area the need to fly slowly over the target disappears, so that one has more freedom in carrying out the procedure. The most obvious procedure for area attack, with single propulsive period and return home, consists in the bomber being catapulted from its home base, and then driven until it gets sufficient energy to get to the vicinity of the target, turn and get back home. The turn path uses up very large amounts of energy, so that this attack procedure remains limited to small distances and bomb loads.

Area attack over great distances is very much simplified, if an auxiliary field exists not too far from the target, so that the bomber can land and take on new fuel for the return trip. In this case the area attack goes as follows: after release the bomber makes a partial turn through an angle less than 180° (this requires smaller energy consumption than for a complete turn), then flies to the auxiliary field on its residual energy. This area attack with single propulsion, partial turn and auxiliary field is applicable to all distances on the earth; it assumes, however, that within at most a few thousand km. from the target there is a suitable auxiliary field, for landing, and which has a takeoff apparatus. In view of the large number of possible targets for area attack, this requirement can be fulfilled only in exceptional cases.

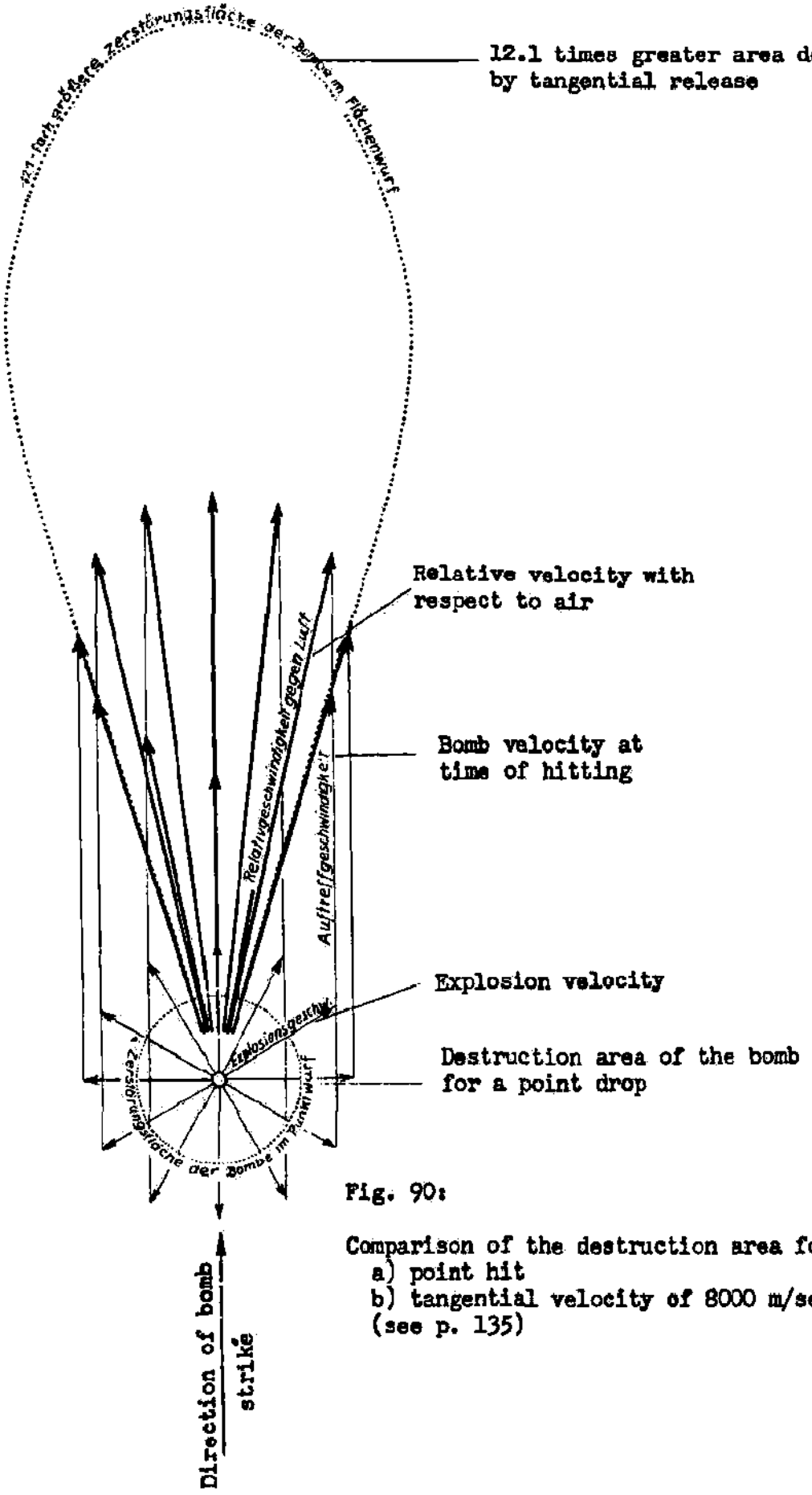

Fig. 90:

Comparison of the destruction area for same bomb
a) point hit
b) tangential velocity of 8000 m/sec.
(see p. 135)

The value of the auxiliary point can vary considerably, not only according to its distance from the target, but also because of the size of the required angle of turn. Since large angles of turn are much more harmful than great distances, an obvious idea is to provide auxiliary points beyond all forseeable targets; e.g. beyond the two population concentrations outside of Europe (North America and S. E. Asia), say on the Marianas in the Pacific Ocean or on the islands of that ocean off the Mexican coast; or to secure a single auxiliary point at the antipodes of the home base, say in New Zealand or on the islands east of it. This auxiliary point at the antipodes can always be reached by straight flight without turning, no matter what point on the earth is attacked. Its distance from the target can be very large. On this discussion is based the method of area attack with single propulsion and auxiliary point at the antipodes. Such a single auxiliary point also has the advantage that it can easily be fully equipped to enable aircraft also to make bombing attacks on their journey back to the home base, and that its island location can be easily protected against enemy attacks; against the most dangerous attacks by enemy fleet units, this could be done by the rocket bombers.

If such an auxiliary point at the antipodes is not available, area attacks over large distances can be carried out by having the bomber, after release, fly a straight course all the way around the earth till it reaches the home base. This is the procedure for area attack with single propulsion and Circumnavigation of the globe.

Summarizing: all possible procedures for area attack coincide in what happens up to the bomb release; they differ only in the manner of bringing the bomber home after it releases its bomb load.

2. Point Attack with Two Propulsion Periods and Reversal of Path

If we denote the weight of the bomber in the separate phases of this attack procedure by G_0 for the fully loaded bomber weighing 100 tons, G_1 after consumption of fuel for the outward trip, G_2 after bomb release, and G_3 the empty weight of 10 tons after consumption of the fuel for the homeward flight, then the identical distances of outward flight and return are determined by identical ratios G_1/G_0 and G_3/G_2 according to Fig. 80, while the bomb load $B = G_1 - G_2$. Thus we obtain for each bomb load $G_1/G_0 = G_3/G_2 = \sqrt{B^2/4 + 10000} - B/2$ and the relation between bomb load and range shown in Fig. 82, which also gives the range of this attack procedure. Figs. 91, 92, 93 show these ranges of attack, for three exhaust speeds $C = 3$, 4, and 5000 m/sec and with approximate inclusion of the earth's rotation, as contours of equal permissible bomb load, on a map of the earth's surface. The pictures show the effectiveness of the rocket bomber in a very persuasive fashion. Despite the unfavorable double propulsion the bomber, for the intermediate exhaust speed, is able to carry out point attacks within a radius of 2000 km., which includes all the strong points in Europe between Moscow and Madrid, Northern Sweden and Tripoli, Ireland and Ankara; these attacks can be carried out with extreme accuracy on any no matter how small object on land or sea, with a bomb load of 30 tons, which bomb load will stove in all except specially reinforced structures within 300 m; penetrate earth works 100 m. thick, and steel armor 1 meter thick; and then the bomber can return home without a stopover! With a smaller bomb load the same bomber can carry its attacks to over 6000 km; from Germany to Central Africa, Hindustan, Eastern Siberia, the North polar regions, to the east coast of North America and over the whole North Atlantic.

For $C = 3000$ m/sec, this range shrinks to Europe and the immediately adjacent regions; for $C = 5000$ m/sec it expands beyond the hemisphere with Europe as center. The procedure of point attack with two propulsion periods thus appears to have extraordinary practical importance, and is applicable to all actions inside Europe or in neighboring regions. In its favor is the fact that, though the bomber during a point attack comes into the enemy defense zone at the target at low velocity and altitude, the attack will generally be such a surprise that even a warship on the alert will scarcely have sufficient time to bother the bomber, much less to ward off the attack.

3. Point Attack with Two Propulsion Periods, Partial Turn and Auxiliary Point

This method of point attack differs from that of the preceding section only because the return flight can be shorter than the outward trip from the home base to the target since the landing is to be made at a suitable auxiliary location other than the home base. Because of the small kinetic energy over the target, the angle of turn is unimportant; the only important quantity is the distance from the target to the auxiliary point, measured as a fraction k of the distance a from takeoff point to target. With the notation of the preceding section, one has

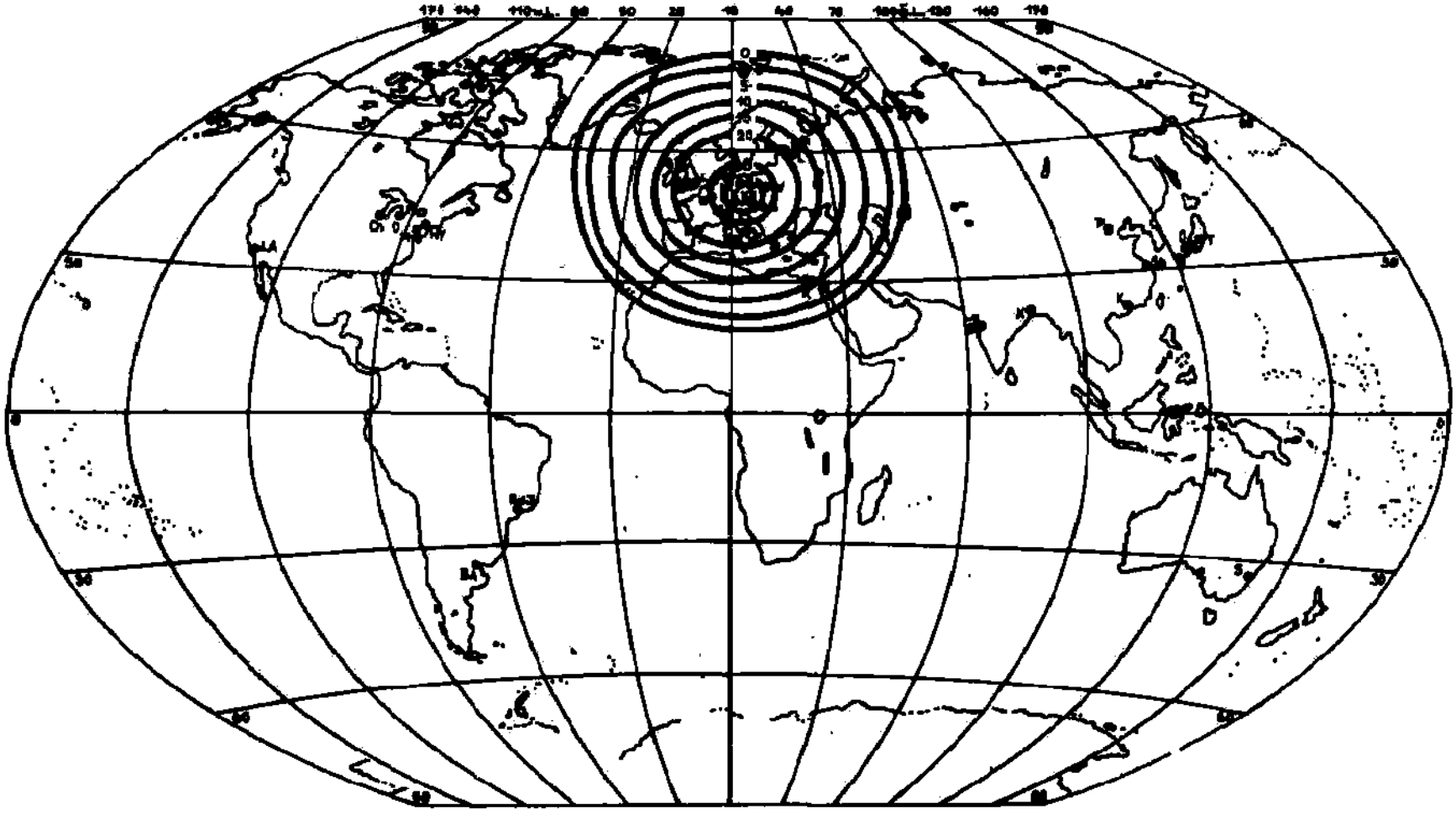

● Cities of more than one million.
× Home base

Fig. 91: Bomb load in tons (i.e. percentage of the initial flight weight) of the Rocket Bomber in the case of point attack - double propulsion with intermediate turn around - and with exhaust velocity c = 3000 m/sec.

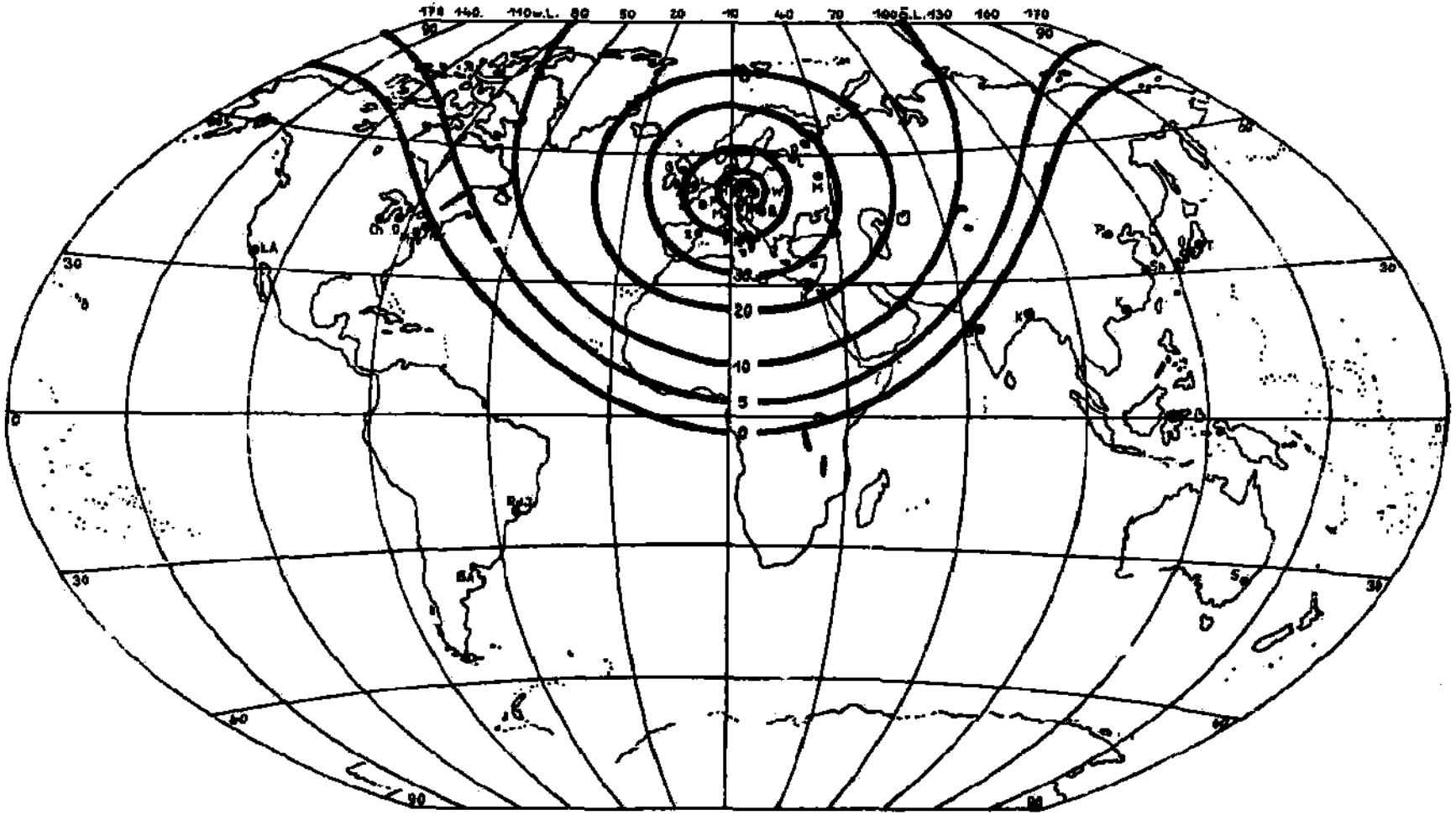

● Cities of more than one million
x Home base

Fig. 92: Bomb load in tons (i.e. percent of the initial flight weight) of the Rocket Bomber in the case of point attack - double propulsion with intermediate turn around - and with exhaust velocity c = 4000 m/sec.

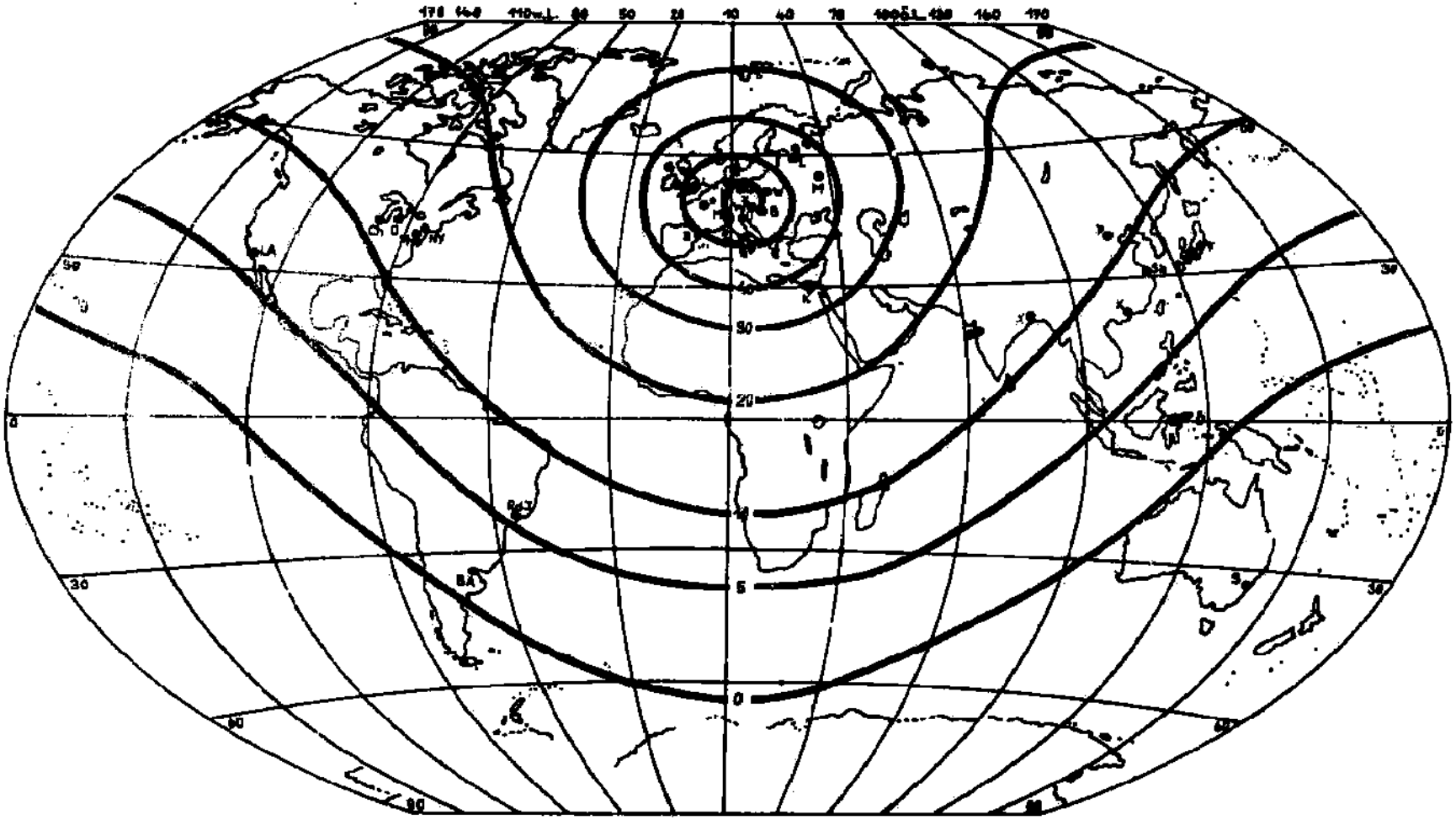

● Cities of more than one million

× Home base

Fig. 93: Bomb load in tons (i.e. percent of the initial flight weight) of the Rocket Bomber in the case of point attack - double propulsion with intermediate turn around - and with exhaust velocity c = 5000 m/sec.

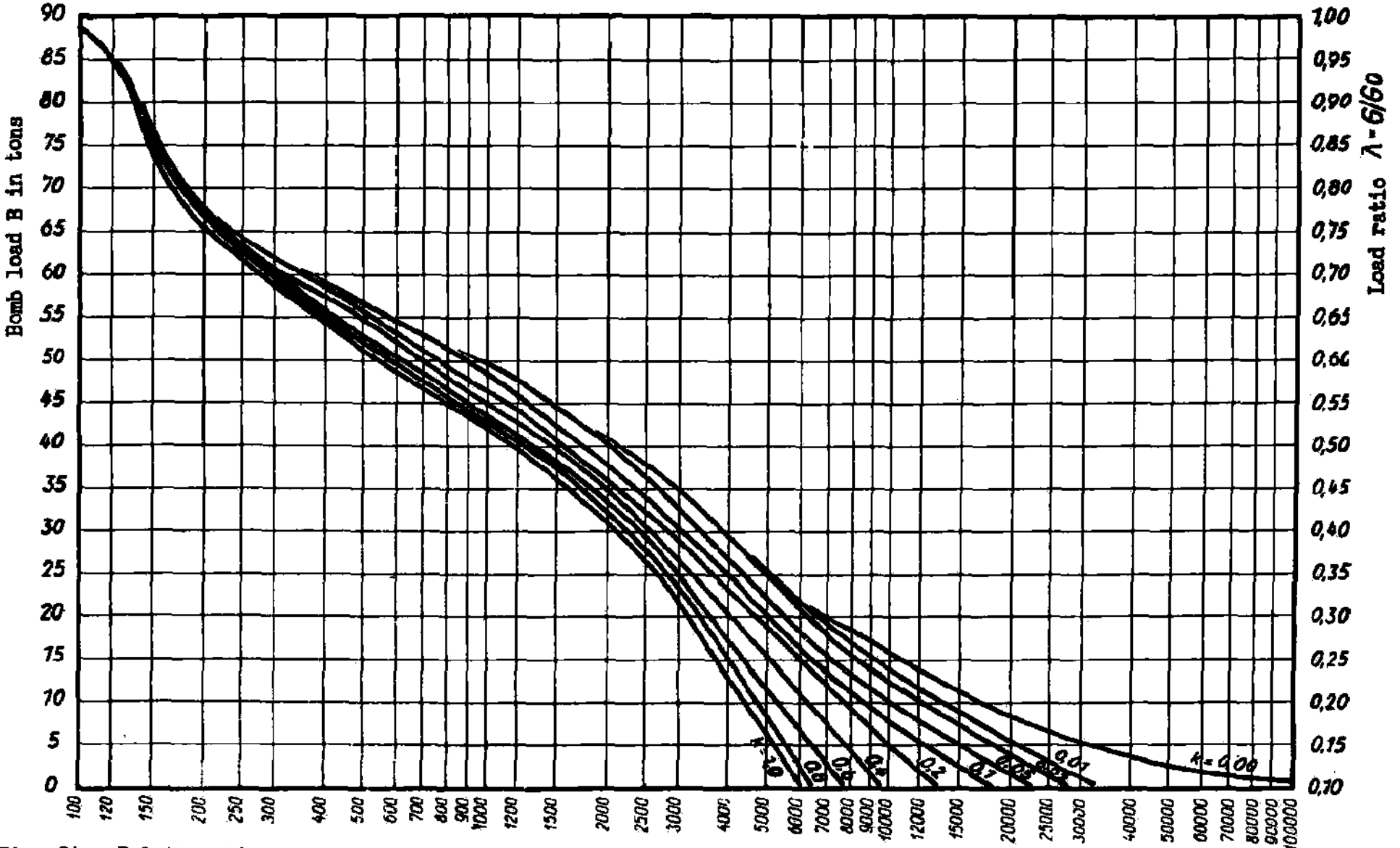

Fig. 94: Relationship between attack range a, and return range k.a and bomb load B, that is load ratio, in case of a point attack and a second propulsion at the knee of a dog leg path to a secondary base, c = 4000 m/sec. (see p. 138, sec. 3)

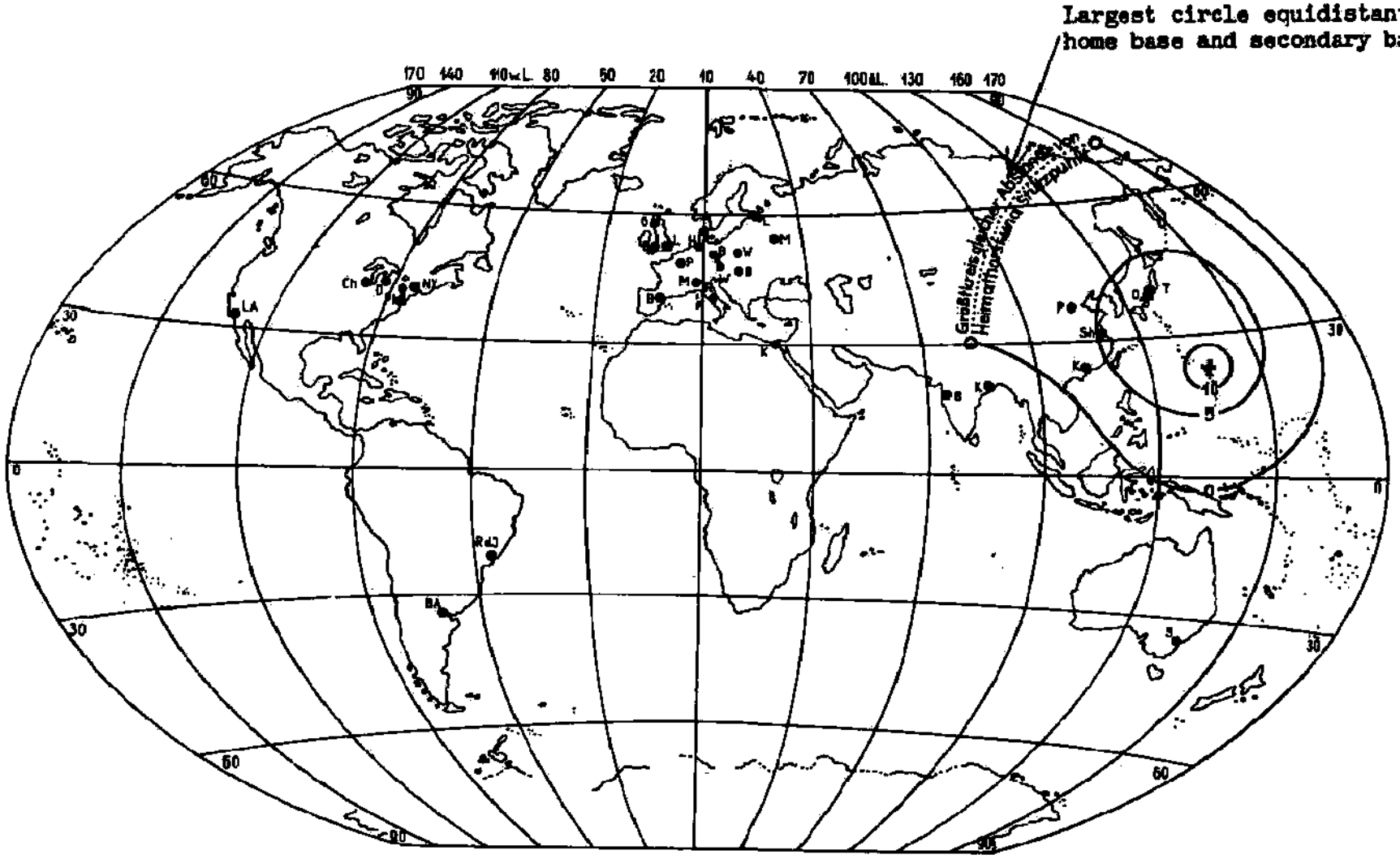

Fig. 95: Bomb load of a Rocket Bomber in tons (percent of the take-off weight) in the case of a point attack, dog leg path, second propulsion at the knee, and a secondary base in the Marianas Islands. Exhaust velocity c = 4000 m/sec.

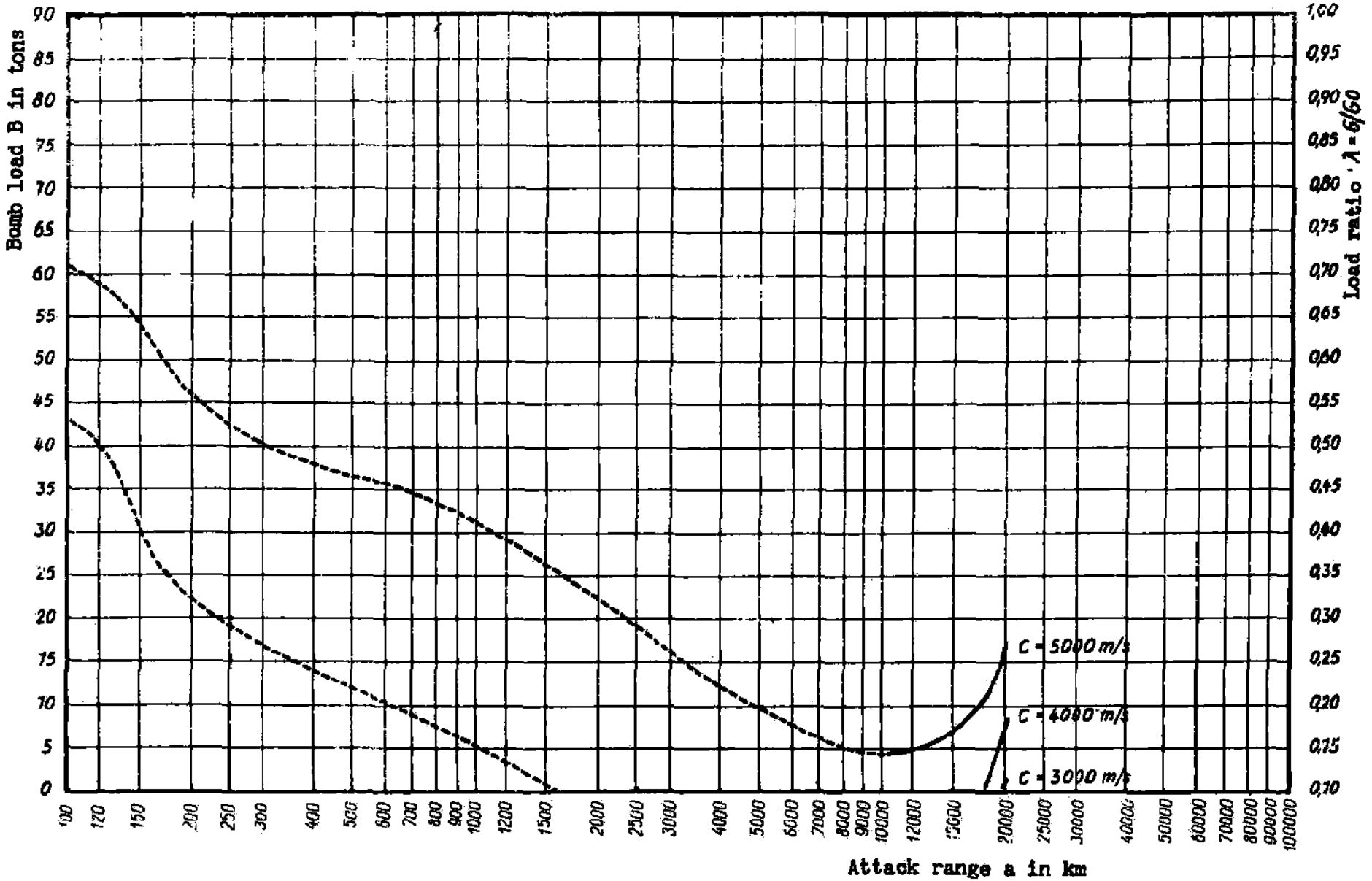

Fig. 96: Relationship between attack range a and bomb load B, i.e. load ratio , in the case of point attack with double propulsion and landing at the antipodal point for c = 3000, 4000 and 5000 m/sec.

two characteristic weight-ratios $G_{1/100}$ and $^{10}/G_2$ for the outward-bound flight and the flight to the auxiliary point, respectively. Thus to each distance of attack a and to the corresponding return distance ka, the required weight-ratios and the possible bomb load $B = G_1 - G_2$ can be gotten from Fig. 80. For k = o, we get the curves of Fig. 80; for k = 1, those of Fig. 82, and for all other values of k we get intermediate values, which for the case of $c = 4000$ m/sec, are shown in Fig. 94. Compared to the previous maximum possible range of attack of 5000 km, we now have unlimited ranges of attack up to 20000 km. if an auxiliary point is available sufficiently near near the target. Fig. 95 shows the contours of constant bomb-load in using an auxiliary point in the Marianas - i.e. when a landing is made at the auxiliary point after the attack. Since a point attack with two propulsions and use of an auxiliary point is sensible only for those parts of the earth's surface which are nearer to the auxiliary point than to the home base, the largest circle whose points are equidistant from home base and auxiliary point has been marked on Fig. 95. The bomb lines are limited to the region of the earth's surface beyond this. The possible range of attack in this case includes all of East Asia and a large part of the Western Pacific. For $c = 3000$ m/sec, the bomb-load curves shrink to small circles around the auxiliary point; for $c = 5000$ m/sec, they spread out over practically the whole hemisphere opposite Europe. When using an antipodal auxiliary point, a + ka = 20000 km, and the possible bomb loads have the values shown in Fig. 96. In this case bomb loads are possible only for quite large ranges of attack - for $c = 4000$ m/sec, only beyond 17,800 km, i.e. in a small circle around the antipodal point with a 2200 km. radius. Whereas an antipodal auxiliary point can be important for area attacks, it is of value for point attacks only when the point itself is to be protected (say against attacks by a fleet) by rocket bombers from the home field.

As an example of point attack with two propulsions and auxiliary point, an attack on the locks of the Panama Canal and landing at an auxiliary field on the American West coast will be described briefly. For $c = 4000$ m/sec, the bomb load is 2 tons; the characteristic numbers for the attacking flight are: Takeoff: time 0 sec, weight 100 tons, velocity 0m/sec, altitude 0 km, distance travelled 0 km; Climb from takeoff track to northwest; 11 sec. after takeoff; weight 100 tons, velocity 500 m/sec, altitude 0 km., distance 3 km. End of the motorless flight: time 36 sec, weight 100 tons, velocity 284 m/sec, altitude 3.7 km, distance travelled 12 km; End of Climb Period: time 332 sec, weight 26 tons, velocity 4560 m/sec, altitude 60 km, distance travelled 5/2 km; End of Supersonic descent: 3882 sec., weight 26 tons, velocity 300 m/sec., altitude 14 km., distance 9390 km. End of Subsonic Descent: the subsonic descent ends with the start of the diving attack; the final altitude is thus determined by the succeding dive. Since for an attack on the Canal-locks maximum accuracy of hits is more important than high impact velocity of the bomb, the end of the subsonic descent is chosen as 2 km. altitude. From this we get the other numbers: time 4162 sec, weight 26 tons, velocity 142 m/sec, distance travelled 9450 km; End of Dive-attack: the dive-attack goes from 2 km. to about 0.5 km. altitude; the final velocity of the dive is about 200 m/sec; then the bombs are released and the aircraft goes off with small loss in velocity, approaching to within negligible distances from the earth's surface. From this we get the values: Time 4172 sec, weight 24 tons, velocity 200 m/sec, altitude 0 km, distance travelled 9450 km;
End of the Second Climb Period: time 4405 sec, weight 10 tons, velocity 2800 m/sec, altitude 22 km., distance travelled 9710 km;
End of the Second Supersonic Glide-Flight: time 6125 sec, weight 10 tons, velocity 300 m/sec, altitude 20 km., distance travelled 12550 km;
End of the Second Subsonic Glide-Flight: time 6785 sec, weight 10 tons, velocity 80 m/sec, altitude 0 km., distance travelled 12648 km;
Landing: time 6810 sec, weight 10 tons, velocity 0 m/sec, altitude 0 km., distance travelled 12650 km.

4. Point Attack with Sacrifice of the Bomber

According to the previous considerations the rocket bomber with moderate exhaust speed can carry out attacks against small individual targets up to 6000 km. distance from the home base; if there is an antipodal auxiliary point, the range extends to 2000 km. from this point; for arbitrary auxiliary points distributed over the earth's surface, the range is the same distance from each of the points. If however the point attack is to be directed at a target in whose vicinity there is no auxiliary point, there is the possibility that the bomber proceeds exactly as described in the previous section, and lands at a corresponding point near the target even though the technical installations of an auxiliary point do not exist there. In this case it will no longer be able to take off from this point under its own power but will not in general be lost if the landing does not occur in enemy territory. If there is no other possibility than landing in enemy territory, then we are left with a last, not to be neglected, way out-point attack with single propulsion and sacrifice of the bomber.

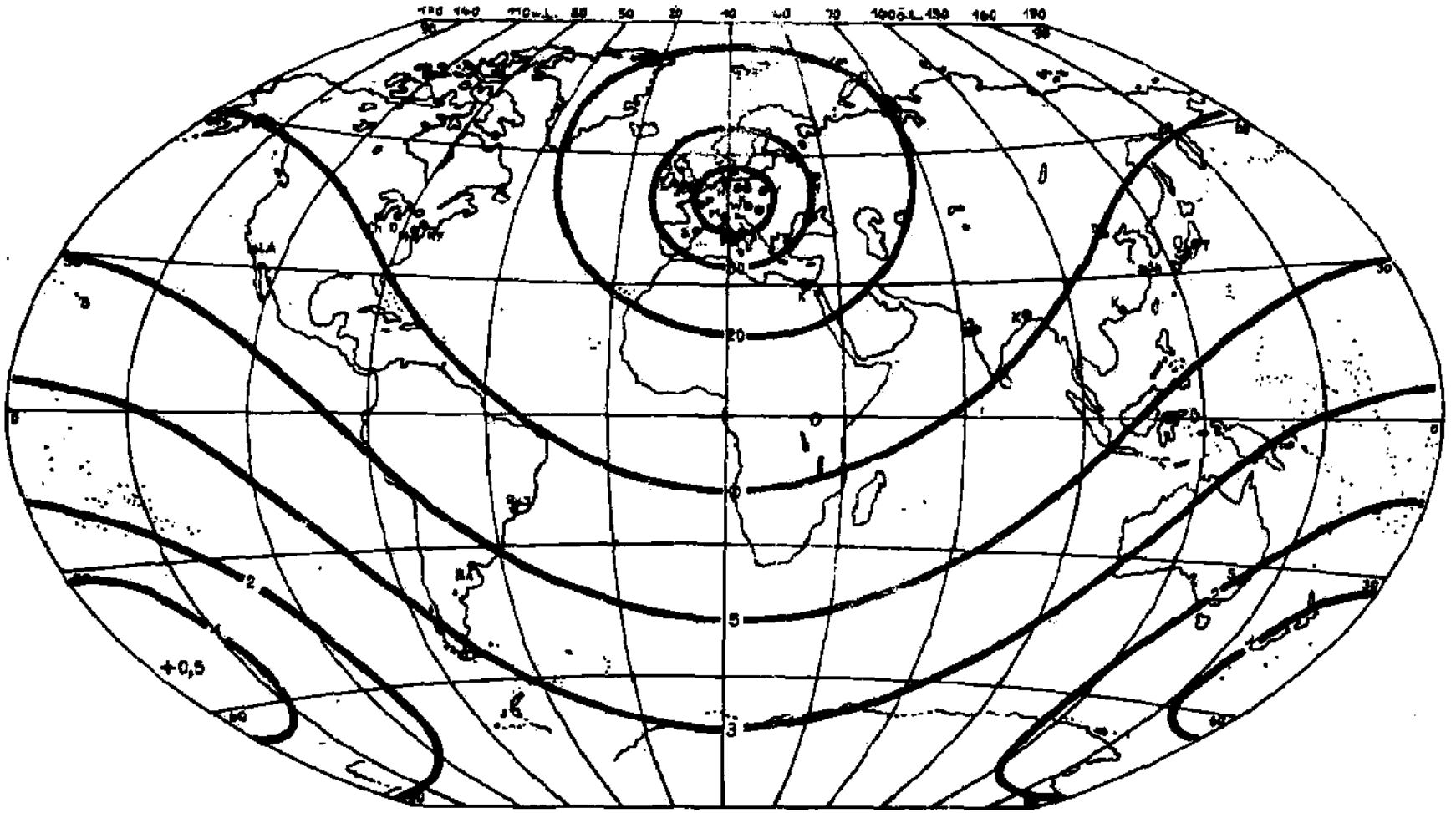

● Cities of more than one million

+ Antipodal base point

× Home base

Fig. 97: Bomb load of a Rocket Bomber in tons, that is percent of the initial weight, in the case of point attack with a single acceleration and sacrifice of the bomber and with exhaust velocity c = 3000 m/sec.

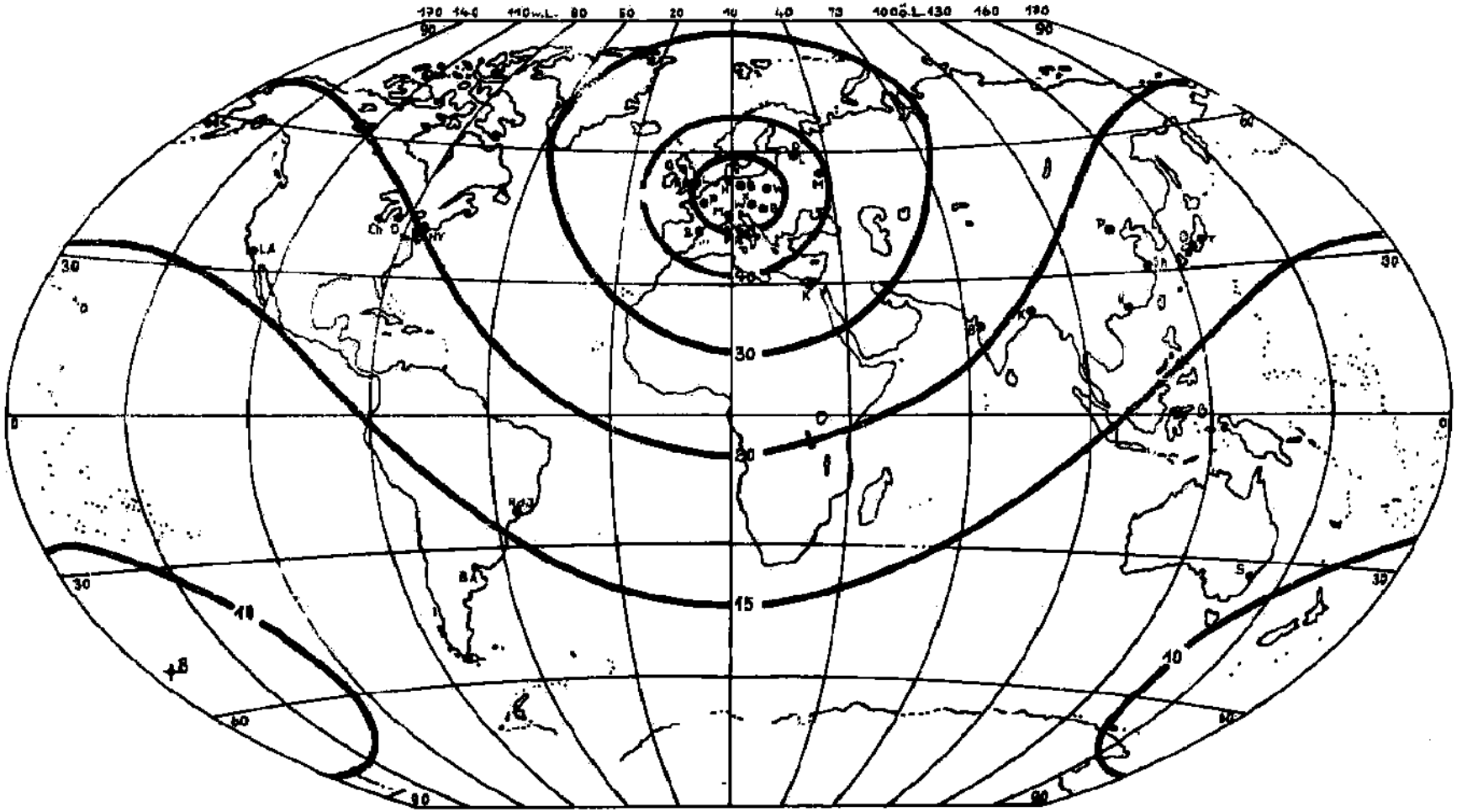

● Cities of more than one million

× Home base

\+ Antipodal base point

Fig. 98: Bomb load of a Rocket Bomber in tons, that is percent of the initial weight, in the case of point attack with a single acceleration and sacrifice of the bomber and with exhaust velocity c = 4000 m/sec.

Since the aircraft gains altitude rapidly after bomb release in a point attack, the pilot can, at the end of this brief climb, parachute from the plane and destroy the empty aircraft to keep it from getting into the hands of the enemy. He will land a few km. away from the point of the impact of his bombs, and be captured. From the point of view of performance this procedure represents the limiting case of the point attack procedure described in the previous section, for which k = o, i.e. the return flight distance is zero. Figs. 97 and 98 show the possible bomb-loads for this method of attack. In all cases, the attacking range covers the entire surface of the earth; at c = 3000 m/sec. 0.5 tons of bombs can still be carried to points most distant from the home base; for c = 4000 m/sec. this figure increases to 8 tons, and for c = 5000 m/sec. to 17 tons. This procedure is naturally also suited to unpiloted use of the rocket bomber.

5. Area Attack with Full Turn

This first procedure for area attack corresponds to the first point attack procedure described, with the difference that the energy supplied at the start of the flight must suffice for the outward flight and the entire return trip to the home base; thus large kinetic energy is present over the target, and considerable fractions of this energy are lost in turning. An outline of the entire flight path including the path of the bomb is included as a sketch in Fig. 99. In order to calculate the relation shown between bomb-load B and range of attack a, one can proceed as follows: from IV 3, S_5, the length of the subsonic glide is known. From Fig. 79, we get the value of V_{w2} for $(a - S_5 - W)$; from Fig. 99 we get V_{w1}. Now the length of the climb, S_3, must be estimated by reading off from Fig. 64 a first value of G/G_o for an assumed V_1, and then getting from this a first estimate of S_3. Then $(a - S_3 - W)$ is given from $S_5 + (a - S_5 - W) - S_3$. The initial velocity V_1 on the supersonic descending path, in order to have velocity V_{w1} after a length of glide of $(a - S_3 - W)$, can be obtained as described from Fig. 79. This value is to be compared with the estimated value and improved, if necessary. From Fig. 64 we now get the desired G and B = G - 10. From Fig. 83, the stationary altitude H_2 for given V_{w1} and G, is known, and finally the range of projection of the bomb, W, corresponding to V_{w1} and H_1 is read from Fig. 87. The range of attack, a, is thus $a = S_5 + (a - S_5 - W) + W$. This calculation contains a few assumptions which should be considered briefly. First, the assumption is made that relations between velocity and distance calculated for particular flight paths can be transferred, unaltered, to similar flight paths. More important is the assumption that the supersonic descending path, during the flight before bomb release and during the turn, is carried out at the stationary altitude, rather than in the strongly oscillating dynamical flight path. This is necessary for the decisive third phase of aiming, in order to attain the necessary aiming accuracy for the bomb release and in order to release the bombs during horizontal flight. Stationary altitudes of flight are also necessary for the period of turn in order to set up the aerodynamic turning-forces.

This last circumstance is connected with the fact that turning is possible only up to definite velocities of flight below the velocity of points on the earth's surface; for higher velocities, other methods of attack must be used. For this reason the procedure of area attack with single propulsion and full turn is limited to the ranges (up to 12000 km.) marked in Fig. 99. Inside this space it proves to be extremely effective despite the very costly turning process.

Figs. 100 and 101 show the lines of equal bomb-weight dropped at the target by this area attack procedure, for c = 3000 and 4000 m/sec. For the former value of exhaust speed, the domain of attack is bounded by a closed curve which deviates from a circle because of the earth's rotation, and whose periphery touches the North Pole, Newfoundland, Central Africa, and Central Asia. For c = 4000 m/sec, the ring expands so that now only Australia, the South polar regions, the South Pacific and the southern tip of South America do not lie within it. For c = 5000 m/sec. it would cover the whole surface of the earth.

As an example of area attack with single propulsion and full turn, we use the attack on New York at a range of 6500 km. For c = 4000 m/sec, the bomb load is 6 tons, and the detailed attack runs as follows: the motor starts to work 36 seconds after the take-off at 12 km. distance from the take-off point, and consumes the total fuel supply of 84 tons in the next 336 sec. At the end of the climb process, the aircraft reaches a velocity of 6370 m/sec, an altitude of 91 km, a distance of 736 km. from the point of take-off, and a weight of 16 tons. Using only its store of potential and kinetic energy, the bomber flies on to the point of bomb release, 5550 km. from the take-off point, and 950 km. in front of the target. At this point, which is reached 1150 sec. after take-off, the velocity has decreased to 6000 m/sec, and the stationary altitude to 50 km. After the bomb release the weight is 10 tons. Then the aircraft goes into a turn and in 330 sec. goes through a turn-spiral 1000 km. in diameter until it has reached the direction for the return flight to the home base. During turning, the altitude is greatly decreased in order to develop

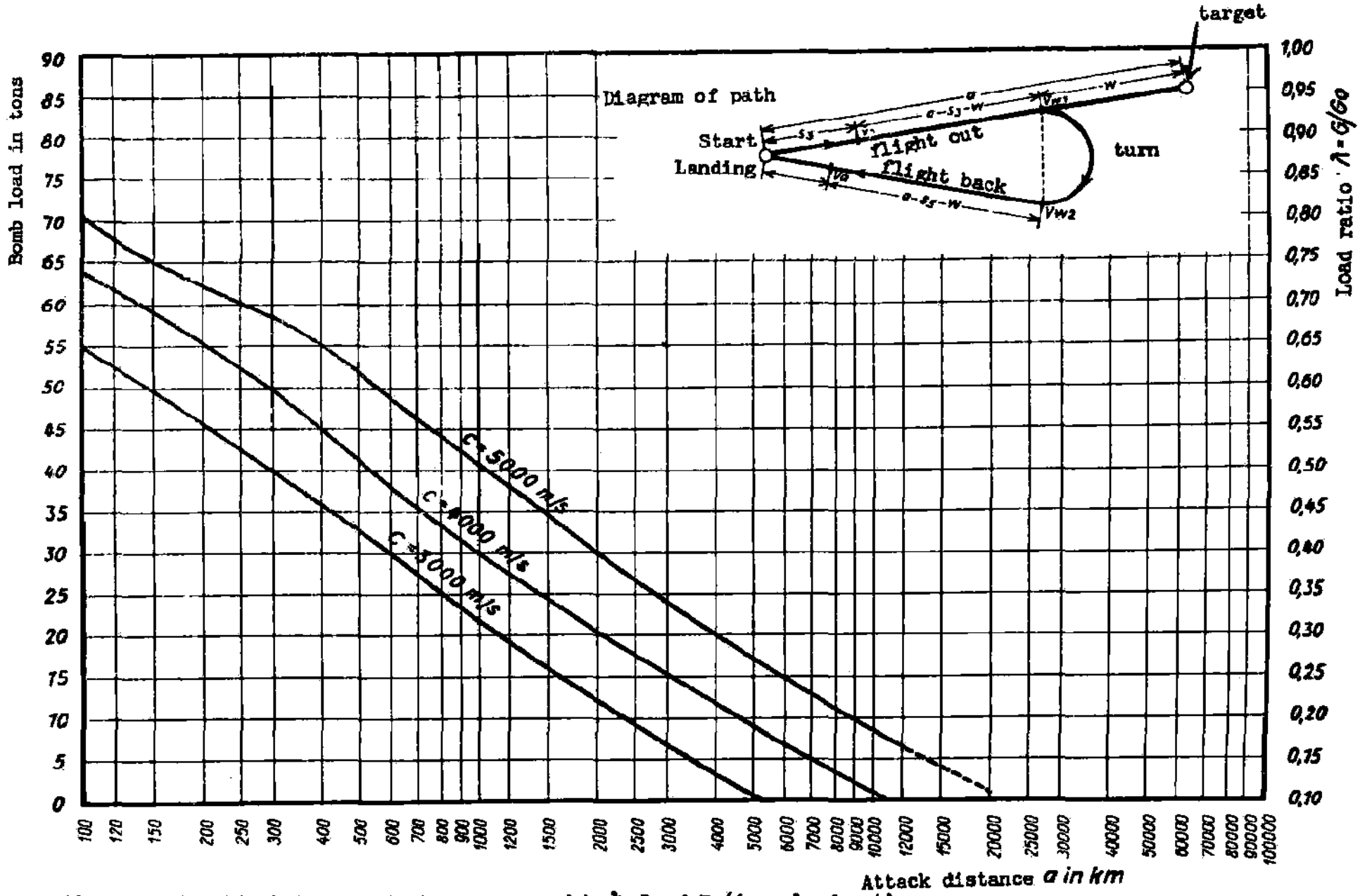

Fig. 99: Relationship between attack range a and bomb load B (i.e. load ratio G/G_o) in the case of area attack with turn around for the exhaust velocities c = 3000, 4000 and 5000 m/sec.

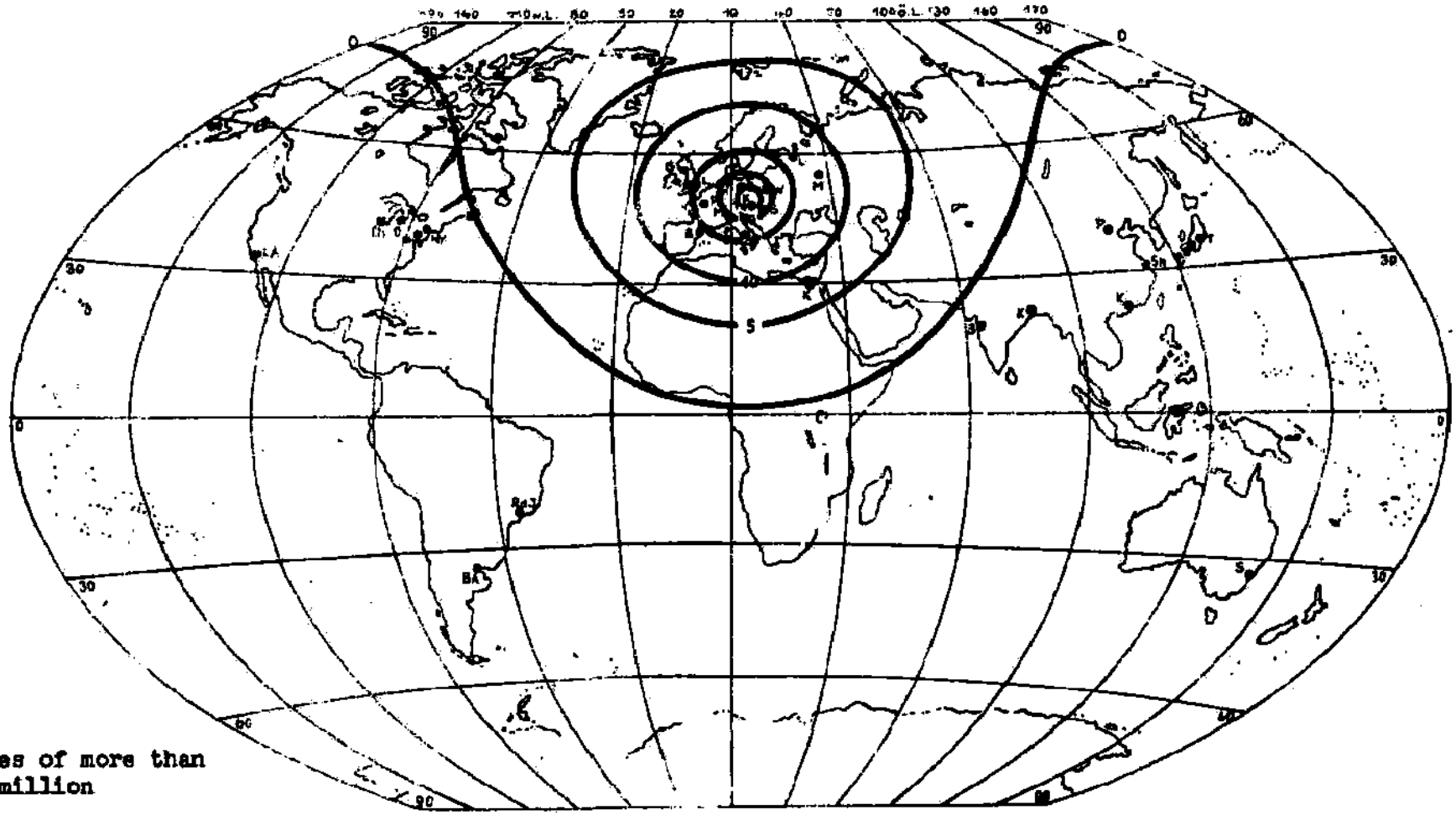

Fig. 100: Bomb load of a Rocket Bomber in tons (i.e. percent of the take-off weight) in the case of area attack with turn around and an exhaust velocity c = 3000 m/sec.

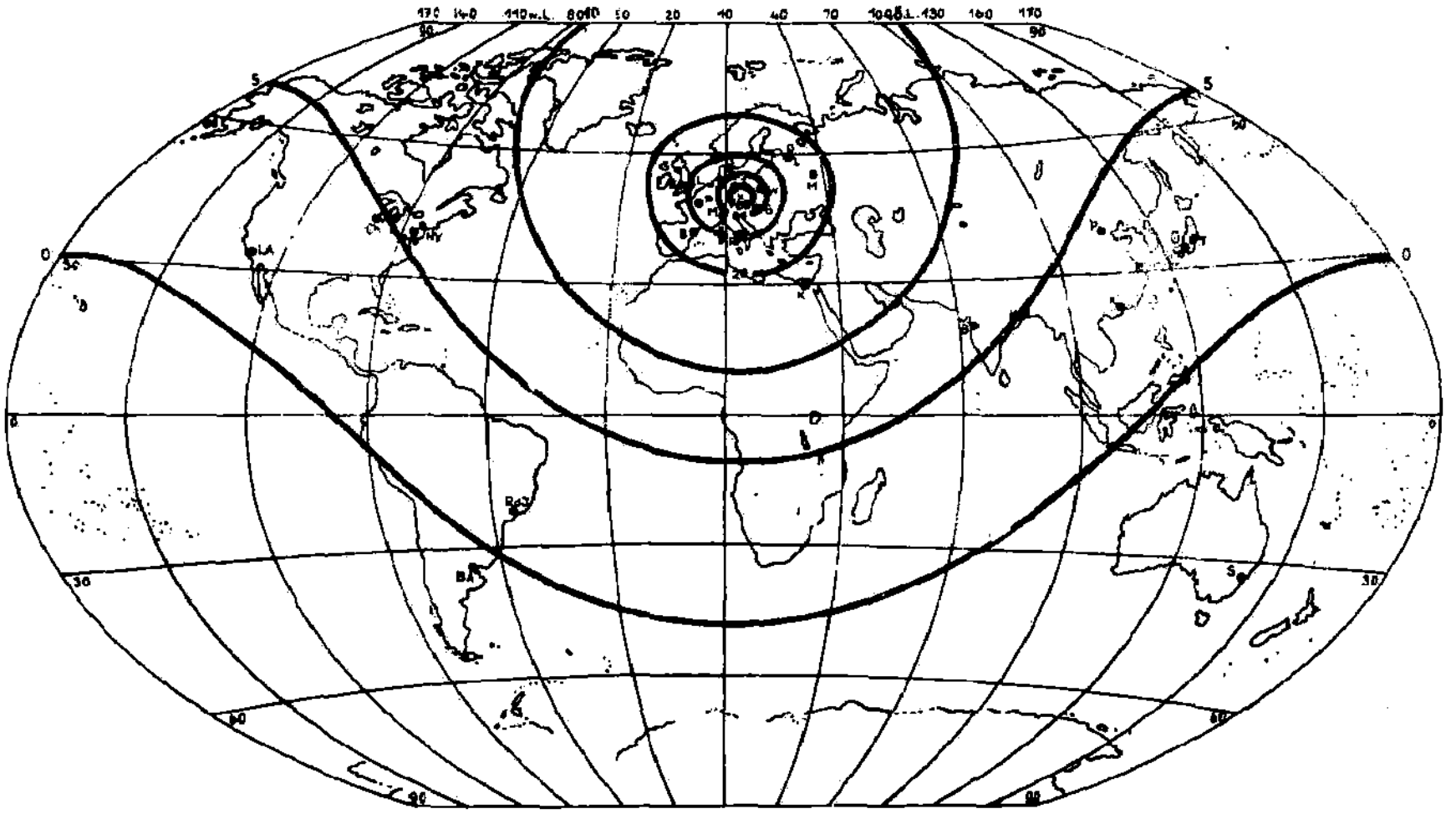

● Cities of more than one million

× Home base

Fig. 101: *Bomb load of a Rocket Bomber in tons (i.e. percent of the take-off weight) in the case of area attack with turn around and an exhaust velocity c = 4000 m/sec.*

the aerodynamic forces necessary for the turn. At the end of the turn path, the velocity is still 3700 m/sec. and the corresponding stationary altitude is 38 km. The supersonic glide-path in the direction of the home base goes over 5450 km. in 2600 sec. and ends 100 km. before the home base at an altitude of 20 km. and velocity 300 m/sec. Subsonic glide and landing are completed in customary fashion. The whole flight lasts 4755 sec.

6. Area Attack with Partial Turn and Auxiliary Point

This type of attack corresponds to the point attack with two propulsion periods, partial turn and auxiliary point. Like the latter, the area attack discussed here represents the most general case in its class, and includes all other procedures for area attack as special cases.

The course of an area attack with single propulsion, partial turn and auxiliary point consists essentially of first giving the bomber, during a single propulsion period, all the power which it requires until landing at the predetermined auxiliary point, having the bomber release its bombs in front of the target, at high altitude and flight velocity, as for area bombing, then carry out a turn at the existing high speed immediately after the bomb release, which takes it into the direction of the auxiliary point at which a landing is contemplated, and finally glides with its residual energy to this auxiliary point and lands there.

The first thing to determine is the relation between bomb load B and attack-range $\underline{a}$. This relation is affected by the distance $\underline{ka}$ between target, and auxiliary point, the angle of turn σ through which the bomber goes after release, and the exhaust speed c. Because of the large number of independent variables, the relations are many-sided. For example, Fig. 102 shows the relation between $\underline{a}$ and B for a large number of distances of return flight, ka, and for a definite angle of turn, $\sigma = 60°$. The procedure of computation which gave these curves was the following: Assuming a definite c, a bomb-load B was chosen. To this there corresponds a mass-ratio $G/G_0 = (10 + B)/100$, a length S_3 of climb path, and from Fig. 59 a final velocity V_1. For this maximum velocity V_1, one can now choose various ranges of attack $a = S_3 + S_4 + \Psi$ in such a way that before the bomb release, (i e. at the end of the outward flight over $S_1 + S_2 + S_3 + S_4$), a sufficient supersonic speed still exists. For this velocity and various turn-angles σ, we can, with the aid of Fig. 81, calculate the loss of speed and the distance S_w travelled during the turn, and from the residual velocity finally calculate the " distance of return " from release point to landing-point. By several repetitions of this procedure, and interpolation between the rough S_H - values found, the ka -curves of Fig. 102 were obtained.

Fig. 103 again shows the lines of constant bomb load for a rocket bomber using this procedure of attack, if an auxiliary point on the west coast of America is used. It should be pointed out that for turn-angle $\sigma = o$, there is a definite bomb-load with which the bomber reaches the auxiliary point and can release its load at any point enroute without altering the range, provided the release occurs after the motor is turned off. Thus for $\sigma = o$ the range of is anywhere between take-off point and auxiliary point. According to Fig. 103, this bomb load is 5 tons for $c = 3000$ m/sec. With smaller bomb loads the possible area of attack stretches over all of North America and considerable portions of South America and the Pacific Ocean.

7. Area Attack with Antipodal Auxiliary Point

A special case of the area attack described in the previous section occurs if the auxiliary point is at the antipodes of the home base. In this case the turn-angle is zero for all targets. Thus there are no energy losses due to turning at speeds above that of sound. The relation between bomb-load B and attack-range $\underline{a}$ can be obtained from the equations of the preceding section for $\sigma = o$ and $a + ka = km$. For a rectilinear flight with total distance $a\,(1 + k) = 20000$ km, with the present approximations it does not matter at what place on the glide-flight the bombs are released. Thus, within the 20000 km. range of flight, the range of attack is arbitrary and independent of bomb load. From Fig. 80, the possible bomb load is 0.7 tons for $c = 3000$ m/sec, B = 8 tons for $c = 4000$ m/sec, and B = 17 tons for $c = 5000$ m/sec.

8. Area Attack with Circumnavigation

Another special case of the general method of area attack discussed in Section VI 6 - the area attack with single propulsion period and circumnavigation - results for $\sigma = 0$ and $a + ka = 40000$ km. The relation between bomb-load $\underline{B}$ and attack-range $\underline{a}$ can be read off from Fig. 80,

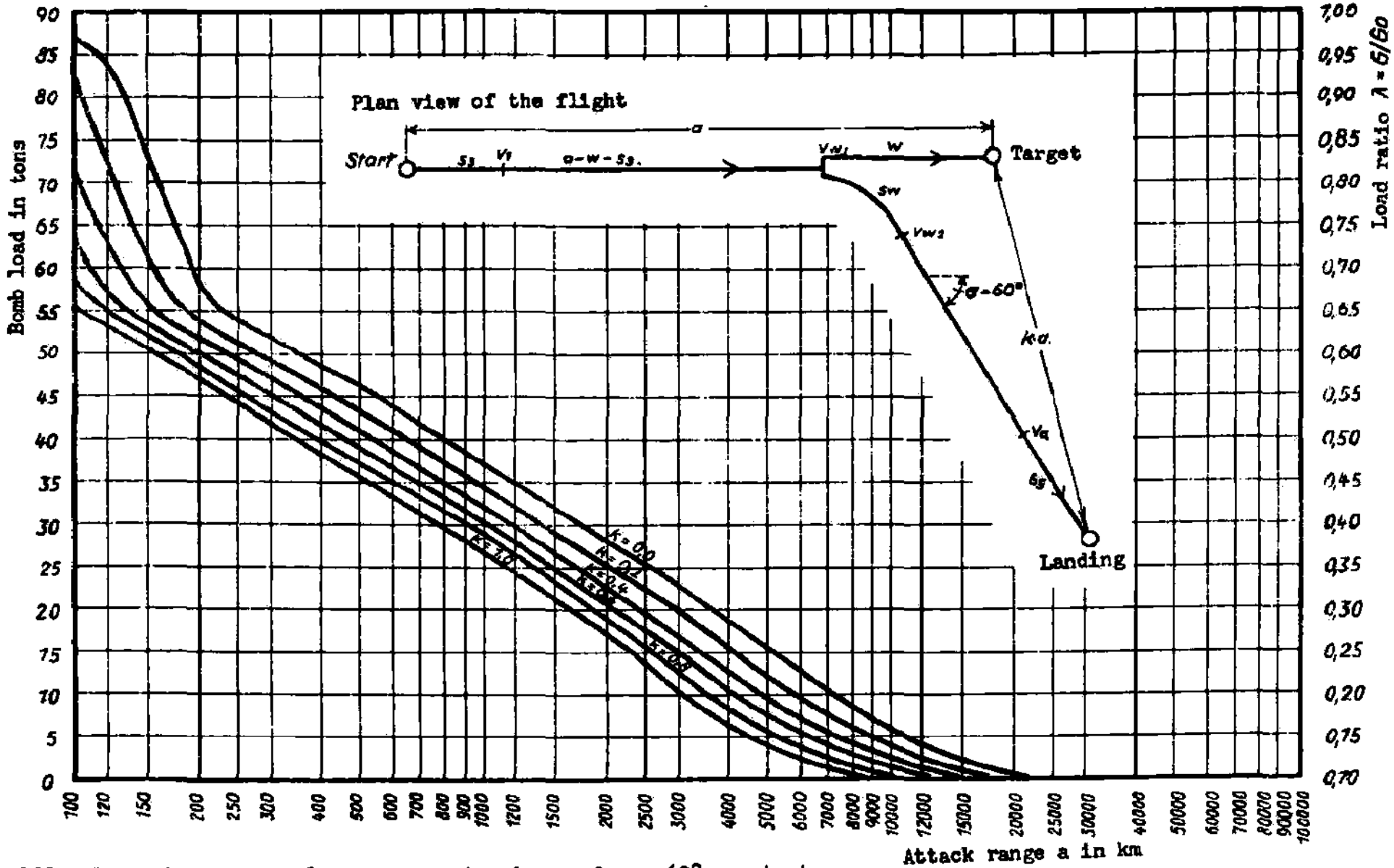

Fig. 102: Area attack - dog leg course - turning angle = 60°=constant. Return flight range, k x a, various fractions, k, of the distance a, to the target. Exhaust velocity = 3000 m/sec.

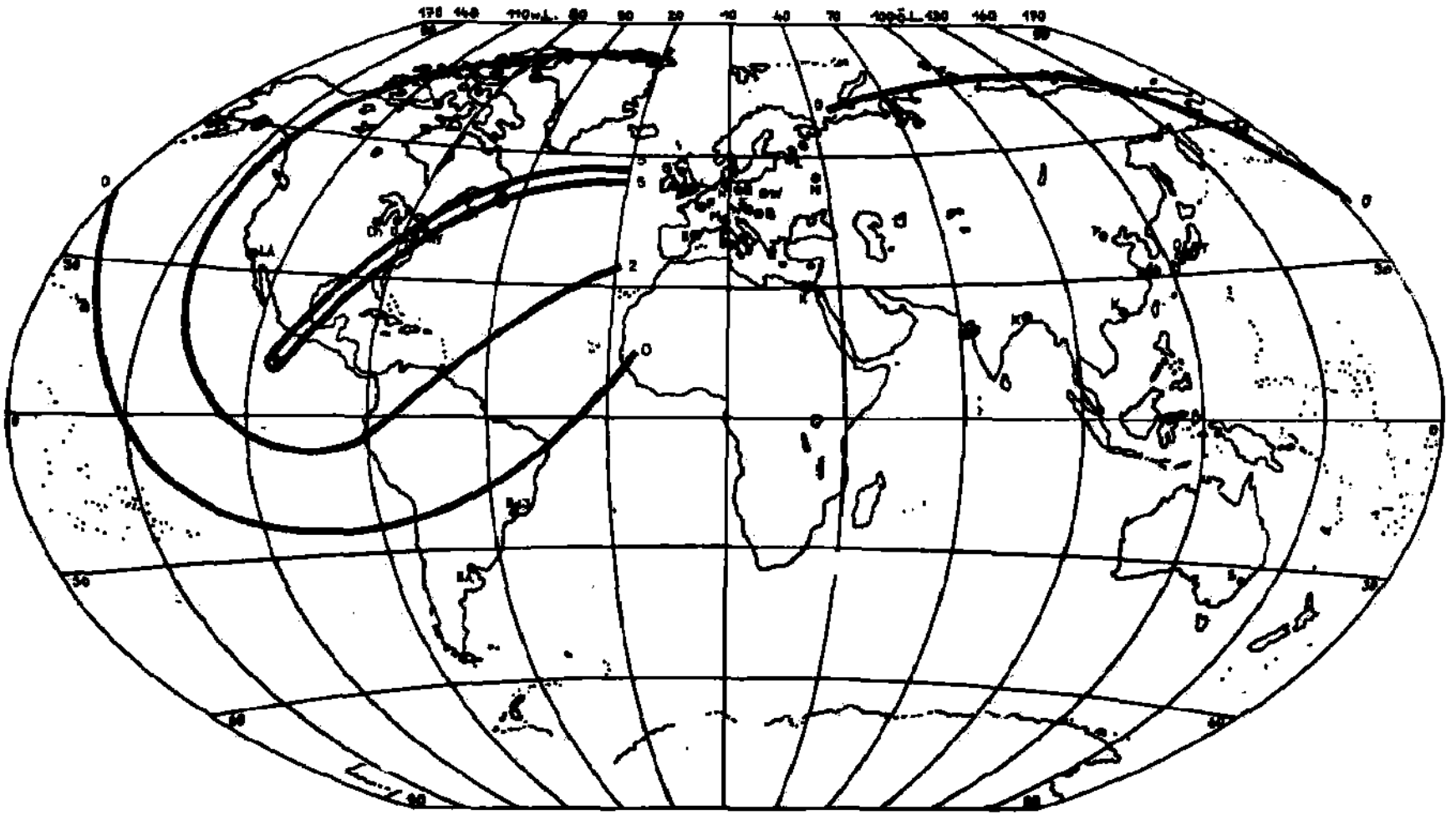

+ Secondary base on American West Coast

● Cities of more than one million

X Home base

Fig. 103: Bomb load of a Rocket Bomber in tons (i.e. percent of the initial weight) in the case of area attack using a secondary base on the American west coast and an exhaust velocity c = 3000 m/sec.

where the rule again holds that the place of bomb release has no effect on the range, so that the range of attack, a, is completely arbitrary and independent of the bomb load. From this figure, the largest bomb load with which circumnavigation is still possible is B = 3 tons for $c = 4000$ m/sec, B = 12 tons for $c = 5000$ m/sec, while for $c = 3000$ m/sec, circumnavigation cannot be achieved even without a bomb load. This method of attack shows most clearly the extreme technical superiority of the rocket bomber which with a size and empty weight equal to that of a medium military craft can, at moderate exhaust speeds, reach every point on the earth's surface with a bomb load of 3 tons, and flies 40000 km. all around the earth without an intermediate landing.

As an example of an area attack with single propulsion period and circumnavigation, we shall use the attack on the city with a million population most distant from Germany - Sidney in Australia. In this case the range of attack is 16500 km., the possible bomb load is 3 tons. The flight goes as follows: Take-off and motion after take-off do not differ from the same phases of previous examples. 36 sec. after take-off the motor begins to operate and consumes the 87 tons of fuel on board in the next 348 sec. At the end of this climbing process the velocity is 7200 m/sec., the altitude 101 km., distance from takeoff-point 815 km. and weight 13 tons. This very high initial speed drops to 300 m/sec. in the course of the supersonic descent which is 39185 km. long. After a 10000 km. journey, the strongly oscillating descent must be damped sufficiently so that at the release point, 15400 km. from take-off, it runs smoothly enough at the stationary altitude to enable accurate aiming for the bomb release. At the release point the altitude is 49 km., the velocity is 6400 m/sec., and the range of projection of the bombs is 1100 km. After release the bomber starts its supersonic glide with only 10 tons weight, during which the course which was previously in a plane has to be altered slightly in order to lead back to the home base. There the bomber lands 13060 seconds after take-off, having travelled 40,000 km.

9. Evaluation of Procedures for Attack

Procedures of point attack are directed against individual houses railroad stations and tracks, tunnel entrances, streets, bridges, dams, single ships, canals, dikes, breakwaters, gas-water-and oil-tanks, munitions depots, magazines, power stations, transformer stations, air-dromes, harbors, factories, troop concentrations, etc; they are limited to a radius of several thousand km. around the home base, except for special cases where the bomber is sacrificed or flies on to an auxiliary field, when the range of attack can extend over the whole of the earth's surface.

Procedures of area attack can be directed against the entire earth's surface. The probable scatter of bombs over several kilometers limits them to target areas of this magnitude, e.g. cities with over a million population, large industries, fleets, etc. If in an area attack, the total energy Z in kcal is released against a single target with a probable scatter $W_r = 2$ km., then half the hits lie in a circle of 2 km. radius; the average density of hits on this unit surface is $\bar{z} = Z/2w_r^2\pi$ the actual density follows a Gauss error curve $z_r = 1{,}398\,\bar{z}\,e^{-0.69\,r^2/w_r^2}$ has the value 1.4 $\bar{z}$ at the center, and is ½ of this at the boundary of the area 4 km. in diameter. Fig. 104 shows such a distribution curve of bomb hits over a map of New York. If larger connected surfaces than the unit surface described are to be attacked, several points of the target can be aimed at, so that the individual Gauss error curves partially overlap somewhat like those of Fig. 105, where the distance between aiming-points was chosen as $w_r\sqrt{2\pi}$ so that the average density over the whole surface is $\bar{z}$, while the local densities are shown as contour lines.

From the appropriate literature the following relations can be gotten between average density of destructive energy $\bar{z}$ in kcal/km^2 and the resultant destructive effect; $\bar{z} = 7\times10^6$ $\frac{kcal}{km^2}$. puts industrial installations completely out of operation for several days. (Degree of destruction I)

$\bar{z} = 1.4\times10^8$ $\frac{kcal}{km^2}$ destroys cities so that all except specially reinforced buildings collapse, and only cellars and foundations are usable (Degree of destruction II)

$\bar{z} = 1.4\times10^9$ $\frac{kcal}{km^2}$ destroys cities so that cellars are also smashed in, all people inside the area are killed and only foundation walls remain standing (Degree of destruction III)

$\bar{z} = 7\times10^9$ $\frac{kcal}{km^2}$ makes cities so flat that their location is no longer discernible against the background. (Degree of destruction IV).

If the energy content of the bomb at rest is assumed to be $E_0 = 700$ $\frac{kcal}{kg}$, then with E =

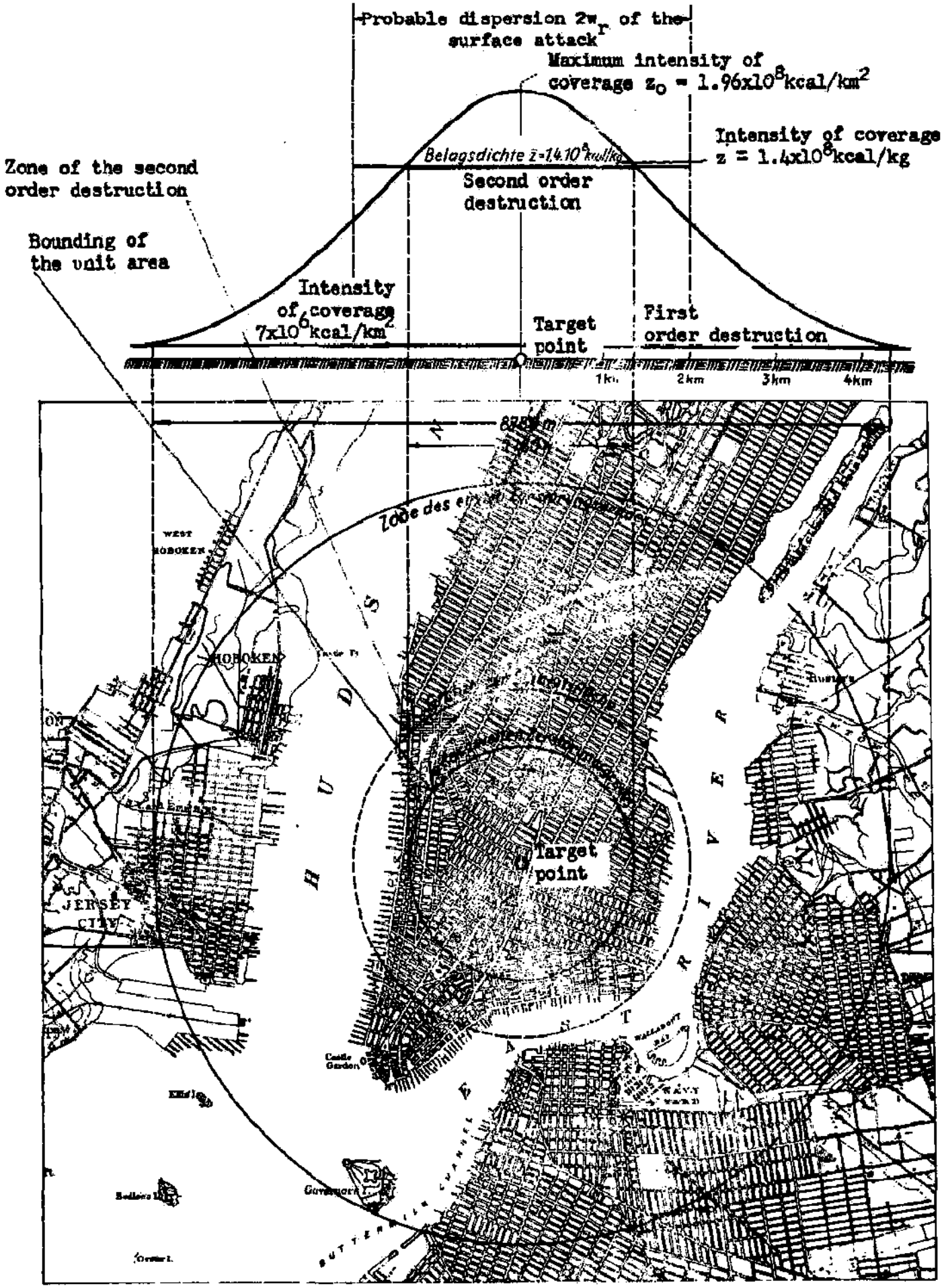

Fig. 104: Hit distribution in area attack against a target point in the center of New York.

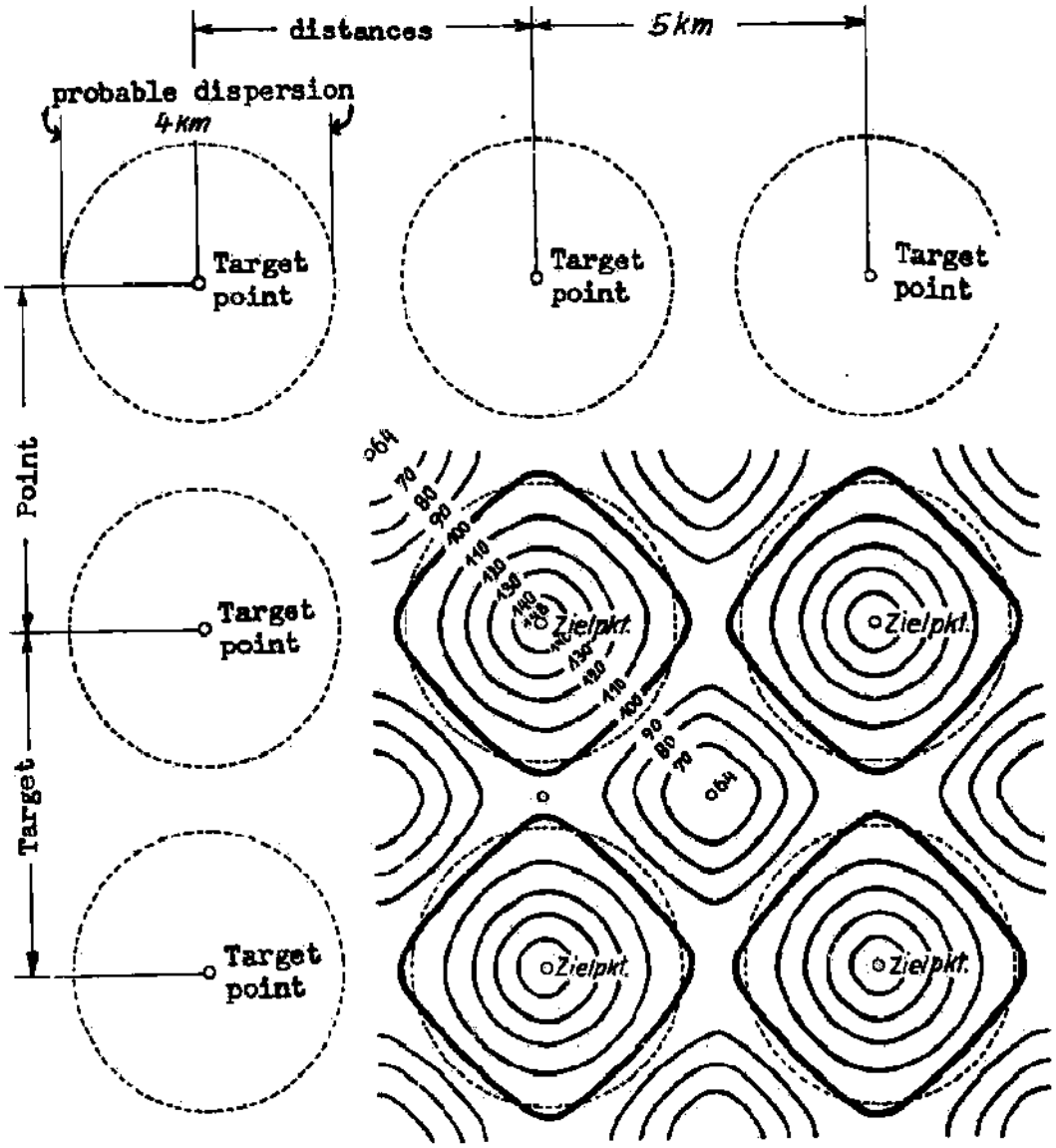

Fig. 105: Target distribution in the case of attack on very large surfaces and contour lines of equal bomb hitting density in percent of average value

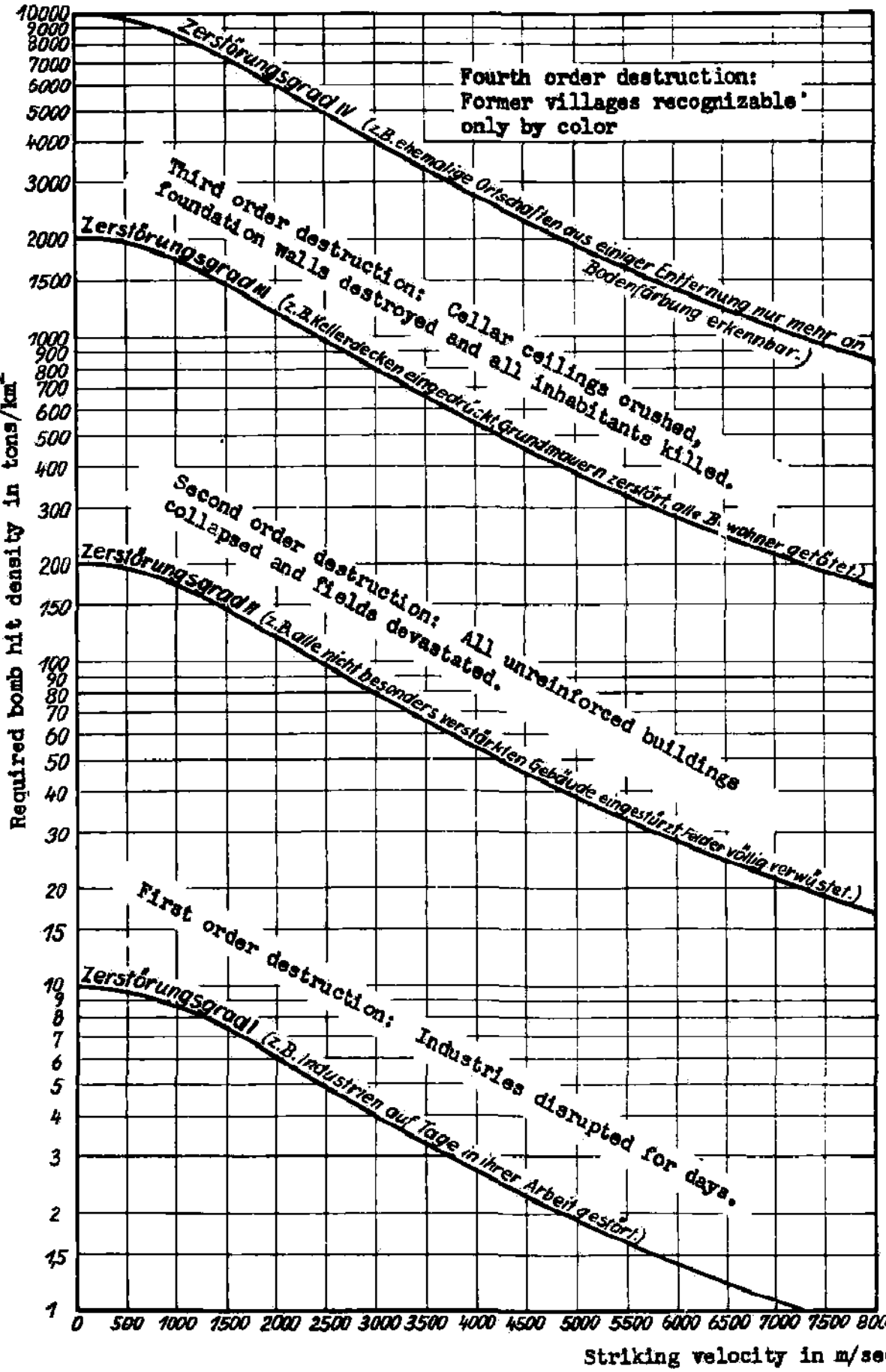

Fig. 106: Required bomb hit density to produce first to fourth order destruction as a function of the striking velocity of the bomb.

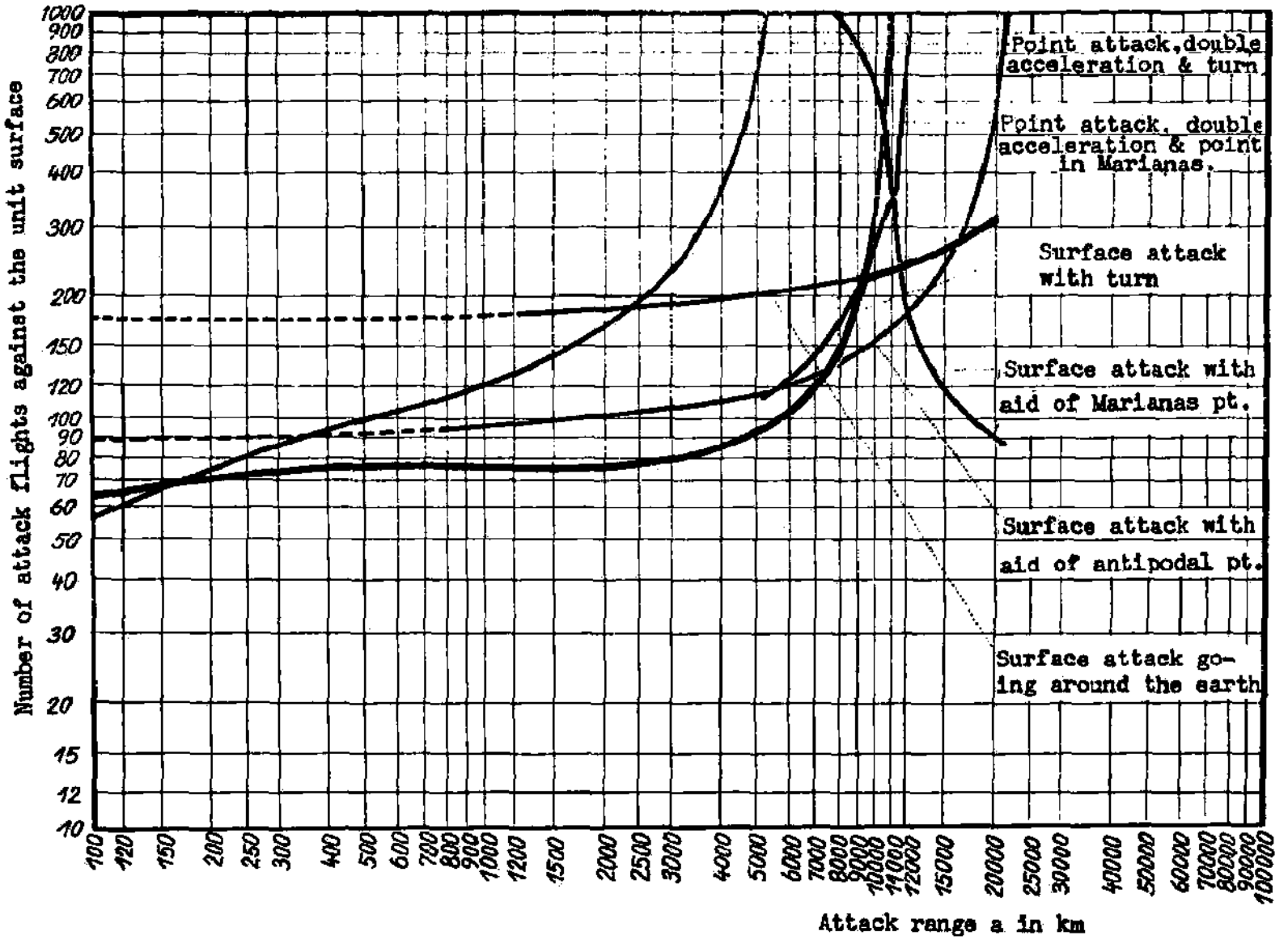

Fig. 107: Number of required sorties to cover the unit area and its surrounding, using various methods of attack, with a total of 3.52×10^9 kcal destructive energy, as a function of the attack range a.

$700 + Av^2/2g$, the density of bomb hits in tons/$_{km}2$, independent of the impact velocity V of the bomb is obtained from Fig. 106.

In order to destroy, to the 2nd degree, the surface of a city having an area equal to the previous unit surface, one must release against the target $Z = 2 \times 12.56 \times 1.4 \times 10^8 = 3.52 \times 10^9$ kcal of destructive energy, corresponding to 5000–420 tons of bombs depending on the velocity of impact. Then the concentration, as shown in Fig. 104, rises to $1.96 \times 10^8 \frac{kcal}{km2}$ near the aiming-points, is $0.98 \times 10^8 \frac{kcal}{km2}$ at the edge of the unit circle, and $1.14 \times 10^8 \frac{kcal}{km2}$ at 4 km. distance from the aiming point.

The number of flights necessary for dropping this amount, Z, of destructive energy on the unit surface is 84 if the bomb load is 60 tons and the impact velocity is low, or 420 if we assume the smallest bomb load - 1 ton -, and an impact velocity of 8000 m/sec. Fig. 107 shows plot of the number of attacks necessary against the unit surface, for various procedures of attack, against range of attack, for $c = 4000$ m/sec. If the unit surface is to be attacked with the minimum number of flights, then the procedure of point attack with double propulsion and full turn is best. If a single unit surface is to be bombed, this superiority is doubled, because then all the energy lies inside the unit circle, and only half as many bombs need to be dropped. For greater ranges of attack up to 8000 km., the procedure of area attack with single propulsion and full turn is far superior to all other procedures, especially since it does not depend on the use of an auxiliary point. A remarkable thing about the curve for this procedure is that the required number of flights does not increase monotonically with the range of attack, but rather that the decreasing bomb load is completely compensated by the increasing impact energy. Corresponding to the full curve, the number of flights actually required when using area attack with full turn or circumnavigation fluctuates between 64 at 1000 km. and 322 at 20000 km. range of attack. The evaluation of attack procedures shown in Fig. 107 assumes that the total consumption of take-off fuel, fuel for the aircraft, and of bombs, which together represent a constant amount of 133.7 tons per flight, shall be a minimum. Since the bombs are much more valuable per unit weight than the fuel, one can also set a requirement of minimum consumption of bombs. In Fig. 108 several procedures of attack are plotted from this viewpoint; we see here the point attack procedures are very inferior while area attack procedures, which operate with high impact velocities of the bombs, are most favorable, especially, area attack with circumnavigation and - at long ranges -, with full turn, which requires in this region the least total consumption as well as least consumption of bombs.

Fig. 109 shows an idealized distribution of hits, according to the laws of probability, over a city map of Berlin, where it is assumed that 84 bombs of 60 tons weight are dropped on the aiming point with low impact velocity; the half shown lies in the 50% circle; about each point of impact a circle of destruction of diameter 618 m results in which the energy density 1.4×10^8 kcal/$_{km}2$ required for degree II exists.

Fig. 110 shows the corresponding distribution of hits for 140 releases with 8000 m/sec. impact velocity and 3 tons weight per release; again the average energy in the unit circle is 1.4×10^8 kcal/$_{km}2$, but the area of destruction for the same energy per release is now drop-shaped and includes 180000 m^2, as previously derived.

VII. THE LINE OF DEVELOPMENT OF THE ROCKET BOMBER

The development of the rocket bomber project will follow roughly the sequence of 12 stages outlined below:

1. Development of the Combustion Chamber and Jet of the Motor

The main problems in this stage concern the introduction of the solid, liquid, or already vaporized fuel and the combustion-maintaining material, into a combustion chamber through injection nozzles; then the rapid distribution, mixing, heating and ignition of the fuel, its most complete combustion at more or less constant high pressure to a combustion gas at very high temperature; then the expansion of these gases in a jet to convert them to a beam of gas with as high streaming velocity and as low temperature as possible. The very high pressures and temperatures in the combustion space have the consequence that not only the tubes for the streaming process in the motor, but also the construction of all walls in contact with the flame, becomes a very serious problem, whose solution as regards choice of materials, methods of cooling, and constructional arrangement, should be a main point of study. Also important are questions of shape and relative size of combustion chamber and jet, choice of most suitable flame pressures, measurement of stream temperature and velocity, arrangements for rapid heating and mixing of the fuel, optical and acoustic phenomena, mixing of the jet with the surrounding air behind the motor, dissociation- and detonation-problems, and numberless others.

2. Development of Special Fuels for Rocket Motors

In many respects quite different requirements are to be set for rocket motor fuels than for the fuels of ordinary aircraft motors. In the first place, what counts is the available energy content per unit mass of the combustion mixture of fuel and, say, oxygen, and not the heating value of the fuel alone Thus a combustible material which has a lower heat of combustion than the usual hydrocarbons, but consumes much less oxygen in burning, can develop a far superior heat output of the mixture. In addition to the heat output of the mixture, other combustion characteristics such as ease of ignition, rate of combustion, tendency to detonate, degree of dissociation, state of aggregation of the combustion products, reaction temperatures, etc., are important. One must also consider properties not so directly connected with the combustion, such as procurement and cost, ease of storage in tanks on the aircraft, density, danger, ease of feeding of the fuel, etc. If one enumerates the problems of atomic hydrogen and nitrogen, of nuclear reactions and of takeoff fuels, then one has outlined in broad strokes the scope of fuel research which should lead to the development of new and more suitable rocket fuels.

3. Development of the Auxiliary Engines of the Rocket Bomber

Just as with ordinary aircraft motors, the rocket motor requires for its operation a few auxiliary engines, of which the most important are those for feeding fuel and coolant and the associated driving assemblies. These additional installations present some not-too-simple problems, since the feeding rates are very high, of order of magnitude 50-100 H.P. per ton of thrust, and the material to be conveyed can be in altogether unusual states, say a liquefied gas, a metallic suspension or even solid or liquid metal - and must be very accurately proportioned as well as being fed against very high pressures. A complication arises because the feeding installations must be designed under extreme limitations on weight of construction. In addition to these arrangements for feeding of fuel and coolant, ignition systems and in some cases intake and regulator systems require consideration.

4. Development of Test Model of Complete Rocket Motor

Even if the development of the previously enumerated most important parts of the motor had been achieved taking account of their interactions, putting them together into a ready-to-fly rocket motor and examining their interplay is still a separate and important step. Only now, on the apparatus ready for flight can a bench study be made of the mutual interactions of the combustion chamber, jet, fuel and auxiliary engines, so that by suitable adjustments the best results are obtained for exhaust speed, reliability of performance and construction weight. These bench tests of the complete rocket motor are especially important and thorough because they reproduce the conditions during flight very closely; this is in contrast to the ordinary aircraft motor where these conditions can be imitated only with difficulty and not even completely by altitude tests. This is mainly connected with the fact that the rocket motor accomplishes the jet formation, combustion and cooling only with its own fuels, and without use of the surrounding atmosphere, so that the differences of velocity, temperature and pressure of surrounding air between the bench test and actual flight can scarcely alter the conclusions. One of the few places where the rocket motor comes in contact with the surrounding air is the mouth of the jet. There the

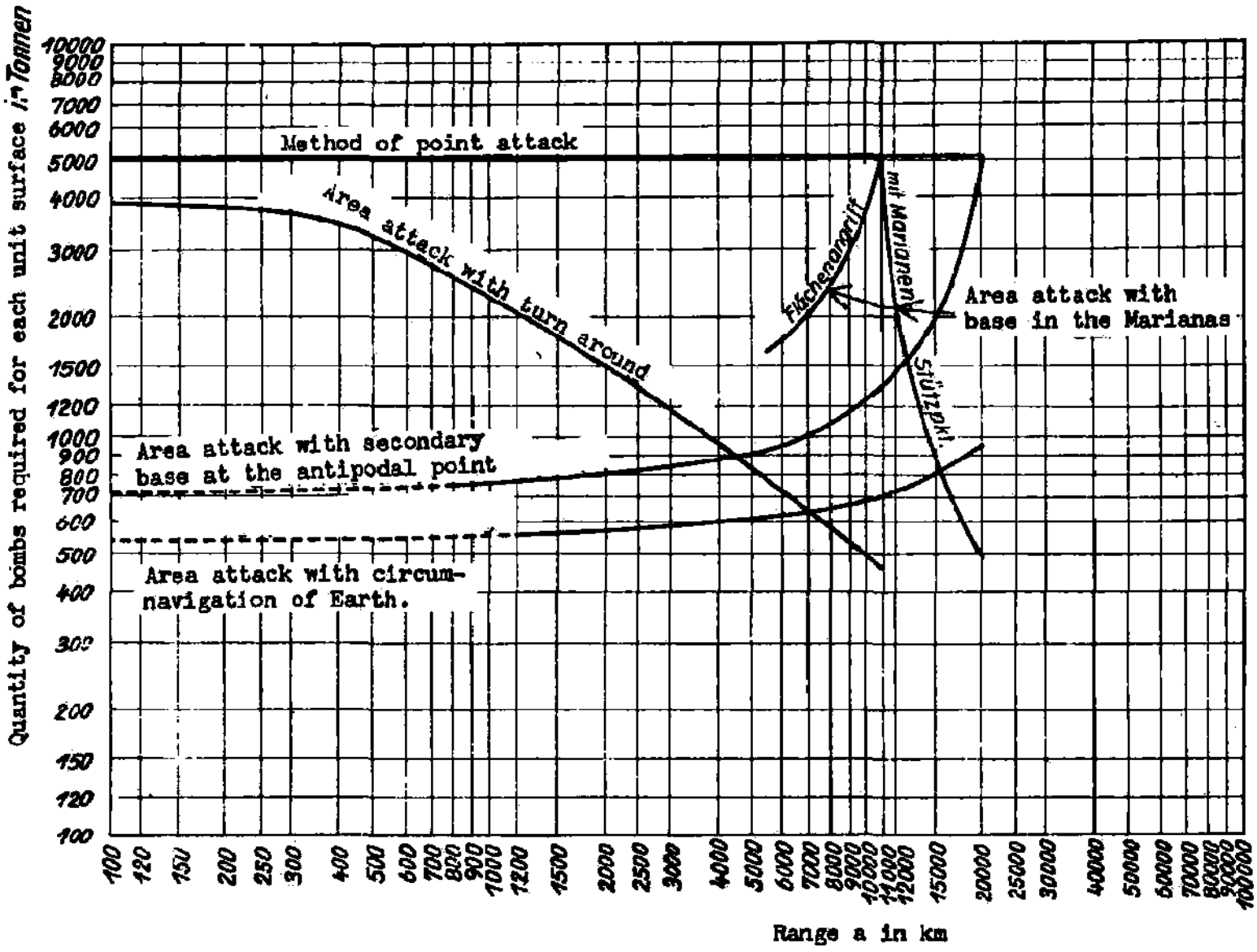

Fig. 108: Amount of required bombs in tons in order to cover the unit surface and the environment by various methods of attack with a total of $3.5? \times 10^{9}$ kcal destructive energy as a function of attack distance a.

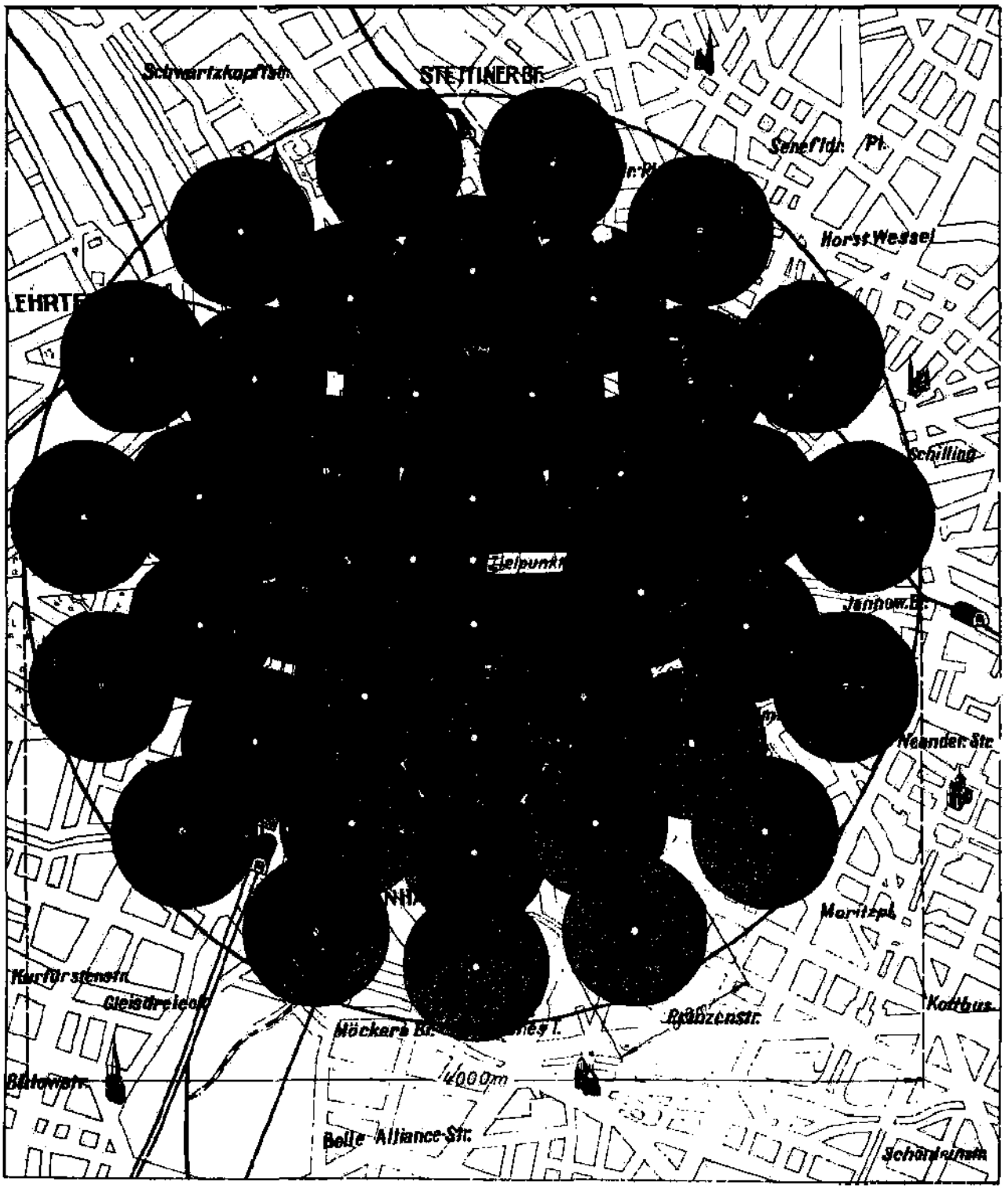

Fig. 109: Ideal Gaussian hit distribution of 42 hits, each of 60 tons of bombs, with small striking velocity in the unit circle in case of surface release against the target, and with area of destruction for each bomb (for example, bombardment of Berlin).

Fig. 110: Ideal Gaussian hit distribution of 70 hits, each of 3 tons of bombs, with small striking velocity in the unit circle in case of surface release against the target, and with area of destruction for each bomb (example, bombardment of Berlin).

combustion gas expands to the pressure of the air behind the aircraft; in flight this pressure is practically zero whereas in the open bench test the jet can expand only to the pressure of the still air around it. Still the differences are not very great, are largely amenable to calculation, and are moreover such that the bench test considers the more unfavorable case. A reaction of the slip-stream and the jet on the aircraft (in particular on the control surfaces) need not be considered for the rocket bomber, because operation of the motor and subsonic velocities of flight never occur together. Aside from the purely developmental and test studies on the model, a whole series of physical researches on the rocket motor can be carried out most advantageously during this phase of the development: more careful investigation of atomizing of the fuel, the actual behavior of the pressure in the combustion chamber, the temperature distribution in the combustion gas, the actual streaming speeds, the conditions of heat transfer from the combustion gas to the walls and from them to the coolant, the jet formation and sound emission in the furnace-jet, as well as numerous other questions. Only when in the course of these studies the motor has proven its complete reliability of performance, can one consider installing it in an aircraft. The development of this aircraft will have to be done alongside that of the motor, so that both may be ready for flight at the same time.

5. Wind-Tunnel and Tow-Tests on Models of the Air-Frame

The external shape of the rocket bomber is determined by the requirements that existing experience on screw-propelled aircraft shall be used as much as possible, that the special conditions of supersonic flight and rear installation of the motor must be considered, that the glide-number of the aircraft shall be as good as possible at very high Mach numbers, where the aerodynamic forces are proportional to the square of the velocity and angle of attack. Under these general requirements models of the rocket bomber can be designed; these cannot be tested in the most interesting region of very high Mach numbers, in the upper part of which actual chemical changes of the streaming medium are possible, because as yet such artificial air-blasts are not available; one can perform wind-tunnel tests in the range of Mach numbers from 0.08 to 4. In the range of velocities below that of sound, which is important for the landing process, using models of reasonable size one can carry out measurements on the aerodynamic forces, and especially on the maximum lift of the aircraft, and its improvement by the use of aerodynamic aids suited to the particular profile. In this range tunnel-tests on stability, vibration conditions and manoeuvrability of the vehicle are important. In the supersonic domain, aerodynamic forces, distribution of air pressure, stability and manoeuvrability, vibration conditions, air temperatures at the stagnation points, and heat transfer to the aircraft are of interest. A whole series of these tests on very small models can be carried out in a supersonic wind tunnel.

For tests on larger models the takeoff track of the rocket bomber is itself a very convenient towing-track; on it even very large models can be towed up to any desired high speed with the aid of rocket propulsion, and then studied. Such tow tests can be carried out at reasonable cost on a 15-30 km. long track, with models scaled 1:10 up to 1:1 at the original speeds of 800 up to 5000 km/hr, so that the Mach number is duplicated exactly and the Reynolds number approximately. Such tests would especially consider the general behavior of the aircraft in the neighborhood of the velocity of sound, i.e. between 800 and 1800 km/hr, for various shapes, angles of attack, arrangements and tilts of control surfaces, etc.; also the distribution of air pressure and temperature on the surface of the aircraft by means of taps, thermoelements, etc., for all velocities; measurement of the location and magnitude of the forces acting on the aircraft, direct tests of stability by means of a Cardan suspension of the moving model at its center of gravity, studies of the reaction of the jet on these conditions - especially on the aerodynamic forces and the stability investigation of the elastic properties on elastically-similar models; e.g. as regards vibration of the wings and control surfaces, etc.; takeoff and free-flight characteristics of self-stable or remotely controlled models especially during the passage of the velocity from values below the sound velocity to values above, and others. A special problem in such tow-tests, aside from the track itself, is the relative sliding behavior of lubricated surfaces at sliding speeds up to 5000 km/hr. For flight at arbitrary speeds in regions of very rare atmosphere, in which the so-called gas-kinetic laws are valid, and where neither tow tests or ordinary wind-tunnel tests are feasible, an extension of the theory is desirable, as well as its experimental justification, say by extension of the well-known molecular-beam methods to the present problem.

6. Constructional Development of the Vehicle

Once a preliminary decision as to the whole arrangement and shape of the rocket bomber has been made on the basis of wind-tunnel- and tow-tests, one can commence the construction of the fuselage, wings, control surfaces, and important installations such as the pilot's cabin, the tank installations and auxiliary equipment. In view of the fixed external shape, the decisive factor for the construction of the fuselage, wings and control surfaces is the fact the air pressures which occur are far greater than those on ordinary aircraft. The air pressures on the rocket bomber will certainly be in the neighborhood of 3000 kg/m^2, and will therefore lead to types

of wing construction like those used in buildings or ships. The problem of the pressurized cabin has already been treated in other connections. The results assembled there can be made use of. There are no prototypes on which to base tank installations for large quantities of fuels like liquefied gases, metallic suspensions, etc., and these must be suited to the special conditions. An especially extensive group of apparatus requiring development is the auxiliary equipment of the rocket bomber, including velocity-, altitude-, and acceleration-meters, instruments for steering, navigation and aiming of bombs, optical instruments and many other apparatuses and instruments connected with the special characteristics of rocket flight.

7. Bench Tests on Interaction of Motor and Air-Frame

These tests represent the last stage before the first flight tests, and should check the satisfactory operation of the motor (which has so far only been bench-tested) under the conditions where all the parts have been assembled into a vehicle. The exact relation between the driving force and the centers of mass and air pressure of the aircraft should be checked to avoid instabilities caused by incorrect placement of the engine; and finally during these tests the pilot can become accustomed to some of the peculiarities of the new aircraft.

8. Development and Test of the Takeoff Arrangement

The several kilometers long takeoff path with its arrangement of rails represents a relatively simple engineering construction which presents no special problems. On the other hand, the takeoff sled, which under a load of several hundred tons must be accelerated in a very short time to 1 1/2 times the velocity of sound and then slowed down even more rapidly, requires special development. This will be concerned especially with the extraordinarily powerful takeoff rocket, the sliding contacts of the sled and the method of braking. Completely reliable operation of the takeoff track will have to be carefully tested by catapult trials on dead weights comparable to the weight of the aircraft.

9. Takeoff and Landing Tests on the Bomber

The takeoff tests begin with small fuel load on a taxi-strip which is as long as possible the practically empty bomber, after very brief operation of its own rocket motor obtains the velocity required to float, after which it rolls on its own landing gear. After a short hop it drops down again and carries out its first landing, which does not differ from the later landings after long flights. These takeoff tests should be carried out in such a large space that the landing can occur immediately after the takeoff without turning the aircraft, in order not to endanger the aircraft by manoeuvers near the ground when its flight characteristics are still uncertain. If after many such tests, the takeoff and landing characteristics are understood, then by using more fuel the aircraft can be brought to somewhat higher altitudes, say a few hundred meters, and then glided back to earth. Thus the essential flight characteristics at low speed will be determined, the arrangement of the control surfaces will be undertaken, the trimming, stability and manoeuvrability will be checked, and thus the airworthiness of the craft in all flight attitudes at not too high altitudes will be determined and eventually improved. If during these tests the aircraft acts reliably for the pilot, then the takeoff tests on the track can be repeated, by placing the empty aircraft on the takeoff sled, catapulting it and landing it. If these tests are satisfactory the trials can be extended to higher flight speeds. This phase of the trials will best begin by tow tests on a very long tow path, so that the aircraft doesn't get to fly but is only accelerated on the towing path and then immediately slowed down again. These tow tests on the actual aircraft at gliding speeds of 800 to 1600 km/h are to be devoted especially to the following individual problems: rechecking and refinement of the results of the tow tests on models concerning pressures, temperatures, aerodynamic forces, stability, vibrations, effects of the driving jet, etc.; studies of the behavior of instruments, apparatus and jet engines under the influence of high accelerations and velocities, development of suitable safety devices, e.g. special seats, getting the pilot accustomed to the new phenomena of high accelerations, high velocities, special engines and new arrangements of the aircraft.

10. Flight Tests of the Bomber

Finally one can go over to flight tests in which one catapults the aircraft with an initially small but gradually increasing supply of fuel, and lets the motor operate for longer and longer periods. Thus longer and longer climb paths will be traversed; one will soon surpass the velocities attained up to now by the fastest aircraft, and go up to altitudes never previously reached. The takeoff speeds also increase at the same time. Now begins the most difficult part of the flight studies, since the flight conditions depart farther and farther from any known at present and checked by experience; completely new aeronautical territory must be conquered. As far as can be visualized at present, the flight tests will extend to maintenance of requirements of life in the pilot's space taking account of the high altitudes, accelerations, and temperatures, the effect of the aerodynamic forces on the wings and controls of the aircraft, testing of the heating of the walls at many points of the aircraft, maintenance of stability and manoeuvrability beyond the velocity of sound, etc. This part of the flight tests will have to be done very

circumspectly and with stepwise increase in velocity, since at very high altitudes, low air densities and high speeds, any slight accident can lead to a catastrophe since it is practically impossible to leave the aircraft by parachute. These tests of flight characteristics will be continued up to speeds not yet reached by projectiles, i.e. about 6 times the velocity of sound. Finally the actual trial flights will be completed with performance tests. They will serve first to determine simple performance data such as takeoff speeds, takeoff distances, landing distances, landing speeds, climbing performance, consumption of fuel, etc., and later to determine the maximum speed, ceiling and range of the rocket bomber. Since these three limiting performance figures are interdependent, they can be determined during the same flight. As the velocity is increased from the values attained during the tests of flight characteristics up to the maximum value, the temperature distribution on all windward surfaces will have to be carefully checked by means of a remote-reading thermometer system, in order to catch in time any dangerous heating as a result of air friction and stagnation. Too great heating, especially of projecting parts, such as the sharp end of the fuselage, the sharp wing edge, etc., is most dangerous because the slightest melting or other deformation of these carefully shaped critical points and their consequent blunting leads to instantaneous enormous increase of the stagnation temperature at those places and then in steadily spreading molten regions, and would result in immediate burning up of the whole aircraft. If the performance flights are carried out until these expected limiting values of 7000 m/sec velocity, 150 km altitude and 40000 km. length of flight are reached, then the flight studies can be considered completed.

11. Navigation Tests on the Rocket Bomber

The next important task of development concerns arrangements for navigation, which, after propulsion has ceased, give the rocket craft exact knowledge of its path, enable corrections of its course, and permit an exact calculation of the moment of bomb release. This precision navigation will have to be checked in a very large number of flight tests, since the success of any attack depends on its accurate and rapid performance.

12. Bomb Release Trials

These constitute the last phase of the research and development work on the rocket bomber and should give a practical verification of the preliminary theoretical work on the processes occurring during the fall of the bombs and their contact with the earth. So far as the relation between point of impact and point of release from the aircraft for various heights and speeds of flight is concerned, the oceans of the whole earth provide a suitably large testing areas. The study of impact of the bomb on land will be somewhat more troublesome, since very large uninhabited areas are required. However a few tests in the Arctic regions untrodden deserts or in our own possessions will suffice for this purpose.

BIBLIOGRAPHY

(1) C r a n z, C.: Lehrbuch der Ballistik. Springer, Berlin.

(2) D i r i n g s h o f e n, H. v.: Bis zu welcher Stärke kann der Mensch im Flugzeug Zentrifugalkräfte vertragen und welchen Einfluss hat hierauf die Änderung der Körperhaltung. Jahrbuch 1937 der Deutschen Luftfahrtforschung, Ausgabe Ausrüstung, S. 128.

(3) F l ü g g e, S.: Kann der Energieinhalt der Atomkerne technisch nutzbar gemacht werden. Naturwissenschaften 27, S. 402, 1939.

(4) F r e n k e l, I.: Theorie der Adsorption und verwandter Erscheinungen. Zs. f. Physik 26, S. 117, 1924.

(5) G e i b, K. H.: Atomreaktionen. Ergebnisse der exakten Naturwissenschaften Bd. 15, S. 44, 1936.

(6) G l i w i t z k y, W.: Messung des Druckverlaufs bei Aluminiumstaubexplosionen. Zs. d. VDI Bd. 80, S. 689. 1936.

(7) G ü m b e l, L. und E v e r l i n g, E.: Reibung und Schmierung im Maschinenbau. Berlin 1925, Krayn.

(8) J o s t: Explosions- und Verbrennungsvorgänge in Gasen. Berlin 1939, Springer.

(9) K n e s e r, H.O.: Der aktive Stickstoff. Ergebnisse der exakten Naturwissenschaften. Bd. 8, S. 229, 1929.

(10) K n e s e r, H.O.: Die akustischen Relaxationserscheinungen. Phys. Zs. 39, S. 800, 1938.

(11) L a n d o l t - B ö r n s t e i n: Physikalisch-chemische Tabellen, Berlin 1923 - 1936, Springer.

(12) R a n k e, O.F.: Kreislauf unter Beschleunigung; Versuche über die Wirkung der Beschleunigung auf der Zentrifuge an Mensch und Tier. Jahrbuch 1937 der Deutschen Luftfahrtforschung, Ausgabe Ausrüstung, S. 123.

(13) R o t h, W.A., W o l f, U. und: F r i t z, O. Die Bildungswärme von Aluminiumoxyd und Lanthanoxyd. Zs. f. Elektrochem. 46, S. 42, 1940.

(14) R u f f, O. und K o n s c h a k, M.: Verdampfungswärme des Al_2O_3, Zs. f. Elektrochem. 32, S. 32, S. 518, 1926.

(15) R u f f, S.: Die physiologische Wirkung hoher Beschleunigungen. Luftwissen 7, S. 24, 1940.

(16) S ä n g e r, E.: Über Bau und Leistungen der Raketenflugzeuge. Deutschösterr. Tageszeitung, Folge 35, S. 11 und Folge 38, S. 9, 1933.

(17) S ä n g e r, E.: Der Entwicklungsweg der Raketenflugtechnik. Zs. Flug, Heft 5 - 10, Wien 1933, Pittner.

(18) S ä n g e r, E.: Raketenflugtechnik. München 1933, Oldenbourg.

(19) S ä n g e r, E.: Neuere Ergebnisse der Raketenflugtechnik. Zs. Flug, Sonderheft 1, Wien 1934, Pittner.

(20) S ä n g e r, E.: Der Raketenantrieb für Flugzeuge. Der Pilot, Heft 1, S. 5, 1935.

(21) S ä n g e r, E.: Raketenmotor und Verfahren zu seinem Betrieb. Oe. P. 144 809, Wien 1935.

(22) S a n g e r, E.: Expansionsdüse mit gekühlter Wand für die Feuergase von Raketenantriebsmaschinen. Oe. P. 146 000, Wien 1935.

(23) S ä n g e r, E.: Der Verbrennungs-Raketenmotor. Schweizer Bauzeitung, Bd. 107, Nr. 2, S. 1, 1936.

(24) S ä n g e r, E.: Kurze Darstellung der Raketentechnik. Deutsche Luftfahrtforschung, Bericht 828, Berlin 1936.

(25) S ä n g e r, E.: Hohe Auspuffgeschwindigkeiten beim Raketenantrieb. Deutsche Luftfahrtforschung, Bericht 829, Berlin 1936.

(26) S ä n g e r, E.: Raketenmotor. D.P. 44/39, Berlin 1937.

(27) S ä n g e r, E.: Verfahren zum Betrieb eines Raketenmotors mit Dampfkraftmaschinenhilfsantrieb. D.P. 380/40, Berlin 1938.

(28) S ä n g e r, E.: Gaskinetik sehr hoher Fluggeschwindigkeiten. Deutsche Luftfahrtforschung, Bericht 972, Berlin 1938.

(29) S ä n g e r, E.: Gleitkörper für sehr hohe Fluggeschwindigkeiten. D.P. 411/42, Berlin 1939.

(30) S ä n g e r, E.: Verfahren zum Betrieb eines Raketenmotors mit Sonderbrennstoffen. D.P. a.S. 143 284, Berlin 1940

(31) S c h u b e r t, G.: Physiologie des Menschen im Flugzeug. Berlin 1935, Springer.

(32) S é f é r i a n, M.D.: Flamme d'hydrogène atomique; recherches sur la dissociation des gaz dans l'arc. Chaleur et industrie 19, S. 80, 1938.

(33) Z e n n e c k, J.: Physik der hohen Atmosphäre. Ergebnisse der kosmischen Physik, Bd. 3, S. 1, 1938.

TABLE OF MOST IMPORTANT SYMBOLS

a.....attacking distance (m, km), sound velocity (m/sec)

a.....critical sound velocity (for example, in nozzle throat)

b.....acceleration (m/sec^2)

b_n.....normal acceleration (m/sec^2)

b_t.....tangential acceleration (m/sec^2)

c.....effective exhaust velocity (m/sec)

c_{max}.....maximum flow velocity of fire gases (m/sec)

c_{th}.....theoretical maximum flow velocity of fire gases (m/sec)

c_m.....fire gas(exhaust) velocity at the mouth (of nozzle) (m/sec)

c_H.....probable velocity of the air molecules before they strike a wall (m/sec)

c_R.....probable diffuse rebound velocities of the air molecules from a wall (m/sec)

c_a.....lift coefficient (C_L)

c_{ao}.....initial lift coefficient (C_{Lo})

c_{amax}.....maximum lift coefficient

c_{aF}.....lift coefficient of wings

c_w.....drag coefficient (C_D)

c_{wr}.....frictional component of C_D, drag coeff.

c_f.....surface drag coefficient

c_v.....specific heat at constant volume ($kcal/kg^o$)

c_{vtrans}.....specific heat at constant volume, portion due to molecular translation ($kcal/kg^o$)

c_{vrot}.....specific heat at constant volume, portion due to molecular rotation ($kcal/kg^o$)

c_{vosc}.....specific heat at constant volume, portion due to molecular vibration ($kcal/kg^o$)

d.....wall strength, caliber, diameter (m)

d_m.....diameter of nozzle mouth (m)

d.....nozzle throat diameter (m)

f.....cross-sectional areas (m^2)

f.....cross-sectional areas of throat of fire nozzle (m^2)

f_m.....area of surface bounding mouth of nozzle (m^2)

g.....acceleration due to gravity (m/sec^2)

h.....length of projectile (m)

h_o.....smallest thickness of lubricating layer (m)

i_{pH}.....vertical shock impulse which in unit time is transmitted to surface of plate by impinging air molecules (kg/m^2)

i_{pR}.....vertical rebound impulse which in unit time is given by surface of plate to rebounding air molecules (kg/m^2)

i_r.....impulse parallel to wall, of the air molecules which impinge in unit time on a unit area of the wall (kg/m^2)

l.....free path length of molecules (m)

m.....mass ($kgsec^2/m$)

p.....air pressure, gas pressure, pressure (kg/m^2)

p_a.....external pressure of static air (kg/m^2)

p_o.....initial pressure, gas pressure in furnace, stationary gas pressure (kg/m^2)

p_m.....mouth pressure (kg/m^2)

q.....dynamic pressure, heat flow ($kcal/m^2sec$)

r.....trajectory radius of horizontal turning curves (m)

s.....flight distance (m,km) (pathlength)

s_1.....starting distance (m,km)

s_2.....length of partial distance after starting (m,km)

s_3.....length of accelerated climb (m,km)

s_4.....length of unaccelerated supersonic glide path (m,km)

s_5.....subsonic glide path length (m,km)

s_w.....length of turning distance (m,km)

t.....time (seconds), wing depth, sliding slipper depth (m)

t_f.....hot side temperature of fire wall(^oC)

t_k.....cool side temperature of fire wall (^oC)

v.....flight velocity (m/sec)

$\mathfrak{H}$.....velocity vector (m/sec)

v_a.....absolute velocity (m/sec)

v_o.....initial flight velocity (m/sec)

V_e.....velocity of a point on the earth's surface (m/sec)

v_{w1}.....flight velocity at beginning of turning arc (m/sec)

v_{w2}.....flight velocity at end of turning arc (m/sec)

w.....bomb range (m,km) (literally "throwing distance")

w_r.....probable scattering of bomb trajectories (km)

$\bar{z}$.....average density of bomb hits for surface attack (kcal/km^2)

A.....mechanical equivalent of heat (1/427 kcal/kg), lift (kg)

B.....bomb load (kg)

C.....coriolis force (kg)

D.....dissociation energy (kcal/kg)

E.....reaction heat of fuels, upper mixture coefficient, total energy content (kcal/kg)

E_v.....spacial energy concentration (kcal/Liter)

F_R.....rebound energy of air molecules per unit time and unit wall surface (kcal/m^2 sec)

F_W.....energy of air molecules remaining in walls after impact (kcal/m^2 sec)

F_A.....energy carried by air molecules per unit time and unit surface to wall (kcal/m^2 sec)

F.....aerodynamic supporting surface (m^2)

F_F.....carrying wing surface (m^2)

F_R.....carrying fuselage surface (m^2)

G.....weight (kg)

G_o.....initial weight (kg)

G_1.....weight of bomber after using up fuel required in approach of target (kg)

G_2.....weight of bomber after release of bombs (kg)

G_3.....empty weight of bomber (kg)

G_s.....starting weight (kg)

G_{os}.....initial starting weight (kg)

H.....flight altitude (m,km)

J.....heat content (kcal/kg), impulse (kgsec)

J_o.....heat content in state of rest, state of furnace, initial state (kcal/kg)

J_m.....mouth impulse (kgsec)

K.....evaluation number of rocket fuels

M.....molecular weight

P.....effective thrust, load on one of a sliding slipper (kg)

P.....free thrust measurable by dynamometer (kg)

Q.....quantity of heat (kcal/kg)

R.....individual gas constant (m/°), radius of earth (m)

R_e.....Reynold's number

R_{io}.....internal height of evaporation at 0°K (kcal/kg)

T.....temperature (°K), d'Alembert's inertial force (kg)

T_o.....initial temperature, furnace temperature, static temperature (°K)

T_m.....mouth temperature (°K)

T_G.....temperature of air molecules before impact with wall (°K)

T_W.....temperature of a wall surface struck by air molecules (°K)

T_R.....temperature of air molecules after rebounding from wall (°K)

U.....internal energy (kcal/kg)

V.....specific gas volume (m^3/kg)

V_o.....furnace volume (m^3)

W.....resistance (kg)

W'.....resistance measured in wind tunnel (kg)

Z.....total energy thrown at a target (kcal)

α.....angle of attack (^{o}), coefficient of accommodation

α_s.....angle of attack of leading edge of a curved surface

γ.....specific weight (kg/m^3)

γ'.....specific gas weight at the critical velocity (kg/m^3)

γ_o.....specific gas weight at rest, or in the neighborhood of Earth's surface (kg/m^3)

ε.....glide number, numerical eccentricity of a Keppler ellipse

ϵ_a.....optical absorption coefficient

ξ.....compass rose angle (i.e. "heading") (^{o})

η.....viscosity ($kgsec/m^2$)

η_a.....maximum efficiency, external efficiency

η_n.....nozzle efficiency

η_i.....internal efficiency

η_o.....furnace efficiency

η_{therm}.....thermal efficiency

$\varkappa$.....adiabatic exponents

$\bar{\varkappa}$.....average adiabatic exponents

λ.....thermal conductivity ($kcal/mh^o$)

μ.....coefficient of friction

ρ.....density, radius of path, ($kgsec^2/m^4$) (m)

$\bar{\rho}$.....mass of gas striking unit surface area of a plate each second ($kgsec/m^3$)

ρ_m.....gas density at the mouth ($kgsec^2/m^4$)

ρ_o.....gas density in furnace, initial state, rest state ($kgsec^2/m^4$)

σ.....strength, turning angle (kg/cm^2) (^{o})

τ.....tangential stress due to air or gas drag (kg/m^2)

φ.....path inclination (^{o})

ω..... angular velocity (1/sec)

Δ.....change in a quantity

θ.....characteristic temperature of vibrational excitation of a gas molecule (^oK)